The geology of the Blouberg Formation, Waterberg and Soutpansberg Groups in the area of Blouberg mountain, Northern Province, South Africa

by

ADAM JOHN BUMBY

Submitted in partial fulfillment of the requirements for the degree

DOCTOR OF PHILOSOPHY

in the Faculty of Science
University of Pretoria

PRETORIA

November 2000

THIS THESIS REPRESENTS THE ORIGINAL WORK OF THE AUTHOR, EXCEPT WHERE SPECIFIC ACKNOWLEDGEMENT IS MADE TO THE WORK OF OTHERS

November 2000

ABSTRACT.

The geology of the Blouberg mountain area, Northern Province, South Africa is characterised by a number of successor basins developed over a region which is underlain by a cratonic suture (the Palala Shear Zone). The suture was formed during the Limpopo Orogeny, due to oblique convergence of the Kaapvaal Craton and the Central Zone of the Limpopo Mobile Belt at either 2.65Ga or 2.0Ga. Post-collisional brittle reactivation along the Palala Shear Zone in the Blouberg study area is accommodated on the parallel Melinda Fault.

The earliest basin developed in this area was that of the Blouberg Formation, which is preserved in an area restricted to the eastwards extension of the Palala Shear Zone. The Blouberg Formation can be divided into Lower and Upper Members. The widespread Lower Member is thought to have been deposited in a pull-apart basin, is characterised by braided fluvial sheetflood deposits, and is generally steeply-dipping or overturned, reflecting a subsequent southwards-vergent basin inversion. The Upper Member contrasts with the Lower Member in that it is preserved only rarely, is generally flat-lying, and is composed of conglomerates with sub-angular cobbles of foliated basement rocks with rare granulestone beds, reflecting deposition in debris flows and braided rivers respectively. The tectonic event responsible for the southwards-vergent basin inversion of the Lower Member probably also uplifted proximal basement sources to the north and east, leading to deposition of the Upper Member in localised basins close to the southern strand of the Melinda Fault scarp.

The syn-tectonic deposition of the Blouberg Formation was followed by a period of relative tectonic quiescence, and deposition of the Waterberg Group. The fluvial Setlaole Formation was succeeded by the predominantly aeolian Makgabeng Formation. Strata of these two formations are not preserved north of the Melinda Fault, probably due to the syn-Blouberg tectonic activity, which had led to development of high topography in this area. This palaeohigh gradually denuded throughout Waterberg sedimentation.

Ultimately, the Mogalakwena Formation, the youngest of the Waterberg units in the study area, onlapped northwards over these denuding highlands.

After the end of Mogalakwena deposition, renewed tectonic activity led to approximately north-south orientated extension. Syn-Blouberg northwards-dipping reverse faults along the southern strand of the Melinda Fault were locally reactivated as normal faults, resulting in a half-graben type environment. A depository was created above the hanging wall, which filled with the strata of the Soutpansberg Group; initially volcanics of the Sibasa Formation erupted, followed by the clastic deposition of the Wyllies Poort Formation.

Late-stage reactivation along the Palala Shear Zone is represented by the northern strand of the Melinda Fault, which is generally a dextral strike-slip fault, with up to 17km of total displacement.

SAMEVATTING.

Die geologie van die Blouberg omgewing in die Noordelike Provinsie van Suid-Afrika word gekenmerk deur die teenwoordigheid van 'n aantal opeenvolgende sedimentêre komme wat ontwikkel is oor 'n kratoniese sutuursone (die Palala skuifskeursone). Die sutuur het gevorm tydens die Limpopo Orogenese (2.65 of 2.0 Ga) en was die gevolg van skuins konvergensie van die Kaapvaalkraton en die Sentralesone van die Limpopo Mobiele Gordel. Bros heraktivering van die Palala skuifskeursone in die Blouberg studiegebied, na die botsing, het plaasgevind op Melindaverskuiwing.

Die eerste kom wat ontwikkel het in die studiegebied, is gevul deur die Blouberg Formasie, wat gepreserveer is in 'n gebied wat beperk is tot die oostelike verlenging van die Palala skuifskeursone. Die Blouberg Formasie kan onderverdeel word in 'n Onderste en Boonste Lid. Die wydverspreide Onderste Lid is klaarblyklik in 'n ooptrekkom afgesit en word gekenmerk deur gevlegde fluviale plaatvloed afsettings wat algemeen steilhellend tot oorgeplooi is deur 'n jonger, suidwaarts gerigte kominversie. Die Boonste Lid verskil van die Onderste Lid deur dat dit swak gepreserveer is, oor die algemeen horisontaal gelaagd is, en bestaan uit konglomeraat met sub-hoekige rolstene van gefolieerde vloergesteentes en korrelsteenlae. Laasgenoemde sedimente dui respektiewelik op puinvloei en gevlegde riviere. Die tektoniese gebeurtenis verantwoordelik vir die suidwaarts gerigte kominversie van die Onderste Lid het ook proksimale vloergesteente bronne in die noorde en ooste opgehef. Dit het gelei tot die afsetting van die Boonste Lid in gelokaliseerde komme naby die suidelike vertakking van die Melindaverskuiwingseskarp.

Die sintektoniese afsetting van die Blouberg Formasie is gevolg deur 'n relatief tektonies-statiese tydperk waartydens die Waterbergkom gevul is. Die fluviale Setlaole Formasie is gevolg deur die eoliese Makgabeng Formasie. Sedimente van hierdie twee formasies is nie noord van die Melindaverskuiwing gepreserveer nie, waarskynlik as gevolg van die sin-Blouberg tektoniese aktiwiteit wat hoë topografie in die gebied tot gevolg gehad het. Hierdie paleohoog is geleidelik tydens Waterberg sedimentasie vernietig. Uiteindelik het

die Mogalakwena Formasie, die jongste van die Waterberg eenhede in die studiegebied, hierdie hooglande na die noorde oordek.

Na die einde van Mogalakwena afsetting het hernude tektoniese aktiwiteit gelei tot noord-suid korsverlenging. Sin-Blouberg noordwaartshellende oorskuiwings, langs die suidelike vertakking van die Melindaverskuiwing, is plaaslik geheraktiveer as afskuiwings wat 'n halwe-graben omgewing tot gevolg gehad het. 'n Afsettingskom is gevorm op die dakkant en is gevul deur gesteentes van die Soutpansberg Groep, bestaande uit vulkaniese gesteentes van die Sibasa Formasie gevolg deur klastiese gesteentes van die Wyllies Poort Formasie.

Laat-stadium heraktivering van die Palala skuifskeursone word deur die noordelike vertakking van die Melindaverskuiwing verteenwoordig en aanduidings is dat daar sowat 17 km regs-laterale strekkingsglipverplasing is.

TABLE OF CONTENTS.

LIST OF FIGURES.

LIST OF TABLES

CHAPTER 1: INTRODUCTION.

1.1: Location of the Study Area:

The area investigated in this thesis is situated in the Northern Province of the Republic of South Africa (Figure 1.1). The study area lies approximately 100km north-west of Pietersburg and 120km W.S.W. of Louis Trichardt, and covers approximately 2200km^2. This area, and the scope of the study, was determined by the project sponsors. The northern border of the area under investigation is 23°S, the western border is 28°30'E, the southern border 23°25'S, and the eastern border forms a N.N.E.-trending diagonal line from 23°25'S - 28°55'E to 23°S - 29°10'E (Figure 1.2). Much of the study area is flat-lying, with a height, typically, of 900m above sea level. There are, however, two notable topographic features within the study area: the Makgabeng plateau, which covers c. 225km^2 in the south of the study area and averages 1200m in altitude, and Blouberg mountain in the north east of the study area, which rises to 2051m (Figure 1.2). Whilst the flat-lying portions of the study area are readily accessible by gravel or sand roads, access to the more mountainous areas can only be gained on foot.

Flat, relatively low-lying areas of the study area are generally covered by Quaternary Kalahari sand or calcrete. Outcrop quality is considerably better around Blouberg mountain and on the Makgabeng Plateau, and consequently these areas form the main focus of this study.

1.2: Regional Geology:

Within the study area, outcrops can be assigned to five different lithological units. The *basement rocks* are comprised of Archaean granulite-grade gneisses of the Limpopo Mobile Belt, which are overlain by a series of younger, generally non-metamorphosed volcano-sedimentary and sedimentary Proterozoic successions: the *Blouberg Formation*, the *Waterberg Group* and the *Soutpansberg Group*. Some strata of the Phanerozoic *Karoo Supergroup* also occur locally, but the extent of their outcrop is minor. Before

considering the detailed geology of the strata within Blouberg mountain and its surrounding area (Chapters 2,3,4,5, and 6), this section will provide an outline of the general characteristics of the lithological units which are most important to this study. During this chapter, the existing stratigraphic names and classifications used by the South African Committee for Stratigraphy (S.A.C.S., 1980) will be retained. However, in later chapters, evidence will be proposed for a revised stratigraphic nomenclature, which will be used throughout the remainder of this work.

1.2.1: The Limpopo Mobile Belt:

The 250 km–wide, E.N.E.–W.S.W. -trending Limpopo Mobile Belt is thought (Treloar *et al.*, 1992) to represent a Himalayan-style collisional event between the Kaapvaal Craton in the south and the Zimbabwe Craton in the north (Figure 1.3). Within the Mobile Belt, a central zone and two marginal zones can be identified by their individual geological signatures (van Reenen *et al.*, 1992). The Southern Marginal Zone (S.M.Z.) is composed of granite-greenstone material from the Kaapvaal Craton, metamorphosed under at granulite facies conditions. It is separated from the remainder of the Kaapvaal Craton by a northward-dipping shear zone, which contains down-dip lineations, and is thought to have formed by southward-verging thrusting of the Kaapvaal Craton during syn-collisional crustal thickening (van Reenen *et al.*, 1992). The Central Zone (C.Z.) of the Mobile belt is characterised by granulite-grade gneiss of the Beitbridge Complex (S.A.C.S., 1980). Generally the Beitbridge Complex is composed of quartzo-feldspathic gneiss, with highly altered meta-sediments such as metapelitic gneiss, marble, quartzite and magnetite quartzite. Mafic protoliths are represented by amphibolites (van Reenen, 1992). The boundary between the S.M.Z. and the C.Z. is marked by the Palala Shear Zone, which is composed of mylonitised C.Z. and Bushveld Complex (c. 2.05 Ga) rocks. Structures within the 10 km-wide Palala Shear Zone suggest sinistral strike-slip displacement (McCourt and Vearncombe, 1987). Similarly, the Northern Marginal Zone (N.M.Z.) is separated from the Central Zone by the Tuli-Sabi Shear Zone, which is interpreted as a gently-dipping dextral strike-slip fault (McCourt and Vearncombe, 1987). The N.M.Z. is separated from the Zimbabwe Craton by a southward-dipping, northward-

verging thrust, and is composed of granulite-grade rocks, the protoliths of which are thought to have been granite-greenstone rocks of the southern edge of the Zimbabwe Craton. Thus the Limpopo Mobile Belt appears to be symmetrical in structure (Figure 1.3).

Although the structure of the Limpopo Mobile Belt is relatively well understood, there are conflicting interpretations concerning the age of the orogeny. Until recently, it has generally been held that the minimum age of the collision could be gained by dating the crystallisation of granites which cross-cut tectonic fabrics within the belt, and are thus thought to represent decompression melting during post-collisional exhumation. These chronological data suggest that the age of the contractional, late-stage of the orogeny is 2.65 Ga (McCourt *et al.*, 1995).

However, more recently it has been suggested that the age of the Limpopo orogeny may be considerably younger (e.g. Barton *et al.*, 1994; Holzer *et al.*, 1998). Kröner *et al.* (1999) found that granites throughout the Central Zone could be dated as having crystallised at a variety of ages between 3.3 Ga. and 2.5 Ga., all of which show fabrics indicating subsequent polyphase deformation. This, therefore, indicates that much of the tectonic history of the Central Zone took place in the early Proterozoic, rather than in the late Archaean. Undeformed granites in the Central Zone were dated, with an age of approximately 2.0 Ga being proposed (Barton *et al.*, 1994; Holzer *et al.*, 1998; Kröner *et al.*, 1999;). The older dates, including the 2.65 Ga event, are regarded as being related to earlier tectonic events but not to the cratonic collision. However it is argued (Treloar and Blenkinsop, 1995; McCourt and Armstrong, 1998) that such young dates (c. 2.0 Ga) may reflect a later phase of metamorphism, caused, for example, by the proximal intrusion of the c. 2.06 Ga Bushveld Complex in the Kaapvaal Craton, by peripheral mobile events (e.g. the c. 2.0 Ga Magondi orogeny on the northwestern edge of the Zimbabwe Craton, or the coeval -Kheis orogeny, south-west margin of the Kaapvaal Craton), or by the c. 2.0 Ga (Therriault et al., 1997) Vredefort impact event in the central Kaapvaal Craton. It is also argued that structures such as the Palala Shear Zone (which cuts the Bushveld

Complex) do not necessarily represent sutures between the zones of the Limpopo Belt, but may have formed during later events (McCourt and Armstrong, 1998).

1.2.2: The Blouberg Formation:

The Blouberg Formation is regarded (Jansen, 1976) as a siliciclastic and volcanic succession, which lies nonconformably on the gneiss of the Limpopo Mobile Belt, which is unconformably overlain by medial to upper formations of the Waterberg and Soutpansberg Groups (Jansen, 1976, 1982; Brandl, 1986). The extent of the outcrop is small, and occurs in isolated exposures approximately on the projected line of the Palala Shear Zone through the study area. The Blouberg Formation can therefore be considered to outcrop on the suture between the northern edge of the Southern Marginal Zone and the southern edge of the Central Zone. There is little evidence for metamorphism or mylonitisation of the Blouberg strata, suggesting that they post-date the Limpopo orogeny (Jansen, 1976,) and movement on the Palala Shear Zone (Callaghan and Brandl, 1991). The lithostratigraphic subdivision of the Blouberg Formation (S.A.C.S., 1980) is presented in Table 1.1, and the location of the outcrops of these constituent members is shown in Figure1.4.

Jansen (1976, 1982) considered the various members of the Blouberg Formation to have been laid down within partially isolated basins within a block-fault zone. This accounts for the variety of lithologies mapped within the Blouberg area and their isolated pattern of outcrops (Figure 1.4), and for the fact that the Blouberg Formation cannot be recognised as a continuous succession (Jansen, 1982). The lowermost, feldspathic clastic members of the Blouberg Formation generally outcrop in the southern foothills of Blouberg mountain, whereas non-feldspathic clastic sediments and volcanic members outcrop generally to the north and west of Blouberg mountain (Figure 1.4) (Jansen, 1976).

Jansen (1976, 1982) correlated the feldspathic Blouberg members (Basehla Arkose Breccia, Mananka Arkose, Thalalane Feldspathic Sandstone and Mmallebogos Grit

members) with the middle Waterberg strata (in particular the Setlaole Formation (Section 1.2.3) correlates well with the feldspathic Blouberg members). The non-feldspathic and volcanic Blouberg members (Mositone Conglomerate, Varedig Sandstone, Semaoko Grit and My Darling Trachyandesite members; Table 1.1) were correlated by Jansen (1976, 1982) with the late Waterberg (in particular the Mogalakwena Formation (Section 1.2.3) correlates well with the non-feldspathic members). Callaghan and Brandl (1991) suggested that the non-feldspathic and volcanic members of the Blouberg Formation should rather be considered as a part of the Soutpansberg Group (Section 1.2.4).

1.2.3: The Waterberg Group:

The Waterberg Group is comprised dominantly of red coloured, coarse clastic strata, and outcrops mainly in the west of the Northern Province, and in eastern Botswana, with smaller outcrops in Gauteng and Mpumalanga Provinces, South Africa (Figure 1.5). The Waterberg Group is composed of twelve formations, some of which grade laterally into each other (Table 1.2). The formations are preserved in two basins, the Middelburg basin and the Warmbaths basin; the latter is sometimes considered to be made up of a Main basin, and the southern Nylstroom protobasin (Jansen, 1982; Callaghan *et al.*, 1991) (Figure 1.5). The thickness of the Group may locally be as much as 7km (du Plessis, 1987), though other workers (e.g. Cheney and Twist, 1986) argue that the thickness is less, up to 5km. A thickness of 5km or less is also supported by geophysical investigations (Stettler, 1991). The age of the Group is estimated as 1900-1700 Ma (Jansen, 1982), though no radiometric dating has been done on Waterberg lithologies, and ages are largely based on relationships with surrounding, dated lithologies (Barker *et al.*, in press).

The Waterberg Group (Warmbaths basin) is considered to have been deposited within a continental fault-bounded basin, which developed in the northern part of the Kaapvaal Craton and the southern edge of the Limpopo Mobile Belt. Important faults which appear to have controlled the location of the edge of the basin are the Murchison Fault Zone (part of the Thabazimbi-Murchison Lineament) in the south and the Melinda Fault Zone

in the north (Callaghan *et al.*, 1991) (Section 1.2.5; Figure 1.5). Generally, the basin seems to have been filled by prograding sedimentary systems from south to north, as successively younger formations outcrop towards the Melinda Fault Zone (Jansen, 1976), although northern source areas are important locally.

The red colour of the Waterberg sediments is produced by haematite grain coatings, which appear to be early diagenetic in origin, as coatings themselves are deformed by late-diagenetic compaction, and are often covered by late diagenetic quartz overgrowths (Eriksson and Vos, 1979). This suggests that the sediments were deposited within an oxidizing environment, within 30° of the equator (Turner, 1980).

The Swaershoek, Wilge River and the lowermost part of the Sterk River formations (Figure 1.6) are thought to have been deposited in fan deltas and alluvial fans, which prograded into lakes, where they were subsequently reworked by lacustrine tides (Jansen, 1982; Callaghan *et al.*, 1991). The upper portion of the Sterk River Formation and the Alma Formation reflect synsedimentary fault activity along the Murchison Fault Zone, producing a steep fault scarp at the southern margin of the basin. North of the scarp, alluvial fans prograded northwards, composed of detritus eroding from the newly formed highlands to the south (Callaghan *et al.*, 1991). Fine detritus was washed further north where it either settled in lakes or was deposited in the distal parts of prograding lacustrine fan deltas (Callaghan *et al.*, 1991).

The Skilpadkop Formation (Figure 1.6) is interpreted as having been deposited in braided rivers. Local soft-sedimentary overturning and slumping within the Formation are thought to reflect either dragging by heavily laden, fast-flowing water above newly deposited sediment, or shock dewatering cased by activation of basin-bounding faults (Callaghan *et al.*, 1991). The Setlaole Formation (Figure 1.6) has also been interpreted as reflecting proximal braided river deposition, based on the immature clast-supported sedimentary rocks and a lack of planar bedding (Callaghan *et al.*, 1991.). The Setlaole Formation also locally contains tuffaceous beds. Thus the palaeoenvironmental

conditions inferred for the Setlaole and the laterally equivalent (Table 1.2) Skilpadkop Formation are very similar (Callaghan *et al.*, 1991).

The Aasvoëlkop Formation (Figure 1.6) is generally upward-coarsening, and is interpreted to have been deposited within a lacustrine environment, with coarse fluvial detritus, washed into the lake, becoming increasingly common towards the top of the Formation (Callaghan *et al.*, 1991). The base of the Aasvoëlkop Formation is marked by a lahar deposit (Callaghan *et al.*, 1991), indicative of volcanic activity within the Waterberg basin at this time, possibly associated with faulting at the margins of the depository. The fluvial upper part of the formation exhibits contorted bedding, indicating movement along a nearby (Murchison) fault zone (Callaghan *et al.*, 1991).

The Makgabeng Formation (Figure 1.6) is laterally equivalent to the Aasvoëlkop Formation, and outcrops in the northern part of the Waterberg basin. It is characterised by very large-scale cross-bedding, and uniformly-sized fine- to medium-grained sandstones, lacking clay matrix (Meinster and Tickell, 1975). Also, local tabular bodies of massive sandstone are reported (Callaghan, 1987a). These facies associations are thought to reflect an aeolian palaeoenvironment. The multimodal palaeocurrent pattern, derived from the dip direction of the large cross-beds reflects superposed longitudinal dunes deposited during changing seasonal wind directions (Callaghan, 1987b); alternatively, they probably also reflect barchanoid dune forms (Simpson *et al.*, 1999). Small scale aqueous, or partly aqueous structures observed in the Makgabeng Formation, such as ripplemarks, interference ripplemarks, adhesion warts and desiccation cracks, may indicate gradational change to the lacustrine conditions of the Aasvoëlkop Formation to the south (Callaghan *et al.*, 1991), or could reflect interdune deposition (Eriksson *et al.*, 2000).

Both the Sandriviersberg and the Mogalakwena Formations (Figure 1.6) comprise trough and planar cross-bedded arenites, though the Mogalakwena Formation is more coarse, suggesting that it is more proximal. Both formations contain common pebble washes, with boulder conglomerates present in the most northerly outcrops of the Mogalakwena

Formation (Jansen, 1976). The average palaeocurrent direction for the two formations is from E.N.E. to W.S.W., whilst grain size generally decreases towards the south. (De Bruiyn, 1971). Both formations are interpreted to have been deposited in a braided stream palaeoenvironment; the consistent palaeocurrent directions, and the presence of matrix-poor coarse-grained sandstones with poorly rounded grains indicates that sedimentation was rapid, though not chaotic, and was deposited within a steadily deepening basin during uplift of a provenance to the north-east (Callaghan *et al.*, 1991).

The Cleremont Formation (Figure 1.6), characterised by texturally and mineralogically mature medium- to coarse-grained sandstones with local rounded pebble washes, is thought to have been deposited within a littoral palaeoenvironment (Callaghan *et al.*, 1991). The Vaalwater Formation (Figure 1.6) is very mature, suggesting that it may have been reworked from earlier Waterberg Group strata, and the greyish colour of these arenites indicates a less-oxidizing environment than the remainder of the Waterberg Group (Callaghan *et al.*, 1991). The postulated palaeoenvironment was a shallow siliciclastic sea, although the association of ripplemarks and trough cross-bedding may rather indicate estuarine conditions (Callaghan *et al.*, 1991). The Vaalwater Formation thus suggests fluctuating base levels within the late-Waterberg basin (Callaghan *et al.*, 1991).

The palaeoenvironmental interpretations suggested for the Waterberg Group reflect at least one major reactivation of the fault zones bounding the basin, as two fining-up sequences can be identified within the succession (Callaghan *et al.*, 1991), from the Swaershoek (basal) to the Aasvoëlkop/Makgabeng Formations, and from the Mogalakwena Formation to the Vaalwater Formation (Figure 1.6). The mid-Waterberg resumption of rapid erosion appears to coincide with extension of the basin to the north, and the increased supply of detritus from northerly source areas (Callaghan *et al.*,1991).

1.2.4: The Soutpansberg Group:

The volcano-sedimentary Soutpansberg Group outcrops in the far north of South Africa, mainly in the Soutpansberg mountains. The mountains form a long south-facing escarpment from Kruger National Park in the east to Vivo in the west. The Soutpansberg Group is preserved in an elongated basin, which extends from the western end of the present study area to Punda Maria (Figure 1.7). The lithostratigraphic subdivision of the Soutpansberg Group is shown in Table 1.3, and the distribution of the units in Figure 1.7. Generally, the Soutpansberg strata have a moderate to steep northerly dip, and are cut by several E.N.E.-W.S.W.-trending faults (van Eeden *et al.*, 1955).

The basal Tshifhefhe Formation is only locally developed at the eastern end of the Soutpansberg basin, and is only a few metres thick. It is comprised of strongly epidotised clastic sediments, including shale, greywacke and locally-derived conglomerate (Barker *et al.*, in press). The Sibasa Formation comprises subaerially extruded basalt, with intercalated pyroclastic and sandstone lenses. Generally the basalts are massive, epidotised and locally amygdaloidal (Barker *et al.*, in press). The pyroclastic lenses locally reach a thickness of 200m, whereas the laterally persistent clastic lenses locally attain a thickness of 400m (Barker *et al.*, in press).

The generally siliciclastic Fundudzi Formation is only developed at the eastern end of the basin (Figure 1.7). It is mainly comprised of arenaceous and argillaceous sedimentary rocks, though there are rare pyroclastic horizons, and basaltic lavas are intercalated with the sedimentary lithologies close to the top of the Formation (Barker *et al.*, in press). The Wyllies Poort Formation is composed of red-pink quartzite with minor pebble washes. The base is marked by a prominent agate pebble conglomerate, and in the east, minor basaltic and pyroclastic intercalations are present (Barker *et al.*, in press). The uppermost unit of the Soutpansberg Group is the Nzhelele Formation, which is volcanic at the base (400m), followed by argillaceous sedimentary rocks in the middle, and arenaceous rocks at the top (Barker *et al.*, in press).

The preponderance of inferred fluvial sediments and subaerial lavas suggest that the Soutpansberg Group was deposited within a continental setting. Although originally no unconformities were identified between the formations (Jansen, 1974), more recent work (Cheney *et al.*, 1990) identified a regionally-developed, low-angle unconformity beneath the Wyllies Poort Formation. Figure 1.7 shows that the base of the Wyllies Poort Formation lies on successively older rocks towards the west, indicating that the Soutpansberg Group may not represent continuous continental deposition (Cheney *et al.*, 1990).

1.2.5: The Melinda Fault Zone:

The Melinda Fault Zone strikes E.N.E.-W.S.W. across the region. In the west, it bounds the northern edge of the Palala Shear Zone at 23°22'S; 27°57'E, and in the east it appears to merge with several sub-parallel faults cutting the Soutpansberg strata and Karoo strata east of Vivo (Figure 1.7). In the Blouberg area, the fault bifurcates into two strands, which pass to the north and south of Blouberg mountain (termed the *northern* and *southern* strands respectively in this work). The northern strand, in turn, bifurcates into several splays in the north-eastern foothills of Blouberg mountain, where it cuts the Wyllies Poort Formation (Geological Survey 1: 250000 sheets 2326; Ellisras, 2328; Pietersburg and 2228; Alldays). The fact that the Melinda Fault displaces strata in an area situated approximately above, and parallel to the projected line of the Palala Shear Zone, may imply that the Melinda Fault Zone is a manifestation of reactivation along the Palala Shear Zone. It is thought that the Melinda Fault comprises two distinct phases of movement. Pre-Karoo movement along the fault caused Waterberg strata to the south to be downthrown, with a vertical displacement of about 1000m, and reactivation in post-Karoo times caused a downthrow to the north, with a vertical displacement of at least several hundred metres (Brandl, 1986).

1.3: Previous work in the Blouberg area:

Throughout sections 1.3 and 1.4, previously published work which has bearing on the present study will be examined, and many of the conclusions of earlier workers will be highlighted. Although the Blouberg area in Northern Province has not received much attention from workers during the last century (Section 1.3), more work has been done in surrounding areas, and on related lithologies, which have bearing upon the strata within the Blouberg area (Section 1.4).

The most detailed published work directly concerning the geology of the area around Blouberg mountain was that of Jansen (1976), and the discussion of that paper by Meinster (1977). Jansen (1976) based his paper on field data obtained from the Blouberg area by B. Meinster and S.J. Tickell between 1972 and 1974. The following sections summarise the reasoning and conclusions of the work of Jansen and Meinster.

1.3.1: Summary of the work of Jansen (1976):

Jansen (1976) recognised that the Blouberg area was located at the intersection of two major sedimentary basins on the Kaapvaal Craton: the Waterberg basin, which developed progressively from south to north, and the Soutpansberg basin, which developed progressively from east to west. As such, the Blouberg area presented an ideal opportunity to consider the relative ages of the Waterberg and Soutpansberg Groups, as the Blouberg area provides the only location where these two groups of strata are developed in close proximity to each other. Additionally, Jansen (1976) identified that this location appeared to be coincident with the northern margin of the Kaapvaal Craton.

1.3.1.1: Stratigraphic units examined by Jansen (1976):

Jansen (1976) considered three stratigraphic units within the Blouberg area: The Blouberg Formation, the Waterberg Group (in particular the Setlaole, Makgabeng and Mogalakwena Formations), and the Soutpansberg Group (in particular the Wyllies Poort

Formation). His paper aimed principally at solving age-relationships between these three units, and examining their depositional conditions and structural patterns.

Jansen (1976) proposed that the Blouberg Formation consists of an association of eight members (Table 1.1). The lowermost four members, which outcrop on the southern slopes of Blouberg are generally feldspathic siliciclastic sediments (Basehla Arkose Breccia, Mananka Arkose, Thalalane Feldspathic Sandstone, Mmallebogos Grit Members). The northern slopes of Blouberg, however, are underlain by three non-feldspathic siliciclastic sedimentary units (Mositone Conglomerate, Varedig Sandstone, and Semaoko Grit Members) which are overlain locally by a volcanic unit (My Darling Trachyandesite Member).

He proposed that the members of the Blouberg Formation were laid down within an active block-faulted terrain along the uplifted northern rim of the Waterberg basin (the 'Limpopo Rise'). The variability in maturity, inferred variability in distance from source area, variance in depositional conditions, and the patchy occurrence of the outcrops of the Blouberg Formation sediments could thus be explained by the varying presence of localised basins, by deposition within partially isolated basins, or 'negative fault blocks' (Jansen, 1976). As block-faulting was continuous throughout the deposition of the Blouberg members, small depositories were created at different times and in different places along the southern edge of the Limpopo Rise (Jansen, 1976).

Within the Waterberg Group, Jansen (1976) identified three formations: The arkosic, partially conglomeratic Setlaole Grit Formation, the Makgabeng Sandstone Formation, (which wedges out rapidly to the north, so that it is not present within the Blouberg block-fault zone), and the Mogalakwena Conglomerate Formation, characterised by the locally developed basal Sesalong Boulder Conglomerate Member, overlain by conglomerate and sandstones.

Jansen (1976) assigned all Soutpansberg Group strata in the Blouberg area to the Wyllies Poort Formation, which is characterised by light-coloured quartzite, with locally

developed pebble washes, conglomerates and mudstone pellets. The presence of interbedded lavas, tuffs, argillaceous rocks and diabase sills was only inferred by the presence of rubble, as outcrop quality is exceptionally poor. Rarely outcropping lavas are coarse-grained, epidotised and often amygdaloidal. Significantly, Jansen (1976) assigns none of the lavas in the Blouberg area to the volcanic Sibasa Formation of the Soutpansberg Group.

1.3.1.2: Stratigraphic relationships proposed by Jansen (1976):

The only direct stratigraphic relationships that Jansen (1976) was able to observe between the three units in the field were:
1.) The Wyllies Poort Formation (Soutpansberg Group) unconformably overlies the non-feldspathic members of the Blouberg Formation on the northern slopes of Blouberg, and also unconformably overlies the basement.

2.) The Mogalakwena Formation (Waterberg Group) unconformably overlies the feldspathic members of the Blouberg Formation on the southern slopes of Blouberg, and also the basement.

3.) The Blouberg Formation unconformably overlies the basement.

4.) The contacts between the Waterberg and Soutpansberg Groups are faulted.

With such incomplete data (especially regarding the age relationship between the Waterberg and the Soutpansberg Groups), Jansen (1976) attempted to invoke other methods in order to draw up a stratigraphic column. His conclusions regarding stratigraphic relationships were based on lithological similarities between strata, palaeogeographical data, and age determinations on the basement.

Jansen (1976) correlated the four lowermost (feldspathic) members of the Blouberg Formation with the Setlaole Formation of the Waterberg Group, based on the fact that the

Setlaole is also locally feldspathic and conglomeratic, and lithologically similar to some of the members in the lower Blouberg Formation. Jansen (1976) suggested that a correlation of Blouberg units with the Magkabeng Sandstone Formation (Waterberg Group), which is aeolian in origin (Meinster and Tickell, 1975), and which is generally an arenaceous mature sandstone, is untenable.

Jansen (1976) noted that the feldspathic members of the Blouberg Formation, on the southern slopes of Blouberg, are unconformably overlain by the basal boulder conglomerates (Sesalong Member) of the Mogalakwena Formation. However, to the west of Blouberg, on the farm Kranskop 278 LR (23°09'S; 28°42'E to 23°09'S; 28°41'E: Appendix 1), Jansen recorded the presence of an abnormally thick succession of Blouberg strata (1200m of the Basehla Arkose Breccia Member). This succession is unconformably overlain by the sandstone and grit of the Mogalakwena Formation, rather than being overlain by the lowermost boulder conglomerate that typically marks the unconformity on the southern slopes of Blouberg. Jansen (1976) therefore suggested that the anomalously thick Kranskop strata may correlate with the Setlaole, the Makgabeng, and the lowermost part of the Mogalakwena Formations.

Jansen (1976) argued a syn-Mogalakwena age for the non-feldspathic members of the Blouberg Formation. He suggested that the southerly dip of the older feldspathic members of the Blouberg Formation indicated an area of positive relief to the north, thus providing evidence against contemporaneous deposition of the feldspathic and non-feldspathic Blouberg members. The fact that the non-feldspathic members cannot be obeserved to be overlain by the basal Sesalong Conglomerate Member of the Mogalakwena Formation, and the similarity between the non-feldspathic members of the Blouberg Formation and the upper sandstone and grit of the Mogalakwena Formation led Jansen (1976) to suggest that they could be correlated. Jansen (1976) also suggested a syn-Sibasa age for these rocks, as an alternative, as the non-feldspathic members can be observed to be unconformably overlain by the Wyllies Poort Formation of the Soutpansberg Group.

Thus, Jansen (1976) concluded that the feldspathic members of the Blouberg Formation are of middle Waterberg age (syn-Setlaole) and the non-feldspathic members are of late Waterberg age (syn-Mogalakwena) and also contemporaneous with the volcanic Sibasa Formation of the Soutpansberg Group. The Wyllies Poort Formation was considered to be younger, thus providing evidence that the Soutpansberg Group strata represent deposition over a relatively long period of time.

1.3.1.3: Mode of deposition proposed by Jansen (1976):

With a complete, ordered stratigraphical column of the lithologies in the Blouberg area, Jansen (1976) examined the inferred mode of deposition and palaeogeography of the Blouberg area at the time of deposition. As previously mentioned, Jansen strongly favoured the deposition of the feldspathic members of the Blouberg Formation within a block-faulted terrain positioned parallel to, and immediately south of the 'Limpopo Rise'. This rise, an area of strongly positive relief, was envisaged to have formed the north-eastern edge of the Waterberg basin, and to have been the source of many of the sediments within the Blouberg area. Sedimentation of the feldspathic members within the small isolated basins was inferred to have resembled that of yoked basins, with thick arkose wedges. Areas where there is no outcrop of Blouberg strata were explained by localised rises within the palaeotopography, and the 1200m-thick succession of arenaceous and arkosic strata on Kranskop 273LR (23°09'S; 28°42'E to 23°09'S; 28°41'E: Appendix 1) was explained by the encroachment of the main Waterberg basin into the localised Kranskop basin during Setlaole deposition.

Similarly, the main Waterberg basin was envisaged to have encroached over the entire block-faulted terrain upon the onset of Mogalakwena deposition, as the Sesalong Conglomerate Member outcrops above the feldspathic Blouberg strata. Evidence for the continued activity of the block-faulted terrain beneath is given by the irregular thickness and distribution of the Sesalong conglomerate, and by localised tilting of this stratum. Continued erosion of the Limpopo Rise mountain belt led to its progressive retreat northwards as Mogalakwena Formation deposition continued. Thus the Mogolakwena

rocks are less rich in feldspar, reflecting erosion of increasingly distant source areas. Current directions within the Mogalakwena Formation were interpreted by Jansen (1976) to reflect fluvial currents both longitudinal and transverse to the Limpopo Mobile Belt (E.N.E.-W.S.W.) trend , and indicate an overall transport from the N.E., from an area occupied by the most elevated terrain of the Limpopo Rise. The now denuded area west of Blouberg was subjected to localised downwarping, creating a depository for the non-feldspathic members of the Blouberg Formation (the 'Lebu trough'). Deposition in the Lebu trough was thought to have been contemporaneous with the deposition of the sandstone and grit of the upper-Mogalakwena to the south. Following peneplanation of the Limpopo Rise, down-faulting continued, localised rifting provided conduits for lavas (My Darling Trachyandesite Member), and eventually culminated in the development of the Soutpansberg trough, previously envisaged by Jansen (1975b) to represent an aulacogen. Current directions recorded within the Wyllies Poort Formation were generally north to south, and S.W. to N.E. within the east-west trending Soutpansberg trough. Jansen (1976) interpreted this as reflecting, in part, longtitudinal current directions within the trough, and hence indicating a partial reversal of the Waterberg current directions.

Having dealt with the primary aim of his work (that of solving the enigmatic stratigraphic relationships and mode of deposition within the Blouberg area), Jansen (1976) used this as a basis to speculate on the basin evolution and structural patterns in the Blouberg area.

1.3.1.4: Basin evolution of the Blouberg area proposed by Jansen (1976):

Jansen (1976) noted that, in comparison to the relatively undisturbed nature of the Waterberg and Soutpansberg strata, the feldspathic members of the Blouberg Formation are frequently steeply tilted, and locally overturned. He interpreted this deformation as representing the first post-Limpopo deformational event in the Blouberg area, and ascribed the deformation to localised down-faulting within the block-fault zone. This earliest deformational event is envisaged to have continued from mid-Waterberg (syn-

Blouberg/Setlaole Formations) until the late Waterberg (syn-Sesalong Conglomerate Member), as the basal Mogalakwena is also tilted locally.

Similar down-warping and faulting is thought to have formed Jansen's (1976) next deformational phase in the area west of Blouberg. This led to the widening of the fault zone, and ultimately to the creation of horsts and grabens, most notably that of the 'Lebu trough', into which the non-feldspathic Blouberg members were deposited, and in which the My Darling trachyandesitc lavas were erupted. These rocks are locally unconformably overlain on the southern margin of the Lebu trough by the Wyllies Poort Formation. The Lebu trough is considered by Jansen (1976) to be a proto-trough to the main Soutpansberg trough. Continued regional down-warping and down-faulting culminating in the creation of the main Soutpansberg trough is the third structural event proposed by Jansen (1976) for the tectonic evolution of the Blouberg area. The developing Soutpansberg trough extended farther south than the Lebu trough, into the earlier Blouberg block-fault zone, now occupied by overturned feldspathic Blouberg members and sub-horizontal, locally-dipping Mogalakwena strata. Continued reactivation of the trough-bounding faults was envisaged to have occurred while regional down-warping of the Soutpansberg aulacogen proceeded. On account of this, the strata close to the trough-bounding faults are locally steeply tilted; the Blouberg strata bordering the faults on the southern edge of the trough became overturned, while Wyllies Poort quartzite on the northern margin attained dips up to 80° (Jansen, 1976).

1.3.1.5: Conclusions (Jansen, 1976):

On a cratonic scale, Jansen's model for the geological evolution of the Blouberg area can be considered in terms of the extension of a rift zone (Soutpansberg trough) into the domain of a cratonic basin (Waterberg Group), thus creating an intersection of two zones of crustal weakness. In turn, the development of the Soutpansberg and Waterberg basins was probably controlled by crustal events within the Limpopo Mobile Belt. Mobilisation within the Limpopo Mobile Belt between 2100-1800 Ma (the youngest U-Pb zircon ages to have been recorded in the basement in the Blouberg area at that time) led to isostatic

uplift and the deveopment of a crustal arch over the Limpopo Mobile Belt (the Limpopo Rise). This was the main source of sediment for the developing Waterberg basin to the south. The isostatic uplift of the Limpopo Belt is envisaged to have promoted the sub-crustal flow towards it, and encouraged both the creation of the Blouberg block-fault terrain, and the northwards propagation of the Waterberg basin towards the Limpopo Belt. The Soutpansberg trough was presumed to have formed as a result of the foundering of the crustal arch, producing volcanic centres in the eastern Soutpansberg (Sibasa basalt) and at Blouberg (My Darling trachyandesites).

Jansen ended his work by proposing that the structural features examined should not be considered in terms of plate tectonics, as he was of the opinion that the Limpopo Mobile Belt was non-collisional in origin. Jansen (1976) rather favoured an intra-plate environment as the setting for the Waterberg and Soutpansberg basin development.

1.3.2: The work of Meinster (1977):

Meinster, who had performed much of the initial mapping on which Jansen (1976) had based his work, did not agree with many of Jansen's (1976) proposed age relationships. Rather than consider the Blouberg Formation as containing eight individual members, Meinster (1977) proposed that the non-feldspathic members be termed the 'Lebu Complex', and the feldspathic members be termed the 'Blouberg Complex', and Jansen's (1976) individual members be considered as formations.

Meinster (1977) recognised clasts of the Varedig Formation (Lebu Complex) within the Basehla Arkose Breccia Formation (Blouberg Complex). Additionally, the presence of well-rounded quartz pebbles within the otherwise immature Blouberg Complex was thought to be due to reworking of primary conglomerates within the Lebu Complex (e.g. Semaoko and Mositone Formations), and soft green material within the Blouberg Complex was thought to be highly weathered lava from the My Darling Formation. Thus, Meinster (1977) suggested that the Blouberg Complex was younger than the Lebu Complex, reversing the stratigraphy of Jansen (1976). Meinster (1977) did not look

favourably upon the idea of block-faulting being a potential cause for overturning of the Blouberg Complex, suggesting that overturning caused by drag folding is a rarity, whilst overturned beds in the Blouberg and Lebu Complexes are common. Thus, he argued for a major deformational phase, postulating that steep upthrusts and overthrusts caused folding and overturning in the Lebu Complex, and created localised downwarping for the Blouberg Complex depository. Meinster (1977), however, was not able to show field evidence for such thrusts. The uplifted Lebu Complex was rapidly eroded into the nearby depository, accounting for the immaturity of the Blouberg Complex sediments, and the presence of the Lebu Complex detritus therein (Meinster, 1977). As compressional tectonics continued with time, the Blouberg Complex itself became tilted and overturned. Peneplanation of both the Lebu and Blouberg complexes following compression is regarded as having removed most of the evidence for such a deformational event. Significantly, Jansen (1977), in a reply to Meinster, argued that the Lebu Complex (non-feldspathic Blouberg members) was not particularly folded or tilted compared to the strata of the Blouberg Complex.

With regard to other correlations made by Jansen (1976), Meinster (1977) questioned the suitability of correlating the Blouberg Complex with the Setlaole Formation of the Waterberg Group, based solely on the presence of feldspars in both units. Correlation based upon such a common sedimentary mineral as feldspar was not, Meinster argued, sound practice. Additionally, with regard to this correlation, Meinster brought attention to the point that the geological map of the Blouberg area provided by Jansen (1976) shows Blouberg Complex strata unconformably overlain by Setlaole Formation rocks at 'Hill 3970' on the farm Beauley 260 LR (23 06.80'S; 28 59.40'E: Appendix 1). Meinster also noted the relative lack of deformation in the Setlaole Formation compared with the Blouberg Complex, and the lack of mudstones in the Setlaole, whilst observing that they are present (although rare) in the Blouberg Complex. Meinster (1977) did, however, propose that the Lebu Complex might correlate with the sediments of the Koedoesrand Complex in the Palala Shear Zone (located about 100km W.S.W. of the Blouberg area), as these rocks also show good evidence for having been affected by a strong phase of deformation. The fact that the Koedoesrand strata are intruded by the Bushveld Complex

(c.2050 Ma) provided Meinster with evidence that the Lebu and Blouberg complexes were considerably older than the ages proposed by Jansen (1976).

The erosion and peneplanation of the Lebu and Blouberg Complex mountains was followed by deposition of what Meinster (1977), somewhat ambiguously, terms 'transitional strata' (they are not marked on his map), reported as flat-lying strata between the Lebu Complex and the Soutpansberg Group. These transitional strata appear on Jansen's (1976) map as part of the Varedig Member.

Of critical importance regarding the age-relationships in the Blouberg area, are Meinster's (1977) opinions regarding the relative ages of the Soutpansberg and Waterberg Groups. Meinster (1977) proposed that the similarity between the Lebu Complex and the Soutpansberg Group in terms of inferred mode of deposition, cyclicity, sedimentary rocks, lavas and their close spatial relationship, indicate their close relationship in time. Meinster (1977) refers to them as 'a single entity....separated from each other by a strong compressional phase, vigorous erosion, and subsequent deposition of the Blouberg Complex. Additionally, as the Soutpansberg strata are regarded as having been preserved, rather than having been deposited, in grabens, Meinster (1977) argues that rifting related to the graben formation would have produced plateau lavas over any pre-existing strata. The lack of plateau lavas within the Waterberg Group shows that these strata had not been deposited at this point. Therefore the logical succession of strata in the Blouberg area according to Meinster (1977) is:

5. Karoo Sequence
4. Waterberg Group
3. Soutpansberg Group
2. Blouberg Complex
1. Lebu Complex

With regard to the age of the Soutpansberg Group, Meinster refers to an age of lavas in the upper portion of the Group dated at ±2000 Ma, indicating a much earlier age for the

Soutpansberg Group than the Waterberg Group. Meinster (1977) argued that this age could be re-set, e.g. by the Bushveld intrusion, at 2050Ma from an even earlier date, and hints that the Soutpansberg Group may, in fact, correlate well with the Ventersdorp Supergroup. Such an early age is considered unlikely by Jansen (1977) in a reply to Meinster, due to the fact that the Soutpansberg sediments are generally red beds, thus reflecting sedimentation and diagenesis in an oxidising environment and thus within a younger time period (post c. 2000 Ma)(Jansen, 1977).

The contrasting stratigraphic and structural relationships proposed by Jansen (1976) and Meinster (1977), derived from the same field data, serve to illustrate the structural complexity and the lack of good stratigraphic markers across the study area, which has hampered previous work within the Blouberg region.

1.3.3: The work of Brandl (1991):

The contrasting views on issues concerning the geological history of the Blouberg area remained largely dormant until Brandl (1991) briefly re-examined the outcrops. He suggested that the non-feldspathic and volcanic strata within the Blouberg Formation/Complex (i.e. the Lebu Complex of Meinster, 1977) should rather be considered as part of the Soutpansberg Group. The My Darling Trachyandesite Member would therefore correlate with the Sibasa Formation (Brandl, 1986; Cheney *et al.*, 1990). The Blouberg Formation would thus only consist of feldspathic strata, and Brandl (1991) proposed that these should not be classified as separate members.

1.4: Relevant previous work in surrounding areas:

1.4.1: Previous work on the Limpopo Mobile Belt:

The Limpopo Mobile Belt has been subjected to intense study during the last sixty years, although early European miners began exploiting copper at Messina as early as 1904 (Barton, 1983). Söhnge (1945) began to map the rocks around Messina in 1940, and was

the first to consider the high-grade metamorphism of those lithologies (Söhnge, 1940; Söhnge *et al.*, 1948). MacGregor (1953) coined the term 'Limpopo Orogeny', having identified that the metamorphic rocks formed a belt. Holmes and Cohen (1957) determined an approximate age of 2 Ga for the Limpopo Orogeny. Cox et al. (1965) termed it the 'Limpopo Orogenic Belt', and were the first to identify the Northern, Central, and Southern zones within the Belt, which terminology still remains in usage. Anhaeusser *et al.* (1969) applied the name 'Limpopo Mobile Belt' in order to avoid analogies with Alpine tectonic models. Bahnemann (1971) recognised basement and supracrustal successions within the Messina area, with deformed mafic dykes also present in the basement rocks.

Mason (1973) examined the Limpopo Belt as a whole, and envisaged the belt as being "a zone of crustal weakness throughout geological time and characterised by repeated shear deformation, igneous intrusion and extrusion". He recognised that the zones of the Limpopo Mobile Belt were separated from each other by shear zones (e.g. the Palala Shear Zone), and also proposed a faulted relationship between the Southern Marginal Zone and the Kaapvaal Craton. The Northern Marginal Zone was, however, believed to grade transitionally into the Zimbabwe Craton. In contrast, Coward *et al.* (1973) identified the northern margin as a dextral shear zone with up to 200km of displacement, which was also the view of Hepworth (1977).

Between 1973 and 1982, The South African Council for Scientific and Industrial Research (C.S.I.R.) sponsored the Limpopo Working Group as part of the National Geodynamics Project (N.G.P.) A summary of the work of the Limpopo Working Group is presented in Table 1.4. In 1983, the Geological Society of South Africa produced a special publication (van Biljon and Legg, 1983), which drew together much of the work of the Limpopo Working Group. The work in this publication is summarised in Table 1.5. and more recent work (1983 to 1999) is summarised in Table 1.6. The results of previous work on the Limpopo Mobile Belt which are most relevant to this study, were presented in the section on general geology (Section 1.2.1) and are not repeated here.

1.4.2: Previous work on the Waterberg Group:

1.4.2.1: Early work on the Waterberg Group (1872-1982):

Very early work on the Waterberg Group (1872-1965) is summarised in Table 1.7. The most relevant previous work began in the mid-sixties, when the Geological Survey of South Africa began a comprehensive study of the Waterberg strata. Much of the work in this large-scale study also concerned the investigation of the Blouberg Formation (Jansen, 1976; Meinster, 1977) and the Soutpansberg Group (Jansen, 1975b) which are dealt with separately in Section 1.3 and Section 1.4.3. The more recent work by the Geological Survey of South Africa (1965-1982) is summarised in Table 1.8, where publications which are of particular importance to the present study are highlighted in bold type. The work of Meinster and Tickell (1975), and Tickell (1975) are particularly relevant to the present study area.

Meinster and Tickell (1975) investigated the Makgabeng Formation on the Makgabeng Plateau. They reported the ubiquitous presence of fine- to medium-grained sandstone with rounded to well-rounded, spherical sand grains, with little or no matrix. Of particular importance are the sedimentary structures present within the Formation. Meinster and Tickell (1975) reported that the Formation is characterised by pronounced fine-scale laminations within very large-scale cross-bedded units. The large cross-bedded units are between 2 and 10m in set thickness, and their maximum recorded extent was recorded as 200m along foreset strike, and 400m perpendicular to strike. Meinster and Tickell (1975) also noted that the lower bounding surface of the cross-bedded units is typically marked by enigmatic 20cm to 8m-thick massive sandstone beds. Generally, they found that bounding surfaces between cross-bedded units were curved, though these were also observed to be irregular on a small scale, indicating erosion prior to deposition of the next cross-bedded unit. Foresets were reported to be generally tabular or shaped like very broad troughs. In cross-section, the foresets are concave, and typically dip at around 19°, though a maximum dip of 38° was recorded (Meinster and Tickell, 1975). The foresets flatten and merge towards the bottom of the set, so that the bottomsets are confomable

with the massive beds beneath. Sparse ripple marks were reported on bottomset and foreset beds within the Makgabeng Formation. These are generally asymmetric, though many show truncated tops. Parting lineations were observed on the tops of massive beds. Rare mudstone lenses, up to 2 or 3 metres in width and only a few centimetres thick, were also recorded by these two researchers in their 1975 paper.

Meinster and Tickell (1975) considered, but rejected a sub-aqueous origin for the Makgabeng sediments, and favoured an aeolian palaeoenvironment. Massive beds were interpreted as having formed during temporary changes in wind direction, causing the dune to become aerodynamically unstable, and to be rapidly reworked. Such an interpretation was strengthened by the presence of anglar unconfomities between the massive bed and the earlier cross-bedded dune beneath, and the contrasting dip directions of subsequent dunes, reflecting changing wind directions (Meinster and Tickell, 1975). The presence of parting lineations on the top surface of the massive beds is not easily reconciled with the aeolian model of Meinster and Tickell (1975). They suggested that parting lineations may be able to form in subaerial conditions, due to rotating cellular vortices of air, in a similar way to parting lineations that are produced in fast-flowing water. The generally tabular shapes of the foresets in the Makgabeng Formation were taken to indicate that cross-bedded units represented fossil transverse dunes, and broad trough-shaped foresets were thought to be barchan dunes. Palaeowind directions, inferred from foreset dip directions, were thought to be dominantly from the N.E, (Meinster and Tickell, 1975).

Tickell (1975) examined the generally horizontally-dipping coarse sandstone and conglomerate of the Mogalakwena Formation. He found that the Mogalakwena Formation conformably overlies the Makgabeng Formation, with a 20m thick zone of transitional rocks developed between the two formations. However, Tickell (1975) also noted that in the immediate area of the Melinda Fault (Figure 1.5) there is a disconformity developed between the two formations. In the south-west, the Mogalakwena Formation is reported to grade laterally into the Sandriviersberg Formation, which is generally more yellowish in colour than the Mogolakwena, and

contains no conglomerates. The maximum preserved thickness of the Mogalakwena Formation was reported to be 1250-1500m.

The Mogalakwena Formation is generally comprised of coarse sandstone, with several subordinate conglomerate members locally developed at a variety of stratigraphic heights (Tickell, 1975). The Tafelkop member is developed just beneath the base of the overlying Cleremont Formation, the Marken Member is developed about 50m above the base of the Mogalakwena Formation, and the Sesalong Member, at Blouberg, lies directly at the base. All of the conglomerate members were estimated to be about 100m in thickness, and Tickell (1975) reported that the Sesalong Member wedges out about 10km south of Blouberg.

The sandstone member of the Mogalakwena Formation was observed to be purplish brown in colour with pale pink patches, and with the presence of cross-bedding being highlighted by dark laminae within the foresets. Tickell (1975) reported an average composition of 64% detrital quartz, 33% matrix, and 3% lithic fragments, with feldspars generally being absent. The conglomerates were reported to contain rounded to well-rounded clasts of high sphericity, composed mainly of vein quartz, quartzite and quartz-mica schist. Clasts of quartz-haematite schist (banded iron formation pebbles), jasper and fuchsitic quartzite were found to be less common, and clast diameters between 3 and 10cm, and locally up to 80cm were recorded. The matrix in the conglomerate is similar to the sandtone member (Tickell, 1975).

Trough cross-bedding was reported to be present throughout the Formation, up to 2m in width, 60cm in set thickness, and up to 4m long. The dimensions of cross-bedded units were found to vary considerably within individual outcrops. Cosets were reported to be up to 3m in thickness, and were followed laterally by Tickell (1975) for up to 1km. The base of each unit was observed to be irregular, although the development of channels was not noted. Tickell used trough cross-bedding to define palaeocurrent directions, and suggests an overall direction from north-east to south-west, though trends in the Steilloopbrug (40km south-west of Blouberg mountain) area are more westerly. The

conglomerate members were observed to consist of laterally persistent, sheet-like pebble layers, up to 3m in thickness, interbedded with sandstones. It was noted that there is a regional decrease in clast size in the Sesalong member, with thick boulder conglomerates developed in the extreme north (in the Blouberg area), decreasing to cobble conglomerates 10-30km to the south-west. The palaeocurrent directions derived from trough cross-bedding present in the interbedded sandstone in the conglomerate members are indistinguishable from those recorded in the sandstone member (Tickell, 1975).

The nature of the trough cross-bedded units, coupled with the lack of ripple marks and fine argillaceous deposits in the Formation led Tickell (1975) to suggest that the Mogalakwena Formation had been deposited in a braided river environment. Tickell (1975) pointed out that the Mogalakwena Formation bore considerable similarity to molasse sediments deposited adjacent to the Himalyas. The northerly source of the sediments led Tickell (1975) to propose that the Mogalakwena developed as a molasse complex from the Limpopo mountains to the north.

A summary of the re-investigation of the Waterberg Group (1965-1982) by the Geological Survey of South Africa was provided by Jansen (1982), which highlights the key issues raised during this period of investigation. The results of this large-scale project greatly improved knowledge of the Group, and formed the basis on which modern work on the various Waterberg strata was undertaken.

1.4.2.2: Recent work on the Waterberg Group (1977 to present):

Other work continued on the Waterberg Group during this time that was independent of the Geological Survey. Coertze *et al.* (1977) proposed that sedimentation of the Transvaal (Supergroup, c. 2.6 – 2.1 Ga) succession and the Waterberg succession may have been at least partially continuous in the Otse basin of Botswana, and that sedimentation was interrupted only by as little as 180 Ma during the intrusion of the Bushveld Complex in the main Transvaal and Waterberg basins. Vos and Eriksson (1977) proposed a fluvial fan model for the depositional environment of the Waterberg Group, and suggested that

the general reddish colour of these rocks was due to authigenic-diagenetic alteration of iron-bearing detrital silicates.

Cheney and Twist (1986) re-interpreted the stratigraphy of the Waterberg Group, proposing the presence of unconformities between each of the major formations in the lower part of the main basin. Only the Mogalakwena, Cleremont and Vaalwater formations were viewed as a continuous succession. Importantly, unconformities were thought to be present between the Setlaole and Makgabeng Formations, and between the Makgabeng and Mogalakwena Formations. This proposal was based on the fact that each of the five identified unconformity-bounded sequences (U.B.S.) rests on one or more older sequences, and also on basement rocks, indicating erosion between each U.B.S. The consequences of these proposed unconformity-bounded sequences within the Waterberg are that the present outcrop of Waterberg may bear little resemblance to the previous extent of the basin (i.e. the present outcrop is preservational rather than depositional). Models involving the northward migration of the depocentre (e.g. Jansen, 1975a) could no longer be applied accurately. Additionally, the presence of proto-basins could be questioned due to obscuring of the original basin architecture by inter-sequential erosion. Cheney and Twist (1986) proposed that the maximum thickness of the preserved Waterberg Group does not exceed 5km.

Cheney and Twist (1986) also provide good evidence constraining the age of some of the Waterberg strata: the Makgabeng Formation unconformably overlies the Abbotspoort Fault, a southern reactivation of the Palala Shear Zone. The Abbotspoort Fault cuts the Palala Granite, and deformation of the granite has been dated at 1770±60 Ma. (Cheney and Twist, 1986). This data indicates that the Makgabeng and younger formations probably post-date 1770±60 Ma, assuming that deformation of granite was coeval with the Abbotspoort Fault.

Du Plessis (1987) re-examined the Gatkop area of the Waterberg basin, east of Thabazimbi. He observed structures present along the Thabazimbi-Murchison Lineament (T.M.L.), a zone of major crustal weakness, that is thought to have actively controlled

basin margins on the Kaapvaal Craton throughout the Late Archaean and much of the Proterozoic. The structures under investigation in the T.M.L. cut Bushveld granite, close to the edge of the Nylstroom protobasin (Figure 1.5), indicating that the T.M.L. may have been active at the time of Waterberg Group sedimentation, producing the Nylstroom protobasin and Alma trough as a pull-apart basin. Du Plessis argued that the unconformities present within the Waterberg Group need not necessarily represent basin-wide erosion, as basin edges are typically associated with marginal unconformities which grade into conformable relationships towards the centre of the basin. If a basin is expanding, each successively younger sedimentary succession will onlap onto the basin floor. Du Plessis therefore postulated that the presence of an unconformity indicates only the proximity of a basin edge, and not basin-wide erosion. It was therefore proposed that the present extent of Waterberg rocks does indeed closely resemble the extent of the Waterberg depositional basin, and that protobasins can be recognised (du Plessis, 1987); as a consequence, models of Waterberg basin evolution involving the northward migration of centres of thermal subsidence (e.g. Jansen, 1975a) were again proposed.

Stettler (1991) used gravitational and aeromagnetic data to determine the thickness of the Waterberg Group. The geophysical data suggested a maximum thickness no greater than 5km, in support of Cheney and Twist (1986). Callaghan (1987b) and Callaghan *et al.* (1991) summarised the sedimentology and petrography of the Waterberg Group strata, and investigated cassiterite–bearing placer deposits. Van der Neut *et al.* (1991) studied the Wilgerivier Formation in the Middelburg basin, and proposed that it had been deposited in a distal alluvial fan-braidplain environment within a graben. Eriksson *et al.* (1997) examined the economic potential of the Waterberg sediments, and discussed palaeoplacer deposits of titanomagnetite-ilmenite-zircon in the Cleremont Formation, cassiterite in the Gatkop area, and U-Cu and manganese deposits close to the T.M.L. Van der Neut and Eriksson (1999) calculated palaeohydrological parameters in the Wilgerivier Formation, and compared tham with calculated parameters from Phanerozoic braided river deposits in South Africa. The calculated palaeohydrological parameters were used to infer the palaeogeography and palaeoclimate. Barker *et al.* (in press)

summarise the present knowledge concerning the Middelberg and Main Waterberg basins.

1.4.3: Previous work on the Soutpansberg Group:

Very early work concerning the Soutpansberg strata (1908-1955) is presented in Table 1.9. Original mapping of the Soutpansberg area was by Van Eeden *et al.* (1955), though the most comprehensive study of the Group is that of Barker (1979). Important work concerning the tectonic setting of the Soutpansberg Group has also been undertaken by Jansen (1975b), Barker, (1983) and Cheney *et al.* (1990).

Although the volcano-sedimentary nature of the succession is accepted by all workers, there has been heated debate in the past concerning the tectonic environment in which the Soutpansberg Group was deposited and preserved. Jansen (1975a) recognised that both the Waterberg and the Soutpansberg basins were intra-cratonic in origin (i.e. both are continental), but saw that there were considerable differences between the two basins. He appreciated that the Waterberg basin was developed in broad undulations in the craton, whereas the Soutpansberg basin appears to be developed within a distinctly narrow, E.N.E.-W.S.W. (Limpopo-parallel) trending trough, which may be partially fault bounded on the northern and southern margins. The apparent lack of internal unconformities within the Soutpansberg Group (Jansen, 1975b) led him to believe that the Soutpansberg Group represented a single sedimentary and volcanic cycle. Jansen (1975b) was also able to identify syn-sedimentary faulting, as some of the faults within the Soutpansberg Group are only developed in older formations.

Considering all the available data, Jansen (1975b) proposed that the Soutpansberg Group was deposited in an aulacogen (failed rift), which had developed due to reactivation between the Central and Southern Marginal Zones of the Limpopo Belt. The onset of rifting was marked by normal faulting (evidence for which is now masked by subsequent reactivation), and widespread volcanism (Fundudzi Formation) which continued sporadically throughout the lifespan of the trough. Jansen (1975b) believed that the older

members of the Soutpansberg Group at the eastern end of the trough pre-dated the Waterberg Group, whereas relationships in the west at Blouberg suggested that the Wyllies Poort Formation was younger than the Waterberg Group (Jansen, 1975b, 1976) (Section 1.3.2). Jansen (1975b) therefore proposed that the aulacogen was long-lived (spanning the Waterberg Group sedimentation) and that the trough spread gradually from east to west through time. The fact that successively younger Soutpansberg strata appear to have been deposited non-conformably on basement strata towards the west seemed to corroborate this suggestion. The Soutpansberg aulacogen compared favourably with aulacogens developed on other cratons.

Jansen's (1975b) work did not remain unchallenged. Barker (1976) suggested that the aulacogen model should be regarded with caution. He noted the absence of chemical and marine clastic sediments within the Soutpansberg succession, providing evidence against aulacogen formation adjacent to a continental margin. Barker also noted that available palaeocurrent data indicated transport generally from the north, whilst aulacogen environments generally favour transport along the axis of the trough. Barker (1976) suggested that the evidence from the Soutpansberg Group favoured a rifted or yoked basin model, rather than an aulacogen. In addition to a rifted or yoked basin, Barker (1983) also proposed that the Soutpansberg Group may have been deposited with a half-graben with a southern hanging wall.

Meinster (1977) did not believe that the mature sediments of the Wyllies Poort Formation (typically recrystallised to quartzite with well rounded quartz pebble washes) could have formed within an active fault-bounded rift, and proposed that these sediments had been transported a considerable distance, rather than from the proximal edges of a graben. To account for such mature sediment, Meinster (1977) proposed that the Soutpansberg had been preserved, rather than having been deposited, in a graben type structure, hinting that the Soutpansberg Group may have been developed over a wider area than the present extent of outcrop suggested.

Such an idea was explored by Cheney *et al.* (1990), who identified a large regional low-angle unconformity below the Wyllies Poort Formation, which had remained unidentified by earlier workers. The presence of the unconformity was based on the observation from maps that the Wyllies Poort Formation rests on successively older strata towards the west, though this could rarely be identified directly in the field (the same relationship had been explained by Jansen (1975b) as being due to westward propagation of the Soutpansberg aulacogen). The presence of such an unconformity provided a strong argument against an aulacogen model, as continuous down-faulting should lead to continuous sedimentation. Major gaps in sedimentation (represented by the unconformity) suggested that the Soutpansberg Group was once, as Meinster (1977) earlier hinted, more widespread, possibly across the Limpopo, Zimbabwe and Kaapvaal provinces. Cheney *et al.* (1990) proposed correlations with other isolated red-bed sequences on the Kaapvaal and Zimbabwe Cratons that had previously been thought of as representing separate basins. The Olifantshoek Sequence in the west of the Kaapvaal Craton, and the Palapye Group in eastern Botswana were proposed as correlates of the Soutpansberg Group.

Barker (1983) considered the development of the Soutpansberg trough from the perspective of its evolution within the Limpopo Mobile Belt. He proposed that rising granite diapirs, formed during anatexis at about 2.7 Ga, were responsible for uplifting the Central Zone of the Limpopo Mobile Belt (granulite-grade gneisses are presently exposed at the surface, indicating around 15 km of uplift). Rapid uplift continued from 2.1 to 1.8 Ga, when isostatic settling along the margins of the Central Zone led to the creation of the Soutpansberg trough within an asymmetrical yoked basin, with a faulted northern boundary. Post -Karoo readjustment is proposed as the tectonic event responsible for the present-day steeply dipping Soutpansberg strata, erosion of which has created the escarpment in the Soutpansberg mountain range.

The geochemistry of the Sibasa and 'Ngwanedzi' (lower Nzhelele) Formation basalts was examined by Crow and Condie (1990). They found evidence that the magmas were derived from multiple mantle sources, which had been enriched in subduction-zone

components during an earlier (Archaean) phase of arc collision. These conclusions were based on the ratios of incompatible trace-elements in the Soutpansberg basalts.

Barton and Pretorius (1997) related the Soutpansberg Group to rifting, possibly associated with mantle plumes. In agreement with Cheney *et al.* (1990), Barton and Pretorius (1997) also envisage the extent of the Soutpansberg Group to be much more widespread than the extent of the preserved basin suggests. Barton and Pretorius (1997) note that the age of the Soutpansberg Group (c. 1.85Ga) is coeval with the emplacement of the Schiel Alkaline Complex, just east of Louis Trichardt (Barton *et al.*, 1996).

Barker *et al.* (in press) propose that the most appropriate explanation for Soutpansberg basin evolution may be a combination of the models outlined above. They suggest that the lower Soutpansberg Group (Sibasa and Fundudzi Formations) represent a graben or rift environment. The upper Soutpansberg Group (Wyllies Poort and Nzhelele Formations), which is unconformable on the lower part of the Soutpansberg Group, was laid down within a more extensive basin, only a portion of which is now preserved, after reactivation of the original Soutpansberg rift (Barker *et al*, in press).

1.5: Aims of the Study:

Although the main basins of the Waterberg and Soutpansberg Groups have been the focus of considerable attention in recent years, the geology of the Blouberg area, (the only location where these two groups are found in close proximity to each other) remains poorly understood . The summary of previous work undertaken in the Blouberg area (Jansen, 1976; Meinster, 1977; Brandl, 1991; discussed in Section 1.3) serves to emphasise the lack of consensus of opinion regarding the Blouberg area. Fundamental geological questions, such as the age-relationships between the strata, remain largely unresolved.

Whilst the previously published data give a good overview of the geology of the Blouberg area, there is an absence of integrated analysis of sedimentary, structural and

geochemical data from the study area. Advances in geological methodology in recent years present the opportunity for a new focus with which to re-examine the geological history of the Blouberg area. The present study therefore aims to collect new field data, including a detailed map of the area, structural data, measurement of sedimentary architectural elements and determination of their component lithofacies and their three-dimensional relationships, and to re-interpret the geological evolution of the Blouberg area.

Unravelling the tectonic and depositional history of the area around Blouberg mountain may help to constrain models for the age of the Limpopo Mobile Belt, which is presently the focus of much debate. Furthermore a model for the geological evolution of the Blouberg area may serve as a model for basin development and basin inversion on or near an inter-continental suture zone (or terrane boundary).

A second focus of attention of this work concerns the strata of the Makgabeng Formation on the Makgabeng plateau. An interpretation as an aeolian deposit has been proposed (Meinster and Tickell, 1975; Callaghan *et al.*, 1991), but the Formation has not been examined in detail. The considerable age of these sediments (c. 1920–1700 Ma; Jansen, 1982) indicates that the Makgabeng plateau may be one of the oldest (e.g., Eriksson and Simpson, 1998) and best preserved records of aeolian deposits.

1.6: Methodology:

1.6.1: Field work:

Field work was carried out between November 1997 and August 1999. The field area shown in Figure 1.2 was mainly mapped on foot, and geological data were recorded in notebooks and plotted on field base maps. Navigation in the field was generally accomplished by use of a G.P.S. (global positioning system) receiver.

General geological data were collected during the course of the fieldwork, and mostly comprised primary (sedimentary) structures and secondary (tectonic) structures. Primary sedimentological features were recorded for the identification of sedimentary facies, in order to attempt to correlate strata in different parts of the study area and characterise the depositional conditions. Directional data from primary structures such as ripple marks and cross-bedding orientation were recorded in order to infer palaeocurrent directions. The sedimentary lithofacies and palaeocurrent directions were considered together to produce a classification of architectural elements (Miall, 1996). Cross-bed set thickness, channel size and clast size were measured in order to calculate palaeohydrologic parameters, such as palaeoslope (Section 1.6.3).

Pebble surveys of conglomerates in the Mogalakwena Formation were undertaken with the use of a $1m^2$ grid, with vertical and horizontal strings stretched at 10cm intervals across the grid, thus producing 100 points of intersection. Counting the presence and composition of pebbles or cobbles at each of these points gave an estimate of the ratio of clasts to matrix, and the variability of clast composition within each m^2. Relative clast size could be estimated by the measurement of the b-axis (intermediate axis) of the largest clast within each m^2. Vertical variability of these parameters in the Mogalakwena Formation could be assessed by choosing accessible vertical profiles and conducting a metre by metre survey through the exposed vertical section. Lateral variation in these parameters could be assessed by comparison of data collected from vertical profiles from different locations.

Plane-table mapping was used for accurate large-scale maps of cross-bedding geometry in the Makgabeng Formation. Borehole data were logged in order to provide details on vertical lithological variation within the Waterberg Group. Dip and dip-direction of bedding were frequently recorded, and the orientation of tectonic structures (e.g. slickenside lineations, foliations, lineations and veins) was measured to aid with the reconstruction of tectonic events.

1.6.2: Photogeology:

A set of 1:50,000 –scale aerial photographs of the study area was used to assist with field-based mapping. The use of aerial photographs was most beneficial in mapping large areas west of the Makgabeng plateau, occupied by flat-lying Mogalakwena Formation sandstones and conglomerates. Outcrops of these lithologies could readily be identified from the surrounding Quarternary cover by stereoscopic examination of an overlapping pair of photographs. Dykes cutting the Waterberg Group could also be examined by the use of aerial photographs. As these basic igneous rocks weather much faster than the siliciclastic sedimentary wall rocks, they give rise to a reddish soil, which appears darker on monochrome aerial photographs. Dykes could therefore be easily identified, followed for many kilometres along strike, and plotted straight onto maps thereby avoiding unnecessarily long periods in the field.

1.6.3: Geological maps and cross-sections:

Collected field data and interpretetations from aerial photographs were transferred to 1:50,000 –scale topographic maps (South African Government Printer) of the study area, and data were then transferred to a digital format and plotted on digitised topographical maps, using ArcView G.I.S. (Geographic Information System) software. The final geological map is presented in Appendix 1, and cross-sections, based on interpretation of the maps in Appendix 1, are presented in Appendix 3.

1.6.4: Calculations of palaeohydrological parameters:

A variety of different formulae have been proposed by several workers with which to measure hydrological parameters in ancient fluvial deposits. Generally the field data required for these formulae are grain size analyses (sandstones) and clast size analyses (conglomerates and gravels) and the set thickness of cross-bedded units (e.g. Ethridge and Schumm, 1978). It is important to emphasise, however, that the calculated results are only estimates of the hydrological conditions at the time of deposition of the fluvial

sediment. Use of different formulae will likely produce different results, and results may also vary considerably with a variety of data set sizes. It should therefore be stressed that the calculated results are most useful for comparative purposes between different fluvial deposits, and should not be considered as quantitative values for the palaeohydrological parameters being considered.

A variety of formulae will be used to calculate palaeohydrological parameters during this work, in order to minimise the error of using single formulae alone. Methods involve both utilisation of measurements from clast-filled channels, and the set thickness of cross-beds. The use of multiple methods also provides a range of parameters rather than a single value, which produces a more accurate framework from which to model the palaeogeography and palaeoclimate.

1.6.4.1: Palaeohydrological parameters that can be calculated from clast-filled channels:

Clast sizes can be used to calculate the average velocity of water and the unit stream power, according to the following equations:

$$v = 0.2 \times (di)^{0.455} \quad (1)$$

$$W = 0.009(di)^{1.686} \quad (2)$$

(where v is velocity of water in ms^{-1}, W is the unit stream power, measured in Watts/m^2, and di is the length of the intermediate axis of the largest visible clast) (Costa, 1983).

Provided that the cross-sectional surface area of a channel containing a clast can be measured (or estimated), the discharge can be calculated by the following equation:

$$Q = \bar{v} \times A \quad (3)$$

(where Q is the discharge in m^3s^{-1}(cumecs), and A is the cross-sectional surface area of the channel (approximated by $d_m \times w$) in m^2, where d_m is the mean depth of the channel measured in metres, and w is the width of the channel in metres)(Costa, 1983).

When the intermediate axis of a clast in the channel is measured, then palaeoslope can be calculated by the following equation:

$$W = \left(\frac{9800 \times Q \times S}{w}\right) \quad (4)$$

(where S is the palaeoslope, measured in m/m) (Costa, 1983).

1.6.4.2: Palaeohydrological parameters that can be calculated from cross-bed set thickness:

The mean water depth can be calculated by the following formula:

$$h = 0.086(d_m)^{1.19} \quad (5)$$

(where h is the mean set thickness of cross-beds in metres (Allen, 1968).

The ratio between channel width and depth can be estimated by:

$$F = 225M^{-1.08} \quad (6)$$

(where F is the ratio between channel width and depth, and M is the sediment load variable, i.e. the percentage of silt and clay in the channel perimeter, which can be assumed to be a constant of 5% for such coarse bedload as inferred from the sedimentary rocks of the Blouberg area (Schumm, 1968a,b; Van der Neut and Eriksson, 1999)). This gives a fixed channel width to depth ratio, $F = 40$.

The estimation of the width of channel, w, can be calculated by:

$$w = Fd_m \quad (7)$$

(Schumm, 1968a).

It is then possible to estimate the average daily discharge (also called the mean annual discharge by some workers):

$$Q_m = vA \quad (8)$$

where Q_m is the average daily discharge, measured in m^3s^{-1}, and A is the mean cross-sectional surface area (approximated by $d_m \times w$) in m^2; v is the velocity of water in ms^{-1}, and can range between 0.5 and 1 ms^{-1} in conditions where large subaqueous dune bedforms migrate (i.e. when cross-bedding is formed). (Leopold *et al.*, 1964). For the purposes of this study, an intermediate velocity of 0.75 ms^{-1} is assumed.

Mean bankfull channel depth can be estimated by:

$$d_b = 0.6M^{0.34}Q_m^{0.29} \quad (9)$$

(where d_b is mean bankfull channel depth in m) (Schumm, 1969).

Calculation of bankfull channel width can be estimated by:

$$w_b = 8.9d_b^{1.40} \quad (10)$$

(where w_b is the bankfull channel width in m) (Leeder, 1973).

This allows for a recalculation of Q_m (average daily discharge), which can be compared to the results of equation 8, when the following equation is applied:

$$Q_m = 0.027w_b^{1.71} \quad (11)$$

(Osterkamp and Hedman, 1982).

Palaeoslope can be calculated by:

$$S = 60M^{-0.38}Q_m^{-0.32} \quad \text{(Schumm, 1968a)} \quad (12)$$

and by

$$S = 30\left(\frac{F^{0.95}}{w^{0.98}}\right) \quad \text{(Schumm, 1972)} \quad (13)$$

(where S is the palaeoslope).

Assuming that the estimation of Q_m is gained only from equation 11 (which is likely to be more accurate than that derived from equation 8), two different estimates of palaeoslope can be obtained from equations 12 and 13. Thus an approximate range of palaeoslope can be gained.

Using the two values of palaeoslope derived from equations 12 and 13, two estimates of bankfull water discharge can be made, using the equation:

$$Q_b = 4.0 A_b^{1.21} S^{0.28} \quad (14)$$

(where Q_b is bankfull water discharge, and $A_b = d_b \times w_b$) (Williams, 1978).

The drainage area (catchment area) of a river system can be estimated by:

$$Q_b = A_d^{0.75} \quad (15)$$

(where A_d is the drainage area in km^2) (Leopold *et al.*, 1964).

Principle stream length (from source to depositional site) can be estimated by:

$$L = 1.4 A_d^{0.6} \quad (16)$$

(where L is the stream length in km) (Leopold *et al.*, 1964).

By substituting the two different values of Q_b obtained from equations 12 and 13 into equations 15 and 16, two different values for drainage area and stream length can be calculated.

1.6.5: Laboratory methods

Lithological samples from all the main stratigraphic units encountered in the field area were collected for thin section analysis. Additional samples were collected for thin section analysis of sedimentary and tectonic structures, which required closer examination. Orientated samples were taken in order to determine kinematic directions, fault and recrystallisation history.

Orientation data of bedding and tectonic structures were analysed by stereographic projection in order to identify any dominant tectonic trends. Analyses of stereographic

data were undertaken using *Spheristat 2* software. Each stereographic projection presented in this work is a lower hemisphere projection on a Schmidt (equal area) net. Palaeocurrent analyses and dyke trend analyses were plotted on rose diagrams, and vector mean (principal directions) were calculated, also using *Spheristat 2* software. Data concerning the trend of dykes intruding the field area were collected directly from collated maps. A 1.5cm^2 grid was placed over a 1: 150000 geological map, and the trend of each dyke within each grid square was measured with a protractor, and plotted on a rose diagram. Thus, the most laterally extensive dykes are recorded the most frequently within each grid square, and are in turn represented preferentially on the rose diagrams. The azimuth of the principal direction is indicated, where appropriate, on rose diagrams by a single line. The standard deviation away from the principal direction is indicated by small ticks on both sides of the principal direction line.

Geochemical investigation of Sibasa Formation basalts and dyke swarms intruding the Waterberg Group were undertaken by use of the I.C.P.M.S. facility at the University of Cape Town (incompatible trace elements) and by X.R.F. at the University of Pretoria (major and trace elements).

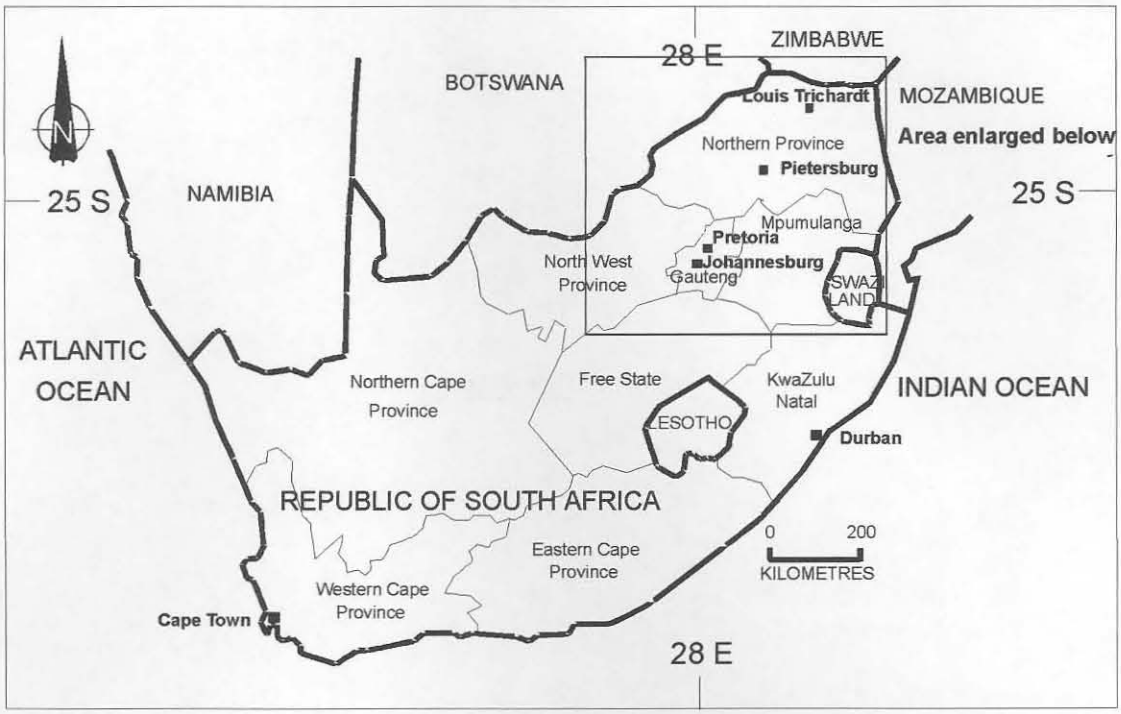

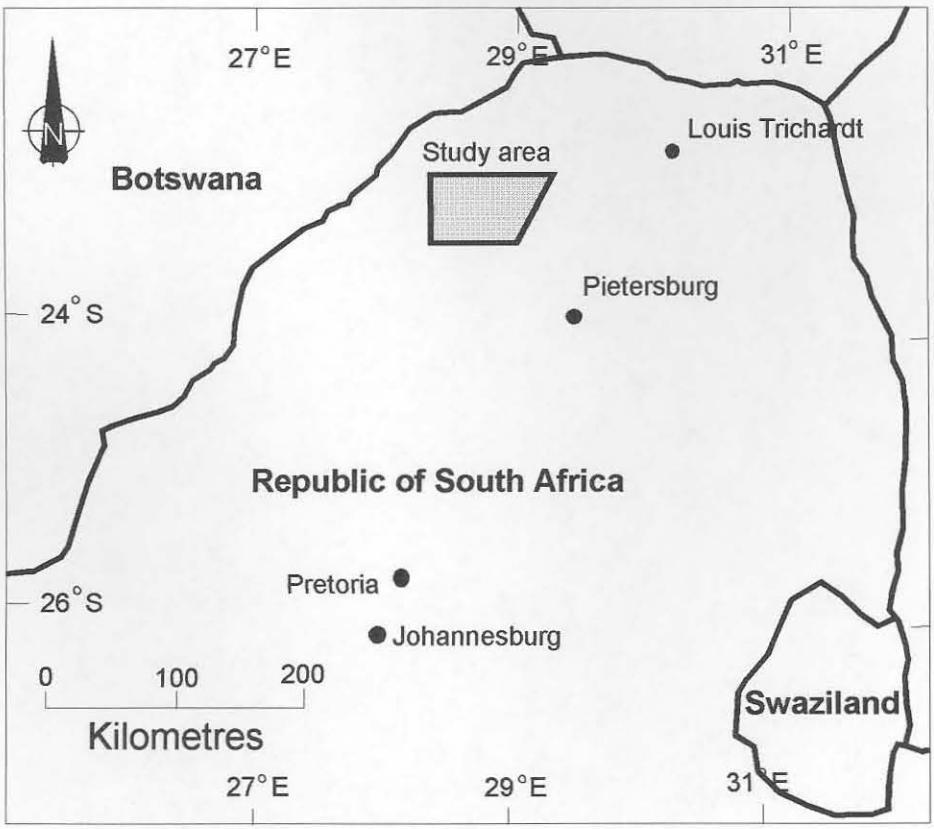

Figure 1.1: Geographical location of the study area.

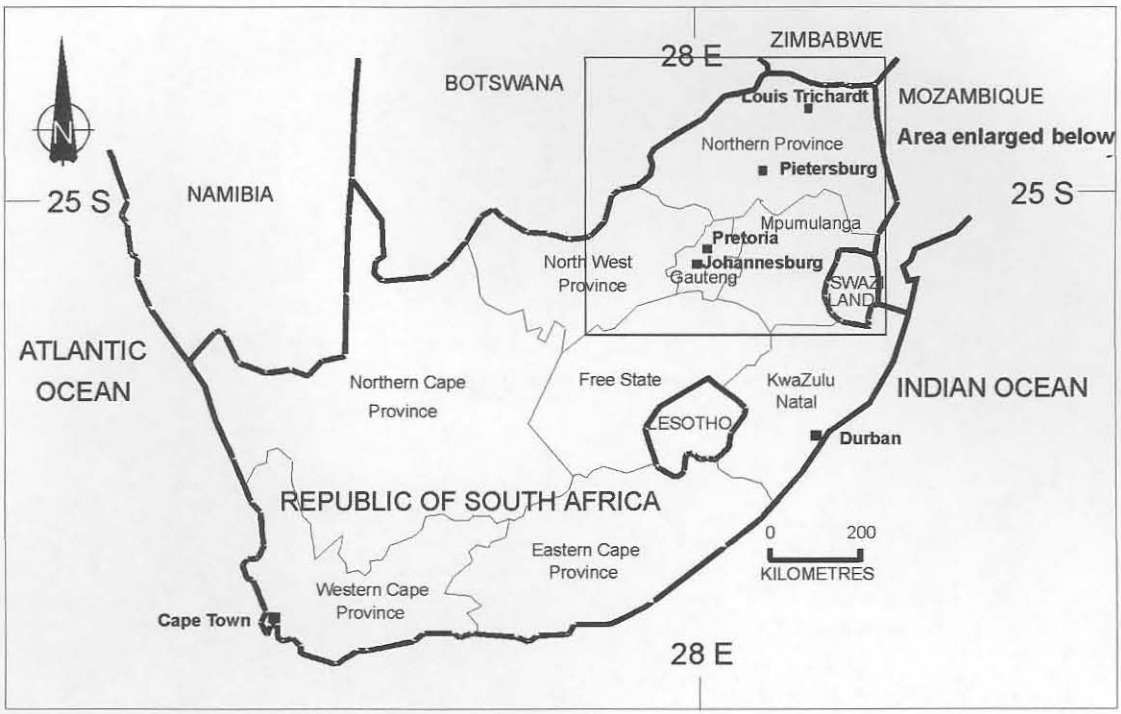

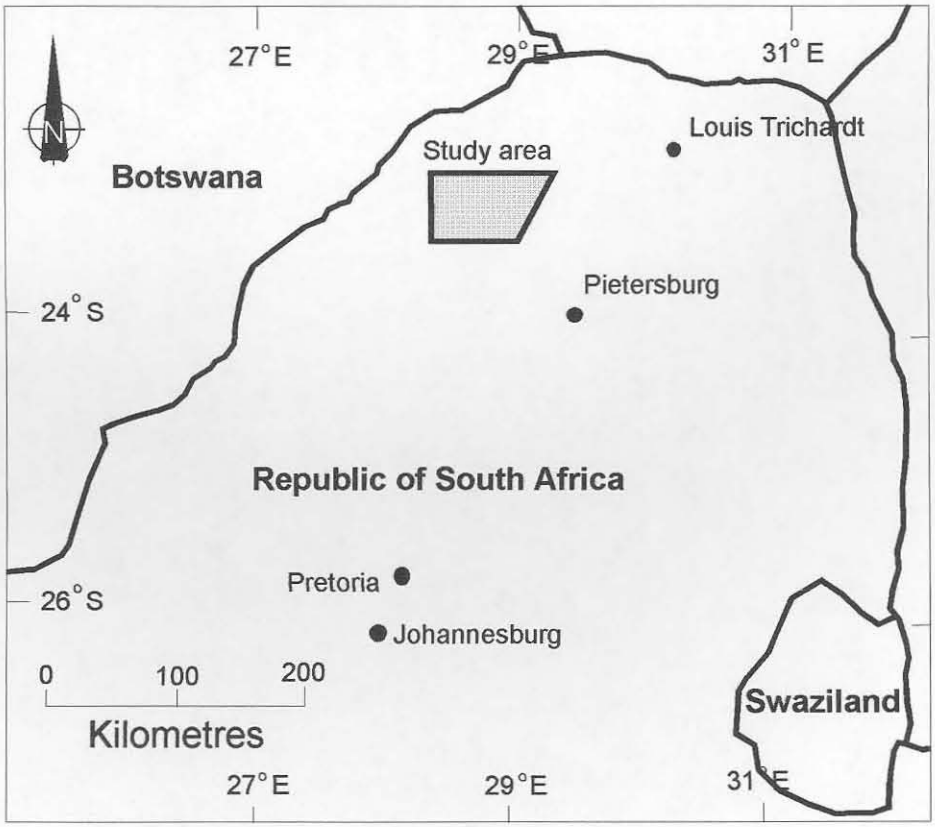

Figure 1.1: Geographical location of the study area.

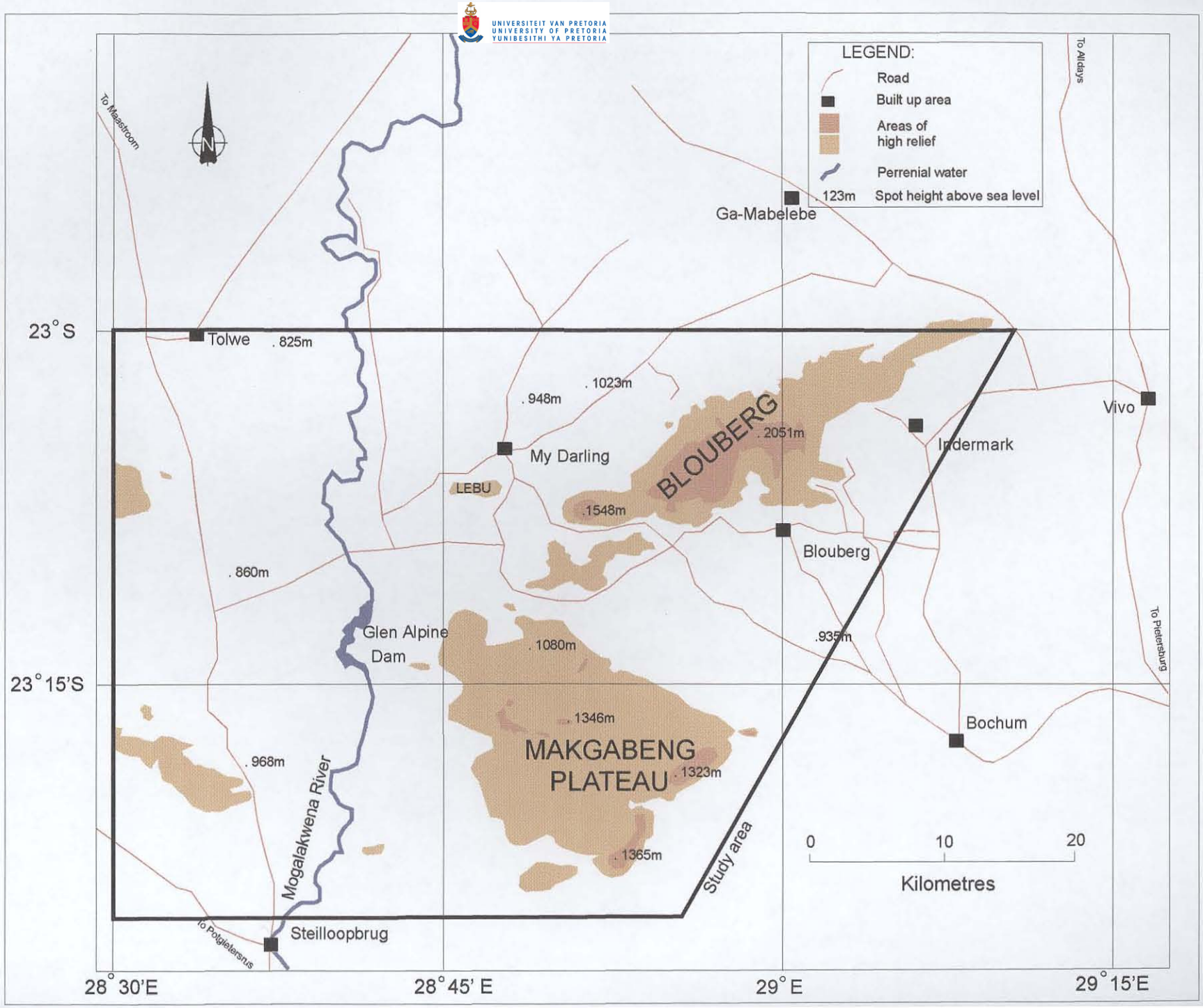

Figure 1.2: Map showing geographical features of the study area.

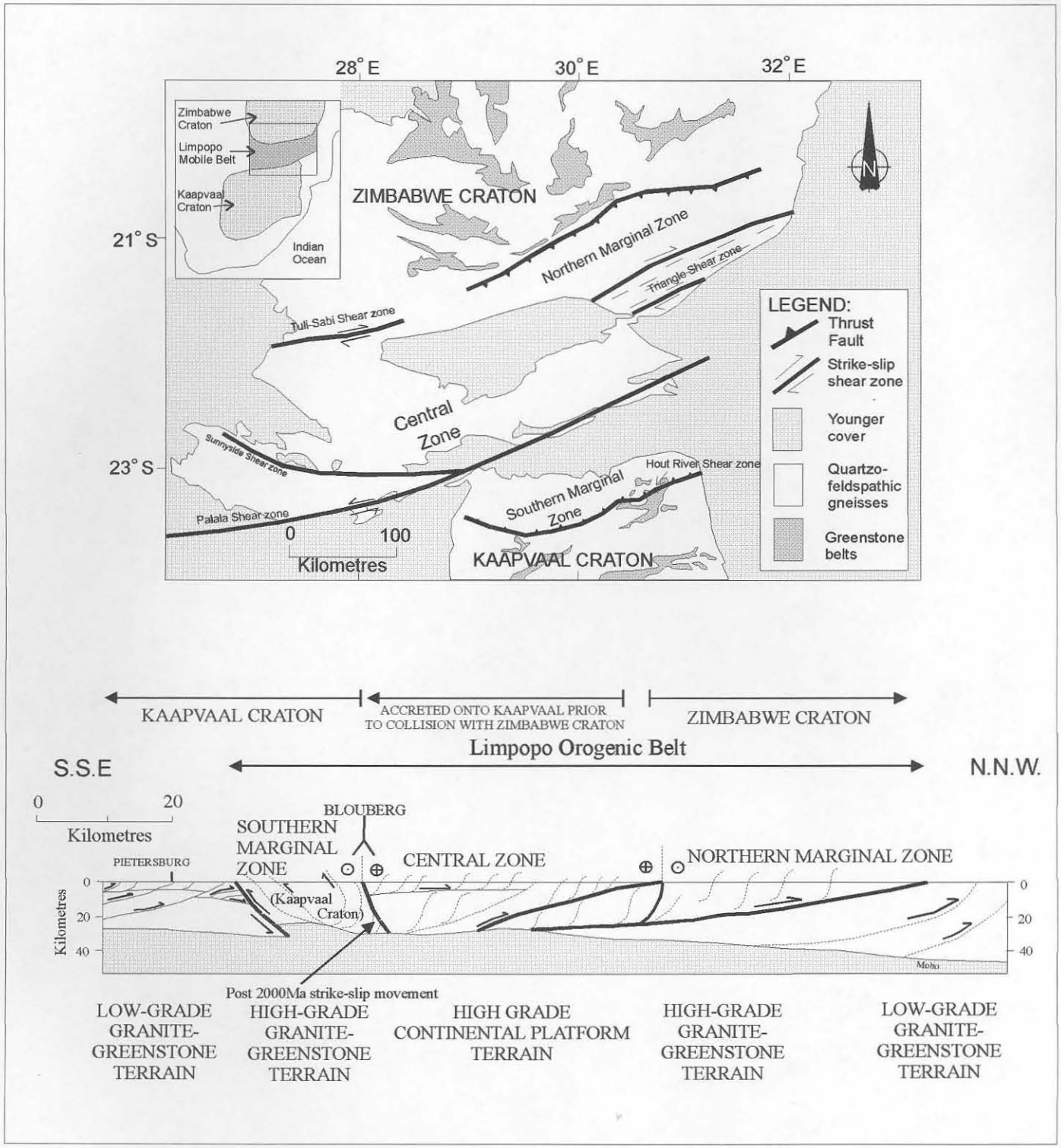

Figure 1.3: Simplified geological map and cross-section showing features of the Limpopo Mobile Belt (after Kröner *et al.*, 1999 and Roering *et al.*, 1992).

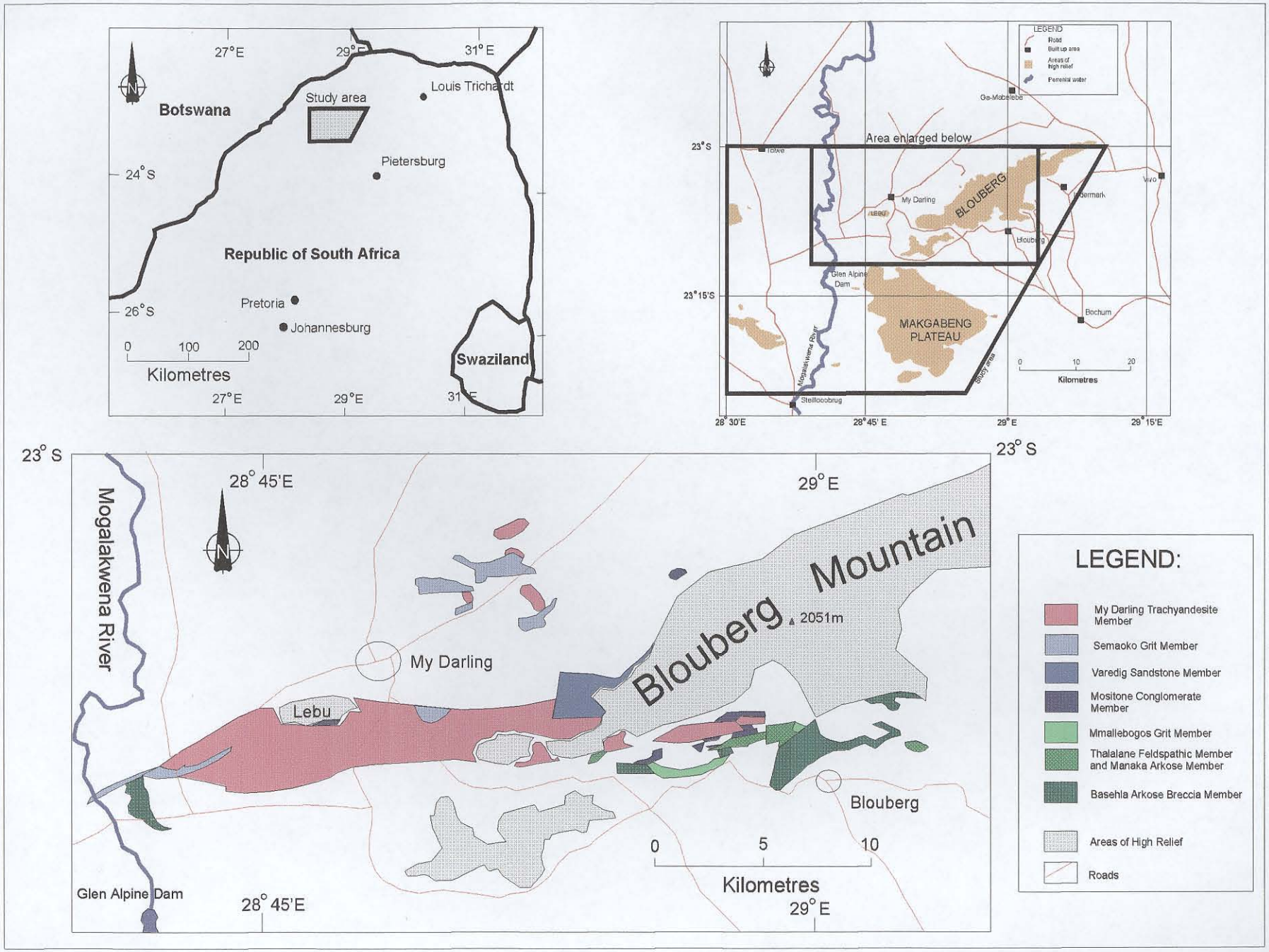

Figure 1.4: Map showing the distribution of the lithostratigraphic units in the Blouberg Formation (after Jansen, 1982).

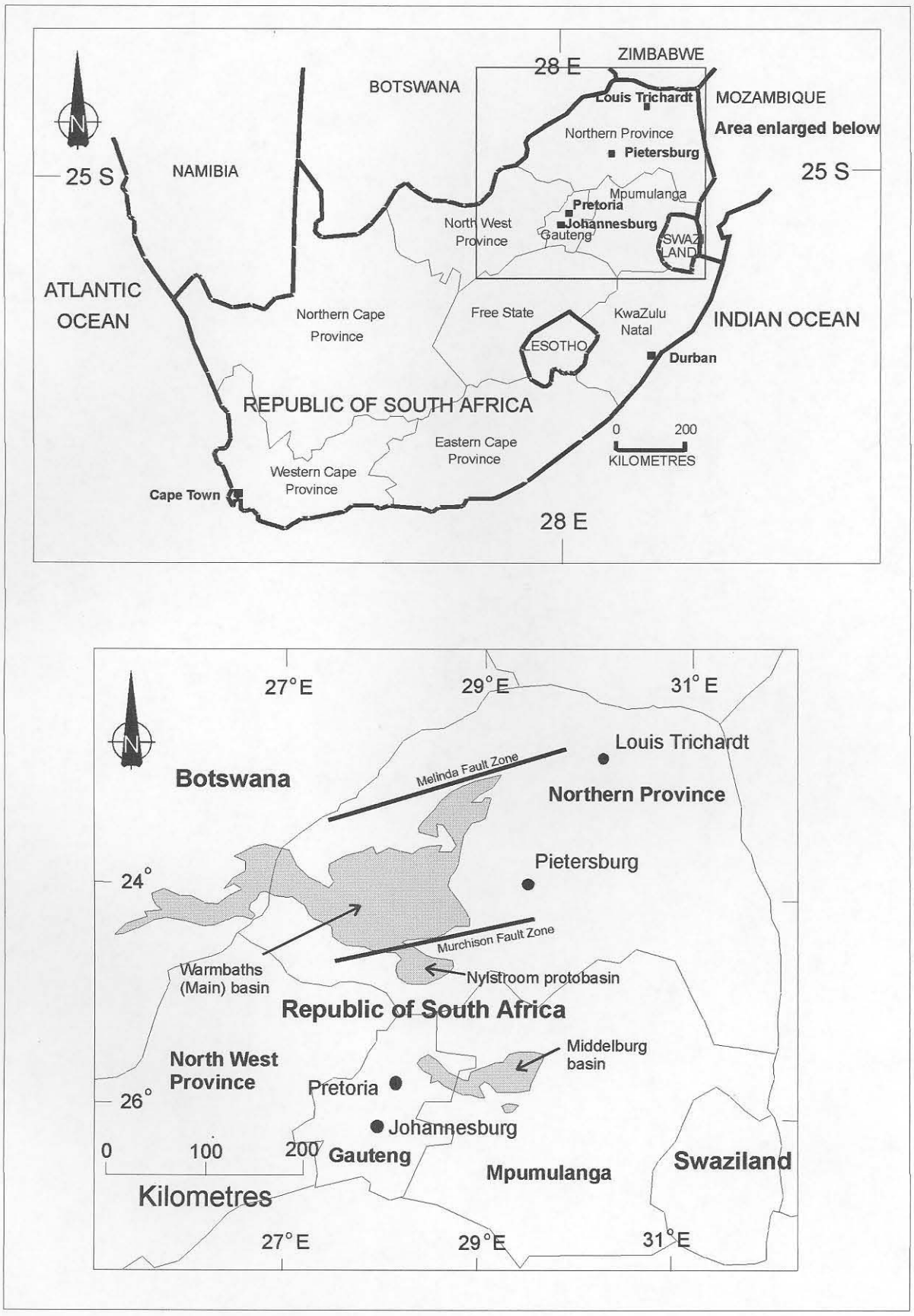

Figure 1.5: The distribution of the Waterberg Group (after Callaghan *et al.*, 1991).

Figure 1.6: Map showing the distribution of the lithostratigraphic units in the main Warmbaths basin of theWaterberg Group (after Callaghan *et al.*, 1991).

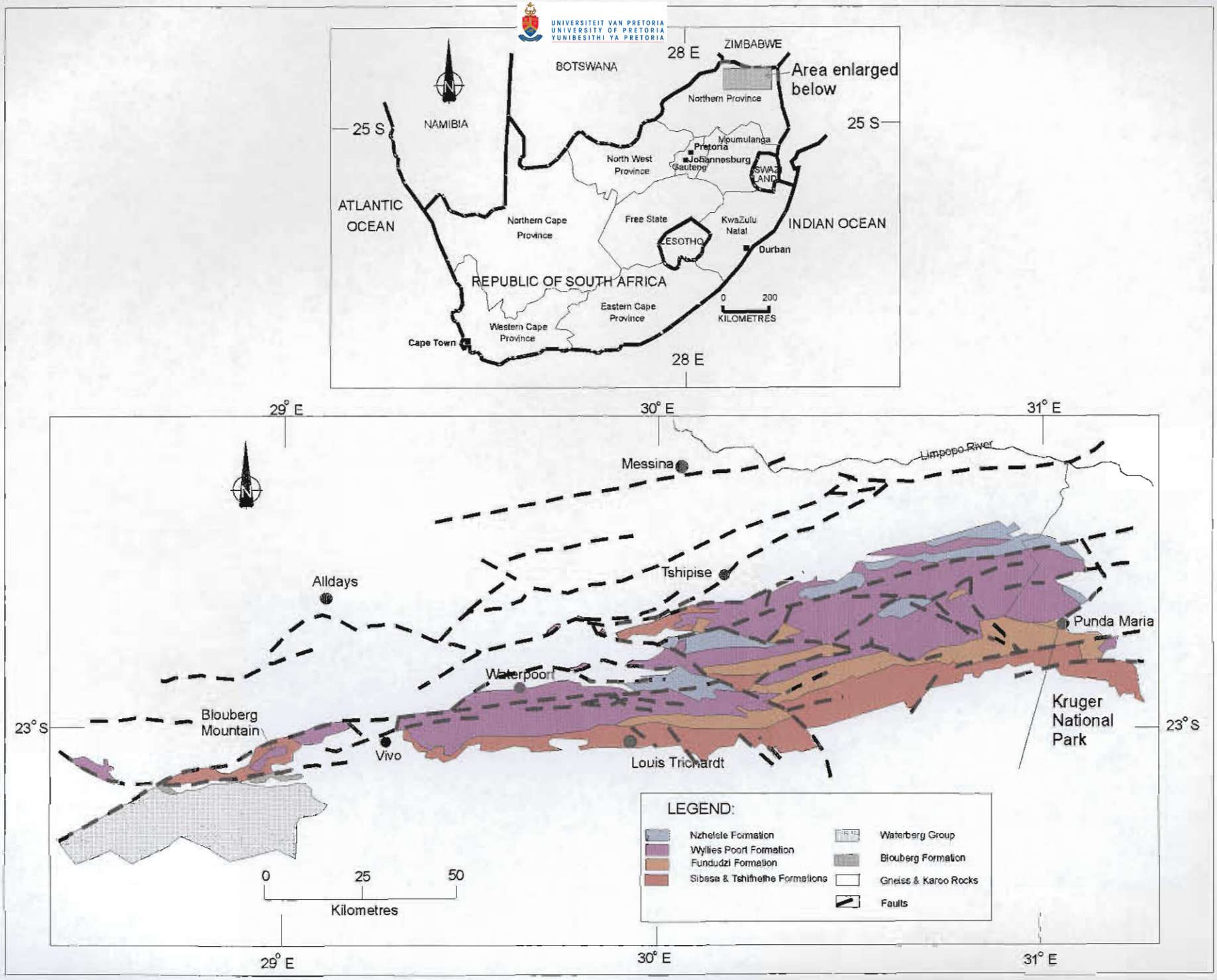

Figure 1.7: Map showing the distribution of the lithostratigraphic units in the Soutpansberg Group (after Barker *et al.*, in press).

FORMATION	MEMBER
BLOUBERG FORMATION	Semaoko Grit (300-400m)
	My Darling Trachyandesite (Max. 800m)
	Varedig Sandstone (350-450m)
	Mositone Conglomerate (100-150m)
	Mmallebogos Grit (400m)
	Thalalane Feldspathic Sandstone (450-600m)
	Manaka Arkose (150-250m)
	Basehla Arkose Breccia (Max. 1200m)

Table 1.1: Stratigraphic subdivision of the Blouberg Formation (after S.A.C.S., 1980).

GROUP	SUBGROUP	South / southwest & central parts	Southeast & central parts	North / northeast & central parts	Nylstroom area	Middelburg area
WATERBERG GROUP	KRANSBERG	Vaalwater Formation (475m)				
		Cleremont Formation (125m)				
		Sandriviersberg Formation (1250m)	Sandriviersberg/ Mogalakwena Formations	Mogalakwena Formation (1250-1500m)		
	MATLABAS	Aasvoelkop Formation (300-600m)	Aasvoelkop/ Makgabeng Formations	Makgabeng Formation (380-1000m)		
		Skilpadkop Formation (450-600m)	Skilpadkop Formation (450-600m)	Setlaole Formation (450m)		
	NYLSTROOM	Alma Formation (3000m)	Sterk River Formation (500-1500m)		Alma Formation	
		Swaershoek Formation			Swaershoek Formation (2500m)	Wilge River Formation

Table 1.2: Stratigraphic subdivision of the Waterberg Group (after Callaghan *et al.*, 1991).

GROUP	FORMATION
SOUTPANSBERG GROUP	Nzhelele Formation (1000-2000m)
	Wyllies Poort Formation (1000-4000m)
	Fundudzi Formation (0-2800m)
	Sibasa Formation (0-3300m)
	Tshifhefhe Formation (0-9m)

Table 1.3: Stratigraphic subdivision of the Soutpansberg Group (after S.A.C.S., 1980).

Date	Author(s)	Nature of investigation
1977	Barton and Ryan	Review of geochronology
1977	Barton *et al.*	Rb-Sr dating of ancient dykes
1977	Du Toit and Van Reenen	Metamorphism and structure in the S.M.Z.
1977a 1977b	Van Biljon	General Introduction Relationship between plate tectonics and ancient mobile belts
1977	Van Reenen and Du Toit	Mineral reactions and timing of metamorphism
1978	Barton *et al*.	Relationship between Rb-Sr and U-Th-Pb dates in Sand River gneiss
1978	Van Reenen	High-grade metamorphic petrology of the S.M.Z.
1978	Van Reenen and Du Toit	Metamorphic petrology of granulites
1979a 1979b	Barton	Geochemistry, Rb-Sr isotopes and tectonic setting of post-kinematic igneous rocks. Crustal evolution
1979a 1979b	Barton *et al*.	Rb-Sr and U-Pb dating of Singelele and Bulai gneisses Geology, age and tectonic setting of the Messina Layered Intrusion
1979	Du Toit	Geology and structure of the Levubu and Bandelierskop intrusions
1979	Fripp *et al.*	Structure and origin of the Singelele gneiss
1980	Barton	Pattern of Archaean crustal evolution
1980	Fripp *et al.*	Deformation in the Archaean Kaapvaal craton
1980	Horrocks	Archaean supracrustal rocks in the L.M.B.
1981a 1981b 1981c	Barton	Status of isotopic investigations Pattern of Archaean crustal evolution Limpopo excursion guidebook
1981	Barton and Key	Tectonic development of the L.M.B., and the Archaean crustal evolution.
1981	Fripp	Sand River gneiss
1981	Horrocks	Geology between Messina and Tshipise
1981	Robertson and Du Toit	General report on Limpopo Belt
1982	Fripp	Geology around Sand River, Messina

Table 1.4: Summary of the work of the Limpopo Working Group, 1977-1982.

Date		Author(s)	Nature of investigation
1983	a	Barton *et al.*	Isotopic studies of the Sand River gneiss
		Barton and Key	Ages and geological setting of Central Zone rocks in eastern Botswana
	b	Barton *et al.*	Ages and chemical composition of deformed mafic dykes in the Central Zone
	a	Barton	Lead isotope evidence for age of Messina Layered Intrusion
	b	Barton	Lead isotope studies of Banded Iron Formation in the Central Zone
		Barton and McCourt	Rb-Sr evidence for the age of the Palala Granite
		Ryan *et al.*	Isotope studies on copper deposits near Messina
	c	Barton *et al.*	Geochronology in the S.M.Z.
		Watkeys *et al.*	Overview of the Central zone
		Horrocks	Geology of the area between Tshipise and Messina
		Fripp	Geology of the area around the Sand River, Messina
		Brandl	Geology and geochemistry of supracrustal rocks of the Beitbridge Complex
		McCourt	Archaean lithologies in the Koedoesrand area
		Du Toit *et al.*	Geology, structure and metamorphism of the S.M.Z.
		Van Reenen	Metamorphic petrology in the S.M.Z.
		Key *et al.*	Evolution of the S.M.Z. In Botswana
		Coward	Tectonics of the Limpopo Belt
		Barker	Geotectonic model for the Soutpansberg Group
	c	Barton	Summary of work

Table 1.5: Summary of the work on the Limpopo Mobile Belt in the Geology Society of South Africa special publication (Van Biljon and Legg, 1983).

Date	Author(s)	Nature of investigation
1982	Light	Continental collision as cause of Limpopo Belt
1985	Watkeys and Armstrong	Deformed lamprophyric dykes in the Central zone
1987	McCourt and Vearncombe	Shear zones bounding the Limpopo Belt
1987	Van Reenen *et al.*	Deep crustal response to collision in the Limpopo Belt
1988	Brandl	Geological setting and southern boundary of the Central zone
1990	Barton *et al.*	Significance of 3 Ga mafic dykes in the Central zone
1990	Boryta and Condie	Geochemistry and origin of the Beitbridge complex
1990	Brandl	Geology of the Alldays gneiss and associated dykes
1990	Brandl and Reimold	Pseudotachylite occurrences in the Palala Shear zone
1990	Retief *et al.*	Zircon ages in the Limpopo Belt
1990	Van Reenen *et al.*	Granulite facies rocks of the Limpopo Belt
1992a	Barton and Van Reenen	Age of the Limpopo Orogeny
1992b		Significance of biotite and phlogopite ages for the thermal history of the Central zone and S.M.Z
1992	McCourt and Vearncombe	Shear zones in the Limpopo Belt
1992	Roering *et al.*	Tectonic model for the evolution of the Limpopo Belt
1992	Stevens and Van Reenen	Origin of metapelitic granulites in the S.M.Z.
1992	Treloar *et al.*	Himalayan-Tibetan analogies for the evolution of Limpopo Belt
1993	Rollinson	Terrane interpretation of the Limpopo Belt
1994	Barton *et al.*	Metamorphic events: implications for P-T pathway application in complex metamorphic terrains
1994	Mkweli *et al.*	Timing of thrusting in the N.M.Z.
1995	Berger *et al.*	Geochemistry, geochronology of charoenderbites in the N.M.Z.
1995	Holzer	Petrology of the Bulai pluton and the 2.0Ga overprint in the Central zone
1995	Ichihashi and Miyano	P-T trajectory of the Central zone
1995	Kamber and Biino	Evolution of high T, low P granulites in the N.M.Z.
1995a	Kamber *et al.*	2.0 Ga event in the Triangle Shear zone
1995b		Proterozoic transpressive deformation in the N.M.Z.
1995	Rollinson and Blenkinsop	Magmatic, metamorphic and tectonic evolution of the N.M.Z.
1995	Tsunogae and Yurimoto	Zircon chronology
1996	Barton	Messina Layered Suite: Crustal contamination of an Archaean anorthosite complex
1996	Blenkinsop and Frei	Mineralisation and tectonics at Renco mine, N.M.Z.
1996	Holzer *et al.*	2 Ga event in the Limpopo Belt
1996	Layer *et al.*	Cooling history of the Central zone
1997	Barton and Sergeev	Discordia in zircon dates
1997	Chavagnac *et al.*	Nd systematics in migmatites
1997	Holzer *et al.*	Granulite facies metamorphism: Evidence for Proterozoic collision
1997	Jaeckel *et al.*	Granitoid magmatism and high grade metamorphism in the Central zone
1998	Hofmann *et al.*	Field relationships of Sand River gneiss
1998	Holzer *et al.*	Pb dating of metamorphic minerals in the Central zone
1998	Kröner *et al.*	Field relationships and age of Beitbridge Complex
1999	Kröner *et al.*	Zircon ages for the granitoid gneisses in the Central zone

Table 1.6: Summary of recent work on the Limpopo Mobile Belt (1982-1999).

Date	Author(s)	Nature of investigation
1872	Moodie	Presence of copper/lead occurrence
1897	Harger	Strata in Middelburg basin (Wilge Rivier Fm) unconformably overlie Transvaal strata, and are, in turn, unconformably overlain by Karoo strata.
1898a 1898b 1901 1904	Molengraaff	Named the rocks the 'Waterberg Sandstone Formation', and later the 'Waterberg Series', after the Waterberg District of Northern Transvaal. Relationship between Waterberg and surrounding strata
1904 1905a 1905b 1907 1908 1909a 1909b 1910	Mellor	Geology of Springbok Flats and Rhenosterkop Geology of Middelburg Discussion of Merensky's paper Geology west of Potgietersrus Description of the basal Alma Formation and its nonconformable relationship to the underlying Bushveld granite. Geology north of Nylstroom
1904	Holmes	General geology of Northern Transvaal
1904	Jorrisen	Mentioned in discussion of the Chuniespoort Group.
1905	Hatch and Corstorphine	General geology of South Africa
1908	Merensky	Tin deposits around the Bushveld granite.
1910	Anderson	General geology between Nylstroom and the Limpopo River.
1912	Kynaston and Mellor	Geology of the Warmbaths area (Map explanation).
1924	Daly and Molengraaff	Refuted claims that the Bushveld granites were intrusive into the Waterberg strata at Gatkop.
1932	Hall	Estimated thickness of Waterberg strata: max. 2700m north of Warmbaths
1942	Le Roex	Geological Survey report, Potgietersrus
1942 1948	Strauss	Dolerite and granophyre near Potgietersrus Geological Survey report, Potgietersrus
1944	Du Preez	Structural geology east of Thabazimbi.
1960	Cullen	Distribution of Waterberg strata in southern Bechuanaland Protectorate (Botswana).
1965	Glatthaar	Pyroclastics south east of Rust de Winter

Table 1.7: Summary of early work on the Waterberg Group, 1872-1965.

Date	Author(s)	Nature of investigation
1963	Wilke	Geology of sheet 2428B
1963	De Villiers	Geology of sheet 2428B
1966		Sedimentary geology around Potgietersrus
1967		Sedimentology of Loskop and Waterberg strata
1969	De Vries	Stratigraphic subdivision (current usage)
1970		Geology of the southern Waterberg
1973		Sedimentary structures in the southern and central Waterberg
1970	Frick	Identified strata in the south east as having been deposited within a littoral, possibly tidal palaeoenvironment
1971		Heavy mineral deposits in the Waterberg basin
1972a		Geology and geochemistry of the south eastern Waterberg
1972b		Heavy mineral deposits in the Waterberg Group
1972c		
1969	Meinster	Waterberg bedding and cross-bedding
1970a		Deformed cross-bedding in the Swaershoek Formation
1970b		Geology between Matlabas and Buffelsdrift
1971		Geology between Heuningfontein and the Makapansberge
1972		Geology of Gatkop, near Thabazimbi
1975		Structures at Gatkop
1975	**Meinster and Tickell**	**Aeolian deposits in the Makgabeng Formation**
1975	**Tickell**	**Braided river palaeoenvironment proposed for the Mogalakwena Formation**
1971a	De Bruiyn	Geology around Vaalwater
1971b		Geology between Mokamole and Blouberg
1972a		Folded cross-bedding in the Waterberg Group
1972b		Report on Nooitgedacht lead mine
1972a	Du Plessis	Relationship between Waterberg Group and Bushveld Complex
1972b		Geology of the area north-east of Warmbaths
1969	**Jansen**	Structural evolution of the southern Waterberg basin
1970a		Volcanic and sedimentary rocks in the south of the Waterberg basin
1970b		Geology of the Nylstroom area
1975a		Sedimentology and structures of Precambrian basins on the Transvaal craton.
1975b		**Aulacogen model for Soutpansberg Group**
1976		**Geology of the Blouberg area (Waterberg and Soutpansberg groups).**
1982		**Review of all available data. Termination of this period of study.**
1970	Jansen *et al.*	Geology between Thabazimbi and Rankins pass
1972		Waterberg tectonics and sedimentation

Table 1.8: Summary of work on the Waterberg Group undertaken by the Geological Survey of South Africa, 1963-1982 (items in bold are most relevant to this study).

Date	Author(s)	Nature of investigation
1908	Mellor and Trevor	Description of some rocks in the Soutpansberg area, and general impressions regarding structure.
1925	Rogers	Geology and petrography of lavas
1931	Janisch	Notes on Fundudzi Lake
1938	Taljaard	Physiographic description
1939	Kent	Description of a copper occurrence on Bosch 407
1955	Van Eeden *et al.*	Explanation of Sheet 42 (Soutpansberg) Geological Survey.

Table 1.9: Summary of early work on the Soutpansberg Group, 1908-1955.

CHAPTER 2: PRE-BLOUBERG, WATERBERG AND SOUTPANSBERG ROCKS.

The lithologies which pre-date the Blouberg, Waterberg and Soutpansberg Group rocks generally outcrop at relatively low altitudes amongst the lower slopes of Blouberg mountain, and more rarely outcrop on the flat-lying terrain to the north and south of Blouberg (Appendix 1). At areas around 23°06.20'S; 29°00.50'E, these rocks underlie areas of relatively high altitude (locally up to 1500m), immediately to the north of the southern strand of the Melinda Fault. Rarely, outcrops of these rocks can also be found in the low-lying area to the east of the Makgabeng plateau, though these lie outside the study area. Generally these rocks consist of a well foliated quartzo-feldspathic gneiss (Fig. 2.1) which can be considered to be a basement complex to the overlying non-metamorphosed or low-grade strata in the field area.

A photomicrograph of a typical gneiss in the field area is shown in Figure 2.2, and shows that minor biotite is also present in addition to quartz and feldspar, which is commonly developed along foliation planes. Amphibolite lenses are also well developed in many areas, with the long axis of the lenses orientated parallel to the strike of the foliation plane (Figure. 2.1). The length of the lenses varies from 10cm to several metres, and can be 2 to 3m wide. A thin section from an amphibolite lens is shown in Figure 2.3, which shows intergrown amphibole, feldspar and quartz. Generally quartz is rare in these amphibolitic rocks.

The feldspar- and amphibolite-rich basement rocks generally weather easily to produce a thick soil, and as a result outcrops of these rocks are rare in the study area, and measurements relating to their structural geology can only rarely be recorded. Outcrops are generally limited to stream beds where weathered material is commonly eroded resulting in fresh surfaces being exposed.

The orientations of foliation planes recorded in basement gneiss throughout the field area are shown in Figure 2.4, which indicates that the foliation planes generally dip vertically to sub-vertically, and generally strike W.S.W. to E.N.E. In many locations (e.g. 23°05.12'S; 29°01.93'E) the sense of shearing within the gneiss can be determined. W.S.W.-E.N.E. -trending boudins formed between the foliated layers (Figure 2.5) indicate shearing in this orientation, and vertically plunging asymmetric 'S' folds suggest sinistral strike-slip movement along an 080° striking, vertically dipping shear zone (Figures 2.6 and 2.7) The orientation of foliation planes in 'S'-shaped folded gneiss are shown in Figure 2.8., which indicates their vertical fold axis. A sinistral sense of movement within the gneiss can also be gained from stair-stepping porphyroclasts (as defined by Passchier and Trouw, 1998) (Figure 2.1). Figure 2.9 shows evidence for multiple deformation: An asymmetric 'S' fold (indicating sinistral movement along an 070°-striking shear zone) is displaced 30 cm by a 080° striking dextral ductile shear zone. Generally, the orientation of foliation planes recorded in the outcrops of gneiss suggests that the foliation is fairly consistent throughout the study area. Due to the paucity of outcrops of basement lithologies, it was not possible to identify any regional variation or discrete domains of specific foliation orientation within the gneiss.

Locally, however, the orientation of foliation planes differs due to folding (Figure 2.6), partial melting, injection of melt or interference folding (Figure 2.10) or due to super-imposed multiple generations of ductile deformation. A large-scale map showing the strike of sub-vertically and vertically dipping foliation planes in basement gneiss at 23°05.21'S, 28°47.53'E, in a stream bed 1km west of My Darling (23°05.21'S; 28°47.53'E) is shown in Figure 2.11. This map, which is divided into a grid of $5m^2$, shows that foliation orientation also varies over a larger scale. Figure 2.11 shows that at least two orientations of foliations are developed in the My Darling area (D_1 and D_2), with evidence locally for the presence of a third (D_3). An earlier sinistral shear zone (D_1) strikes approximately N.E.-S.W., and is subsequently deformed by a secondary cross-cutting shear zone (D_3) which strikes approximately east-west. Drag folding of primary foliation (S_1) along the edges of secondary shear zones (e.g. grid square F/12 in Figure 2.11) can be interpreted to have formed during dextral shearing along the secondary shear

zones. Secondary foliation (S_2) is best developed within a c. 5m wide shear zone in grid squares F/13 and E/14 (Figure 2.11). Evidence can also be seen for locally developed N.W.-S.E.-trending tertiary shear zones (D_3) , which cross-cut secondary foliation planes in grid squares F/6 and F/7. Generally tertiary shear zones also appear to have a dextral displacement, and are sub-parallel to the secondary shear zones. Shear zones cutting primary foliation in grid squares B/9 and B/10 (Figure 2.12) may be either secondary or tertiary. Rose histograms of the strike of foliations in primary and secondary shear zones are provided in Figure 2.13, and show that primary foliation planes dominantly strike N.E. to S.W., whilst secondary foliation planes dominantly strike east-west.

In contrast to the foliated gneiss described above, where distinct banding is visible between the segregated mineral layers, many of the outcrops which have been previously mapped as basement gneiss (e.g. Jansen, 1976; Geological Survey, 1985) differ locally. Rocks which outcrop against along the southern side of Blouberg mountain, and are adjacent to the inferred position of the southern strand of the Melinda Fault Zone (Appendix 1) differ from the common crystalline quartzo-feldspathic and amphibolitic gneiss in the field area. These rocks are more granular, and generally friable when weathered (Figure 2.14), and lack amphibolite-rich layers which are characteristics of the gneiss elsewhere in the field area. Locally, the rocks closely resemble a crush microbreccia (using the classification scheme of fault rocks of Roering *et al.*, 1989). They are, however, generally intruded by narrow (3-4mm) quartz-filled veins (Figure 2.15). Though this rock proved too friable for thin section analysis, such veins may also be locally found intruding the foliated basement gneiss adjacent to the edge of the southern strand of the Melinda Fault, such as that shown in thin section in Figure 2.16. Figure 2.16 shows that the vein quartz is relatively undeformed compared to the neighbouring crystals of quartz and feldspar within the gneiss. The orientation of the pervasive quartz veins in the microbreccias and gneiss are shown in Figure 2.17, which have a comparable orientation to the foliation of the gneiss not affected by quartz veining shown in Figure 2.4. The resemblance of the geometry of veins intrusive within the microbreccia to the foliation in the gneiss may have led earlier workers (e.g. Jansen, 1976; Geological Survey, 1985) to have mapped the veined microbreccia as a foliated gneiss. However, the

differences between these two lithologies suggest that a different mechanism was responsible for the veined microbreccia to that of the banded gneiss. The mechanism responsible for such microbreccia is likely to have been faulting under brittle conditions, in comparison to the highly ductile conditions under which banded, foliated gneiss is likely to have formed. As such, many of the rocks previously mapped as basement gneiss should rather be considered as younger faults and will be considered further in Chapter 7 (map relationships and structural geology).

The contact between the basement gneiss or crush breccia of the southern strand of the Melinda Fault and the overlying strata of the Blouberg Formation is locally marked by the presence of a dark red or brown hydrothermally altered rock containing ubiquitous jasper and quartz veins (Figure 2.18). These hydrothermally altered zones may locally reach a thickness of around 5m.

In addition to the crush-breccia described above, other examples of subsequent brittle structures affecting basement rocks were only rarely recorded. Locally slickensides and evidence for thrust faulting can be found within basement rocks, and these are described more fully in Section 7.1. The general paucity of evidence for brittle reactivation in basement rocks may be explained by the fact that the constituent minerals of basement rocks can be readily weathered (e.g. feldspar and amphibolites), and by the friability of brittle structures, which leads to increased rates of erosion. Brittle structures in basement rocks are therefore likely to form negative relief, and so it is unlikely that these structures will crop out and be recorded.

Figure 2.1: Quartzo-feldspathic banded gneiss with dark amphibolite lenses, exhibiting vertically-dipping, 080°-striking foliation. Sub-euhedral feldspar porphyroclasts show stair-stepping, and suggest sinistral movement along the foliation plane. Compass is 6cm wide, and points north. Recorded at 23°05.40'S; 29°01.53'E.

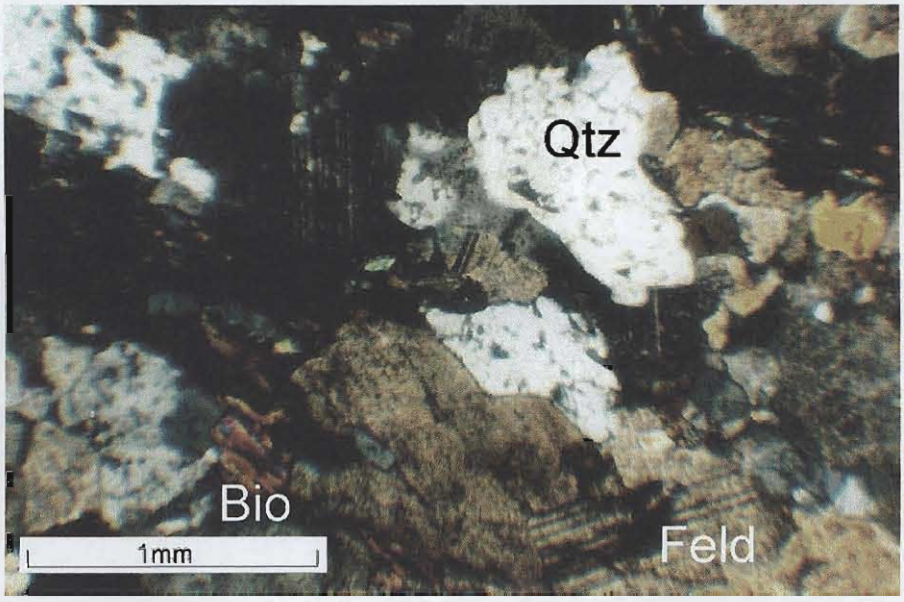

Figure 2.2: Photomicrograph of a thin section of basement gneiss. Constituent minerals are quartz, feldspar and minor biotite.

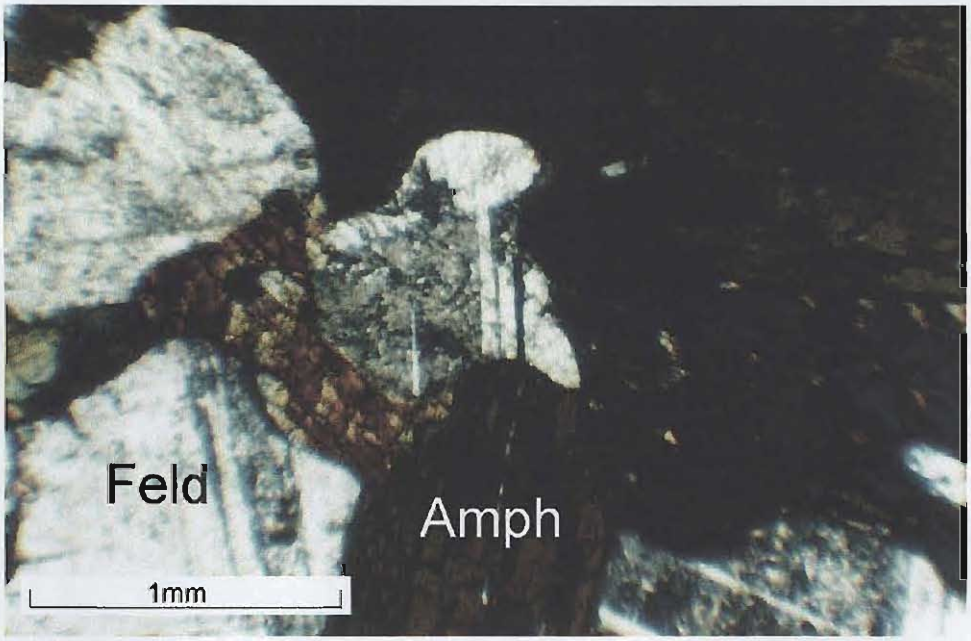

Figure 2.3: Photomicrograph of a thin section from an amphibolite lens in banded gneiss. Constituent minerals are amphibole and feldspar.

Figure 2.5: Banded gneiss at 23°05.12'S: 29°01.53'E, which shows a 080°-striking foliation, exhibiting boudinage of competent quartzo-feldspathic layers within the less competent amphibolite-rich layers. A 4cm-wide pegmatite vein cuts the outcrop. Compass is 6cm wide, and is orientated towards the north.

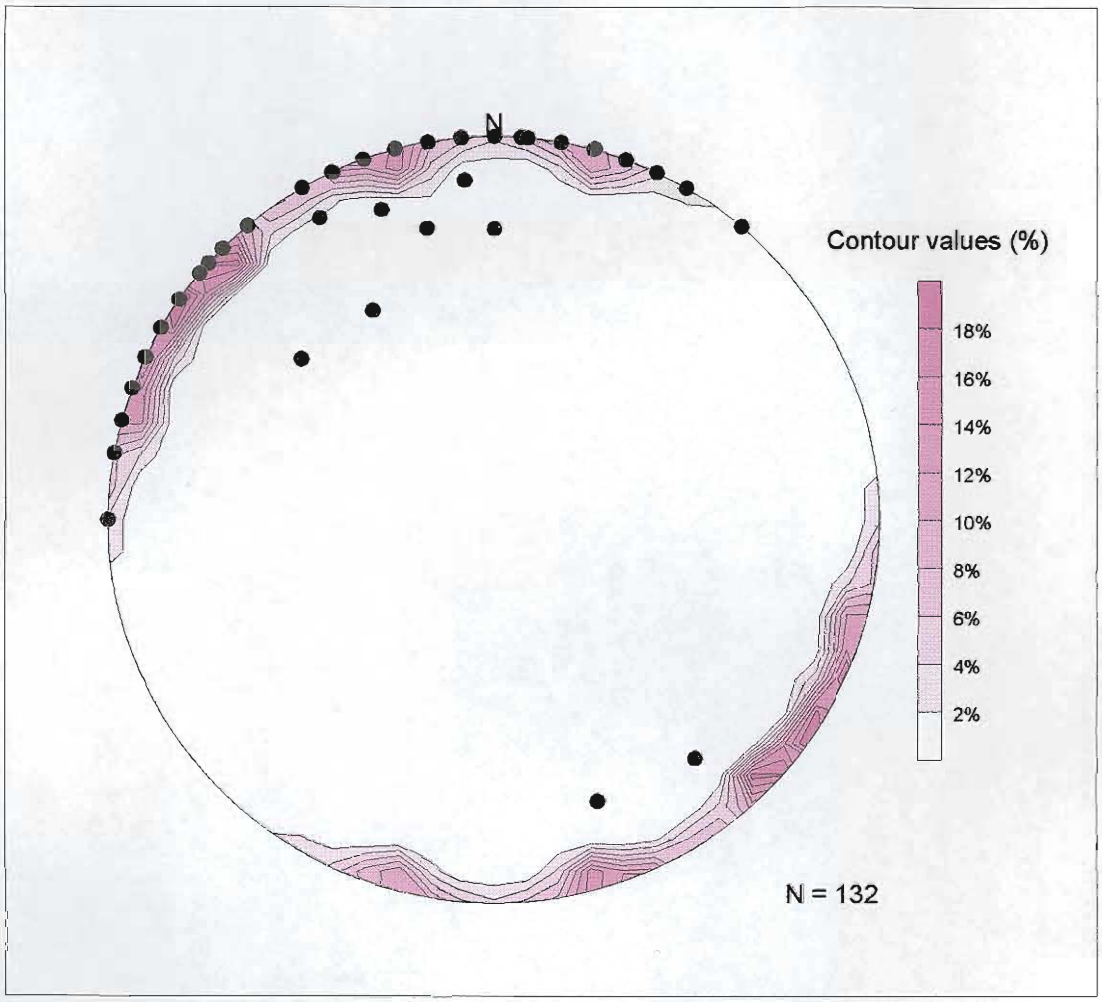

Figure 2.4: Stereographic projection showing the poles of generally vertically-dipping foliation planes recorded in basement gneiss.

Figure 2.6: Local variation in the orientation of foliation planes in the basement gneiss. 'S'-shaped folding of vertically-dipping foliation planes suggests sinistral strike-slip movement. Compass is 6cm wide, and points north. Recorded at 23°06.19'S; 29°00.46'E.

Figure 2.7: An approximately 080°-striking foliation exhibits vertically-plunging folds with asymmetric 'S'-shaped folds, indicative of a sinistral sense of movement. Compass is 6cm wide, and points north. Recorded at 23°05.12'S; 29°01.93'E.

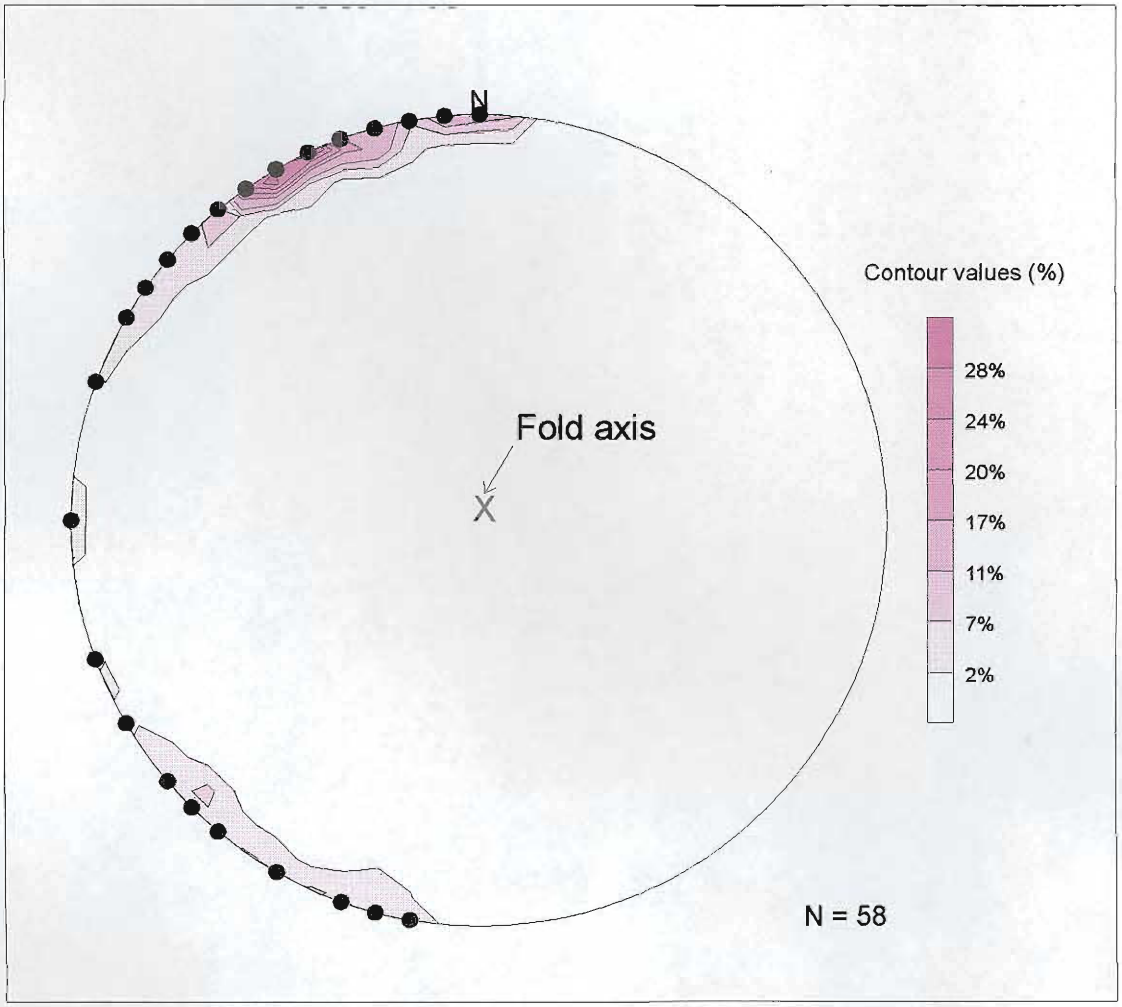

Figure 2.8: Stereographic projection showing poles of foliation planes in 'S' folded basement gneiss.

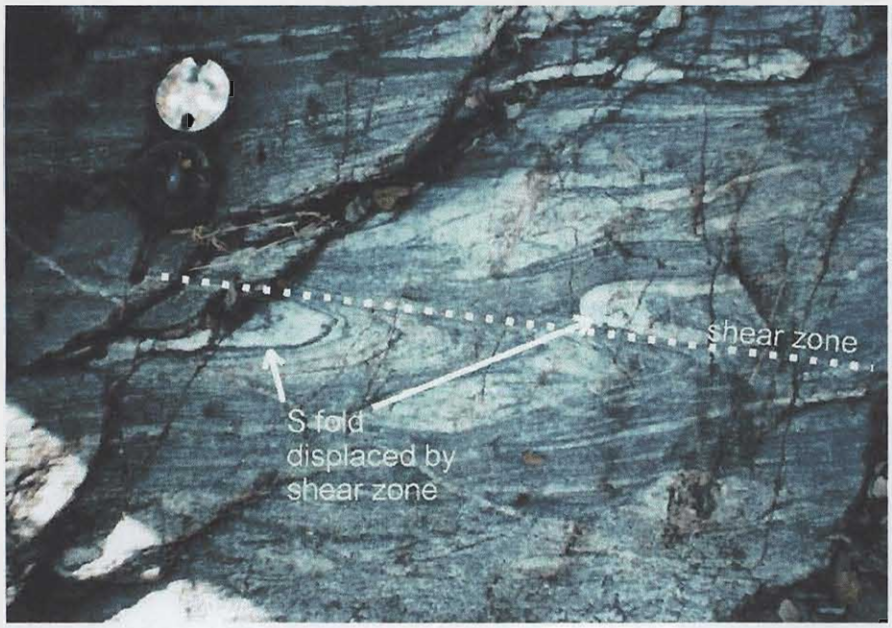

Figure 2.9: A primary foliation, which strikes 042° and shows asymmetric 'S' folds with a vertical plunge is cross-cut by a younger dextral shear zone which strikes 122°. Recorded at 23°05.12'S; 29°01.93'E. Compass is 6cm wide, and points north.

Figure 2.10: Poorly defined foliation in basement gneiss at 23°04.82'S; 28°54.67'E, caused by either partial melting, interferance folding or by injection of melt. Compass is 7 cm wide.

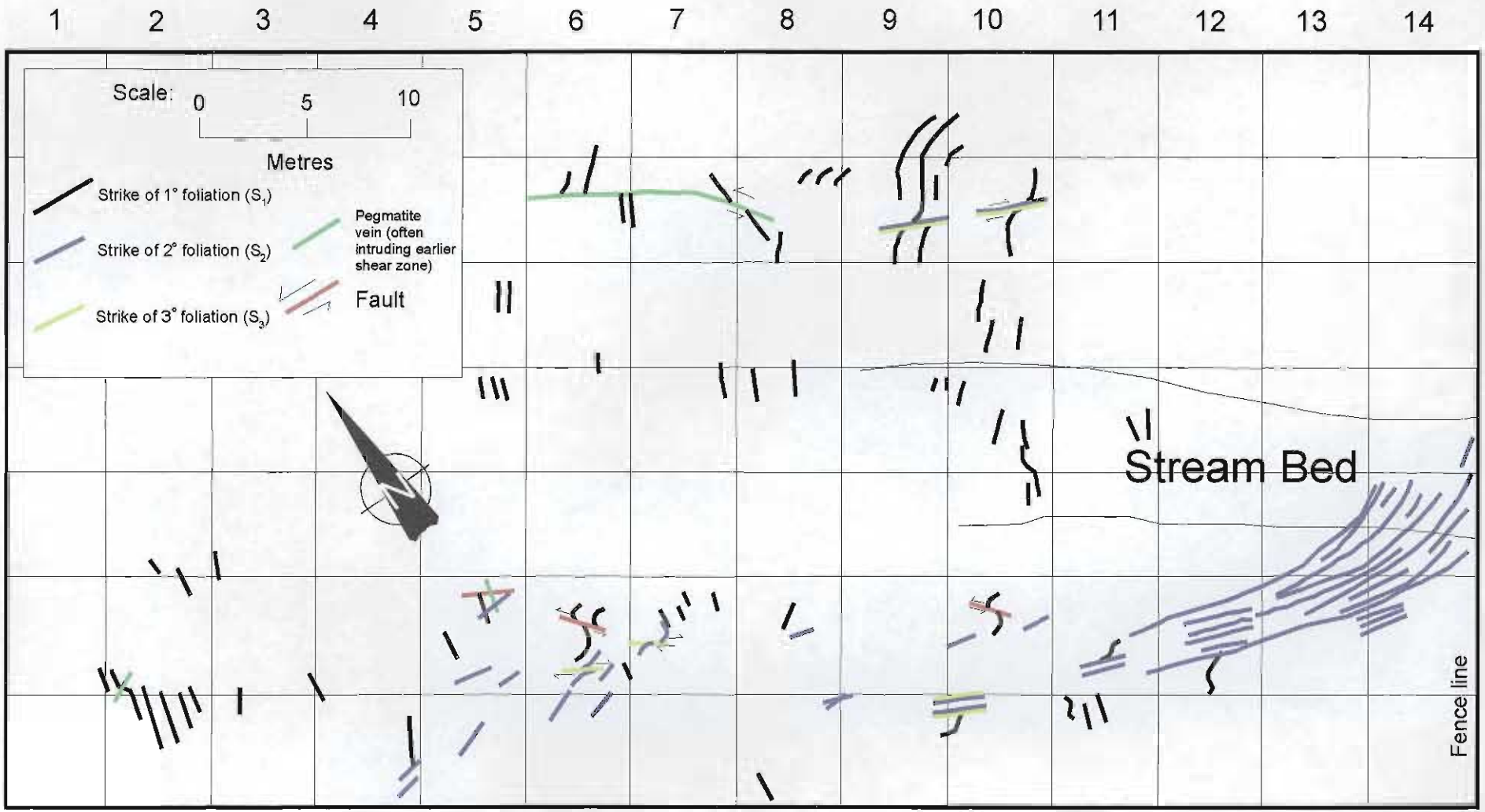

Figure 2.11: Map showing the strike of foliation planes at My Darling (23°05.21'S; 28°47.53'E).

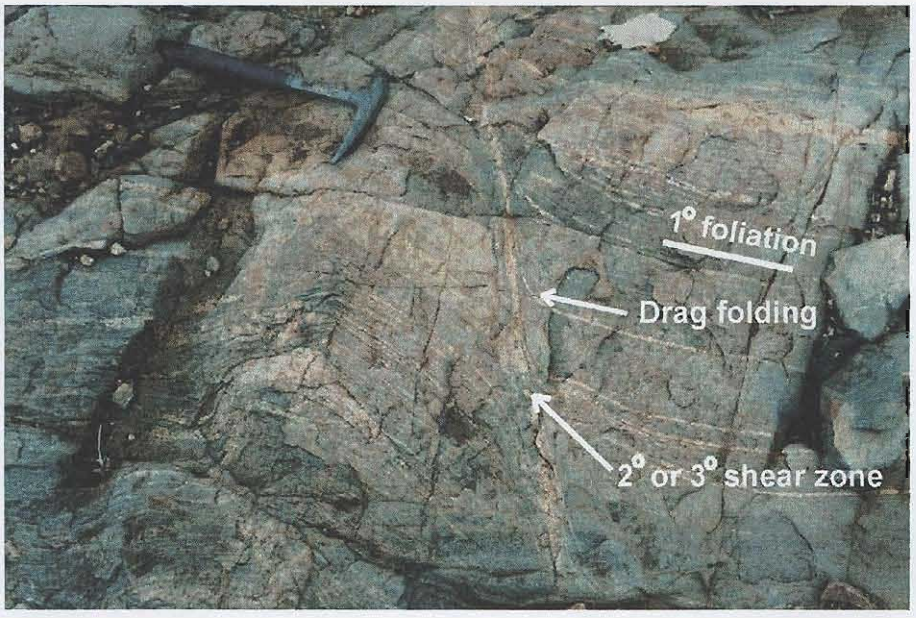

Figure 2.12: Photograph showing detail of grid-square B/10 in Figure 2.11. A primary foliation plane strikes 045°, and is displaced by a secondary or tertiary shear zone, which strikes 115°. Drag folding of the primary foliation suggests that the dextral movement along the later (S_2 or S_3) foliation plane. Hammer is 30cm long.

Figure 2.14: Friable crush breccia from 23°07.39'S; 28°57.46'E, at the southern strand of the Melinda Fault. Lens cap is 5cm wide.

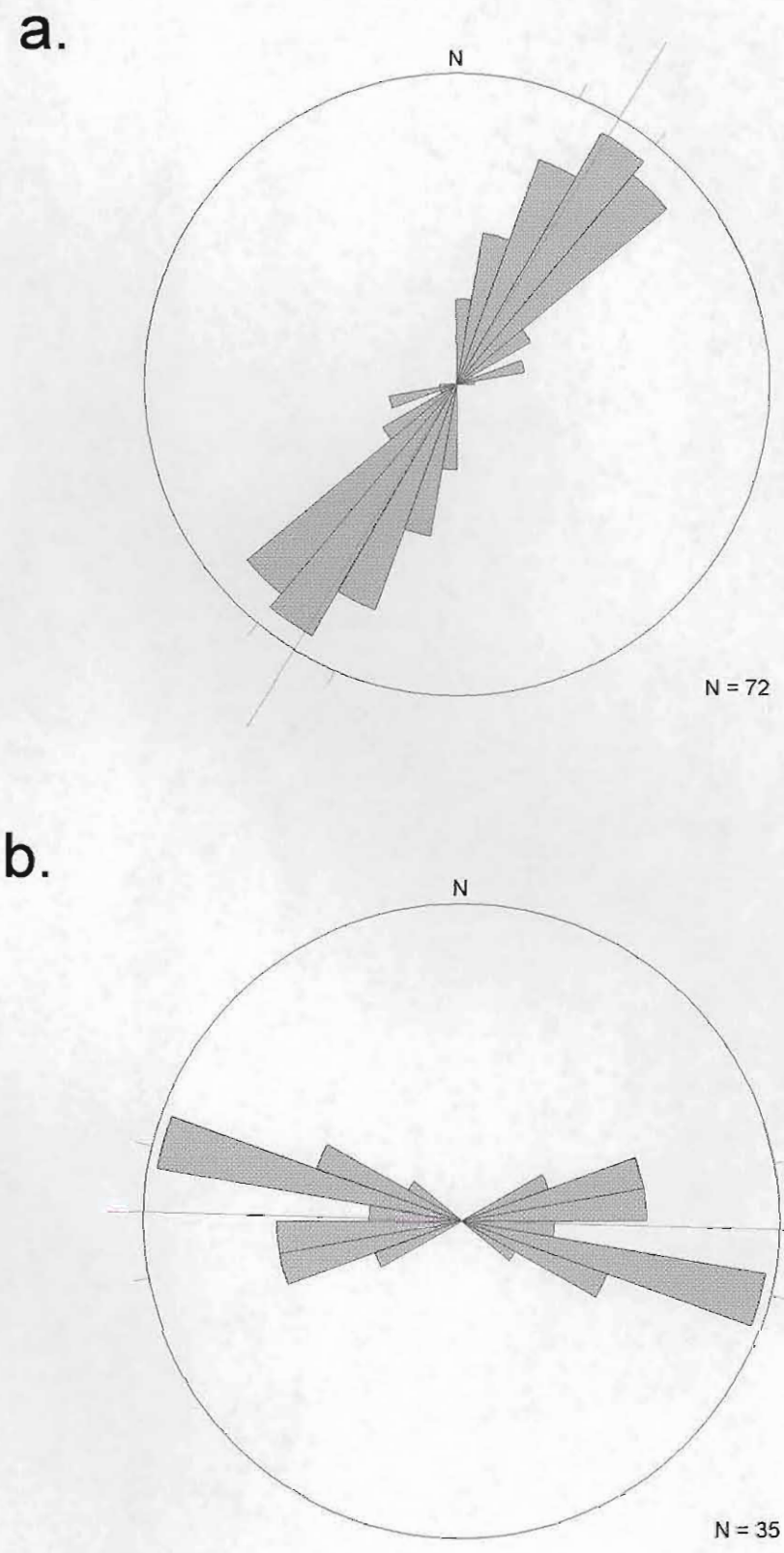

Figure 2.13: Rose histograms showing the strike of (a.) Primary and (b.) Secondary foliation planes in banded gneiss close to My Darling. Principal direction (vector mean) is shown.

Figure 2.15: Crush breccia intruded by thin quartz-filled veins, from 23°07.39'S; 28°57.46'E at the southern strand of the Melinda Fault. Lens cap is 5cm wide.

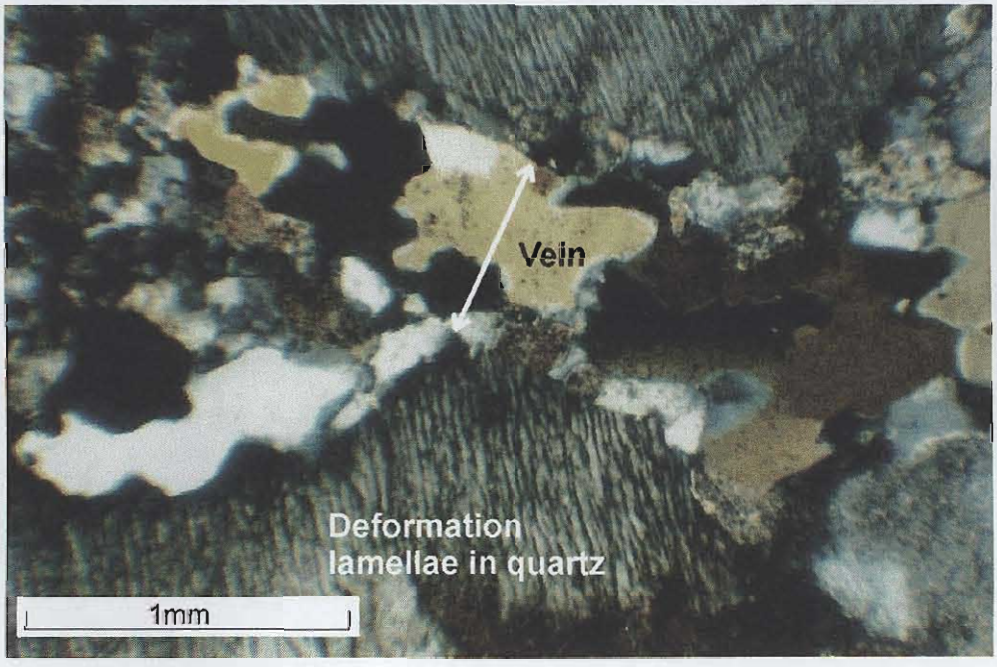

Figure 2.16: Photomicrograph of quarts veins intruding quartzo-feldspathic gneiss at 23°06.31'S; 29°01.16'E. Note that the vein quartz is undeformed compared to deformation lamellae in neighbouring quartz crystals in the gneiss.

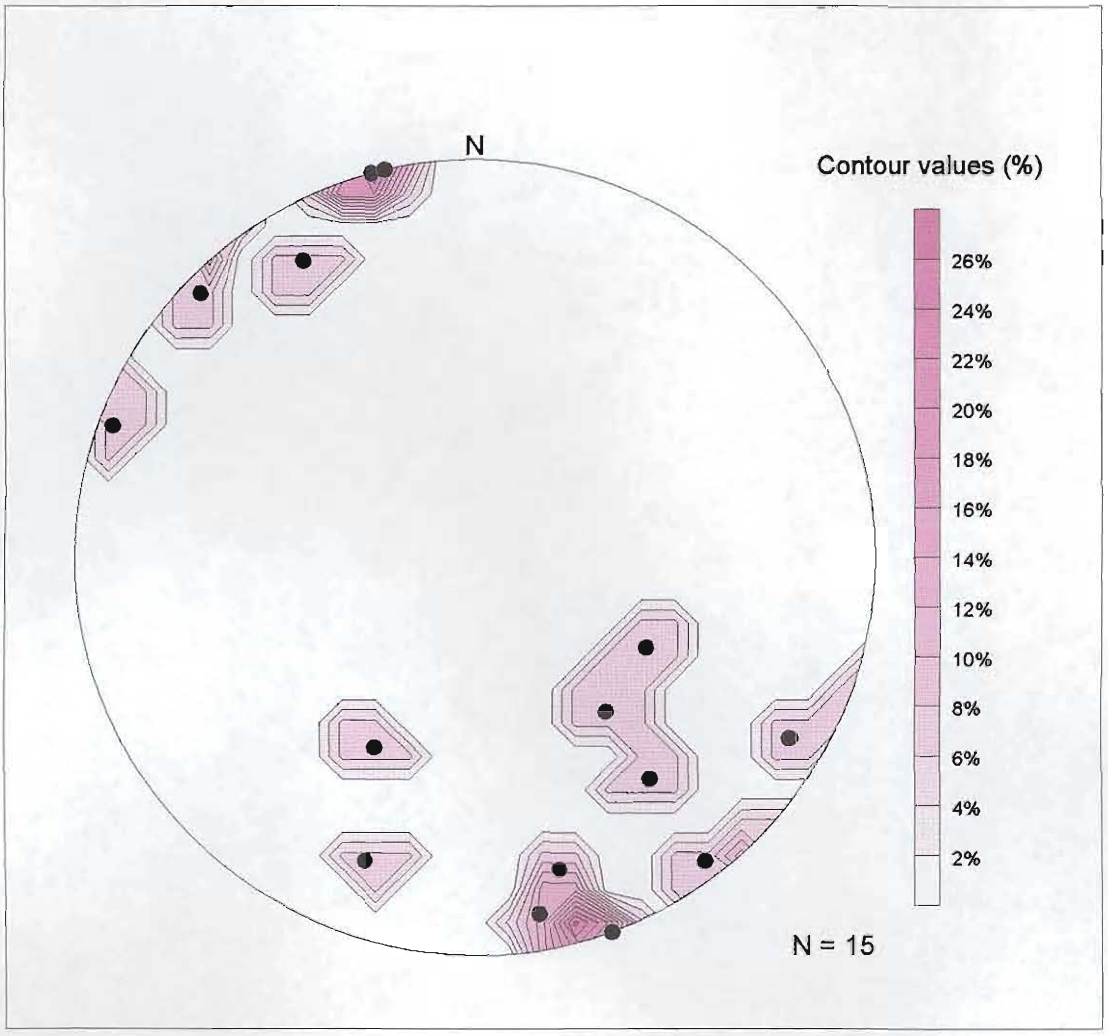

Figure 2.17: Stereographic projection showing the poles to planes defined by quartz-filled veins cutting fault rocks along the southern strand of the Melinda Fault Zone.

Figure 2.18: Hydrothermally altered rock from the contact between the southern strand of the Melinda Fault and the Blouberg Formation at 23°07.39'S; 28°57.46'E. Lens cap is 5cm wide.

CHAPTER 3: THE BLOUBERG FORMATION.

3.1: Introduction:

This chapter includes field data collected from the Blouberg Formation, which outcrops generally on the lower southern slopes of Blouberg mountain south of the southern strand of the Melinda Fault (Appendix 1), and also approximately 25 km west of Blouberg mountain, on the farm Kranskop 278 LR (23°09'S; 28°42'E to 23°09'S; 28°41'E: Appendix 1). The siliciclastic rocks which underlie the northern foothills of Blouberg mountain and which occur on the northern side of the southern strand of the Melinda Fault (Appendix 1), named the Mositone Conglomerate, Varedig Sandstone and Semaoko Grit members by Jansen (1976) (also named the Lebu Complex by Meinster, 1977), are considered in Chapter 4 (Waterberg Group). The volcanic rocks west of Blouberg mountain, named the My Darling Trachyandesite Member of the Blouberg Formation by Jansen (1976) (also part of the Meinster's (1977) Lebu Complex), are considered in Chapter 5 (Soutpansberg Group). The correlations used during this work are presented in Table 8.1.

The outcrops of the Blouberg Formation which occur south of the southern strand of the Melinda Fault (Appendix 1) are generally less than 300m thick. In contrast, in the area between 23°09'S; 28°42'E and 23°09'S; 28°41'E (Appendix 1), on the farm Kranskop 278 LR, a 1400m-thick sequence of Blouberg sediment is preserved, consisting of vertically dipping, north-striking beds exposed in a westwards-trending streambed. This Blouberg succession can be followed from its nonconformable relationship with the basement gneiss at 23°09.01'S; 28°42.01'E, until it is unconformably overlain by the basal conglomerate beds of the Mogalakwena Formation at 23°09.12'S; 28°41.23'E (Appendix 1). This section is thought to represent the most complete record of the Blouberg strata, as it is considerably thicker than any of the outcrops of the Blouberg Formation further to the east. It is thus presented here as the provisional type section of the Blouberg Formation. The extent of the outcrop, which is generally restricted to within the bounds of the stream bed is, however, not suitable for establishing lateral dimensions of architectural elements or any lateral facies variation.

3.2: Description of Type Section of Blouberg Formation:

The Blouberg Formation at the Kranskop type locality is composed of an entirely clastic succession of sedimentary rocks, which are shown in a partially complete sedimentary profile in Figure 3.1. Figure 3.1 shows that the lower part of the Blouberg succession (0m to 675m) is dominated by medium- to coarse-grained sandstone and granulestone, according to terminology for grain size classification on the Udden-Wentworth scale (Wentworth, 1922). This nomenclature will be used to describe sedimentary rocks throughout this work, and medium-grained sandstones are defined as those composed of grains with a diameter between 250 and 500μm. Coarse-grained sandstones have grains between 500μm and 1mm, and granulestones have grains between 2 and 4mm. The upper part of the succession (from 675m to 1400m) is largely conglomeratic, with only minor sandstone and granulestone deposits. Clasts within the upper part of the Blouberg Formation are classified as pebbles and cobbles under the Udden-Wentworth scale, where pebbles are of a clast size between 4 and 64mm, cobbles between 64 and 256mm, and boulders are larger than 256mm. These sedimentary rocks of the Blouberg Formation will be described (in order from bottom to top) in the following section, in terms of architectural elements, facies associations and sedimentary facies.

3.2.1: Architectural elements:

Miall (1985) proposed a system for the classification of fluvial sediments, whereby all fluvial deposits are interpreted as being composed of varying proportions of eight *architectural elements*. This system will be used to classify all fluvial deposits considered in this work (Blouberg, Mogalakwena and Wyllies Poort Formations; Section 8.2). Other workers have broadened the application of architectural elements to other palaeoenvironments, such as shallow marine and fan-delta deposits (e.g., Tirsgaard, 1993; Eriksson *et al.*, 1995). An architectural element is defined as a three-dimensional lithosome, for which bounding surfaces, scale, internal lithofacies (and lithofacies associations), and external geometry are defined (Miall, 1985). The eight architectural elements proposed by Miall (1985) are each made up of a certain combination of facies

associations, which are, in turn, made up of combinations of individual facies (Miall, 1985). The architectural elements for fluvial deposits and their symbols are shown in Table 3.1, together with the symbols for facies classification (Miall, 1978).

Of particular importance in the discrimination of architectural elements is the concept of external geometry. In order to correctly identify the external geometry of an element, its bounding surfaces must be recognised, and in order to fulfil this, outcrops must be present which are sufficiently large, so that the bounding surfaces can be traced over a distance, in order to determine the three-dimensional geometry of the element under investigation (Miall, 1985). The larger the scale of the element, then the larger the size of the outcrop necessary for satisfactory definition of the architectural element. In the Kranskop section, it was difficult to accurately determine the three-dimensional external geometry of the deposits, as only a vertical profile through the sedimentary succession (vertically dipping beds exposed in the essentially horizontal stream bed) was afforded in the area. With the absence of data from the third dimension, and with the vertical profile limited to the width of the stream bed (usually between two and five metres) it was impossible to accurately assess the type of architectural element present, although individual facies and facies associations could still be readily determined.

3.2.2: Facies and Facies Associations:

The term 'facies' as used in this work is defined as a particular set of sediment characteristics, and includes a description of attributes such as lithology, texture, colour, sedimentary structures and palaeocurrent direction. Throughout the vertical section of the Blouberg Formation at Kranskop, a variety of sedimentary facies could be identified, which could be grouped into 4 discrete facies associations within the Formation (Figure 3.1). The sedimentary rocks are usually purplish in colour (red beds), though many beds and cross-beds are creamy-white, presumably where certain horizons have been permeable to circulating reducing fluids (Figure 3.2). In general, the rocks within the Kranskop section are weathered and friable, and cannot be easily sectioned for microscopic analysis. However collected rubble from the Kranskop section can be sectioned after being set in resin.

The lowermost part of the succession consists predominantly of facies of trough and locally planar cross-bedded medium- to coarse-grained sandstone (*Sp* and *St* in Miall's [1985] scheme; Table 3.1), with wedge-shaped sets. These sets vary in set thickness between 15cm and 50cm (Figure 3.2). A third facies also present comprises pebbly granulestones, generally with clasts with long axes smaller than 7cm (Figure 3.3) which commonly occurs as a trough cross-bedded channel-fill (Facies code: Gt; Table 3.1). Channel-fills vary in size between 1.5m and 4m wide, and are generally 15-20cm deep (Figure 3.3). These three facies can be considered together as facies association 1, which reaches a thickness of approximately 300m above the basement nonconformity in the Kranskop section (Figure 3.1). Prepared sections (Figure 3.4), show that, mineralogically, the rocks of facies association 1 are immature and poorly sorted, and contain, on average (300 points from 1 thin section) 43% quartz, 33 % matrix (clays), 21% lithic fragments (mainly quartzite), and 3% muscovite. Grains are sub-rounded to sub-angular, and of generally low sphericity. Given the general immaturity of the sediment, it is likely that feldspars, now weathered, were initially also present, and are represented by areas in photomicrographs where clay patches are prevalent. Quartz pebbles in channel-fills are generally angular to sub-rounded and poorly sorted (Figure 3.3). Large sub-euhedral feldspar crystals are also present amongst the pebbly granulestones of the channel-fills (Figure 3.5). These matrix-supported pebbly granulestones have an orthoclase-rich granule-sized interclast material.

Between 300m and 650m, a second facies association is defined. Facies association 2 consists of coarse and very coarse sandstone- and granulestone-filled channel forms (Gt: Table 3.1) (Figure 3.6), within which planar and trough cross-bedding (Sp and St) of medium set thickness (c.20-30cm), and small (<20cm) set thickness occur (Figure 3.7). Planar-bedded sandstone also occurs locally (Figure 3.1). Generally the channel-fills are less granule- and pebble-rich than those in facies association 1. These facies are arranged cyclically to produce individual fining-up sequences which are typically 70cm in thickness, with the lowermost c. 30cm being composed of granulestone-fill (Figure 3.6). There is also an overall fining-upwards trend displayed by this facies association as a whole, so that towards the top, pebble lag deposits and granulestones become less

common as set thicknesses decrease concomitantly upwards (Figure 3.7). Locally, evidence for soft-sediment deformation can be seen (Figure 3.8). Thin sections prepared from samples from facies association 2 show that the rock is comprised, on average (300 points from 1 thin section) 45% quartz, 24% matrix (=clay, probably replacing orthoclase), 24% lithic fragments (mainly quartzite) and 7% muscovite (Figure 3.9). Sorting and grain shapes are comparable with those of facies association 1.

Between 650 and 675m above the basement nonconformity there is a sudden change in sedimentary facies within the Blouberg Formation (Figure 3.1). The medium- to coarse-grained sandstones with small sets of cross-bedding found in the uppermost portion of facies association 2 are overlain by coarse, matrix-supported conglomerate and breccia. Unfortunately the contact between facies associations 2 and 3 is not exposed in the field (Figure 3.1).

From 675m to 925m (Figure 3.1) facies association 3 is comprised of three facies: bedded, cross-bedded and massive matrix-supported conglomerate, composed of angular feldspathic clasts (pebbles, cobbles and, rarely boulders), and sub-rounded to rounded quartz cobbles (Figures 3.10 and 3.11)(Facies code Gmg; Table 3.1). These large feldspar clasts, which generally range in size from 2cm to 25cm diameter, consist of orthoclase derived from the basement gneisses and have sub-rounded shapes with low sphericity (Figure 3.10); they occur within an arkosic granulestone matrix (Figure 3.11), and can only rarely be seen to be imbricated. Generally, conglomerates are arranged in fining-upwards cycles. Each cycle, which is typically between 50 and 100cm thick, is topped by a fourth facies, comprising small channel forms between 10 and 35cm thick, filled with trough cross-bedded coarse arkosic sandstone (Figures 3.12 and 3.13). Thin sections prepared from interclast material in the conglomerate shows that this portion of the rock is composed, on average, of 38% quartz granules, 34% matrix (=clay), 24% lithic fragments, 2% muscovite and 2% feldspar (100 points from 1 thin section)(Figure 3.14).

From 925m to the top of the succession (1400m), the fourth facies association is also composed of matrix-supported massive, bedded and cross-bedded conglomerate, and is thus similar to facies association 3, except that channel forms appear to be laterally more

extensive, and may, instead, represent laterally extensive sandstone lenses or even sheets (it is generally difficult to establish the extent of this facies on account of the narrow width of river section). These wide channel forms/sandstone sheets are found between conglomerate beds, and contrast with the narrow sandstone-filled channel forms of facies association 3 (Figure 3.15). Red-coloured sandstone clasts can also be found locally in the conglomerate.

The similarity between facies associations 1 and 2 suggests that they should be considered together as an individual, lower member of the Blouberg Formation. The similarity between facies associations 3 and 4, and the dissimilarity between these and the lower facies associations, suggest that they should be considered together as a separate upper member. The lithological contrast between the Lower (sandy) and Upper (conglomeratic) members of the Blouberg Formation is strong, and each member can be readily distinguished in the field.

Having identified a general two-member stratigraphy for the Blouberg Formation from the 1400m Kranskop vertical profile, in the next section other outcrops of the Blouberg Formation from further east will be considered in terms of this apparent type stratigraphy.

3.3: Blouberg Formation in the area of Blouberg mountain:

There is a considerable distance (about 25km) between the Kranskop outcrop of the Blouberg Formation and the outcrops surrounding Blouberg mountain, in which no Blouberg strata are preserved. Nevertheless, outcrops on the southern side of the mountain, which lie south of the southern strand of the Melinda Fault, appear to correlate reasonably well with the Blouberg strata from the Kranskop section. Outcrop is more often exposed in three-dimensions in the Blouberg area than in the Kranskop area, due to the less-steeply orientated dip, and greater topographical relief (Appendix 1).

Despite the fact that three-dimensional outcrop is better in this area, the size of outcrops is, again, insufficient for establishing architectural elements. However, facies and facies associations could readily be recognised. The most westerly outcrops of the Blouberg

Formation in the Blouberg area occur around 23°08.02'S; 28°55.16'E. Generally the outcrop here is quite weathered, and the angle of dip of the bedding is matched by the south-facing slope of the hillside, so the outcrop exposes only about 10m of vertical section. The lithology is characterised by purple and cream coloured coarse sandstone and granulestone, with trough and planar cross-beds. Channel forms filled with small rounded quartz pebbles, with a maximum diameter of 3cm, and angular feldspathic clasts (5-10cm diameter) (Figure 3.16) are locally developed, and reach a maximum of 5m width, 55cm depth. The characteristics observed from this Blouberg Formation locality compare favourably with facies association 1 from the Kranskop section (Lower Member).

Between 23°06.80'S; 28°58.50'E and 23°08.00'S; 28°56.50'E (on the farm Buffelshoek 261LR) an almost continuous ridge runs approximately east-west, which is comprised of the Blouberg Formation, exposed in steeply dipping to slightly overturned rocks. The outcrop may continue further along the ridge to the west as far as 23°08.00'S; 28°55.50'E, though it is covered by talus derived from the Wyllies Poort Formation above. The approximate base of the steeply southwards-dipping Blouberg Formation can be gauged by the presence of basement rocks on the northern side of the ridge, which are nonconformably overlain by the Blouberg Formation. Often this nonconformity is marked by the presence of jasperitic, hydrothermally altered rocks (Chapter 2; Figure 2.17). The total thickness of exposed Blouberg strata along this ridge is less than 300m. The lithology consists of coarse-grained sandstone and granulestone, often with rounded quartz pebbles and cobbles, and sub-angular to angular feldspar grains up to 1cm in diameter (Figure 3.17). Locally cobbles of foliated gneiss are also present (Figure 3.18). Quartz cobbles often exceed 10cm in diameter (Figure 3.19). Generally planar and trough cross-bedded sandstones (Sp and St) are common facies in this area, though channel-fills seem to be absent.

Cross-bedding is often preserved in sets of 30-50cm (Figure 3.20), which build fining-upwards pebbly sandstone cycles. Rounded quartz cobbles often occur on the bedding plane at the base of the set, though they may also occur in foresets (Figure 3.21). Foresets are generally comprised of coarse sandstone and granulestones, which may grade up into

medium-grained sandstone on top-most foresets. Point counting of thin sections of Blouberg rocks from this area show that, on average (500 points per section, 2 sections), rocks are composed of 38% quartz, 35% lithic fragments, 24% matrix (=clay), and 3% feldspar and opaques combined (Figure 3.22). Generally the lithology of the rocks seems to bear much in common with facies association 1 (Lower Member) of the Kranskop section.

Continuing eastwards, the next good outcrop of the Blouberg Formation occurs at 23°06.80'S; 28°59.40'E, on the farm Beauley 260 LR. Again, this consists of steeply dipping to overturned Blouberg strata. Trough and planar cross-bedded medium- to coarse-grained sandstone, containing some heavy mineral drapes on foresets is the common lithology, and this locally exhibits soft-sediment deformation. Pebble- and cobble-sized clasts are conspicuously absent (Figure 3.23). Towards the northern edge of this outcrop (i.e. towards the base of the Blouberg Formation), a c.1m-thick folded muddy sandstone bed is developed (Figure 3.24). The stratigraphic position within the Blouberg Formation (i.e. the height above basement) of this outcrop is unknown, as the underlying contact with the basement is not seen. Though the lithology of this outcrop is not exactly comparable with any seen in the Kranskop section, this Beauley outcrop most readily compares with facies association 2 (Lower Member). In contrast to this relatively fine-grained, steeply dipping Blouberg succession, approximately 1km S.E. of this area, at 23°07.22'S; 28°59.91'E, sub-horizontally bedded strata of coarse sandstone and granulestone are found, which locally contain beds which are conglomeratic. The latter consist of feldspathic basement clasts (Figure 3.25), similar to those found in facies associations 3 and 4 (Upper Member) in the Kranskop section.

From the latter outcrop of conglomerate eastwards until 23°07.15'S; 29°03.00'E, a poorly exposed outcrop of Blouberg strata lies beneath cliffs of the Mogalakwena Formation. Generally this outcrop is covered by talus derived from the Mogalakwena Formation above, but rare good exposures suggest that the sub-horizontal strata (of coarse sandstone and granulestone) contain trough cross-bedding, with preserved set thickness of about 50cm – 1m. Locally rounded quartz pebbles and more angular feldspathic basement clasts can also be found in these coarse sandstones and

granulestones. At 23°07.22'S; 29°01.58'E a good vertical section is exposed on the South-facing hillside, of sub-horizontal Blouberg strata, which is shown in a sedimentary profile in Figure 3.26. The section is comprised of slightly less than 100m of a fairly monotonous sequence of trough cross-bedded medium- to coarse-grained sandstone, with rare channel-fills. The lithology is generally free of granules, though it locally contains quartz and feldspar-rich rock fragments, with clasts up to 8cm in diameter. Again, this facies association compares favourably with facies association 1 (Lower Member) of the Kranskop section.

At 23°06.86'S; 29°02.26'(Farm Dantzig 3LS), on a north facing slope, an outcrop of sub-horizontally bedded matrix-supported conglomerate can be found. The matrix is composed of coarse sandstone and granulestone, and the basement clasts are generally sub-angular and feldspathic, mostly c. 10cm in diameter (Figure 3.27) and commonly contain a foliation. Sub-rounded quartz cobbles of similar dimensions are also common. Bedding and trough cross-bedding is generally visible within these rocks. Locally, clasts of red-coloured sandstone are also present, which vary in diameter from 3 to 8cm. Sand-filled channel forms are developed in this matrix-supported conglomerate, typically around 6m wide, and 60cm deep. Channel forms are filled with trough cross-bedded arkose and feldspathic granulestone and locally contain quartz pebbles. This facies association bears a considerable similarity to facies association 4 (Upper Member) of the Kranskop section. The exposed conglomerates, however, are relatively thin (about 20m), and grade into coarse sandstone and granulestone (similar to the conglomerate matrix and channel-fill beneath) where large clasts are more rare; conglomerates are restricted to channel-fills (preserved channels are typically about 5m wide, 50cm deep). This coarse sandstone with local lenticular conglomerates fines upwards into medium-grained trough cross-bedded sandstone, with set thicknesses, typically, of 50cm. Both the upper and lower margins of this outcrop are marked by intrusions of dolerite sills, so the height within the Blouberg stratigraphy is difficult to determine.

The topography of the area around farm Dantzig 3LS produces an east-west trending valley, flanked to the north and south by ridges. The southern ridge is occupied by previously described sub-horizontal Blouberg sediments, overlain by sub-horizontal

strata of the Mogalakwena Formation (Appendix 1). In contrast, the northern ridge of the Dantzig valley, between 23°06.20'S; 29°01.70'E and 23°06.00'S; 29°02.35'E, is underlain by steeply dipping to overturned strata of the Blouberg Formation. The S.S.E.- and N.N.W.-dipping strata are probably underlain by basement gneiss (the localised presence of jasperitic hydrothermal rocks may be diagnostic of the nonconformity), but the gneiss itself does not outcrop, the area being covered by talus derived from the Wyllies Poort Formation above. The total thickness of Blouberg sedimentary succession exposed here is less than 150m.

The lowermost part of the succession here is composed of 4-6m of reddish-purple, micaceous muddy sandstone and medium-grained sandstone beds, which rapidly grade upwards into coarse arkose, sandstone and granulestone, which dominate the remainder of the succession. Large, sub-rounded quartz pebbles and cobbles occur towards the top, and are absent in the lower parts of the stratigraphy. Rare feldspathic clasts of around 1cm diameter are also present. Generally, the 150m-thick sequence exhibits a coarsening-up character.

The dimensions and style of sedimentary structures also varies with height in the stratigraphy. The lowermost shaley sandstones and sandstones are dominated by small planar cross-bedded sets, between 5 and 10cm in height, which suggest a palaeocurrent direction from west to east. Higher up the succession, large-scale trough cross-beds dominate (Figure 3.28), with granulestone-filled channel forms preserved locally. Set thicknesses of planar cross-beds, which occur locally, are typically between 50 and 180cm (Figure 3.29). Preserved channel forms are typically 4.5m wide, and about 40cm deep, and contain clasts up to 9-10cm in diameter. Thin section analysis of Blouberg Formation rocks from Dantzig shows that, on average, the rocks are composed of 42% quartz, 36% matrix (=clay), 17% lithic fragments (=quartzite), and 4% opaques, feldspar and mica combined (averaged from 2500 counted points, in 5 sections). Palaeocurrent directions gained from trough cross-beds in this location show an average trend towards 260°, almost opposite to the current directions associated with the finer grained sedimentary rocks lower in the succession. Despite considerable differences (i.e. the presence of a muddy sandstone facies, general coarsening-up sequence, and comparably

larger trough cross-bed set thicknesses), this Dantzig outcrop bears some resemblance to facies association 1 of the Kranskop sequence.

All the outcrops described above in the vicinity of Blouberg Mountain underlie areas immediately south of the southern strand of the Melinda Fault. Generally, Blouberg rocks are absent from areas north of the southern strand of the Melinda Fault, with one important exception. At 23°05.76'S; 28°53.47'E (Farm Varedig 265LR), a small outcrop of steeply-dipping and locally overturned Blouberg strata occurs unconformably beneath basal conglomerates of the Mogalakwena Formation. This lithology consists of purple, laminated to thinly bedded, fine- to medium-grained muddy arkosic sandstone (Figure 3.30). Cross-bedding is absent, and the bedding has a sheet-like geometry, though small (c.20cm deep, 70cm wide) channel forms are observed rarely (Figure 3.31). It is important to bear in mind that this is the only outcrop of Blouberg strata which occurs north of the southern strand of the Melinda Fault. Point counting of a thin section of this rock shows that it comprises 34% quartz, 35% matrix (=clay), 23% lithic fragments (=quartzite), 6% opaques and 2% muscovite. The rock from this location shows a general immaturity, which is comparable with that of the Blouberg Formation elsewhere in the Blouberg basin.

The general high percentages of matrix recorded in the Blouberg rocks indicates that they should all be classified as sub-lithic wackes or lithic wackes (after Pettijohn *et al.*, 1973). However, the generally weathered state of Blouberg rocks, and the presence of common feldspars in conglomerate beds, suggests that fresh samples of Blouberg sandstones would be more arkosic. The high proportions of matrix recorded in point counts may be due, in part, to the weathering of feldspars to clay minerals.

3.4: Palaeocurrent analysis:

Indicators for palaeocurrent direction were taken throughout the exposed Blouberg Formation. Ripplemarks are not preserved within the Formation, so dip directions of trough (and locally planar) cross-bedding foresets were used as indicators of palaeocurrent direction.

The steeply-dipping nature of the Kranskop section, and generally two-dimensional nature of the outcrop are not conducive for the accurate measurement of foreset dip-directions. Only rarely, when the stream bed possessed sufficient topography to expose vertically-dipping bedding planes and cross-bedded sets, could the orientation of foresets and bedding be measured. The original (pre-tectonic) foreset orientation was calculated by rotating bedding planes to their original horizontal orientation, and by similarly rotating foreset planes by the same amount. Only rarely was imbrication identified in the clasts of the conglomeratic Upper Member of the Kranskop section. The few foreset orientations within the vertically dipping strata at Kranskop which could be measured, were recorded with a very acute angle (<5°) with the bedding plane. With such shallow angular relationships, when rotational correction for horizontal bedding planes is carried out on a stereo net, a very small error in measurement, plotting or rotation may easily allow for 180° change in palaeocurrent direction. Such a potential error in the palaeocurrent data from the Kranskop strata should therefore be borne in mind, especially in view of the small data set that it was possible to collect. Palaeocurrent data collected from the outcrops of the Blouberg Formation in the Kranskop area are presented in Figure 3.32, and show a wide spread of palaeocurrent directions.

Palaeocurrent data from the Blouberg Formation around Blouberg Mountain are presented in Figure 3.33 (Lower Member) and Figure 3.34 (Upper Member), and show that palaeocurrents dominantly flowed towards the S.W. and west respectively. The geographic distribution of outcrops of the Blouberg Formation and of their palaeocurrent directions are shown in Figure 3.35. Figure 3.35 also shows the location of sites (A to F) at which measurements were taken for palaeohydraulic estimations. These calculations will be discussed in the following section.

3.5: Palaeohydraulics:

The general presence of clast-filled channels and predominance of cross-bedded strata, especially in the Lower Member of the Blouberg Formation, provided measurements from which palaeohydrological parameters can readily be calculated. Measurement of the

length of the intermediate axis of clasts, channel dimensions and the set thickness of cross-bedding were recorded from outcrops throughout the Blouberg Formation, and were used for palaeohydrological modelling (as outlined in Section 1.6.3). Sites for measurement were chosen to illustrate how parameters might vary along the inferred axis of the preserved Blouberg basin. Clast-filled channels could be recorded locally (for calculation of equations 1 to 4 in Section 1.6.3.1), and these results are shown in Table 3.2, and in Figure 3.36. Measurements of the set thickness of cross-bedding could be recorded more frequently, and the calculated palaeohydrological parameters (equations 4 to 16 in Section 1.6.3.2) are shown in Table 3.3. These data are also shown as histograms in Figures 3.37 and 3.38.

It should be stressed that the values calculated for palaeohydraulic parameters should not be considered as absolute values, but rather should be used for comparative purposes between different locations in the basin. For example, parameters calculated using the length of the intermediate axis of the largest clast within a channel of known cross-sectional area (equations 1-4 in Section 1.6.3.1) can only provide a minimum estimate of palaeohydrological parameters, as the initial (pre-erosion) cross-sectional area of the channel is not known. The columns shown in the histograms (Figures 3.36, 3.37 and 3.38) are arranged geographically, so that variation across the approximately East-West trending basin axis can be gauged.

Generally, the histograms in Figures 3.36, 3.37 and 3.38 show little systematic variation across the Blouberg basin, with the largest parameters of discharge, drainage area, and stream length being calculated for the approximate centre of the preserved basin (Location B). Palaeoslope appears to decrease towards the centre of the basin. These calculated parameters are discussed more fully in Section 8.2.1.

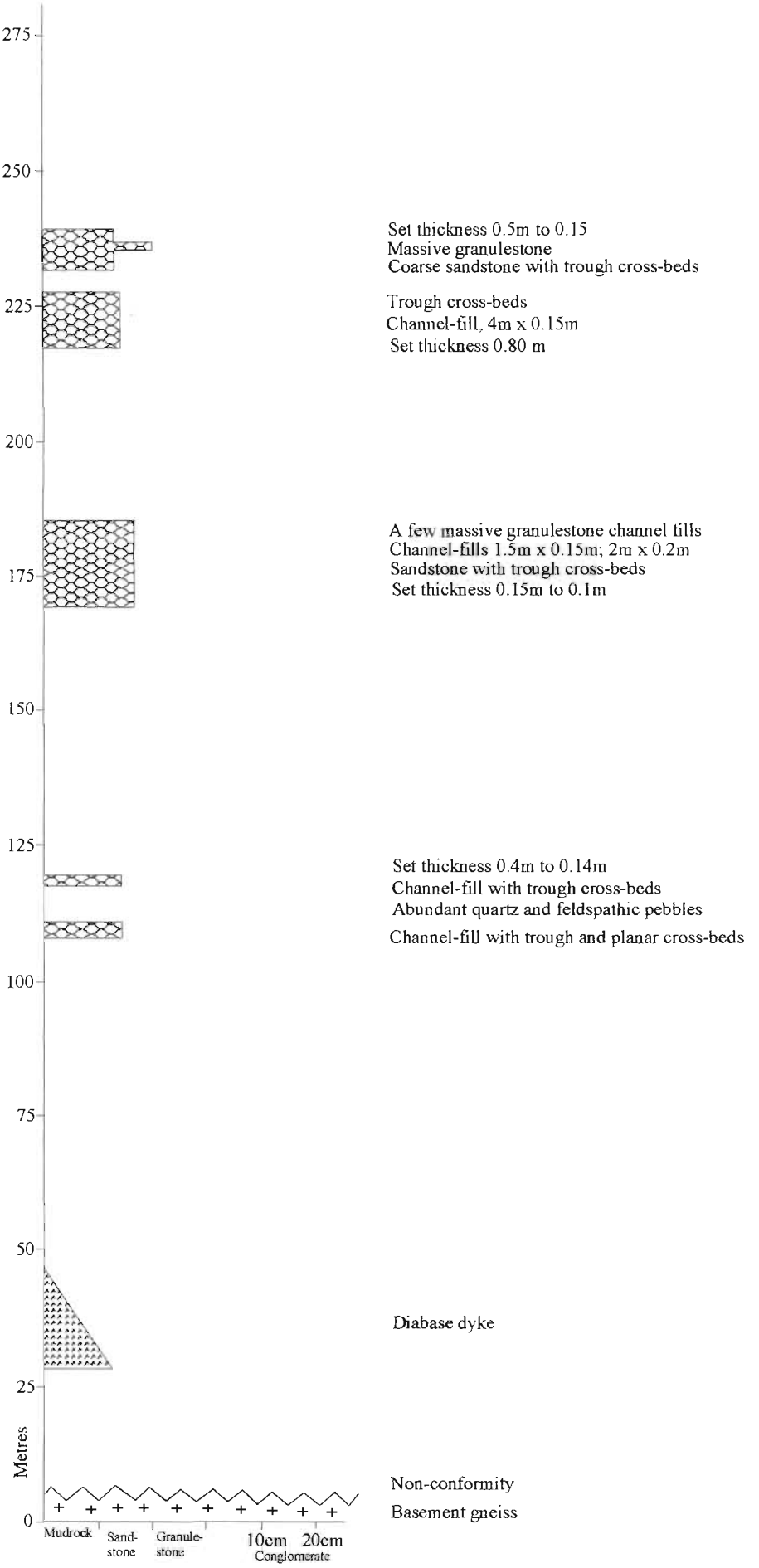

Facies association 1

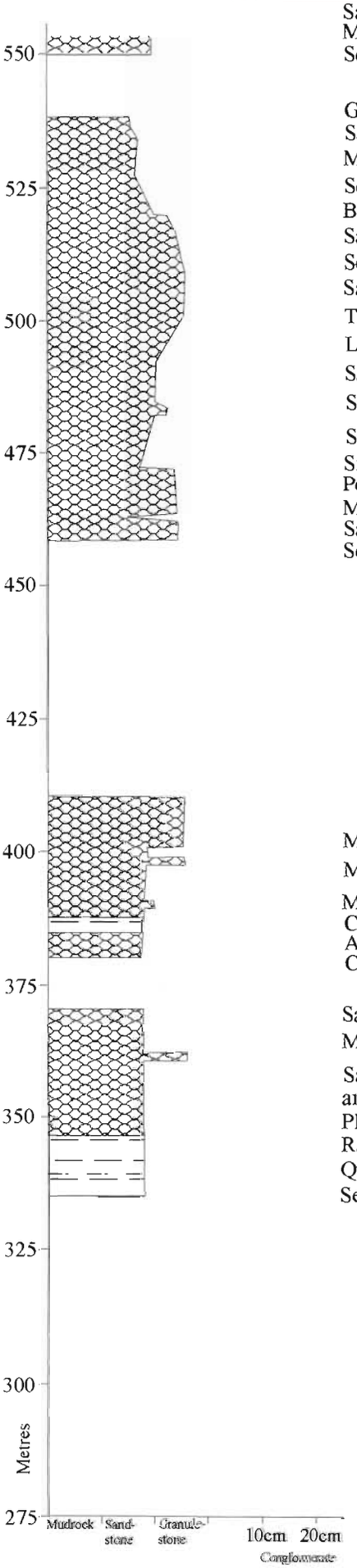

Sandstone with trough cross-beds
Many small massive granulestone channel-fills
Set thickness 0.1 to 0.05m

Granulestone channel-fills 1m x 0.09m
Sandstone with trough cross-beds
Many small massive gravel channel-fills
Set thickness 0.1 to 0.05m
Big and small massive granulestone channel-fills
Sandstone with trough cross-beds
Set thickness 0.2m
Sandstone with trough cross-beds
Thin mudrock layer
Large massive gravel channel-fills, 0.8m x 0.6m
Sandstone with trough cross-beds
Small massive granulestone channel-fills, 1m x 0.13m
Sandstone with trough cross-beds
Small channel-fills
Pebbly sandstone
Massive granulestone channel-fill, 7m x 0.4m
Sandstone with trough cross-beds
Set thickness 0.8m to 0.04m

Massive granulestone channel-fill, 6m x 0.5m
Massive granulestone channel-fill, 4m x 0.45m
Massive gravel channell-fill, 4m x 0.2m
Coarse sandstone with planar and trough cross-beds
Average set thickness 0.2m
Channel-fill; set thickness 1m to 1.5m

Sand with trough cross-beds and rare planar cross-beds
Massive gravel channel-fill, 0.2m to 0.35m
Sandstone with trough cross-beds
and localised channel-fills
Planar cross-beds, rare trough cross-beds
Rare small-scale massive granulestone channel-fills
Quartz pebbles
Set thickness 0.2m to 1m

Facies association 2

Facies association1

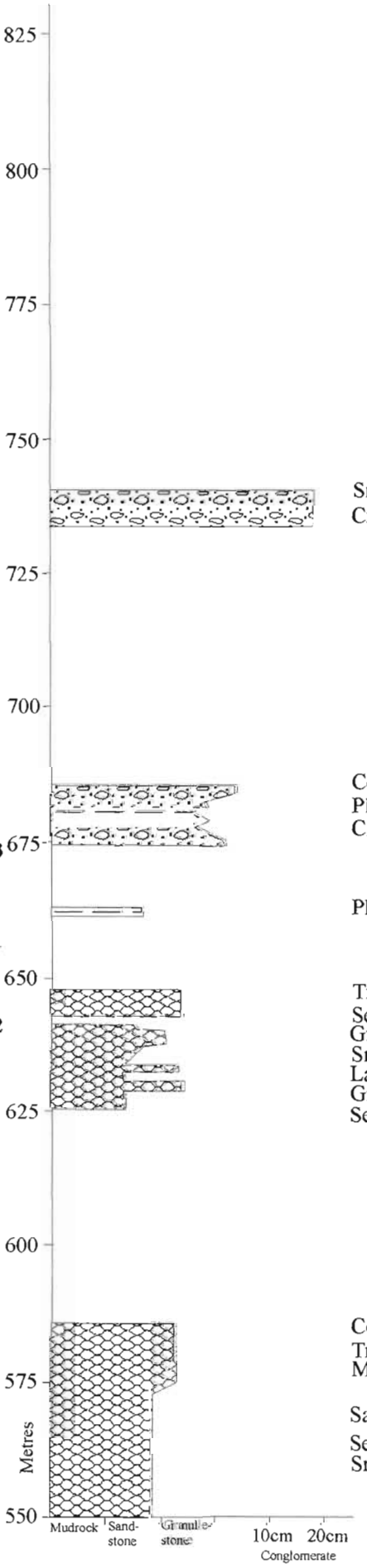

Small sandstone channel-fills
Cross-bedded conglomerate

Conglomerate with imbricate structures
Planar-bedded sand in granulestone
Cross-bedded conglomerate

Facies association 3

Planar-bedded sandstone

Trough cross-beds in sandstone and granulestone
Set thickness 0.3m
Granulestone with trough cross-beds
Small massive granulestone channel-fills 0.5m x 0.05m
Large massive granulestone channel-fills, 6m x 0.5m
Granulestone channel-fill with quartz and feldspar pebbles
Set thickness 0.05m to 0.3m

Facies association 2

Common massive granulestone channel-fills, 4m x 0.02m
Trough cross-beds in sandstone
Massive granulestone channel-fill, 2m x 0.2m

Sandstone with trough cross-beds
Set thickness 0.05m to 0.3m
Smaller massive granulestone channel-fills, 1.2m x 0.14m

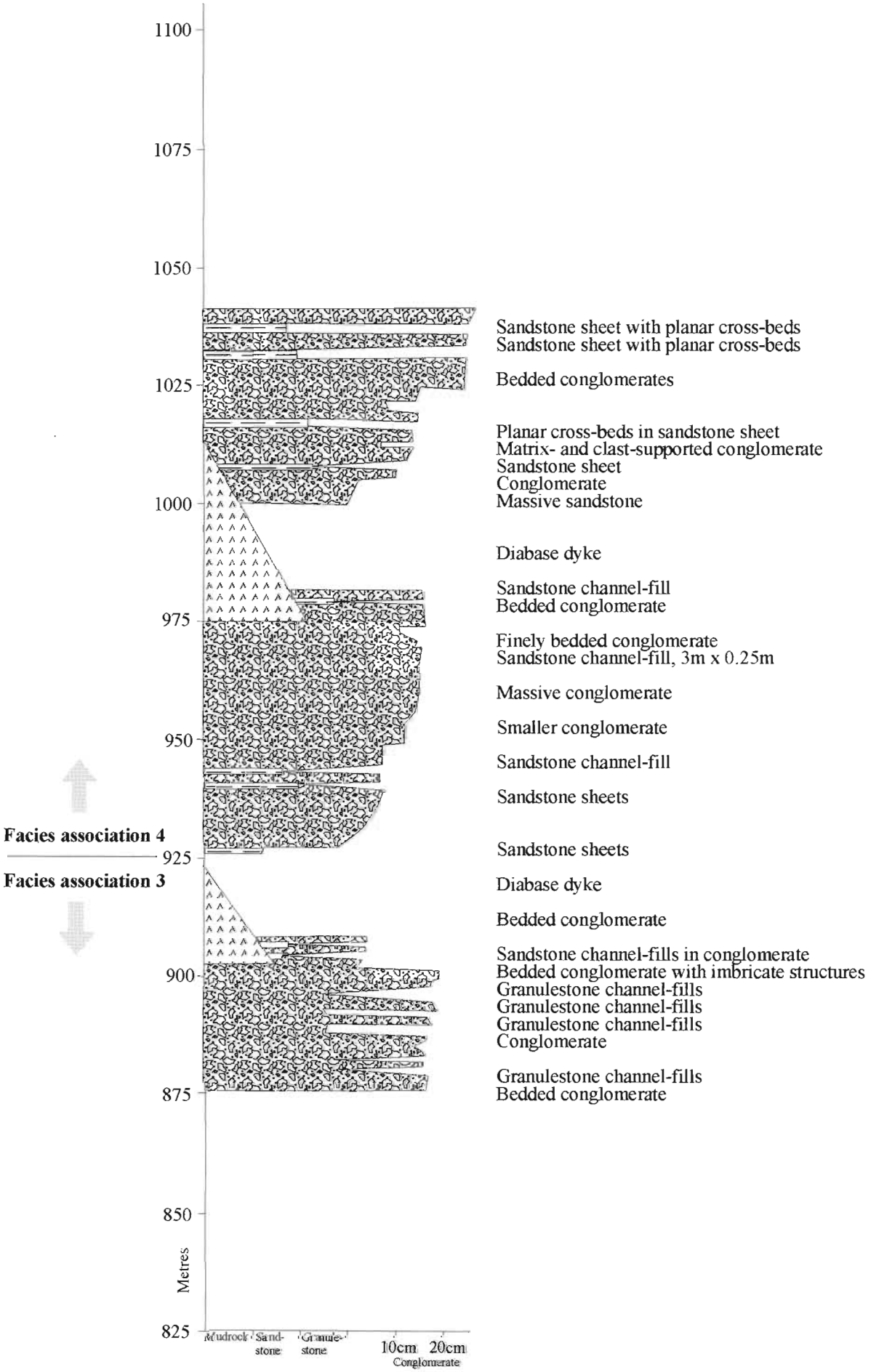
1100
1075
1050
1025
1000
975
950
925
900
875
850
825
Metres
Facies association 4
Facies association 3
Mudrock
Sand-stone
Granule-stone
10cm
20cm
Conglomerate
Sandstone sheet with planar cross-beds
Sandstone sheet with planar cross-beds
Bedded conglomerates
Planar cross-beds in sandstone sheet
Matrix- and clast-supported conglomerate
Sandstone sheet
Conglomerate
Massive sandstone
Diabase dyke
Sandstone channel-fill
Bedded conglomerate
Finely bedded conglomerate
Sandstone channel-fill, 3m x 0.25m
Massive conglomerate
Smaller conglomerate
Sandstone channel-fill
Sandstone sheets
Sandstone sheets
Diabase dyke
Bedded conglomerate
Sandstone channel-fills in conglomerate
Bedded conglomerate with imbricate structures
Granulestone channel-fills
Granulestone channel-fills
Granulestone channel-fills
Conglomerate
Granulestone channel-fills
Bedded conglomerate

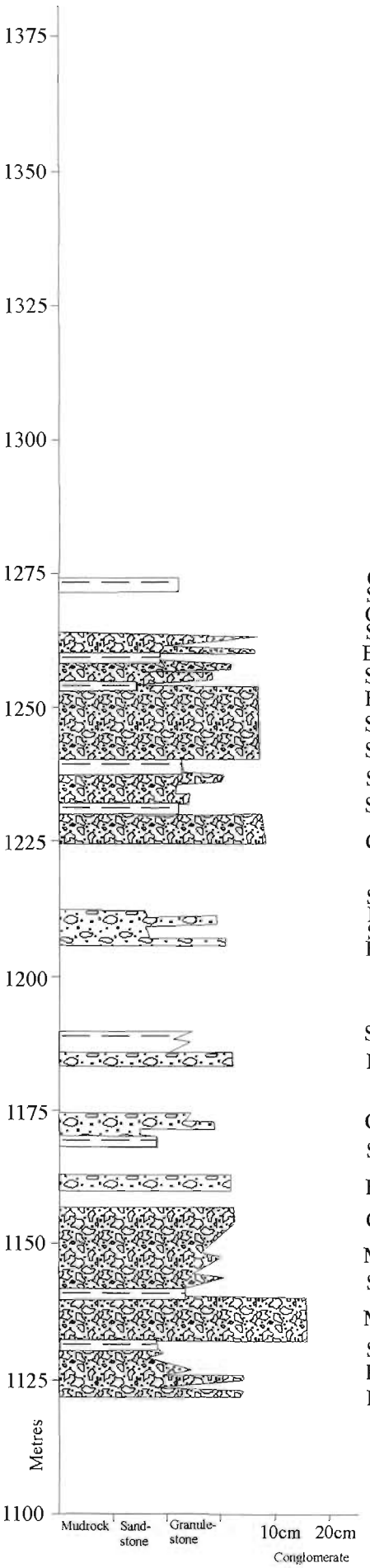
1375
1350
1325
1300
1275
1250
1225
1200
1175
1150
1125
1100
Metres
Mudrock
Sand-stone
Granule-stone
10cm
20cm
Conglomerate
Coarse sandstone and granulestone sheets with planar cross-beds
Set thickness 0.1m
Conglomerate with interbedded sandstone sheet
Sandstone sheet with planar cross-beds
Bedded conglomerate, set thickness 0.8m
Sandstone sheet with planar cross-beds, set thickness 0.12m
Bedded conglomerate, set thickness 2m
Sandstone and gravel sheets with planar cross-beds
Set thickness 0.3m
Sandstone sheet with planar cross-beds
Sandstone and granulestone sheets with planar cross-beds
Conglomerate (max. Clast 25cm)
Sandstone with planar cross-beds
Fine conglomerate
Sandstone with planar cross-beds
Fine conglomerate
Sandstone and granulestone sheets
Fine conglomerate
Coarse granulestone/fine conglomerate
Sandstone sheet
Bedded conglomerate
Cross-bedded conglomerate
Massive granulestone sheets
Sandstone sheet with planar cross-beds
Massive conglomerate
Sandstone and granulestone sheets
Planar cross-beds in sandstone sheet
Bedded conglomerate

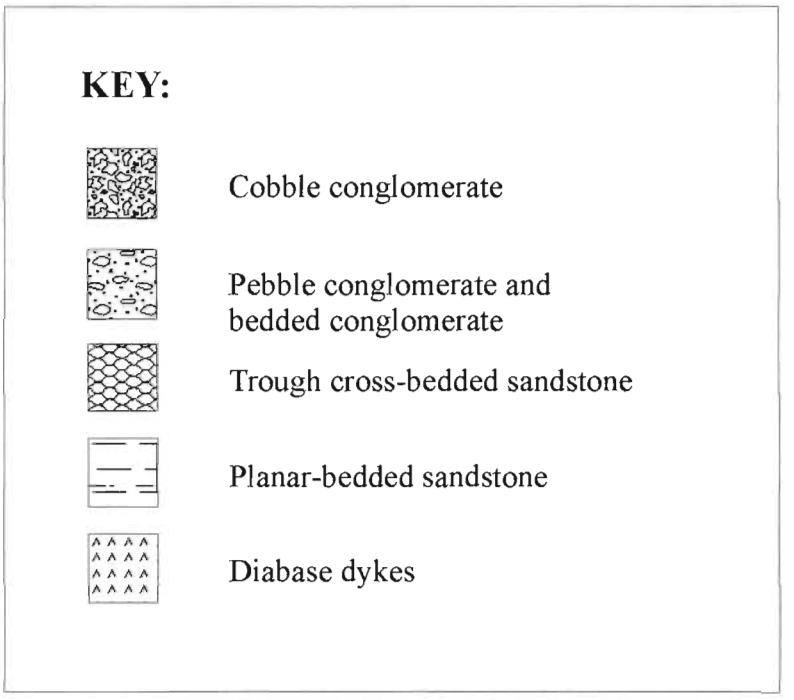

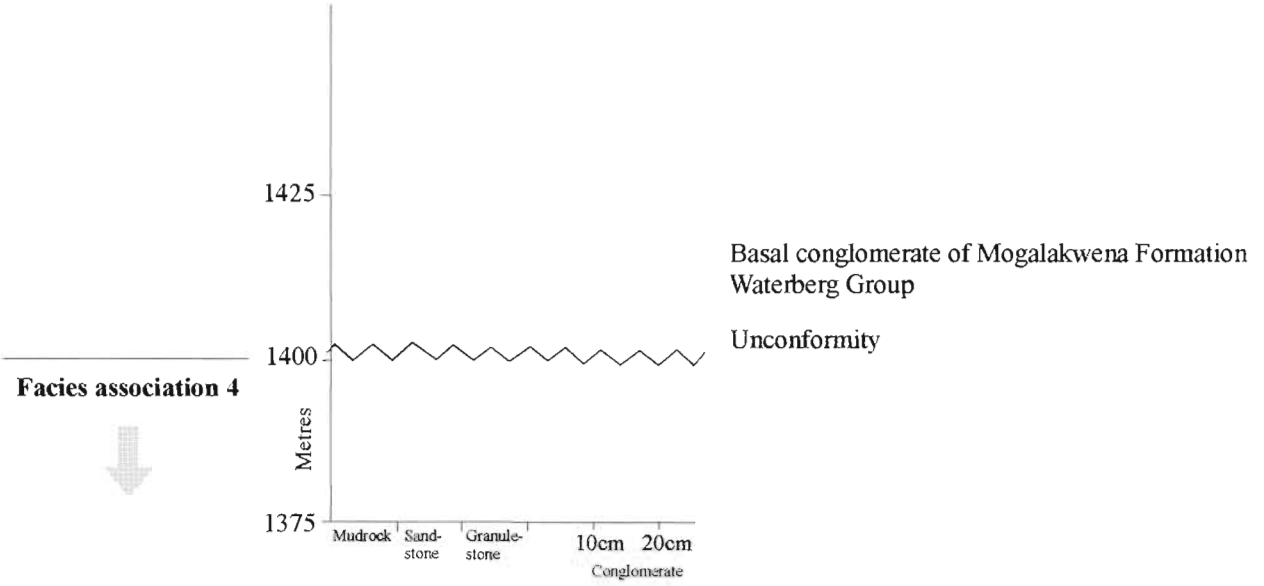

Figure 3.1: Stratigraphic section of the Blouberg Formation in the Kranskop area.

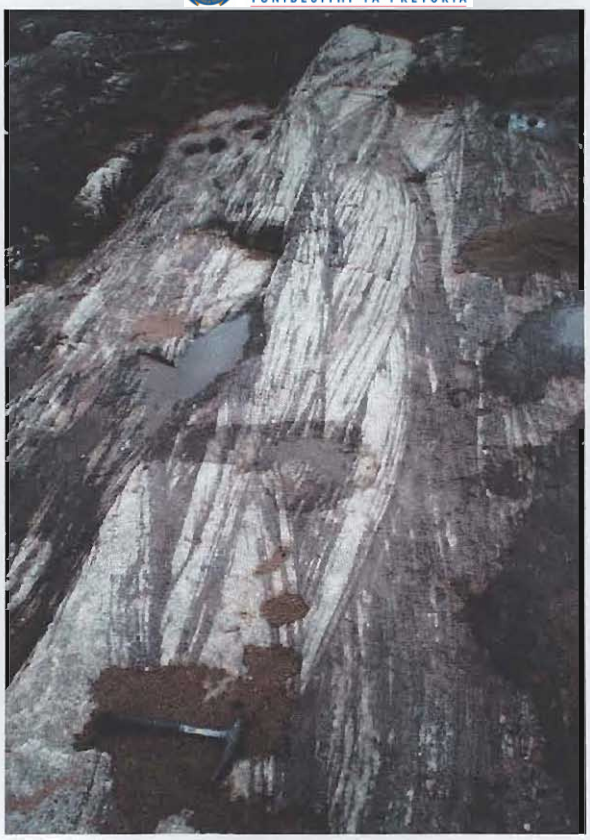

Figure 3.2: Small trough cross-bedded sets (facies association 1; Lower Member, Blouberg Formation). Recorded at 23°09.03'S; 28°41.85'E. Hammer is 30cm long.

Figure 3.3: Pebbly granulestone-filled channel with angular quartz clasts in facies association 1 (Lower Member) of the Blouberg Formation. Recorded at 23°09.03'S; 28°41.85'. Pen is 15cm long.

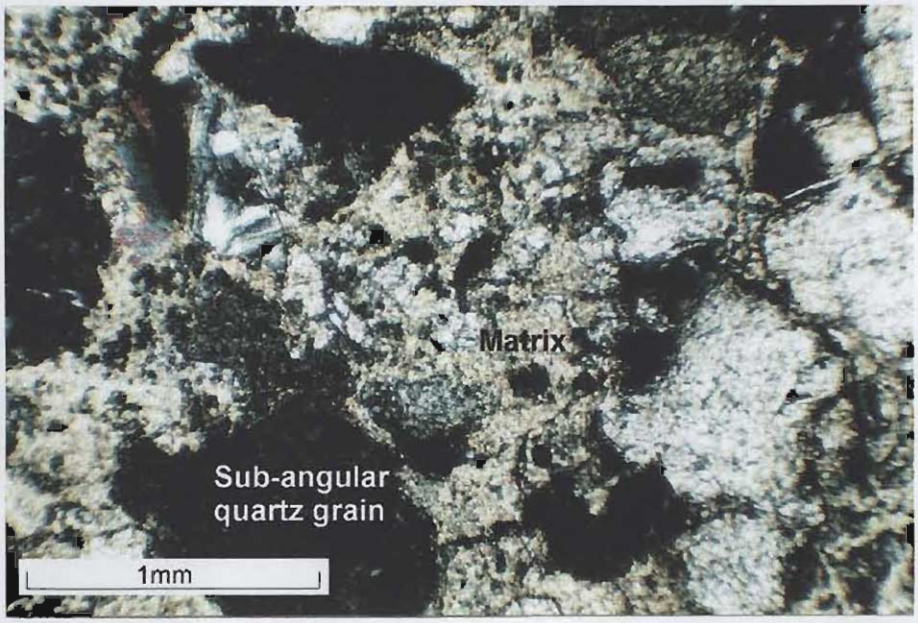

Figure 3.4: Photomicrograph of coarse sandstone from facies association 1 of the Blouberg Formation (collected at 23°09.03'S; 28°41.85'). The sediment is generally immature, with sub-angular quartz grains of low sphericity, with a high percentage of matrix, possibly reflecting weathered feldspar.

Figure 3.5: Detail of pebbly granulestone from Figure 3.3, showing that channel-fill is composed of a highly arkosic (orthoclase) granulestone with pebbles of quartz and feldspathic lithic clasts. Pen is 15cm long.

Figure 3.6: Coarse sandstone- and granulestone-filled channel forms in facies association 2 of the Lower Member of the Blouberg Formation. Recorded at 23°09.05'S; 28°41.65'E. Hammer is 30cm long.

Figure 3.7: Generally small (<10cm) sets of trough cross-bedded coarse sandstone in facies association 2 of the Lower Member of the Blouberg Formation. Recorded at 23°09.05'S; 28°41.76'. Hammer is 30cm long.

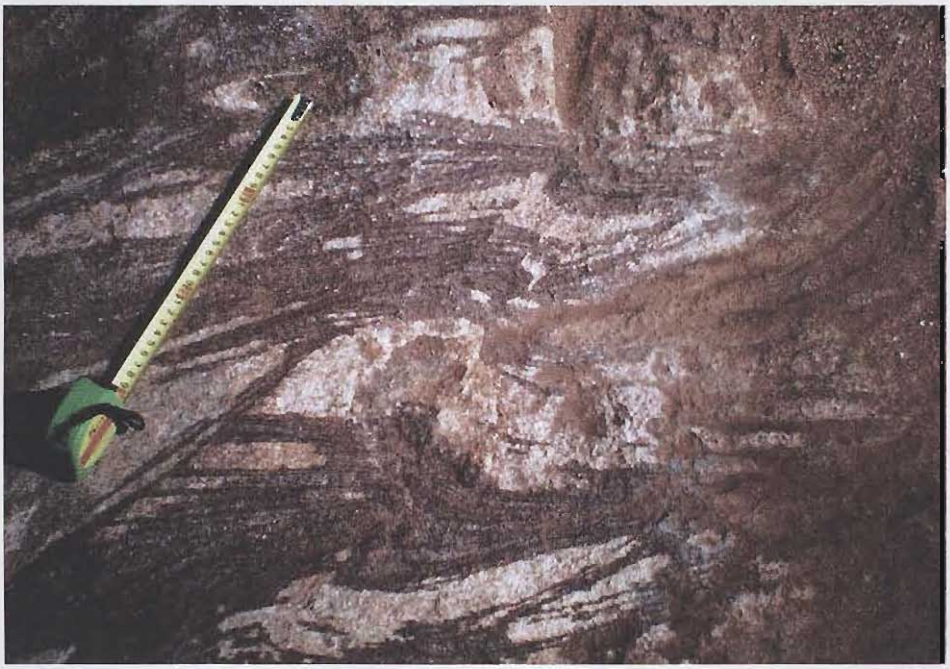

Figure 3.8: Soft sediment deformation in facies association 2 of the Lower Member of the Blouberg Formation. Scale in centimetres.

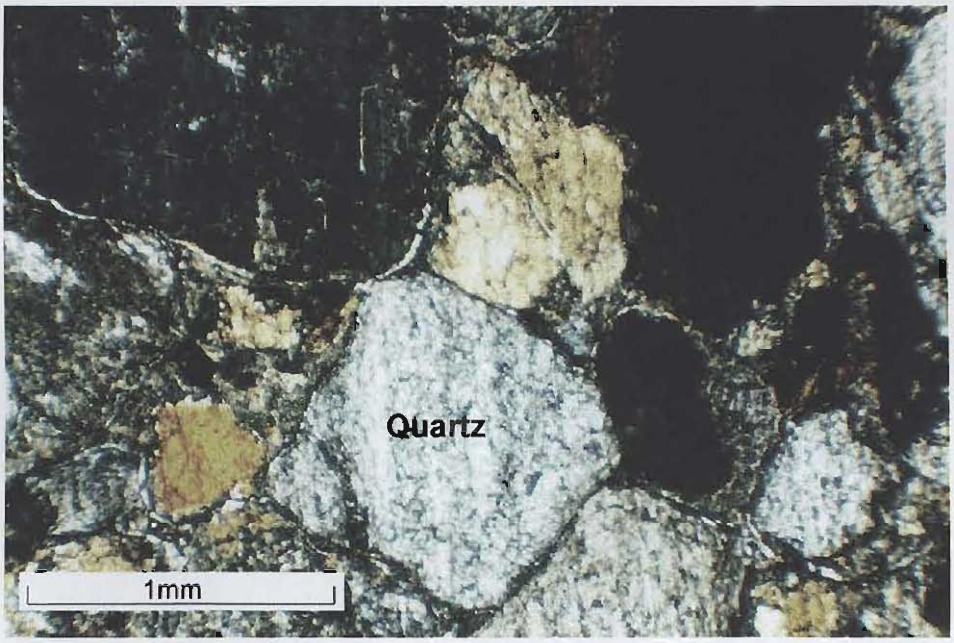

Figure 3.9: Photomicrograph of thin section of coarse sandstone from facies association 2 of the Lower Member of the Blouberg Formation. Quartz grains are sub-angular to sub-rounded, though there is generally less matrix than facies association 1 (Figure 3.4).

Figure 3.10: Facies association 3 of the Upper Member of the Blouberg Formation. Note the presence of large sub-rounded feldspathic clasts of low sphericity in a coarse arkosic matrix. Recorded at 23°09.09'S; 28°41.90'E. GPS receiver is 15cm long.

Figure 3.11: Detail of facies association 3. Note the foliation planes preserved in the cobble of feldspathic gneiss, and the coarse arkosic granulestone matrix. Hammer head is 10cm long.

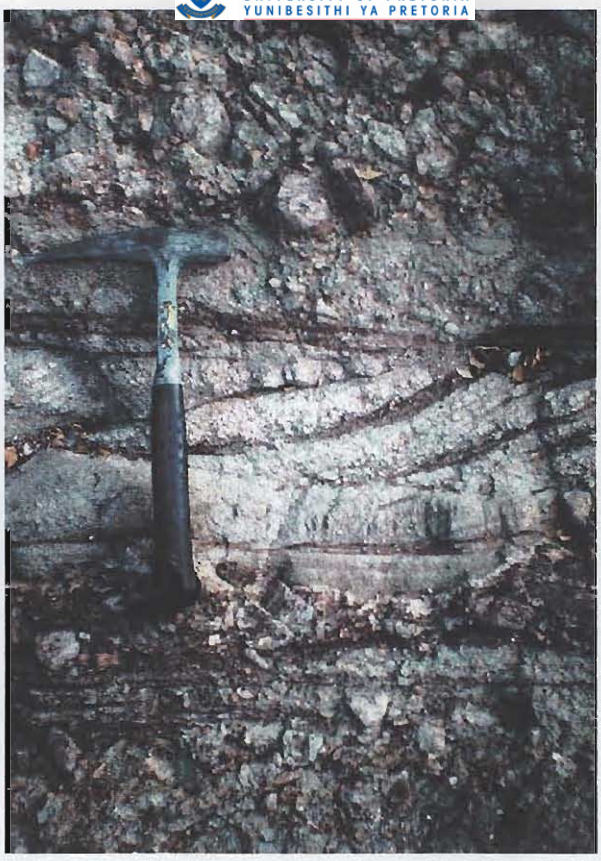

Figure 3.12: Cyclicity in facies association 3. A fining-upwards massive conglomerate grades into an upper trough cross-bedded arkose. The onset of the next cycle is marked by presence of larger cobbles which, in-turn, fine upwards. Hammer is 30cm long.

Figure 3.13: Bedded, clast-supported conglomerates fine upwards into a sandstone-filled channel form, prior to the start of the next cycle, marked by the presence of larger cobbles above. Hammer is 30cm long.

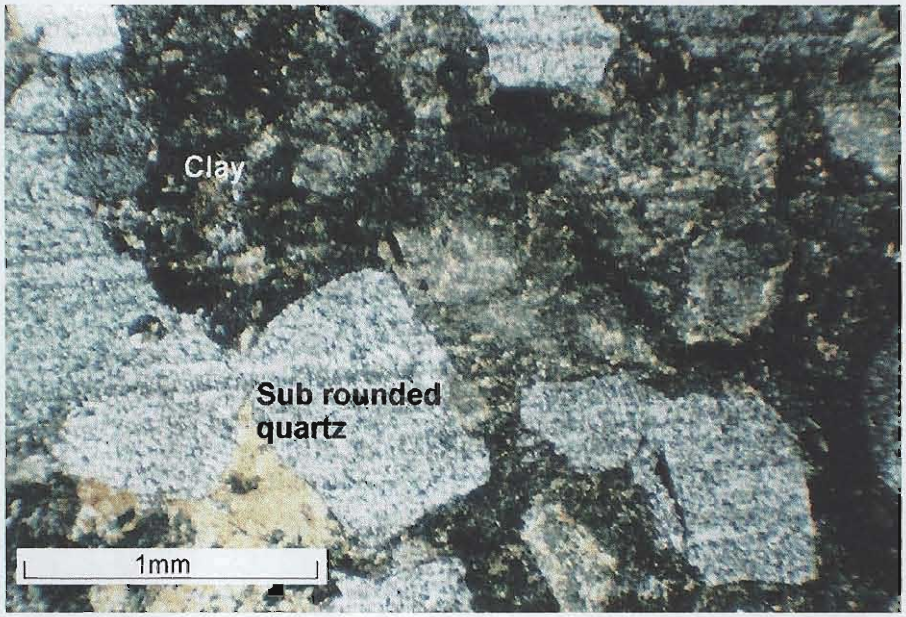

Figure 3.14: Photomicrograph of thin section of interclast material from conglomerate in facies association 3. Quartz grains are sub rounded and of low-sphericity. A high proportion of the grains consist of fine-grained, clayey material, probably reflecting weathered feldspar grains.

Figure 3.15: Facies association 4. Bedded and massive conglomerates are interbedded with trough cross-bedded sandstone sheets or wide channel forms. Recorded at 23°09.05'S; 28°41.30'E. Hammer is 30cm long.

Figure 3.16: Channel-fill in the Blouberg Formation in the Blouberg mountain area. Note the quartz and feldspar granulestone channel-fill (c.f. Figures 3.5 and 3.6 from the Kranskop area). Recorded at 23°07.96'S; 28°55.25'E. Hammer is 30cm long.

Figure 3.17: Detail of coarse, feldspathic granulestone from 23°07.47'S; 28°57.42'E. Pen is 15cm long.

Figure 3.18: Cobbles of foliated gneiss (above and to the right of the pen) in a granulestone matrix in the Blouberg Formation. Recorded at 23°07.47'S; 28°57.42'E. Pen is 15cm long.

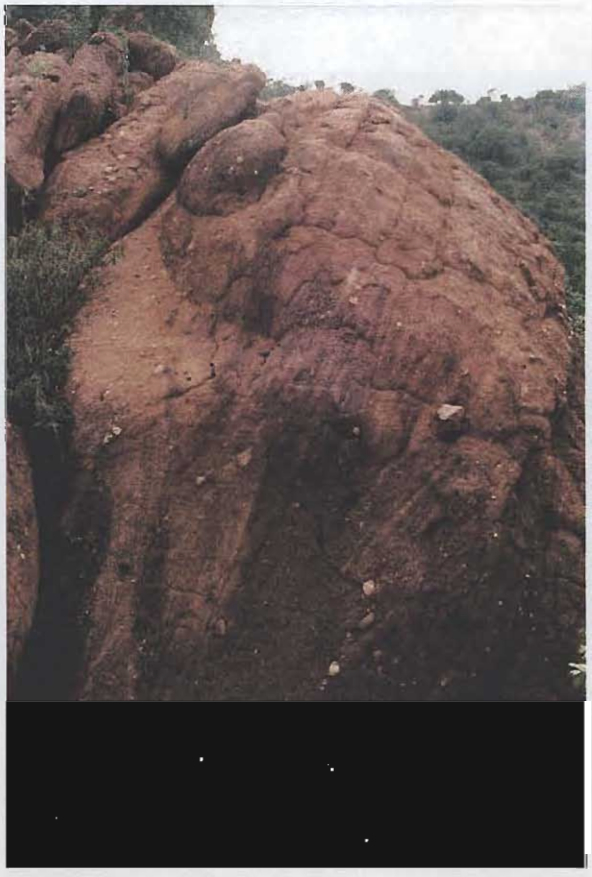

Figure 3.19: Trough and planar cross-bedded sandstone and granulestone, with large (>10cm diameter) quartz cobbles resting on foresets. Recorded at 23°07.71'S; 28°57.08'E.

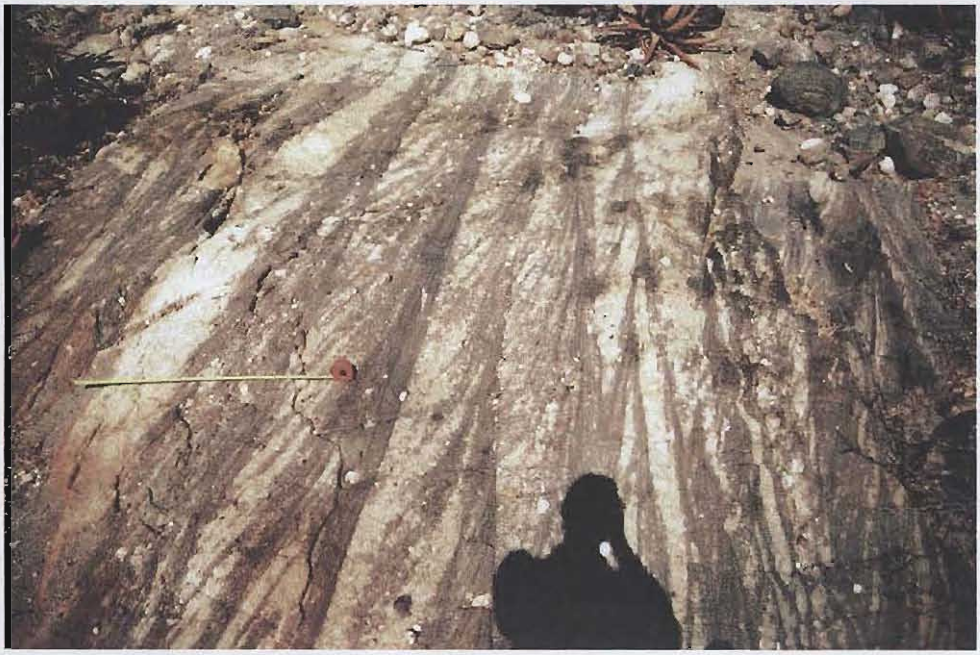

Figure 3.20: Thick (>3m) cosets of cross-bedded sandstone and granulestone in the Blouberg Formation at 23°07.47'S; 28°57.42'E. Cosets are comprised of sets of 30-40cm thickness. Tape measure is 1m long.

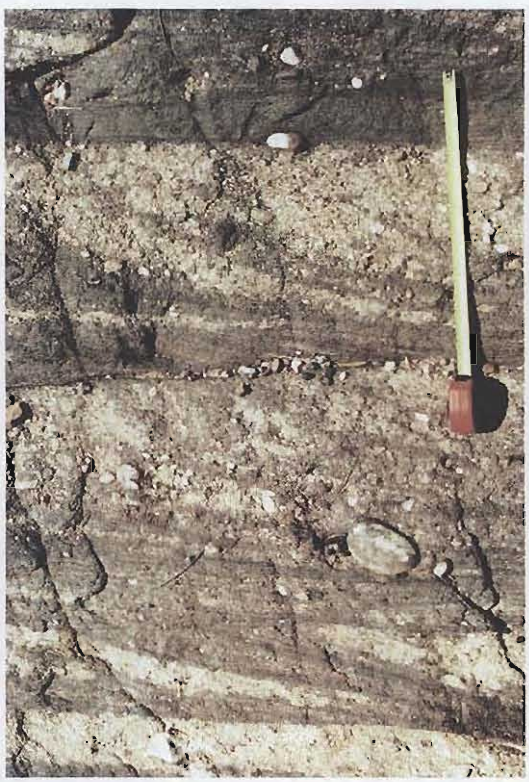

Figure 3.21: Detail of Figure 3.20, showing individual sets with isolated quartz cobbles positioned on foresets. Note fining-upwards cyclicity in each set. Tape measure is 50cm long.

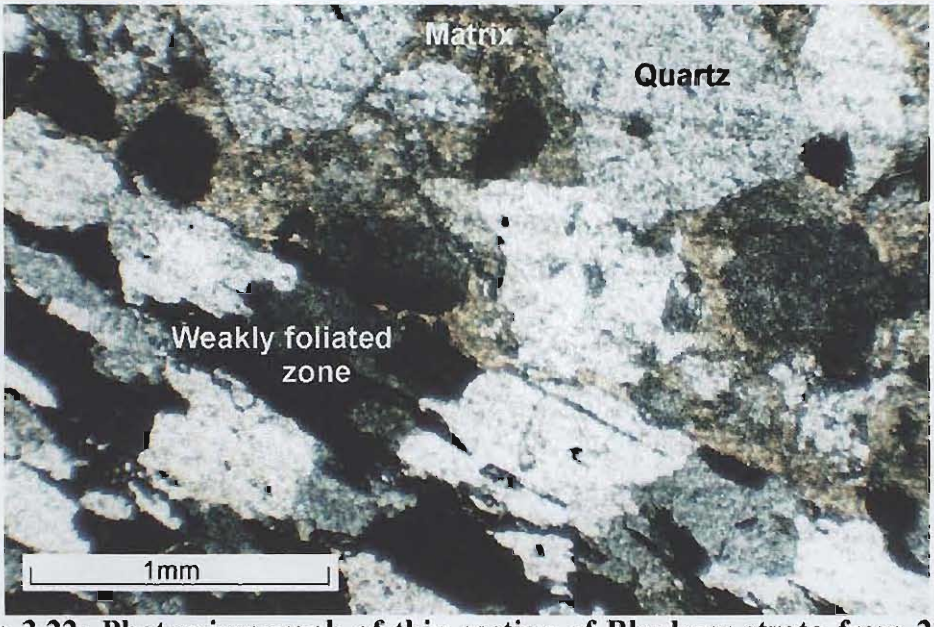

Figure 3.22: Photomicrograph of thin section of Blouberg strata from 23°07.47'S; 28°57.42'E. Sub-rounded quartz grains of low-sphericity have high proportions of interstitial matrix. The lower, left hand side of the photomicrograph shows a weakly developed foliation caused by recrystallisation of quartz grains as a response to stress.

Figure 3.23: The lower half of the photograph shows steeply-dipping trough cross-bedded sandstone in the Blouberg Formation at 23°06.80'S; 28°59.40'E. (Top part of the photograph shows unconformably overlying strata of the Mogalakwena Formation). Hammer is 30cm long.

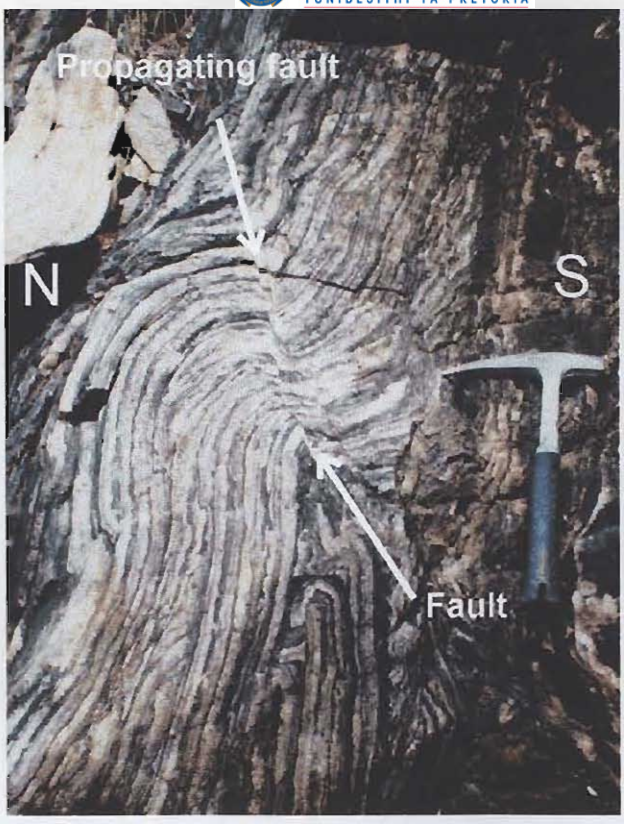

Figure 3.24: Muddy sandstone in the Blouberg Formation at 23°06.80'S; 28°59.40'E. Strata show a fault-propagation fold (fold axis trends 098° and has a plunge of 10° E; Section 7.2). Hammer is 30cm long.

Figure 3.25: Weakly foliated, sub-rounded cobbles of feldspathic basement gneiss in the Blouberg Formation at 23°06.97'S; 28°59.67'E. Pen is 15cm long.

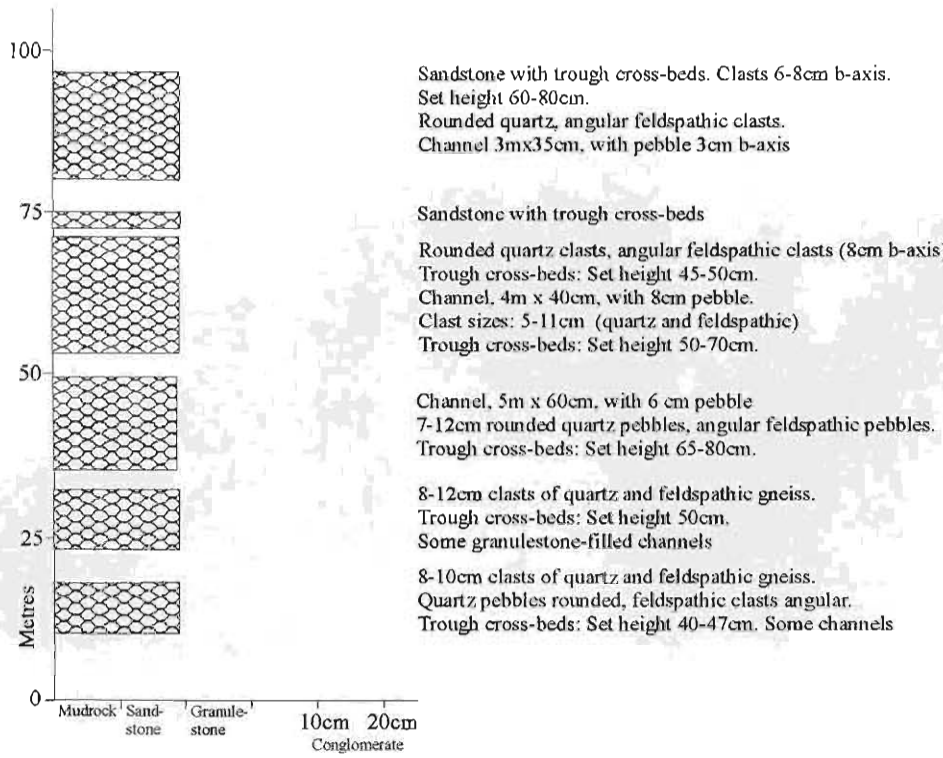

Figure 3.26: Stratigraphic section of the Blouberg Formation in the Dantzig area.

Figure 3.27: Sub-rounded cobbles of highly feldspathic gneiss at 23°06.86'S; 29°02.26'E. c.f. Figure 3.11. Hammer is 30 cm long.

Figure 3.28: Large-scale (<180cm set thickness) trough cross-bedded sets in the Blouberg Formation at 23°06.15'S; 29°01.82'E. Hammer is 30cm long.

Figure 3.29: Vertically-dipping planar cross-bedded granulestone in the Blouberg Formation at 23°06.06'S; 29°02.27'E.

Figure 3.30: Laminated muddy sandstone in the Blouberg Formation at 23°05.76'S; 28°53.47'E. (c.f. Figure 3.24). Hammer is 30cm long.

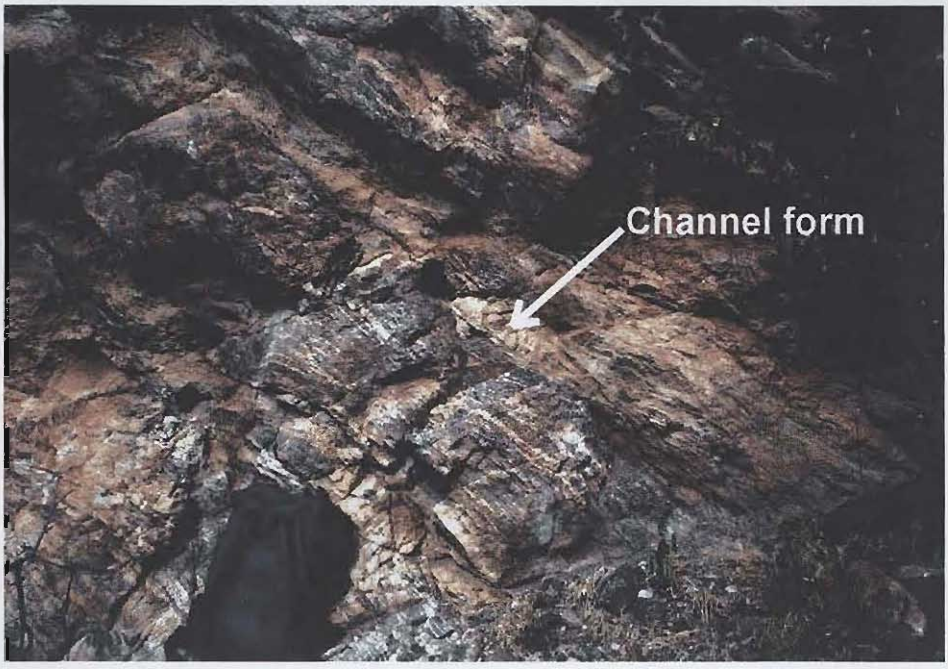

Figure 3.31: Steeply dipping strata of the Blouberg Formation at 23°05.76'S; 28°53.47'E. A poorly defined, small (c.70cm-wide), pale sand-filled channel form is visible c. 1m above and to the right of the rucksack. Rucksack is 60cm high.

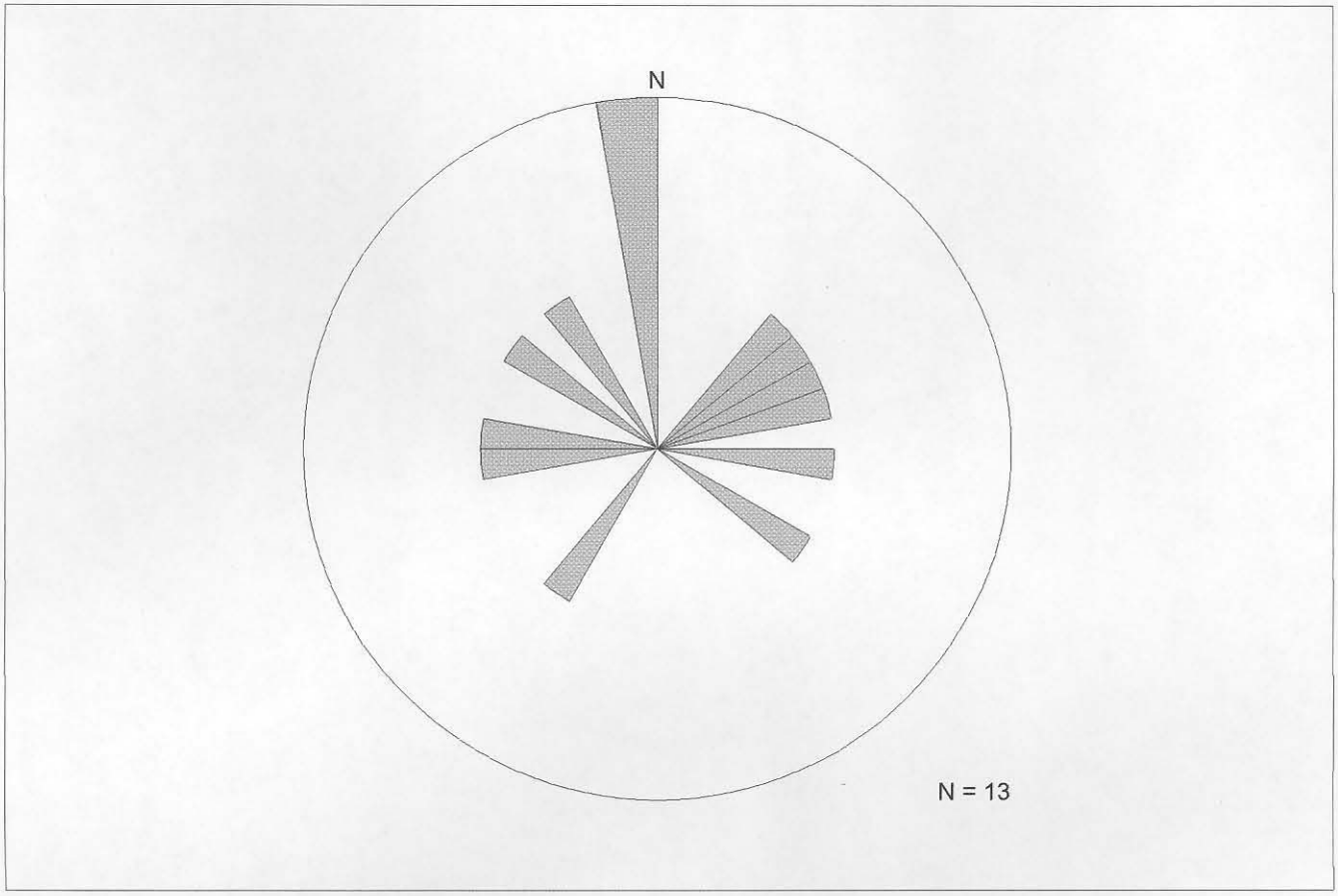

Figure 3.32: Rose diagram showing palaeocurrent directions recorded from steeply-dipping trough cross-beds in the Blouberg Formation (Lower and Upper Members) recorded in the Kranskop area.

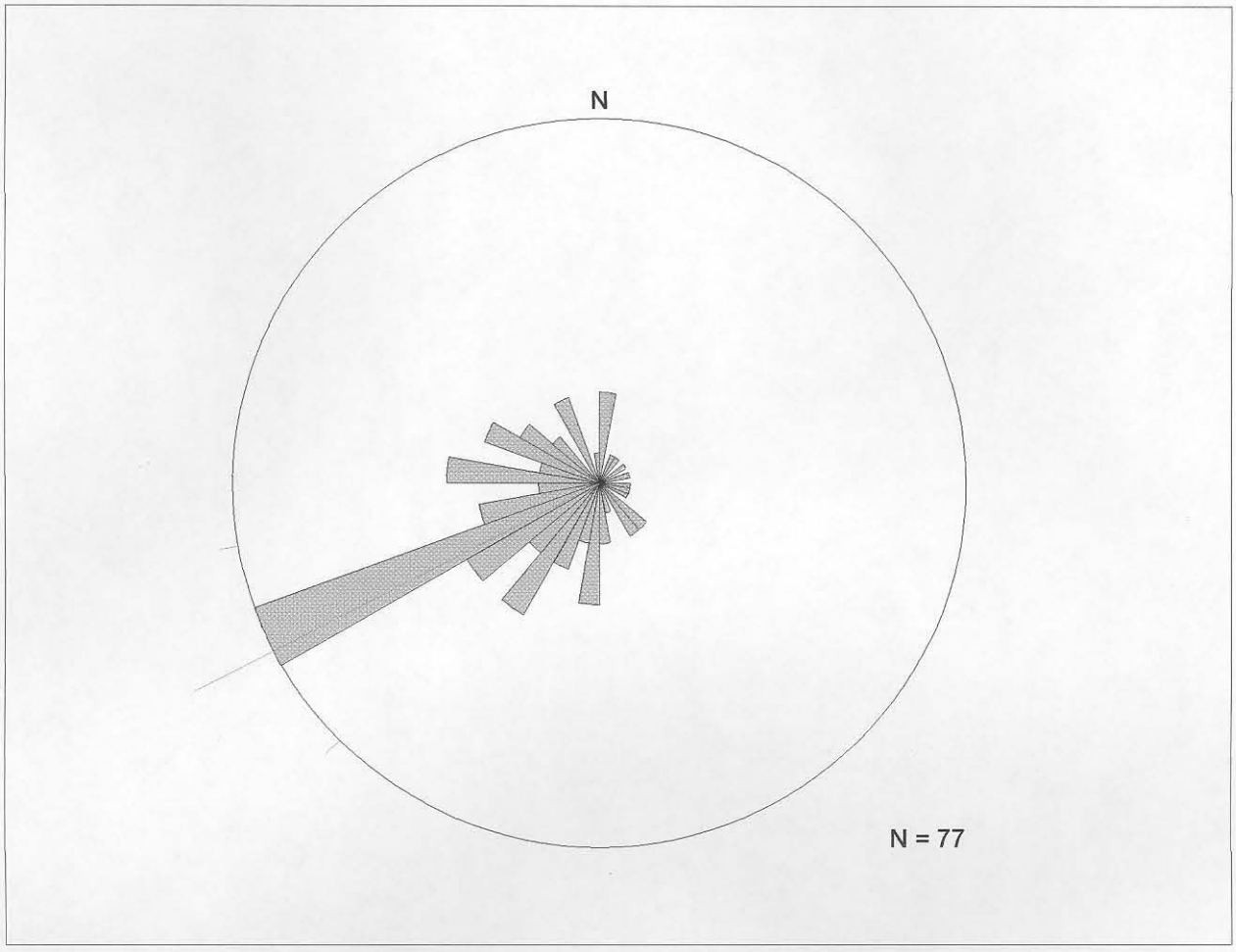

Figure 3.33: Rose diagram showing palaeocurrent directions measured from trough cross-bedding in the Lower Memberof the Blouberg Formation recorded in the Blouberg mountain area. The principal direction (vector mean) is indicated.

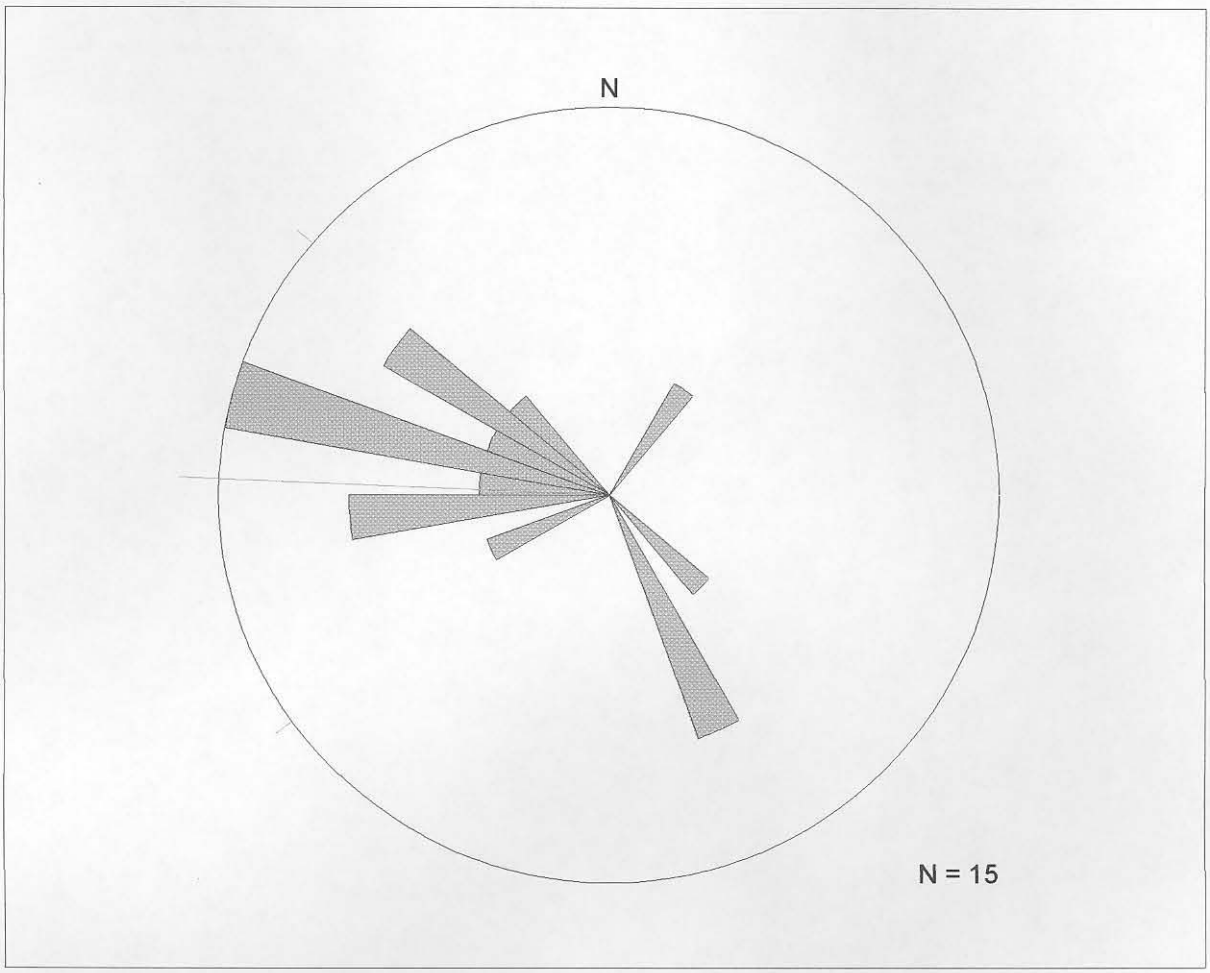

Figure 3.34: Rose diagram showing palaeocurrent directions recorded from trough cross-bedding in the Upper Member of the Blouberg Formation recorded in the Blouberg mountain area. The principal direction (vector mean) is indicated.

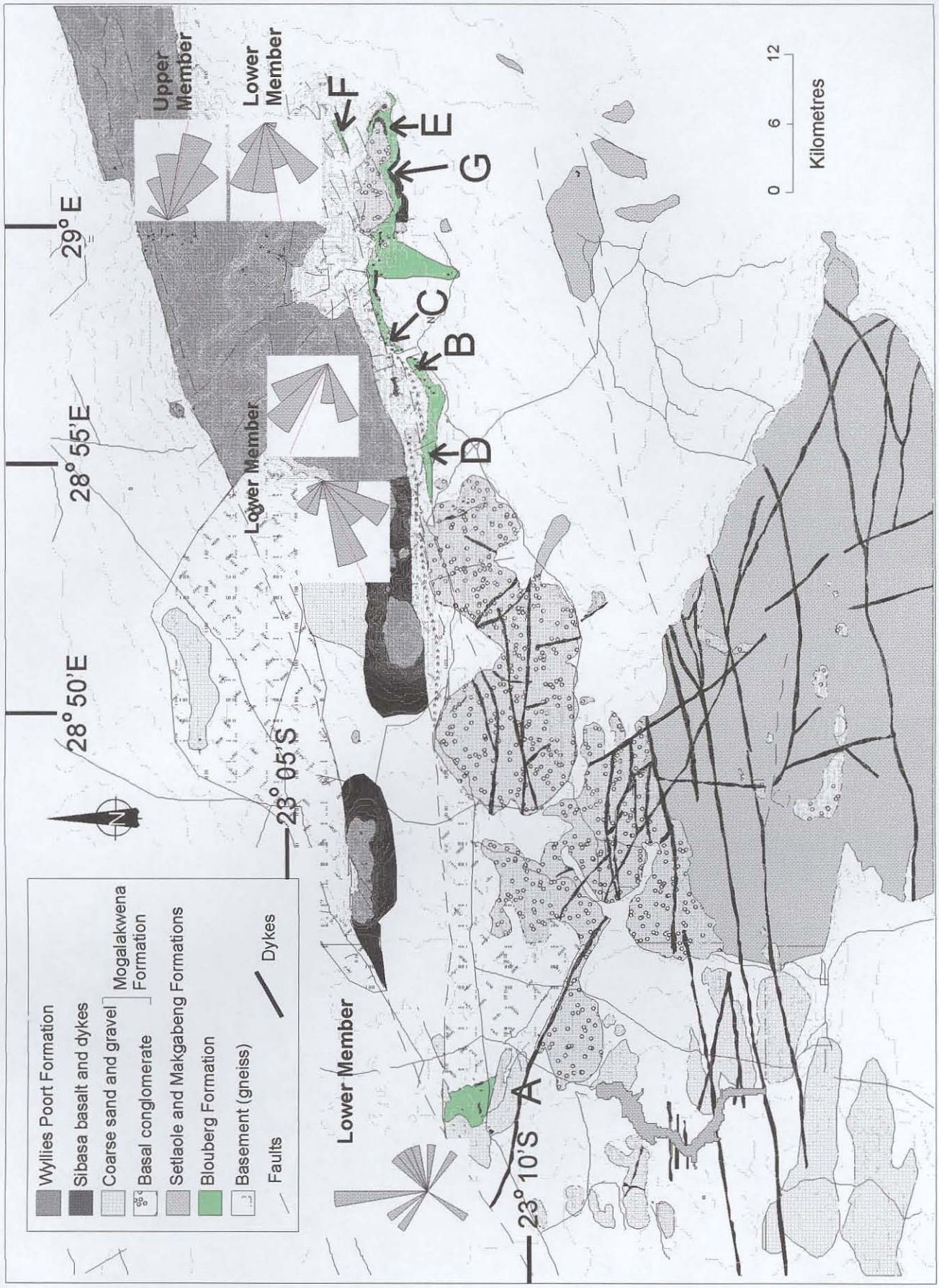

Figure 3.35: Map showing the location of outcrops of the Blouberg Formation, and the variability of palaeocurrent directions across the preserved basin. Letters indicate the location of sites from where palaeohydrological parameters were recorded.

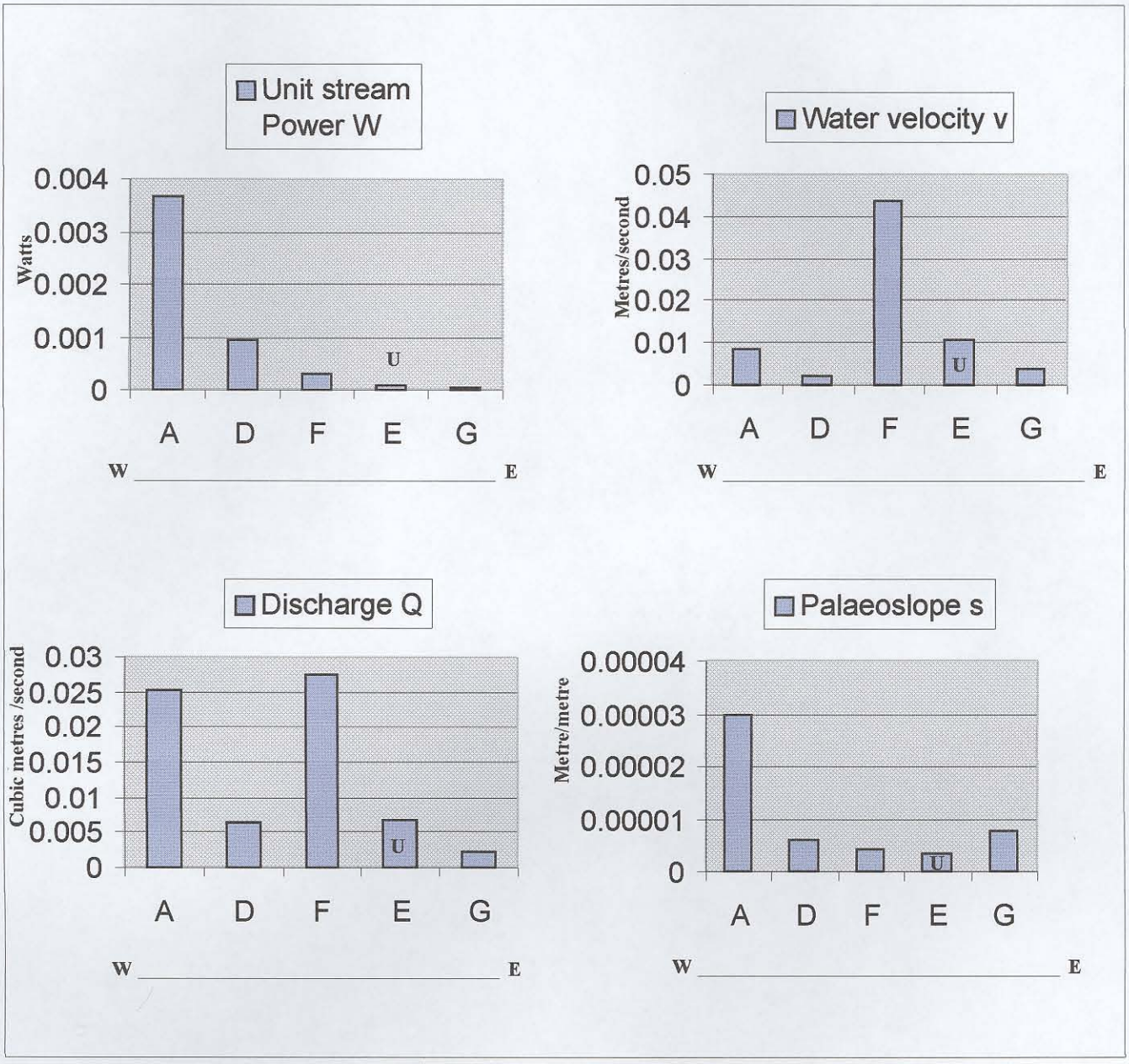

Figure 3.36: Histograms showing variablity in palaeohydrological parameters calculated from clast sizes within channels in the Upper (U) and Lower members of the Blouberg Formation. The location of points A to F are shown in Figure 3.35.

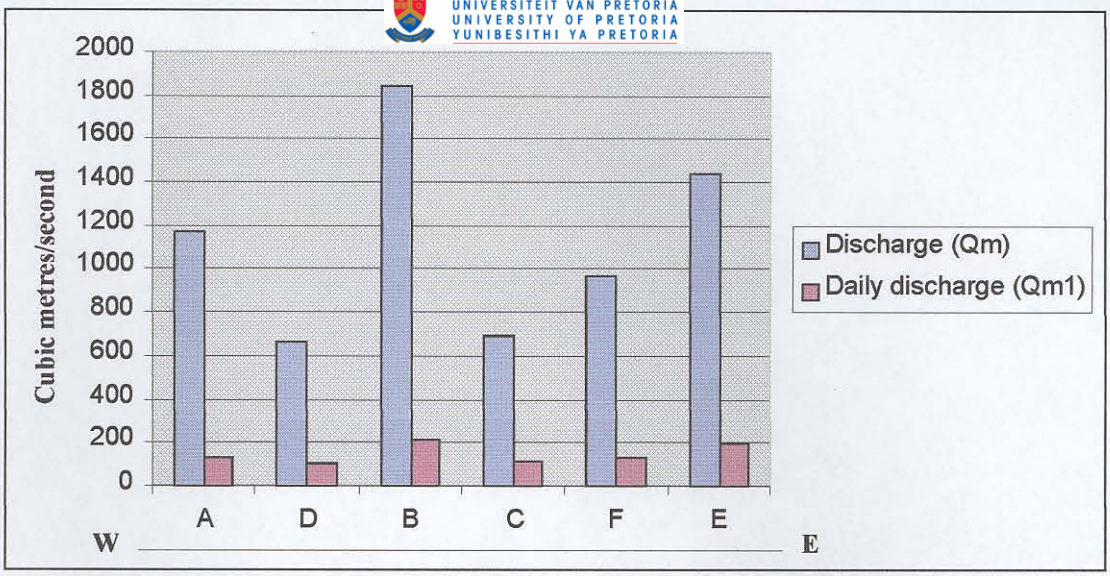

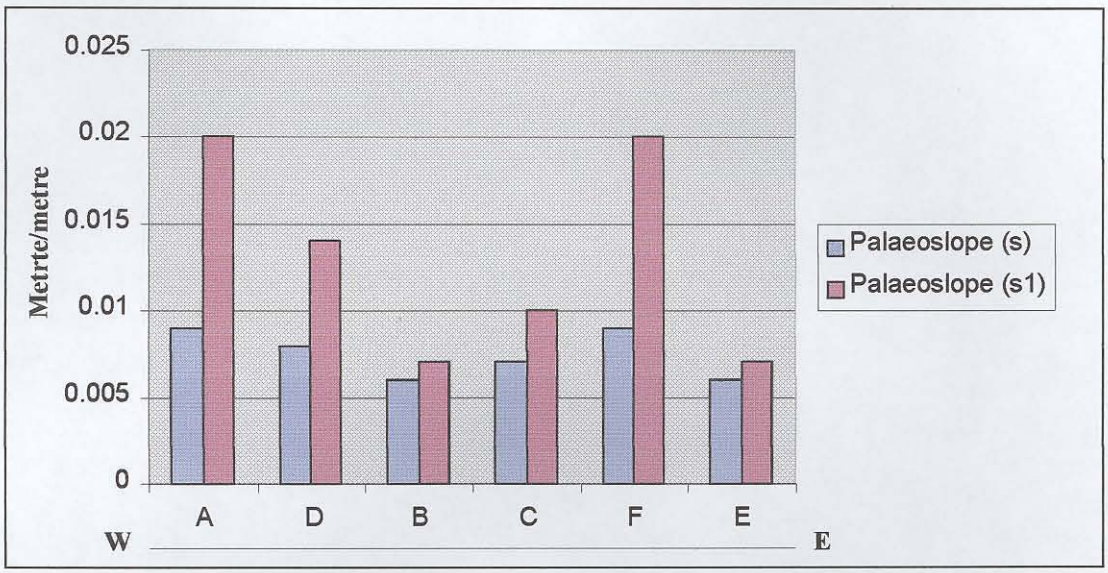

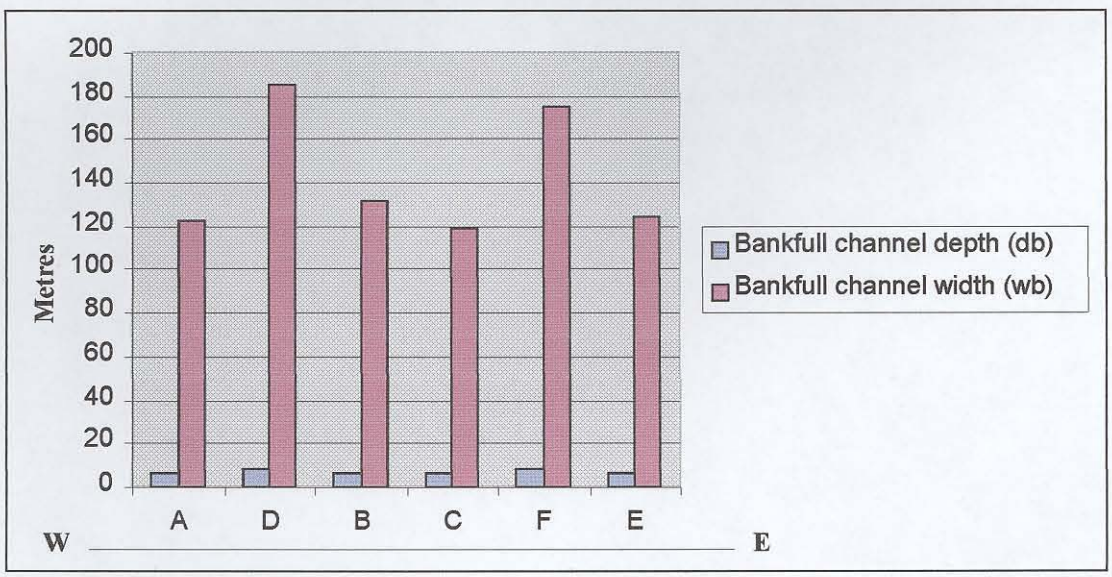

Figure 3.37: Histograms to show variability of calculated palaeohydrological parameters across the Blouberg basin. Location of points A to E is shown in Figure 3.35.

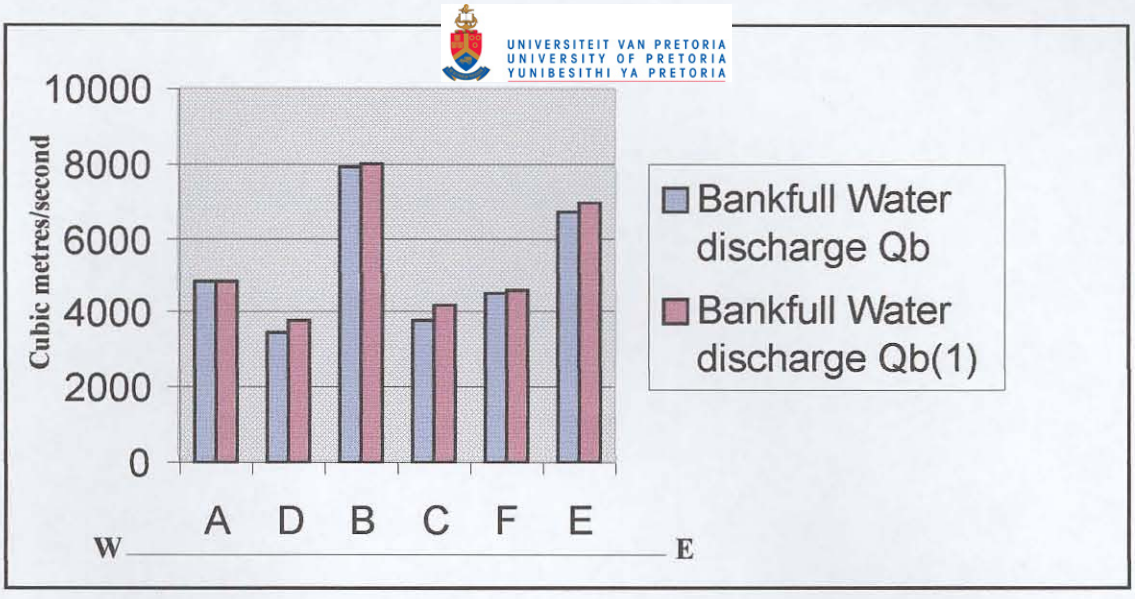

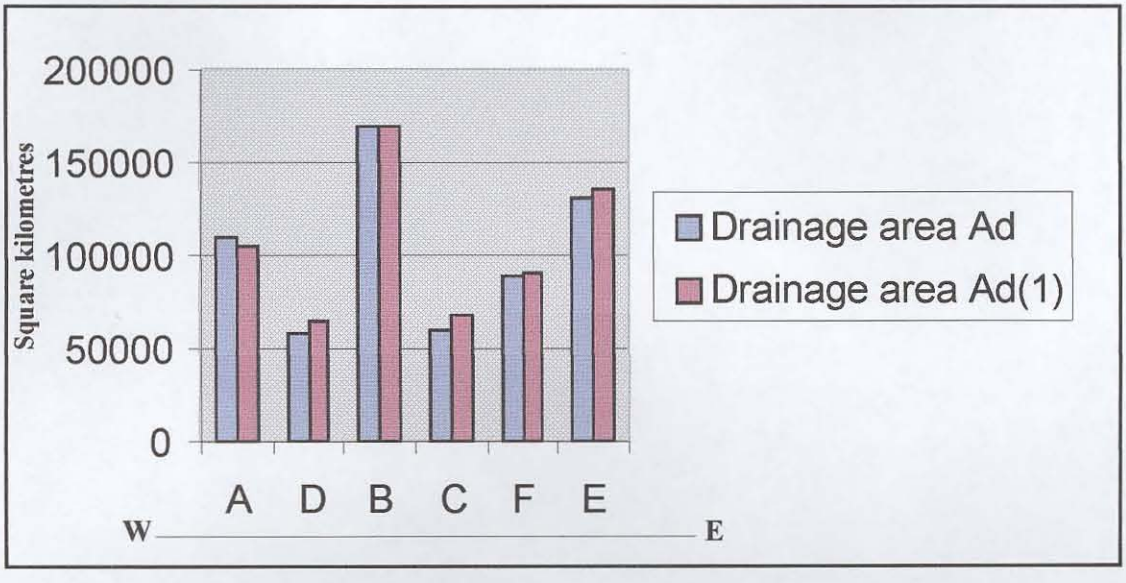

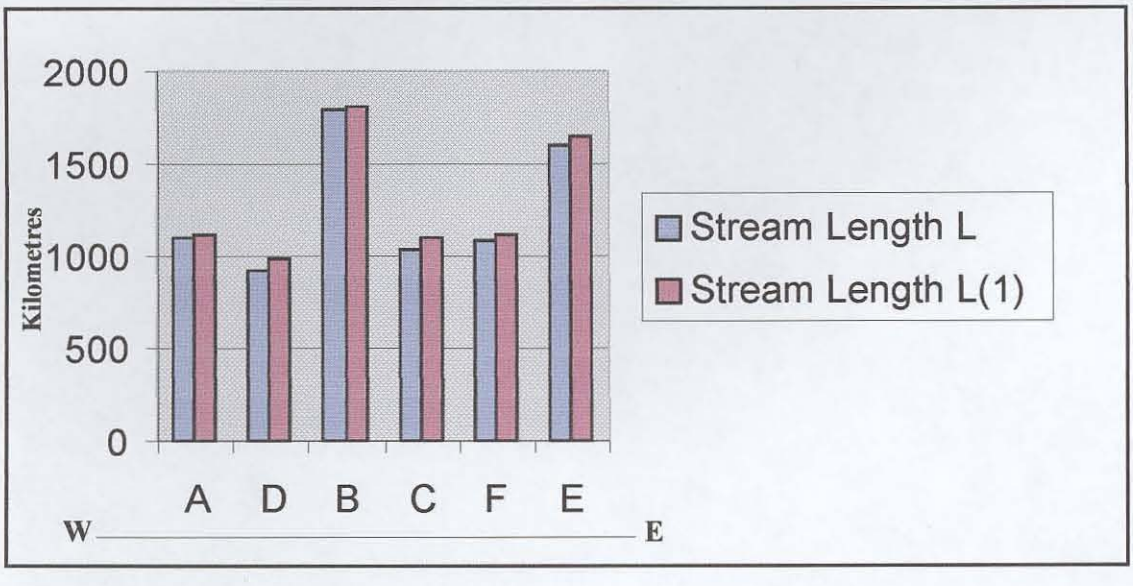

Figure 3.38: Histograms showing the variability of palaeohydrological parameters calculated from set thicknesses in the Lower Member of the Blouberg Formation. See Figure 3.35 for location of points A to E

Element	Symbol	Principal facies assemblage	Geometry and relationships
Channels (Major sandstone sheets)	CH (CHS)-sheet (CHR)-ribbon	Any combination	Finger, lens or sheet; concave-up erosional base; scale and shape highly variable.
Gravel bars and bedforms	GB	Gm, Gp, Gt	Lens, blanket;usually tabular bodies; commonly interbedded with SB
Sandy Bedforms	SB	St, Sp, Sh, Sl, Sr, Se, Ss	Lens, sheet, blanket, wedge, occurs as channel fills, crevasse splays, minor bars
Downstream accretion macroform	DA	St, Sp, Sh, Sl, Sr, Se, Ss	Lens, resting on flat or channelled base.
Lateral accretion macroform	LA	St, Sp, Sh, Sl, Sr, Se, Ss, less commonly Gm, Gt, Gp	Wedge, sheet lobe.
Scour hollows	HO	Gh, Gt, St, Sl	Scoop-shaped hollow with asymmetric fill
Sediment gravity flows	SG	Gmm, Gmg, Gci, Gcm	Lobe, sheet, typically interbedded with GB
Laminated sand sheet	LS	Sh, Sl; minor Sp, Sr	Sheet, blanket
Overbank fines	FF	Fm, Fl	Thin to thick blankets; commonly interbedded with SB; may fill abandoned channels

Facies Code	Facies	Sedimentary structures	Facies Code	Facies	Sedimentary structures
Gmm	Matrix-supported, massive gravel	Weak grading	Sh	Sand, fine to very coarse, may be pebbley	Horizontal lamination parting or streaming lineation
Gmg	Matrix-supported gravel	Inverse to normal grading	Sl	Sand, fine to very coarse, may be pebbley	Low-angle(<15°) cross-beds
Gci	Clast-supported gravel	Inverse grading	Ss	Sand, fine to very coarse, may be pebbley	Broad, shallow scours
Gcm	Clast-supported massive gravel	-	Sm	Sand, fine to coarse	Massive or faint lamination
Gh	Clast-supported, crudely bedded gravel	Horizontal bedding, imbrication	Fl	Sand, silt, mud	Fine lamination very small ripples
Gt	Gravel, stratified	Trough cross-beds	Fsm	Silt, mud	Massive
Gp	Gravel, stratified	Planar cross-beds	Fm	Mud, silt	Massive desiccation cracks
St	Sand, fine to very coarse may be pebbley	Solitary or grouped trough cross-beds	Fr	Mud, silt	Massive, roots, bioturbation
Sp	Sand, fine to very coarse may be pebbley	Solitary or grouped planar cross-beds	C	Coal, carbon-aceous mud	Plant, mud films
Sr	Sand, fine to very coarse	Ripple cross-lamination	P	Palaeosol carbonate (Calcite, siderite)	Pedogenic features; nodules, filaments

b.

BLOUBERG FORMATION

Upper Member	**Facies Association 4**	**Gmg; bedded, cross-bedded, massive, matrix supported conglomerate. Angular feldpsathic clasts (pebbles, cobbles, boulders). Laterally extensive sandstone-filled channel-forms or sandstone sheets define top of each fining-up cycle**	**475m**
	Facies Association 3	**Gmg; bedded, cross-bedded, massive, matrix supported conglomerate. Angular feldpsathic clasts (pebbles, cobbles, boulders). Arranged in fining-upward cycles (c.100cm). Channel forms with St. at top of each cycle.**	**250m**
Lower Member	**Facies Association 2**	**Sp, St; wedge-shaped sets, <20cm Sp, St; wedge-shaped sets, 20-30cm Planar-bedded sandstone Sandstone and granulestone-filled channels**	**350m**
	Facies Association 1	**Sp, St; wedge-shaped sets, 15-50cm medium- to coarse-grained sandstone Gt; Channel fills, 1.5-4m wide, 15-20cm deep. Clasts <7cm. Sub-euhedral feldspars**	**300m**

Stacking patterns within facies association 1 and 2 are comprised predominantly of alternating constituent facies.
Stacking pattens within facies association 3 and 4 are comprised predominantly of fining-upwards cycles.

Table 3.1: Architectural elements, and facies grouping for (a) fluvial deposits (after Miall, 1978; 1985), and (b) for the Blouberg Formation.

Location	Ch width	Ch depth	dm	Member	v	w	Q	A	S
A	2	0.3	0.15	1	0.00844	0.003674	0.02532	0.3	2.96E-05
D	4.8	0.8	0.05	1	0.0512	0.000576	0.0983	1.92	2.95E-06
	2.2	0.2	0.035	1	0.0435	0.000316	0.00957	0.22	7.41E-06
	5	0.55	0.04	1	0.0462	0.000396	0.06353	1.375	3.18E-06
	4	0.4	0.08	1	0.0634	0.001273	0.05072	0.8	1.02E-05
TotalD	16	1.95	0.205	4	0.2043	0.002561	0.22212	4.315	2.38E-05
AverageD	4	0.4875	0.05125	1	0.051075	0.00064	0.05553	1.07875	5.95E-06
F	3.5	0.36	0.035	1	0.0435	0.000316	0.02741	0.63	4.12E-06
E	6	0.6	0.04	2	0.0462	0.000396	0.08316	1.8	2.92E-06
	5	0.5	0.12	2	0.0762	0.00252	0.09525	1.25	1.35E-06
	4	0.35	0.06	2	0.0556	0.000784	0.03892	0.7	8.22E-06
	4.5	0.4	0.01	1	0.0246	0.00038	0.02214	0.9	7.88E-07
TotalE	19.5	1.85	0.23	7	0.2026	0.00408	0.23947	4.65	1.33E-05
AverageE	4.875	0.4625	0.0575	1.75	0.05065	0.00102	0.0598675	1.1625	3.32E-06
F	4	0.4	0.09	1	0.0669	0.001553	0.05352	0.8	1.18E-05
	4.6	0.2	0.01	1	0.0246	0.00038	0.011316	0.46	1.58E-06
	2.2	0.35	0.07	1	0.06	0.001016	0.0231	0.385	9.87E-06
TotalF	10.8	0.95	0.17	3	0.1515	0.002949	0.087936	1.645	2.33E-05
AverageF	3.6	0.316667	0.056667	1	0.0505	0.000983	0.029312	0.548333	7.76E-06

v= water velocity (meters/second)
w=Unit stream power (Watts)
Q=Discharge (Cubic metres/second)
A= Cross sectional area of channel (square metres)
s= Palaeoslope (metre/metre)

Table 3.2: Palaeohydrological parameters calculated from clast size and channel dimensions at locations shown in Figure 3.35 in the Blouberg Formation.

Location		h	dm	w	Qm	db	wb	Qm(1)	s	s(1)	Qb	Qb(1)	Ad	Ad(1)	L	L(1)
South	East	(m)	(m)	(m)	(m3s-1)	(m)	(m)	(m3s-1)	(m m-1)	(m m-1)	(m3s-1)	(m3s-1)	(km2)	(km2)	(km)	(km)
23° 09.12'	28° 41.22'	0.10	1.135124	91.07916	68.30937	3.530208	52.03679	23.24099	0.011894	0.030426	634.9355	825.9283	5457.237	7749.192	244.5185	301.7741
		0.12	1.323068	123.7362	92.80215	3.858272	58.93049	28.75049	0.011112	0.026184	806.351	1025.078	7505.256	10335.76	296.0379	358.7017
		0.19	1.94666	267.8628	200.8971	4.826846	80.63411	49.14858	0.00936	0.017934	1472.764	1766.898	16756.27	21360.69	479.3299	554.4945
		0.20	2.032402	291.9791	218.9843	4.949039	83.50629	52.17994	0.009182	0.017192	1575.194	1877.607	18327.87	23163.61	505.8191	582.119
		0.80	6.515421	3000.664	2250.498	9.726618	215.0486	263.0276	0.005472	0.005489	9694.891	9703.523	206723.8	206969.3	2164.524	2166.065
		0.30	2.857495	577.1697	432.8772	6.03041	110.1224	83.74733	0.007892	0.012312	2680.173	3035.56	37229.21	43952.65	773.8527	854.9074
		2.00	14.07168	13996.65	10497.49	15.20253	401.8575	766.1734	0.003886	0.002581	32224.16	28735.01	1025437	880133.5	5658.135	5162.466
		0.10	1.135124	91.07916	68.30937	3.530208	52.03679	23.24099	0.011894	0.030426	634.9355	825.9283	5457.237	7749.192	244.5185	301.7741
		0.30	2.857495	577.1697	432.8772	6.03041	110.1224	83.74733	0.007892	0.012312	2680.173	3035.56	37229.21	43952.65	773.8527	854.9074
		0.05	0.633982	28.41098	21.30824	2.51814	32.42663	10.35156	0.015408	0.053846	255.9323	363.3122	1624.926	2592.428	118.2029	156.4415
		0.30	2.857495	577.1697	432.8772	6.03041	110.1224	83.74733	0.007892	0.012312	2680.173	3035.56	37229.21	43952.65	773.8527	854.9074
		0.05	0.633982	28.41098	21.30824	2.51814	32.42663	10.35156	0.015408	0.053846	255.9323	363.3122	1624.926	2592.428	118.2029	156.4415
		0.30	2.857495	577.1697	432.8772	6.03041	110.1224	83.74733	0.007892	0.012312	2680.173	3035.56	37229.21	43952.65	773.8527	854.9074
		0.05	0.633982	28.41098	21.30824	2.51814	32.42663	10.35156	0.015408	0.053846	255.9323	363.3122	1624.926	2592.428	118.2029	156.4415
A		0.10	1.135124	91.07916	68.30937	3.530208	52.03679	23.24099	0.011894	0.030426	634.9355	825.9283	5457.237	7749.192	244.5185	301.7741
		0.20	2.032402	291.9791	218.9843	4.949039	83.50629	52.17994	0.009182	0.017192	1575.194	1877.607	18327.87	23163.61	505.8191	582.119
		0.04	0.525581	19.52596	14.64447	2.258637	27.84678	7.978641	0.016747	0.064708	191.0253	278.9076	1100.157	1822.274	93.54073	126.6182
		0.80	6.515421	3000.664	2250.498	9.726618	215.0486	263.0276	0.005472	0.005489	9694.891	9703.523	206723.8	206969.3	2164.524	2166.065
		0.20	2.032402	291.9791	218.9843	4.949039	83.50629	52.17994	0.009182	0.017192	1575.194	1877.607	18327.87	23163.61	505.8191	582.119
		1.00	7.85922	4366.076	3274.557	10.84414	250.4168	341.2544	0.005035	0.004568	12989.04	12640.06	305330.1	294441.3	2735.204	2676.254
		1.50	11.04982	8630.64	6472.98	13.2136	330.2325	547.7036	0.004327	0.003271	22100.7	20435.4	620213.6	558698.6	4184.589	3930.38
		0.25	2.451583	424.8404	318.6303	5.517652	97.24024	67.69872	0.008448	0.014306	2110.417	2445.819	27070.17	32953.31	639.1793	719.2295
		0.20	2.032402	291.9791	218.9843	4.949039	83.50629	52.17994	0.009182	0.017192	1575.194	1877.607	18327.87	23163.61	505.8191	582.119
		1.00	7.85922	4366.076	3274.557	10.84414	250.4168	341.2544	0.005035	0.004568	12989.04	12640.06	305330.1	294441.3	2735.204	2676.254
		0.30	2.857495	577.1697	432.8772	6.03041	110.1224	83.74733	0.007892	0.012312	2680.173	3035.56	37229.21	43952.65	773.8527	854.9074
		0.50	4.38948	1361.942	1021.456	7.735258	156.0467	151.995	0.006522	0.008084	5235.676	5560.152	90913.9	98502.88	1322.228	1387.386
		0.15	1.59595	180.0407	135.0305	4.301563	68.62255	37.30114	0.010223	0.021789	1080.335	1335.293	11085.23	14703.99	374.0888	443.1892
		0.80	6.515421	3000.664	2250.498	9.726618	215.0486	263.0276	0.005472	0.005489	9694.891	9703.523	206723.8	206969.3	2164.524	2166.065
		0.10	1.135124	91.07916	68.30937	3.530208	52.03679	23.24099	0.011894	0.030426	634.9355	825.9283	5457.237	7749.192	244.5185	301.7741
		0.15	1.59595	180.0407	135.0305	4.301563	68.62255	37.30114	0.010223	0.021789	1080.335	1335.293	11085.23	14703.99	374.0888	443.1892
		0.80	6.515421	3000.664	2250.498	9.726618	215.0486	263.0276	0.005472	0.005489	9694.891	9703.523	206723.8	206969.3	2164.524	2166.065
		0.14	1.506052	160.3291	120.2468	4.159321	65.46684	34.41599	0.01049	0.023062	986.9182	1230.484	9825.958	13185.64	347.979	415.1344
23° 09.01'	28° 42.01'	0.40	3.63895	936.0188	702.0141	6.938113	134.0071	117.1527	0.007088	0.009715	3907.855	4268.419	61553.29	69239.84	1046.354	1122.902
		Total	114.7344	51519.75	38639.81	204.5316	4040.599	4331.714	0.300373	0.658085	158963.4	159592.8	3606262	3483592	36169.28	36959.89
		Average	3.476801	1561.204	1170.903	6.197926	122.4424	131.2641	0.009102	0.019942	4817.072	4836.147	109280.7	105563.4	1096.039	1119.997

Table 3.3a: Palaeohydrological parameters calculated from Location A (Figure 3.35) in the Blouberg Formation.

Location			h	dm	w	Qm	db	wb	Qm(1)	s	s(1)	Qb	Qb(1)	Ad	Ad(1)	L	L(1)
South	East		(m)	(m)	(m)	(m3s-1)	(m)	(m)	(m3s-1)	(m m-1)	(m m-1)	(m3s-1)	(m3s-1)	(km2)	(km2)	(km)	(km)
23° 07.61'	28° 57.29'		0.40	3.63895	163.7527	702.0141	6.938113	134.0071	117.1527	0.007088	0.009715	3907.855	4268.419	61553.29	69239.84	1046.354	1122.902
			0.40	3.63895	163.7527	702.0141	6.938113	134.0071	117.1527	0.007088	0.009715	3907.855	4268.419	61553.29	69239.84	1046.354	1122.902
			0.60	5.116252	230.2313	1387.706	8.454099	176.7194	188.0268	0.006092	0.006957	6649.167	6900.827	125032.5	131381.7	1600.818	1649.107
B			0.85	6.85595	308.5177	2491.89	10.01831	224.1311	282.3076	0.005349	0.005222	10496.78	10426.15	229830.8	227771.2	2306.603	2294.179
			0.70	5.823844	262.073	1798.097	9.113745	196.3205	225.079	0.005752	0.006127	8138.124	8283.62	163693.9	167607.5	1881.687	1908.553
			0.40	3.63895	163.7527	702.0141	6.938113	134.0071	117.1527	0.007088	0.009715	3907.855	4268.419	61553.29	69239.84	1046.354	1122.902
			1.30	9.797836	440.9026	5089.252	12.3234	299.5112	463.4789	0.004565	0.00368	18320.59	17248.44	482969.1	445656.1	3601.469	3431.847
			Total	38.51073	1732.983	12872.99	60.7239	1298.704	1510.351	0.043023	0.051131	55328.23	55664.3	1186186	1180136	12529.64	12652.39
			Average	5.501533	247.569	1838.998	8.674842	185.5291	215.7644	0.006146	0.007304	7904.033	7952.043	169455.2	168590.9	1789.949	1807.484

Location			h	dm	w	Qm	db	wb	Qm(1)	s	s(1)	Qb	Qb(1)	Ad	Ad(1)	L	L(1)
South	East		(m)	(m)	(m)	(m3s-1)	(m)	(m)	(m3s-1)	(m m-1)	(m m-1)	(m3s-1)	(m3s-1)	(km2)	(km2)	(km)	(km)
23° 07.35'	28° 57.53'		0.40	3.63895	163.7527	702.0141	6.938113	134.0071	117.1527	0.007088	0.009715	3907.855	4268.419	61553.29	69239.84	1046.354	1122.902
			0.35	3.252695	146.3713	560.8934	6.500943	122.3367	100.2504	0.007451	0.010844	3280.348	3643.827	48740.86	56071.7	909.6282	989.4054
			0.30	2.857495	128.5873	432.8772	6.03041	110.1224	83.74733	0.007892	0.012312	2680.173	3035.56	37229.21	43952.65	773.8527	854.9074
C			0.45	4.017551	180.7898	855.69	7.348062	145.2218	134.4121	0.006783	0.008817	4560.281	4907.642	75623.28	83399.58	1183.917	1255.528
			0.40	3.63895	163.7527	702.0141	6.938113	134.0071	117.1527	0.007088	0.009715	3907.855	4268.419	61553.29	69239.84	1046.354	1122.902
			0.40	3.63895	163.7527	702.0141	6.938113	134.0071	117.1527	0.007088	0.009715	3907.855	4268.419	61553.29	69239.84	1046.354	1122.902
			0.45	4.017551	180.7898	855.69	7.348062	145.2218	134.4121	0.006783	0.008817	4560.281	4907.642	75623.28	83399.58	1183.917	1255.528
			Total	25.06	1,127.80	4,811.19	48.04	924.92	804.28	0.05	0.07	26,804.65	29,299.93	#########	#########	7,190.38	7,724.07
			Average	3.580306	161.1138	687.3133	6.863116	132.132	114.8972	0.007168	0.00999	3829.236	4185.704	60268.07	67791.86	1027.197	1103.439

Location			h	dm	w	Qm	db	wb	Qm(1)	s	s(1)	Qb	Qb(1)	Ad	Ad(1)	L	L(1)
South	East		(m)	(m)	(m)	(m3s-1)	(m)	(m)	(m3s-1)	(m m-1)	(m m-1)	(m3s-1)	(m3s-1)	(km2)	(km2)	(km)	(km)
23° 08.34'	28° 59.045'		0.25	2.451583	110.3213	318.6303	5.517652	97.24024	67.69872	0.008448	0.014306	2110.417	2445.819	27070.17	32953.31	639.1793	719.2295
			0.40	3.63895	163.7527	702.0141	6.938113	134.0071	117.1527	0.007088	0.009715	3907.855	4268.419	61553.29	69239.84	1046.354	1122.902
			0.50	4.38948	197.5266	1021.456	7.735258	156.0467	151.995	0.006522	0.008084	5235.676	5560.152	90913.9	98502.88	1322.228	1387.386
23° 08.02'	28° 55.18'		0.10	1.135124	51.08058	68.30937	3.530208	52.03679	23.24099	0.011894	0.030426	634.9355	825.9283	5457.237	7749.192	244.5185	301.7741
			0.40	3.63895	163.7527	702.0141	6.938113	134.0071	117.1527	0.007088	0.009715	3907.855	4268.419	61553.29	69239.84	1046.354	1122.902
			0.60	5.116252	230.2313	1387.706	8.454099	176.7194	188.0268	0.006092	0.006957	6649.167	6900.827	125032.5	131381.7	1600.818	1649.107
			0.55	4.755507	213.9978	1198.912	8.103066	166.5326	169.8741	0.006294	0.007474	5932.425	6224.852	107393.1	114508.8	1461.214	1518.558
			0.35	3.252695	146.3713	560.8934	6.500943	122.3367	100.2504	0.007451	0.010844	3280.348	3643.827	48740.86	56071.7	909.6282	989.4054
			0.45	4.017551	180.7898	855.69	7.348062	145.2218	134.4121	0.006783	0.008817	4560.281	4907.642	75623.28	83399.58	1183.917	1255.528
			1.00	7.85922	353.6649	3274.557	10.84414	250.4168	341.2544	0.005035	0.004568	12989.04	12640.06	305330.1	294441.3	2735.204	2676.254
			0.06	0.738951	33.25281	28.94845	2.752152	36.72242	12.80549	0.014394	0.046339	325.0272	450.9147	2234.736	3457.742	143.108	185.9532
D			0.30	2.857495	128.5873	432.8772	6.03041	110.1224	83.74733	0.007892	0.012312	2680.173	3035.56	37229.21	43952.65	773.8527	854.9074
			0.20	2.032402	91.45811	218.9843	4.949039	83.50629	52.17994	0.009182	0.017192	1575.194	1877.607	18327.87	23163.61	505.8191	582.119
			0.23	2.285685	102.8558	276.9659	5.297911	91.86213	61.42246	0.008715	0.015323	1891.906	2215.746	23399.12	28886.39	585.663	664.5749
			0.25	2.451583	110.3213	318.6303	5.517652	97.24024	67.69872	0.008448	0.014306	2110.417	2445.819	27070.17	32953.31	639.1793	719.2295
			0.20	2.032402	91.45811	218.9843	4.949039	83.50629	52.17994	0.009182	0.017192	1575.194	1877.607	18327.87	23163.61	505.8191	582.119
			0.32	3.016748	135.7537	482.4717	6.223116	115.0803	90.29747	0.007704	0.011674	2916.784	3276.781	41674.68	48670.21	828.0402	908.8369
			0.50	4.38948	197.5266	1021.456	7.735258	156.0467	151.995	0.006522	0.008084	5235.676	5560.152	90913.9	98502.88	1322.228	1387.386
			0.30	2.857495	128.5873	432.8772	6.03041	110.1224	83.74733	0.007892	0.012312	2680.173	3035.56	37229.21	43952.65	773.8527	854.9074
			0.25	2.451583	110.3213	318.6303	5.517652	97.24024	67.69872	0.008448	0.014306	2110.417	2445.819	27070.17	32953.31	639.1793	719.2295
			0.12	1.323068	59.53806	92.80215	3.858272	58.93049	28.75049	0.011112	0.026184	806.351	1025.078	7505.256	10335.76	296.0379	358.7017
			0.30	2.857495	128.5873	432.8772	6.03041	110.1224	83.74733	0.007892	0.012312	2680.173	3035.56	37229.21	43952.65	773.8527	854.9074
			0.45	4.017551	180.7898	855.69	7.348062	145.2218	134.4121	0.006783	0.008817	4560.281	4907.642	75623.28	83399.58	1183.917	1255.528
			Total	73.57	3,310.53	15,222.38	144.15	2,730.29	2,381.74	0.19	0.33	80,355.77	86,875.79	#########	#########	21,159.96	22,671.45
			Average	3.198576	143.9359	661.8425	6.26735	118.7082	103.5539	0.008124	0.014229	3493.729	3777.208	58804.45	64123.15	919.9984	985.715

Table 3.3b: Palaeohydrological parameters calculated from locations B, C and D (Figure 3.35) in the Blouberg Formation.

Location			h	dm	w	Qm	db	wb	Qm(1)	s	s(1)	Qb	Qb(1)	Ad	Ad(1)	L	L(1)
South	East		(m)	(m)	(m)	(m3s-1)	(m)	(m)	(m3s-1)	(m m-1)	(m m-1)	(m3s-1)	(m3s-1)	(km2)	(km2)	(km)	(km)
23° 07.24'	29° 02.92'		0.20	2.032402	91.45811	218.9843	4.949039	83.50629	52.17994	0.009182	0.017192	1575.194	1877.607	18327.87	23163.61	505.8191	582.119
23° 07.13'	29° 01.64'		0.60	5.116252	230.2313	1387.706	8.454099	176.7194	188.0268	0.006092	0.006957	6649.167	6900.827	125032.5	131381.7	1600.818	1649.107
			0.70	5.823844	262.073	1798.097	9.113745	196.3205	225.079	0.005752	0.006127	8138.124	8283.62	163693.9	167607.5	1881.687	1908.553
			0.80	6.515421	293.1939	2250.498	9.726618	215.0486	263.0276	0.005472	0.005489	9694.891	9703.523	206723.8	206969.3	2164.524	2166.065
			0.70	5.823844	262.073	1798.097	9.113745	196.3205	225.079	0.005752	0.006127	8138.124	8283.62	163693.9	167607.5	1881.687	1908.553
			0.75	6.171474	277.7163	2019.164	9.425422	205.7838	243.9477	0.005605	0.005789	8908.437	8989.195	184672.4	186907.9	2022.876	2037.533
			0.60	5.116252	230.2313	1387.706	8.454099	176.7194	188.0268	0.006092	0.006957	6649.167	6900.827	125032.5	131381.7	1600.818	1649.107
			0.70	5.823844	262.073	1798.097	9.113745	196.3205	225.079	0.005752	0.006127	8138.124	8283.62	163693.9	167607.5	1881.687	1908.553
			0.60	5.116252	230.2313	1387.706	8.454099	176.7194	188.0268	0.006092	0.006957	6649.167	6900.827	125032.5	131381.7	1600.818	1649.107
	E		0.72	5.963357	268.3511	1885.277	9.239743	200.1308	232.6004	0.005692	0.005987	8444.264	8564.769	171955.4	175235	1938.106	1960.201
			0.50	4.38948	197.5266	1021.456	7.735258	156.0467	151.995	0.006522	0.008084	5235.676	5560.152	90913.9	98502.88	1322.228	1387.386
			0.45	4.017551	180.7898	855.69	7.348062	145.2218	134.4121	0.006783	0.008817	4560.281	4907.642	75623.28	83399.58	1183.917	1255.528
			0.50	4.38948	197.5266	1021.456	7.735258	156.0467	151.995	0.006522	0.008084	5235.676	5560.152	90913.9	98502.88	1322.228	1387.386
			0.65	5.472223	246.25	1587.527	8.790432	186.6398	206.4339	0.005913	0.006513	7384.738	7587.305	143807	149090.5	1740.989	1779.091
			0.70	5.823844	262.073	1798.097	9.113745	196.3205	225.079	0.005752	0.006127	8138.124	8283.62	163693.9	167607.5	1881.687	1908.553
			0.80	6.515421	293.1939	2250.498	9.726618	215.0486	263.0276	0.005472	0.005489	9694.891	9703.523	206723.8	206969.3	2164.524	2166.065
			0.65	5.472223	246.25	1587.527	8.790432	186.6398	206.4339	0.005913	0.006513	7384.738	7587.305	143807	149090.5	1740.989	1779.091
			0.50	4.38948	197.5266	1021.456	7.735258	156.0467	151.995	0.006522	0.008084	5235.676	5560.152	90913.9	98502.88	1322.228	1387.386
			0.47	4.167076	187.5184	920.5694	7.505462	149.5955	141.4081	0.006674	0.008507	4827.78	5167.118	81594.95	89330.11	1239.156	1308.358
			0.40	3.63895	163.7527	702.0141	6.938113	134.0071	117.1527	0.007088	0.009715	3907.855	4268.419	61553.29	69239.84	1046.354	1122.902
			Total	101.78	4,580.04	28,697.62	167.46	3,505.20	3,781.01	0.12	0.15	########	########	########	########	32,043.14	32,900.65
			Average	5.088934	229.002	1434.881	8.373149	175.2601	189.0503	0.006232	0.007482	6729.505	6943.691	129870.2	134974	1602.157	1645.032

Location			h	dm	w	Qm	db	wb	Qm(1)	s	s(1)	Qb	Qb(1)	Ad	Ad(1)	L	L(1)
South	East		(m)	(m)	(m)	(m3s-1)	(m)	(m)	(m3s-1)	(m m-1)	(m m-1)	(m3s-1)	(m3s-1)	(km2)	(km2)	(km)	(km)
23° 06.28'	29° 01.83'		0.85	6.85595	308.5177	2491.89	10.01831	224.1311	282.3076	0.005349	0.005222	10496.78	10426.15	229830.8	227771.2	2306.603	2294.179
			0.32	3.016748	135.7537	482.4717	6.223116	115.0803	90.29747	0.007704	0.011674	2916.784	3276.781	41674.68	48670.21	828.0402	908.8369
			0.70	5.823844	262.073	1798.097	9.113745	196.3205	225.079	0.005752	0.006127	8138.124	8283.62	163693.9	167607.5	1881.687	1908.553
	F		0.10	1.135124	51.08058	68.30937	3.530208	52.03679	23.24099	0.011894	0.030426	634.9355	825.9283	5457.237	7749.192	244.5185	301.7741
			0.05	0.633982	28.52919	21.30824	2.51814	32.42663	10.35156	0.015408	0.053846	255.9323	363.3122	1624.926	2592.428	118.2029	156.4415
			Total	17.47	785.95	4,862.08	31.40	620.00	631.28	0.05	0.11	22,442.56	23,175.80	#########	#########	5,379.05	5,569.78
			Average	3.49313	157.1908	972.4153	6.280704	123.9991	126.2553	0.009222	0.021459	4488.511	4635.159	88456.3	90878.12	1075.811	1113.957

Table 3.3c: Palaeohydrological parameters calculated from locations E and F (Figure 3.35) in the Blouberg Formation.

h = set thickness of trough cross-beds
dm = mean water depth
w = channel width
Qm = maximum instantaneous water discharge
db = mean bankfull channel depth
wb = bankfull channel width
Qm(1) = average daily discharge (equation11)

s = stream palaeoslope (equation 12)
s(1) = stream palaeoslope (equation 13)
Qb = bankfull water discharge
Qb(1) = bankfull water discharge (using s(1) values)
Ad = drainage area (using Qb values)
Ad(1) = drainage area (using Qb(1) values)
L = principal stream area (using Ad values)
L(1) = principal stream length (using Ad(1) values)

CHAPTER 4: THE WATERBERG GROUP.

4.1: Introduction:

Within the study area, three Formations within the Waterberg Group have been identified (Appendix 1). These are the Setlaole Formation, Makgabeng Formation and the Mogalakwena Formation. Generally, the Setlaole Formation outcrops poorly, though a few isolated outcrops occur east of the Makgabeng Plateau (Figure 1.2). The Makgabeng Formation has excellent exposure at the type locality, the Makgabeng Plateau, though it is generally absent or poorly exposed in other parts of the study area. The Mogalakwena Formation can generally be found in locations throughout the area, though all Waterberg strata seem to be absent from the far north-western portion (Appendix 1).

4.2: Setlaole Formation:

The extent of outcrop of the Setlaole Formation is insufficient to establish the three-dimensional geometry, and so architectural elements for the Setlaole Formation could not be defined. The most northerly outcrop of the Setlaole Formation in the study area was found at 23°09.67'S; 29°03.50'E, where the unit consists of facies of planar and trough cross-bedded coarse sandstone and granulestone (Figure 4.1), with sub-rounded clasts and pebbles of quartz and quartzite. Many mesoscopic euhedral feldspar crystals and detrital micas are also present. Locally, small cobbles of foliated rocks (probably basement gneiss) can be found (Figure 4.2).

At 23°11.46'S; 29°01.79'E, the lithofacies are comparable to those outlined above, but are generally more mature. The lithology consists of coarse sandstone (granulestone occurs only locally), and there are no feldspars visible in hand specimens. Pebbles, where present, are all well-rounded and quartzitic (there are no feldspar-rich or foliated clasts). Palaeocurrents from both these localities are shown in Figure 4.3, and suggest that currents flowed towards the south.

The type locality for the Setlaole Formation is a low hill (Setlaole) at 23°21.60'S; 28°58.00'E, in the south-eastern corner of the study area, east of the Makgabeng plateau. Here, about 30-40m of sedimentary rocks is exposed on the eastern edge of the hill, which nonconformably overlies basement granite and amphibolite. The top part of the hill at Setlaole is underlain by a thick, sub-concordant diabase sill, which intrudes the Setlaole Formation, and which restricts the vertical extent of the outcrop of the Setlaole strata. At 23°20.36'S; 28°58.00'E, on the northern side of Setlaole, the nonconformity between the basement and the Setlaole Formation is exposed. The basal beds of the Setlaole Formation consist of a thin (c.15cm) quartz and granitic pebble conglomerate, with sub-angular pebbles having a maximum diameter of about 2.5-3cm (Figure 4.4). The pebble conglomerate is overlain by a 50cm-thick hard black mudrock (Figure 4.4). At this locality, less than 1m of Setlaole strata is exposed between the basement and the intruding diabase sill above.

Further to the south on Setlaole hill, at 23°20.90'S; 28°58.00'E, about 30m of Setlaole sedimentary rocks from higher in the Formation crop out. They consist of a coarse- and very coarse-grained sandstone and granulestone facies, with trough cross-beds (Figure 4.5). Sets are between 10 and 30cm in thickness, and preserved troughs are between 40 and 150cm wide. Rare quartz pebbles are present in the sandstones, and have a maximum diameter of 2-3cm (Figure 4.6). The rocks have a purplish colour, though are locally reduced to a pale cream colour, especially in beds composed of coarser sediment grains (Figure 4.6). The quartz grains in the sandstone are generally moderately to poorly sorted, with angular grains of low sphericity. Rare laminatae of medium to fine sandstone, which is moderately sorted, are also present. Palaeocurrent directions at this locality conform to the general southward direction recorded from Setlaole strata further north in the field area (Figure 4.7). Thin sections of the Setlaole Formation, taken from 23°16.33'S; 28°59.94'E show the feldspathic character of the unit in the north (Figure 4.8). Point counting (averaged from 300 points in 1 section) shows that this rock is comprised of 51% quartz, 29% matrix (=clay), 16% lithic fragments (=quartzite), 3% opaque minerals, and 1% feldspar. The rock is poorly sorted, and grains appear to be sub-angular and of low sphericity.

At 23°06.54'S; 28°49.38'E, 2km south east of My Darling (Appendix 1), a low hill is underlain by a white/pale cream pebbly granulestone (Figure 4.9), which bears considerable similarity to the facies observed at the Setlaole type locality (e.g. compare Figure 4.6 with Figure 4.9). Locally, quartz cobbles are also present, and reach a maximum diameter of 15-20cm. Coarse sandstone is interbedded with the pebbly granulestone, and is generally purple in colour. Pale coloured pebbly granulestone deposits are trough cross-bedded, though purple coarse sandstone exhibits planar bedding (Figure 4.10). Locally, clasts also consist of jasper and dark red-coloured coarse sandstone (Figure 4.11). Palaeocurrent directions measured from trough cross-beds suggest that transport was towards the south (an average trend of 197°), parallel with palaeocurrent directions measured from more southerly Setlaole strata (Figures 4.3 and 4.7). This outcrop has previously been mapped as belonging to the Blouberg Formation (Semaoko Grit Member; Jansen, 1976) and to the Soutpansberg Group (Callaghan and Brandl, 1991).

4.3: Makgabeng Formation:

Outcrop of the Makgabeng Formation is limited to an area in the south-eastern portion of the study area (Appendix 1). The most northerly outcrop of the Makgabeng Formation was recorded at 23°10.50'S; 28°52.70'E, about 4km south of the southern strand of the Melinda Fault Zone. Outcrop quality of the Makgabeng Formation is generally good to the south of this area, especially at the type locality, the Makgabeng plateau (Figure 1.2). In the south-western part of the study area, the Makgabeng Formation is overlain and largely obscured by the Mogalakwena Formation, and consequently the western extent of the Formation within the study area cannot be determined, though the most westerly outcrop of the Makgabeng Formation was recorded in the banks of the deeply incised Mogalakwena River at Steilloopbrug (23°25.94'S; 28°37.20'E), where the river has cut down through the thin layer of overlying basal Mogalakwena Formation conglomerate, to expose the upper strata of the Makgabeng Formation. It thus seems likely that the Makgabeng Formation underlies the Mogalakwena Formation throughout the study area.

Within the type locality, a vertical section of the Formation is exposed in cliffs on the northern edge of the Makgabeng plateau. The plateau area itself exhibits three-dimensional outcrops of the upper part of the Formation. In the plateau area, the Makgabeng Formation is between 300 and 400m thick. A borehole drilled through the Mogalakwena Formation 4km south-west of Steilloopbrug (approximately 23°28'S; 28°36'E) intersected 570m of Makgabeng Formation strata, locally intruded by diabase sills (Van der Neut, 1994). The underlying Setlaole Formation was intersected 639m below the surface. The borehole core was also logged during the present study, and a summary of this log is shown in Figure 4.12. As previous workers (Meinster and Tickell, 1975; Callaghan, 1987; Callaghan et al., 1991; Eriksson et al., 2000) are unanimous in their interpretation that the strata of the Makgabeng Formation were deposited in an aeolian palaeoenvironment (Section 1.4.2), a brief discussion of aeolian bounding surfaces is pertinent. This study will focus on a consideration of architectural elements and detailed interpretation of both aeolian and aqueous processes within the Makgabeng palaeo-desert.

Generally, the Makgabeng Formation is preserved as inclined foresets (Section 4.3.3.1), though rare bedding surfaces show horizontal inclination, indicating that the Makgabeng Formation is relatively tectonically undisturbed. The rocks of the Makgabeng Formation are pale coloured red-beds, though these are often reduced along certain foreset and bedding planes and within spherical reduction spots. Reduced areas are pale cream in colour.

4.3.1: Bounding surfaces in aeolian sediments and sedimentary rocks:

The scheme of architectural element analysis (Miall, 1985), developed initially for classification of fluvial sediments cannot be readily applied to aeolian deposits, though previous workers (e.g. Brookfield, 1977; Kocurek, 1988; Blakey *et al.*, 1996) have stressed the importance of the identification of bounding surfaces within aeolian sediments. Brookfield (1977) classified a three-stage hierarchy of bounding surfaces within an aeolian environment. First-order surfaces (largest scale) are flat-lying bedding

surfaces, which are attributed to the passage of draas (large dunes with smaller parasitic dunes migrating on the stoss and lee sides), across an inter-dune area. Second-order surfaces (which may be cut by first-order surfaces) bound individual dunes and are attributed to the migration of dunes across draas (they are, essentially, a cross-bed set boundary; Figure 4.13). Third-order surfaces are 'reactivation surfaces' (McKee, 1966) within an individual dune foreset, caused by temporary changes in transport (i.e. wind) direction, leading to fluctuation in dip direction of the dune foresets (Brookfield, 1977). Third-order surfaces may be cut by first- and second-order surfaces (Figure 4.14a). The three orders of surfaces outlined above may all be climbing surfaces, i.e. the features can move upwards relative to a horizontal depositional surface (Figure 4.14b), due to the prograding-upwards nature of migrating sand dunes (Brookfield, 1977).

Kocurek (1988) identified yet another surface, of lower order than a first-order surface, and which does not climb (i.e. the surface is generally horizontal, apart from localised relict dune topography) formed by a major hiatus in erg (sand sea) deposition (Figure 4.14b). Such surfaces are termed 'super surfaces' and the hiatus in sedimentation can be caused by *climatic change*, *tectonic* and *sea level change* or by the *migration of ergs* (Kocurek, 1988) across an area to a site more favourable for deposition. *Climatic change* can either promote or degrade an aeolian environment by controlling surface vegetation (not applicable to Proterozoic ergs), controlling the input of sand into an erg by fluvial transport (i.e. rainwater runoff) and by changes in wind direction and velocity. *Tectonic* control over super surface formation is influential by means of a greater sediment supply from uplifted source areas (provided, of course, that the tectonically uplifted area is upwind of the erg and weathers to provide grains of suitable size for deflation). It is possible, however that wind direction may be modified by topography, and thus there is an additional, indirect tectonic control over wind direction. Eustatic fall in *sea level* enhances continental freeboard, and promotes erosion of this high-lying continental region, thus maximizing sediment supply. A sea level rise can create intervening water bodies within an erg, which act as barriers to aeolian sedimentation. The *migration of ergs* into, or away from a particular area is controlled by whether the area is suitable for deposition or deflation (i.e. wind erosion). Generally, areas which are sites of deposition

are areas of deceleration of wind speed, such as those caused by wind blowing over a topographical basin, which allows the sediment-laden air to expand vertically, decelerate and become supersaturated with sand, which is therefore deposited from suspension. Erg margins therefore commonly follow topographic contours (Kocurek, 1988), and thus the margins of highland areas act as boundaries for erg deposition. Deceleration may also occur in areas where winds with different directions converge, accounting for an overall drop in wind velocity (Kocurek, 1988). Similarly, areas which have accelerating or diverging winds passing over them (e.g. winds blowing up highland areas, or where wind is forced through a topographical constriction) are undersaturated with sand, and become deflated (Bagnold, 1954; Kocurek, 1988).

Thus, a hiatus in deposition, due to a shift in conditions favourable for deposition to those favourable for deflation, caused by any or several of the reasons outlined above, will result in the creation of a super surface across the erg. The level in the erg at which a super surface develops is often controlled by deflation down to a horizontal surface within the erg at which deflation is impeded. Commonly, such surfaces represent the palaeo-water table (wet sand cannot be wind-blown), an armoured lag deposit within the erg (a layer of rocks too large to be moved by aeolian transport), or the development of a vegetated layer (again, not applicable to Proterozoic aeolian deposits, although microbial mats may have played a role). Alternatively, deflation could simply be stopped by renewed sedimentation (e.g. the migration of a subsequent erg over the deflated erg, or by a change in environment, leading to overlying alluvial or marine deposits; Kocurek, 1988).

Clues as to the cause of the development of the super surface often remain in the geological record. Super surfaces developed at a water table may contain evidence for evaporites, polygonal desiccation cracks and enhanced cementation of sand (i.e. playa lake deposits). Those developed due to a climatic change to more humid conditions show evidence for rapid stabilization of dunes by vegetation, thus leading to relict dune topography, plant roots and soil horizons along the super surface. Importantly these diagnostic features would not be expected in aeolian deposits earlier than the

Phanerozoic. Super surfaces caused by lag deposits are readily identifiable by the presence of the lag at the surface, and those caused by erg migration tend to produce a super surface with planar palaeotopography (no increase in rainfall means vegetation cannot stabilise the dunes). Super surfaces which are drowned by later sediments (i.e. if sedimentation is renewed before deflation down to the water table or a lag deposit) can be identified by the fact that they cut first-order surfaces (in the case of resumed aeolian sedimentation), or by the presence of contrasting sediments (in the case of the onset of marine or fluvial sedimentation) (Kocurek, 1988).

The four-order hierarchy of surfaces within aeolian sediments therefore gives an architectural framework within which an aeolian deposit can be considered, that is comparable to the architectural element scheme applied to fluvial sediments by Miall (1985). In particular the identification of a super surface is important as it gives clues to the causes of development of the surface and, as such, is an important tool for the interpretation of syn-depositional conditions (such as tectonic, eustatic and palaeoclimatic change). Additionally, identification of a super surface acts as a powerful means of correlation between outcrops.

4.3.2: Bounding surfaces present in the Makgabeng Formation:

High-order (i.e. second- and third-order) surfaces are present in most outcrops of the Makgabeng Formation. Figure 4.13 shows a second-order surface developed between two dunes, which reflects deposition in two opposing wind directions. Figure 4.14a shows a third-order surface (a reactivation surface; McKee, 1966) which similarly developed as a result of fluctuating wind direction, though in this case, the angle between the earlier and later wind directions was slight, and did not lead to total destruction of the earlier dune.

First-order surfaces could not be identified within the Makgabeng Formation, though two examples of super surfaces could be identified. The first consists of laterally extensive playa lake deposits, which can be traced horizontally for up to 5km at the northern edge of the Makgabeng Plateau at 23°13.60'S; 28°52.80'E (Section 4.3.3.3).

The second super surface identified marks the contact between the Makgabeng Formation and the overlying Mogalakwena Formation. Regionally, the conglomerates and sandstones of the latter are thought to have a conformable relationship with the aeolian deposits beneath (Callaghan *et al.*, 1991). The contact between the two formations, shown in Figure 4.15, is clearly sharp, and can be mapped for several hundred metres as exhibiting little palaeotopography at the contact. Topmost aeolian dunes in the Makgabeng Formation were generally largely eroded prior to the onset of fluvial Mogalakwena sedimentation (Figure 4.15). Such a non-climbing architecture for these topmost palaeo-dunes therefore clearly represents a super surface.

4.3.3: Facies present in the Makgabeng Formation:

The sedimentary rocks of the Makgabeng Formation, bound by the hierarchy of surfaces outlined above, are composed of five facies associations; (1) large-scale trough and planar cross-bedded sandstone, (2) horizontally bedded and rippled mudstone and sandstone, (3) horizontally and cross-bedded sandstone and mudstone, (4) massive sandstones, and (5) planar bedded and trough cross-bedded pebbly sandstone.

4.3.3.1: Large-scale trough and planar cross-bedded sandstone facies association:

This facies association consists dominantly of inversely-graded foresets of laminated, well sorted, well rounded, fine- to medium-grained, locally rippled sandstone, with minor, thin wedge-shaped strata (Simpson *et al.*, 1999). The inversely graded sandstone occurs in laminations between 2 and 10mm thick (Figure 4.16), though the average thickness of each lamina is around 5mm. Each lamination shows inverse grading from fine-grained sandstone at the lower surface of the lamination to medium-grained sandstone on the upper surface of the lamination, and consists of well-sorted quartz arenites (Figure 4.16). The diagnostic inverse-grading of strata can often only be recognised in the field by examination with a hand lens of exposure faces which have developed at a shallow angle to the lamination plane. Thus a very oblique exposure

section through a thin lamination provides a surface on which changes in grading between fine- and medium-grade sandstones within the lamination can be identified more easily. Asymmetric ripplemarks are rarely preserved in association with low-angled, inversely-graded strata (Figure 4.17). Ripple wavelength averages 7.5cm, and they have an average amplitude of about 3mm. Ripple index (wavelength/amplitude) averages 25, and ripple symmetry index (crest to trough distance/wavelength) averages 0.3.

The inclination of inversely-graded cross-strata varies from horizontal to a high angle of inclination (reaching a maximum preserved angle of about 25-30°) (Figure 4.18). The thin wedge-shaped strata occurring between the inversely-graded foresets taper in the down-dip direction (Figure 4.19), and are generally found in association with high-angled inversely-graded cross-strata, and usually dip in excess of 20°. They are also composed of fine- to medium-grained laminated arenites, though they contain no evidence for internal grading (Figure 4.19). In plan view, wedge-shaped strata extend for between 50cm and 3m across the foresets, and may be up to 30cm thick (Simpson *et al.*, under review). The lower contacts of wedge-shaped sets with underlying inversely-graded strata are irregular to sharp.

The inversely-graded strata and wedge-shaped strata can be found together in both planar and trough cross-bedded sets in the Makgabeng Formation. Large-scale mapping of foresets on the Makgabeng plateau was undertaken by use of plane table and open sighted alidade. This map is shown in Figure 4.20, and identifies a combination of foresets which have a consistent strike (i.e. planar cross-bedding), and foresets which have a variable strike, so that dip-directions converge (i.e. trough cross-bedding), and which are arcuate in plan view. The average dip direction of foresets can be used to determine palaeowind directions. Callaghan (1987) determined an average palaeowind direction of 226° based on foreset directions in the Makgabeng Formation. Similarly, foreset directions recorded in the study area (insert in Figure 4.20) suggest a palaeowind direction towards, on average, 215°.

Preserved planar cross-bedded sets vary in set thickness between 1.5 and 10m, and the strike of planar foresets can be traced for over 150m without appreciable change in strike orientation (Simpson *et al.*, under review). In the down dip direction, foresets can be traced for up to 400m, with little change in the foreset dip angle at a consistent height above the lower set boundary (Simpson *et al.*, under review). Dip angles of foresets vary between horizontal and 28°. Preserved trough cross-bedded sets are between 1 and 6m thick, and can be traced laterally for up to 70m (Simpson *et al.*, under review). Angles of the dip of foresets vary from horizontal to 22° at the set top. Sets of both planar and trough cross-bedded strata are bounded by 2nd order surfaces, and locally contain 3rd order surfaces.

Generally, within the Makgabeng Formation in exposures on the Makgabeng Plateau, it was found that trough cross-bedded sets are dominant in the lowermost half of the Formation, and are then superseded by planar cross-bedded sets towards the top. However, in the uppermost part of the Formation, in common association with the presence of the massive sandstone facies association (Section 4.3.3.4) there is a return to the predominance of trough cross-beds.

4.3.3.2: Horizontally bedded and rippled mudrock and sandstone facies association:

The data presented here were recorded in a cliff section on the northern edge of the Makgabeng plateau at 23°13.60'S; 28°52.80'E, though evidence for this facies association was also found in the core from the bore hole drilled 4km south-west of Steilloopbrug (approximately 23°28'S; 28°36'E; Figure 4.12), and in the top most 2m of the Makgabeng Formation at Steilloopbrug (23°25.94'S; 28°37.20'E).

Four lenses of laminated mudstone and sandstone beds were found on the north of the plateau, which extend laterally for up to 100m, before pinching out or being truncated by large-scale trough cross-bed deposits. The lenticular strata are between 40 and 110cm thick (Eriksson *et al.*, 2000), and together occupy approximately 5m in thickness within the Magkabeng succession exposed within the cliff face. The lower surface of the facies

association is conformable with the upper bounding surfaces of horizontally inclined strata of the large-scale cross-bedded facies association beneath. The beds of this lenticular facies association are internally comprised of facies of massive sandstone, wave, combined flow, current and wind rippled sandstones and mudrocks (Figure 4.21 and 4.22) (Eriksson *et al.*, 2000). Additional minor structures also present locally are adhesion structures, mudcracks (Figure 4.22), rolled-up mud laminations (Figures 4.23 and 4.24), rainspots and evaporite casts, probably of gypsum crystals (Figure 4.25) (Simpson *et al.*, 1999; Eriksson *et al.*, 2000). These structures are arranged with massive, horizontally stratified and current rippled sandstones at the base, followed by wave and combined flow ripples above. In the upper most part of the beds, wind-rippled sandstone, adhesion warts, desiccation cracks and evaporite casts are found (Simpson *et al.*, 1999).

With a general absence of preserved bedding planes in the large-scale trough and planar cross-bedded facies (mostly only inclined foresets are well preserved, with fewer bounding surfaces), horizontally bedded deposits of this facies association offer rare evidence for the direction of tectonic dip of the Makgabeng Formation. Generally, lenticular occurrences of the horizontally bedded and rippled mudrock and sandstone facies association in the Makgabeng Formation retain their horizontal dip (and rarely have a dip in excess of 5°), indicating a general lack of deformation within the Makgabeng Formation.

The rolled-up mud laminations found within this facies association consist of red-coloured silty mudstone laminations between 1 and 2mm thick (Figures 4.23 and 4.24). The laminations are curled into cylindrical, cigar-shaped structures, so that the original upper surface of the lamination is facing towards the centre (Eriksson *et al.*, 2000). The roll-up structures are up to 5cm in length, 2-3cm wide and consist of up to two or three concentric layers (i.e. more than 720° of curvature on the upper surface of the lamination). The long axes of these structures are orientated approximately parallel to each other (Eriksson *et al.*, 2000). The structures show evidence for having been slightly flattened perpendicular to the bedding plane, and are now elliptical in shape. Several

other mudchips, which only show slight curling, are also associated with the roll-up structures (Eriksson *et al.*, 2000).

4.3.3.3: Rippled and cross-bedded sandstone facies association:

This facies association is also observed in the vertical cliff on the northern edge of the Makgabeng plateau at 23°13.60'S; 28°52.80'E, a few metres above the horizontally bedded, rippled mudrock and sandstone facies association previously described, and can be traced laterally for up to 5km, and reaches a maximum thickness of about 30m. This cross-bedded sandstone facies association contains a basal decimetre–thick mudrock, though it is generally sandy for the majority of the sequence above. The sandstone facies above contains the following structures; asymmetric ripples (both strongly and weakly asymmetric), symmetrical ripples, inversely graded laminations in sandstone (identical to that described in Section 4.3.3.1) and, more rarely, massive sandstone and horizontally laminated sandstone (Simpson *et al.*, under review). The beds are arranged in vertical sequences which fine and thin upwards, from medium- to fine-grained sandstone or mudrocks. The structures are commonly arranged from bottom to top in the following manner: strongly assymmetrical ripples, inversely graded laminations, slightly asymmetrical ripples, asymmetrical ripples, inversely graded laminations, symmetrical ripples, inversely graded laminations, symmetrical ripples, massive sandstones, symmetrical ripples, inversely graded laminations, and massive sandstone (Simpson *et al.*, under review).

Thin lenses of large-scale, cross-bedded facies are also present, though they are not laterally continuous. Generally these occurrences of the large-scale, cross-bedded facies association exhibit low to horizontal angles of dip.

In addition to the structures previously described, the top surfaces of the thinning and fining upwards sequences contain small pits, less than 3mm deep. The pits are filled with sandstone, mudstone or siltstone from the overlying bed. The sand grains around the pits

are less well sorted than the surrounding beds, and the area of 2-3mm radius around the pit is a zone of preferential quartz cementation (Simpson *et al.*, under review).

Samples of this facies association taken from the borehole core were analysed by X-ray diffraction, which showed trace amounts of anhydrite and lesser amounts of gypsum present.

4.3.3.4: Massive sandstone facies asscociation:

This facies association is found generally in the upper half of the Makgabeng Formation, and is especially well exposed in good three-dimensional outcrops across the top of the Makgabeng plateau area, beneath the contact with the Mogalakwena Formation. This trend is also shown in the bore hole log (Figure 4.12) which shows that occurrences of this facies association are less common in the lower most half of the Formation. Generally the facies association occurs as planar-based, lenticular bodies, between 5cm and 6m in thickness, and between 1 and 50m in lateral extent in any one direction, and which generally contain no internal structures (Figure 4.26). In thin section, rocks of this facies association appear petrographically identical to those of the large-scale cross bedded sandstone facies association. The lenticular massive sandstone bodies tend to overlie horizontal to low-angle large-scale, cross-bedded facies, and can locally be traced up the foreset, where massive beds may onlap onto 3rd order reactivation surfaces (Figure 4.27). Locally, often in association with medium to high angles of inclination of cross-bed foresets (up to 26^{o}), the geometry of the massive sandstones is channelised, rather than lenticular (Figure 4.28). Bases of the channelised massive sandstones are sharp and erosional into the underlying foresets (4.29). The edges of the channels are generally steep, vertical and rarely overhanging (Figure 4.28). Preserved channel forms may be up to 2m deep and 4m wide, though most are generally smaller. The long-axis of the channel is usually parallel or slightly oblique to the dip-direction of the large-scale foreset that it cuts. Down-dip, channels can be observed to expand into the massive lenticular bodies previously described. As the channel form spreads, the relationship with the substrate changes from channelised and often erosional to either conformable or onlapping, and the

massive body is also likely to thicken. One measured channel axis had an azimuth of 290°, and spread horizontally outwards towards the bottom of the palaeo-dune slip face to form a lenticular body with margins trending 200° to 020°, showing that the lenticular sandstone body is lobate-shaped. Rarely, channels and lenticular bodies can be observed to contain thin layers of wind ripple laminae between two successive massive sands, reflecting two distinct phases of infill, separated by a dry, windy period. In places a few rotated blocks of laminated, large-scale, cross-bedded facies, of between 10 and 50cm diameter, could be observed within massive sandstone bodies. Additionally, at one locality, large-scale cross-beds were over-folded beneath a channelised massive sandstone.

Locally, in close proximity to areas exhibiting massive sandstones, steeply dipping cross-strata of the large-scale cross-bedded sandstone facies association could be seen to have undergone soft sedimentary deformation (Figure 4.30). The deformation appears to be related to slumping, with slumps verging in a down-dip direction. Although the laminations of cross-bedded strata are strongly folded to accommodate the slump, laminae are not destroyed (Figure 4.30).

The upper surfaces of massive sandstones may contain a variety of features including adhesion warts, wind ripple strata, shallow concave-up depressions containing inversely-graded wind-ripple strata, horizontally laminated sandstones with parting lineations, ball and pillow structures, convolute structures and rare desiccation cracks.

4.3.3.5: Pebbly sandstone facies association:

This facies association was only identified locally in the upper most 50m of the Makgabeng Formation. The outcrop is located around 23°16.07'S; 28°52.42'E, and the occurrence of the facies association is about 750m long, 500m wide, and has a stratigraphic thickness of about 30m. The long axis of the outcrop trends approximately N-S. To the south, the facies association erosively overlies large-scale trough cross-bedded facies, and is, in turn, overlain by trough cross-bedded facies to the north. The

eastern and western margins of the exposure show that pebbly sandstones interfinger with the large-scale trough cross-bedded facies. The pebbly sandstone facies association consists of medium- to coarse-grained, locally planar-bedded sandstones, which comprise well-rounded sand grains of generally high sphericity. Sand grains appear well-sorted, and are about 500μm in diameter, though lithic fragments (quartzite) up to 3mm diameter may also be present rarely. Interstitial areas within the coarse sandstone are locally filled with jasper or opaque minerals. The strata of the pebbly sandstone facies association can be easily recognised as it is generally massive compared to the thinly laminated sandstone of the large-scale, cross-bedded facies association (Figure 4.31). The pebbly sandstone facies association of the Makgabeng Formation is also readily identifiable from large-scale, cross-bedded and massive facies associations by the presence of isolated quartz pebbles (Figure 4.32). Individual beds of the pebbly sandstones are about 15cm-1m thick, and are locally normally graded. The bases of the beds may contain isolated quartz or quartzite pebbles, typically with a diameter between 2 and 7cm, within a matrix of coarse-grade sand grains. Towards the top of the bed, no larger clasts occur, and medium-grained sandstone is present. Trough and planar cross-bedding (Figure 4.33), preserved channels and parting lineation on planar bedding surfaces (Figure 4.34) are subordinate characteristics of this facies association, which serve to indicate palaeocurrent direction. Preserved channel forms are typically around 5-11m wide and 50-70cm deep, and are generally sandstone-filled, and free from larger clasts. The rose diagram in Figure 4.35 shows that the transport direction was generally towards the south.

Deeply incised, steep-sided channels generally mark the contact between the pebbly sandstone and the large-scale cross-bedded facies association (Figure 4.31). Such channeling suggests that the cross-bedded facies had not lithified at the time of deposition of the pebbly sandstone, and hence were more easily eroded. Locally, pebbly sandstone facies can be observed to lie directly over very steeply inclined foresets (29-30°) of the large-scale trough cross-beds (Figure 4.36).

4.4: Mogalakwena Formation:

In this section, the Mogalakwena Formation will be considered from two areas: the strata which outcrop south of the southern strand of the Melinda Fault, and the Mogalakwena strata which outcrop north of the southern strand of the Melinda Fault (Appendix 1). These latter rocks have previously been considered as a part of the Blouberg Formation (Mositone Conglomerate, Varedig Sandstone and Semaoko Grit members; Jansen, 1976; Section 1.3.1) and of the pre-Blouberg Lebu Complex (Meinster, 1977; Section 1.3.2), or as part of the Soutpansberg Group (Brandl, 1991; Callaghan and Brandl, 1991; Barker *et al.*, in press; Section 1.3.3).

4.4.1: Mogalakwena strata south of the southern strand of the Melinda Fault:

4.4.1.1: Eastern part of the study area:

The strata of the Mogalakwena Formation south of the southern strand of the Melinda Fault are generally horizontal to sub-horizontal, and only rarely dip at angles in excess of 30° (Appendix 1). Generally, the outcrops are large and provide good three-dimensional exposures (the lithology does not support thick soils and dense vegetation), and commonly the Mogalakwena Formation outcrops as isolated, steep-sided mesas (Figure 4.37). Such outcrops allow for the determination of the large-scale three-dimensional geometry for the identification of architectural elements (Miall, 1985) more readily than other inferred fluvial sedimentary rocks previously discussed.

Generally the elements consist of interbedded sheet-like structures of either coarse sandstone and granulestone or conglomerate (Figures 4.37 and 4.38), which correlate with element CHS (major sandstone sheet) of Miall (1985; 1996; Table 3.1). Sheets are generally 50cm to 1m thick, and hundreds of metres across in lateral extent. Locally these sheets are intersected and cut by large conglomerate-filled channel forms (element CHR of Miall, 1985; 1996; Table 3.1), up to 20-30m in cross section, and 2-5m in depth (Figure 4.39). Where channels are exposed within a steep side of a mesa, the trend of the

palaeocurrent can be determined by the identification of the channel on the opposing side of an adjacent mesa.

Sheet-like elements are comprised of both matrix-supported conglomerate and medium- and coarse-grained sandstone and granulestone. Conglomeratic sheets are generally massive, and internal primary structures (e.g. bedding and cross-bedding) tend not to be present. Figure 4.40 shows rare imbrication of quartz and quartzitic cobbles, which indicates opposing palaeocurrent directions from the trough cross-bedded coarse sandstone facies above.

The conglomerates are generally matrix-supported (Gmm; Table 3.1), with a matrix of coarse sand and granule sized grains, with some opaque minerals also present. Cobbles and pebbles tend to be well rounded and spherical, so imbrication is only rarely detectable (Figure 4.41). Cobbles are mainly composed of quartz, quartzite, green quartz (fuchsite stain) and, locally, pebbles of Banded Iron Formation (B.I.F.) (Figure 4.42).

In sandstone and granulestone sheets, trough cross-bedding (St; Table 3.1) is the only common internal sedimentary structure, with set thickness commonly between 30 and 50 cm (Figure 4.43) and cobble-sized clasts are rare. Grain size is variable from 500μm (medium- to coarse-grained sand) to 3-4mm (granules). Generally granule-sized grains appear most common in thin sections from samples taken from the non-conglomeratic sheets, and are composed of quartz and quartzitic lithic fragments (Figure 4.44). Large granule-sized grains are poorly sorted, angular and of low sphericity, whereas rare patches of medium- to coarse-grained sandstone matrix have grains that are well sorted, sub-rounded and of medium sphericity (Figure 4.45). An average of 500 point counts taken from one thin sections sampled from sandy sheets show that the finer components of these Mogalakwena sedimentary rocks are composed of 40% quartz, 39% matrix (intergranular material) and 21% lithic fragments. A photomicrograph of this rock is also shown in Figure 5.18.

In order to establish variation between interbedded conglomeratic and granulestone sheet-like elements within the Mogalakwena Formation, a systematic survey was made, using a $1m^2$ grid (methodology outlined in Section 1.6.1). Variation in the composition and size of conglomerate clasts and also how these parameters vary with stratigraphic height and distance from the Melinda Fault can also be determined using this method. Granulestone and coarse sandstone beds are indicated by a paucity of recorded conglomerate-sized clasts. The measurements were taken from the following locations: From north to south: 23°11.23'S; 28°52.44'E on Blackhill 317LR; 23°11.52'S; 28°52.28'E at Tsolametse (northern slope); 23°11.66'S; 28°52.21'E at Tsolametse (southern slope); 23°13.60'S; 28°51.65'E at the east side of Sadu, on Gallashiels 316LR and 23°16.20'S; 28°50.50'E, at Masebe, on Montblanc 328LR (Figure 4.46). These five locations are located on a line trending approximately perpendicular to the strike of the Melinda Fault, and lie south of the southern strand (Figure 4.46). Data are presented in Appendix 2. This style of survey was carried out in preference to the calculation of palaeohydraulic parameters, used for the Blouberg Formation (Section 3.5) on account of the paucity of recorded channel forms in the Mogalakwena Formation. Whilst paleaohydraulic parameters could have been calculated from the trough cross-bedded granulestone sheets, such calculations would not have encompassed the palaeohydraological parameters relating to the ubiquitous conglomeratic sheets, and thus would give little indication of the true conditions during deposition of the Mogalakwena Formation.

Measurements of the percentage of pebble- to boulder-sized clasts in the conglomerate (i.e. those larger than about 1cm) relative to matrix, in the basal 90m of the Mogalakwena Formation at these five locations are shown in Figure 4.47. Figure 4.47 shows the overall cyclical nature of the lower Mogalakwena sediments, with peaks corresponding to conglomeratic beds, and troughs (caused by a paucity of larger-sized clasts) representing more sandy beds. Superimposed on this generally cyclical pattern of sedimentation, is an overall trend that the percentage of clasts within the matrix decreases upwards, with a sharp decrease in the percentage of larger-sized clasts about 30m above the unconformity with the Makgabeng Formation.

A general trend that clast frequency decreases towards the south is also evident from these data. Average values for clast frequency from each of the five localities (calculated by the sum of all percentages for each m^2 at each locality, divided by the height in metres of the recorded section) cannot be used as an indicator of relative clast frequency between each locality, as the clast frequency is largely a reflection of stratigraphic height (Figure 4.47).

Therefore, as the stratigraphic height from which data were collected varies between each locality, average values would rather reflect the stratigraphic height from which they were recorded, and not necessarily reflect a north-south trend. (e.g. the northern slope of the Tsolametse locality only contains data from the generally conglomeratic basal 15m of the Formation, so average values would be higher than the Masebe locality, where 67m of less-conglomeratic upper Mogalakwena strata was recorded). Therefore, to avoid such error, regional comparisons between localities should only be made from data recorded at the same stratigraphic height. Figure 4.47 shows that between the stratigraphic heights of 0m and 13m, data are recorded from four out of the five localities (only the Masebe locality is missing data from this stratigraphic height). Therefore this provides the best stratigraphic interval from which comparisons between localities can be made. Average values of clast percentages from within this13m interval are shown in Figure 4.48, which shows a slight overall decrease in clast frequency towards the south, though the trend is not clear.

In addition to the percentage of clasts and matrix within any particular m^2 of exposed strata, the length of the intermediate axis of the largest clast within that m^2 was also measured (Appendix 2). These collected data are presented in Figure 4.49, and again show the cyclical nature of the coarseness of the beds, and that generally clast size varies inversely with stratigraphic height. This relationship is most noticeable in the data from the southern slope of Tsolametse. Similarly, by comparison of clast size from between 0 and 13m height in the stratigraphy, there is also an apparent relationship, which shows that clast size generally decreases from north to south (Figure 4.50).

Multiplication of clast percentage and the length of the intermediate axis of the largest clast within that m^2, gives an overall index of the coarseness of that particular height in the stratigraphy. Highly conglomeratic beds with large clasts have a high resultant product, whereas more sandy beds with fewer, smaller clasts have a low product. Thus any trends of fining upwards and southwards can be exacerbated. Figure 4.51 shows how the overall coarseness of beds varies with stratigraphic height in the Mogalakwena Formation. Figure 4.52 shows the general coarseness of beds recorded in strata from the 0-13m interval. Although there is a general drop in coarseness of beds towards the south, again the southwards-fining trend shown in Figure 4.52 is not strong.

It is important to note that in many instances, the stratigraphic height within the Formation (i.e. the height above the unconformity with the Makgabeng Formation) had to be estimated (e.g. the basal part of the succession was hidden beneath talus at the Masebe location). Additionally the cyclical nature of the strata makes correlations between individual conglomeratic beds difficult between neighbouring locations. It is therefore possible that correlations in stratigraphic height made between localities within the Mogalakwena Formation are inaccurate. As the upper and lower boundaries of each m^2 interval measured do not necessarily coincide with a facies boundary plane, often each m^2 would contain parameters measured from both a sandy and a conglomeratic facies. This has the effect of smoothing the curves plotted in Figures 4.47, 4.49 and 4.51, as more average values are recorded.

Within these five locations the composition of the clasts per m^2 was recorded. Clasts which were recorded are vein quartz, quartzite, with rare clasts of fuchsitic quartz and B.I.F (Appendix 2). Figure 4.53 shows that both quartz and quartzite decline upwards in the stratigraphy (as clast frequency decreases; Figure 4.47). The presence of B.I.F. clasts in the Mogalakwena conglomerate seems to be strongly controlled by stratigraphic height within the Formation (Figure 4.53), with B.I.F. clasts occurring only rarely at stratigraphic heights greater than 20m. Figure 4.54 shows the variability of average percentages of clasts present for each location between the 0 and 13m interval. Percentages of vein quartz clasts are high in the north (an average of 10%), and generally

decline towards the south, whereas percentages of quartzite fragments seem to vary less systematically (Figure 4.54). Due to the lack of outcrop of the basal 20m at the Masebe location, it is difficult to assess the lateral variation in B.I.F. clast presence, though thin basal conglomerates in the Steilloopbrug area (23°25.94'S; 28°37.20'E and at 23°15.38'S; 28°42.39'E) also contain B.I.F. clasts. Thus it seems that the presence of B.I.F. clasts is controlled stratigraphically, rather than by distance southwards from the Melinda Fault.

In summary, the general sedimentary characteristic of the Mogalakwena Formation in the eastern part of the study area embodies interbedded trough cross-bedded coarse sandstones and massive matrix-supported conglomerate. These facies are found as sheet-like architectural elements with rare conglomeratic channel elements. There is a general trend of cyclicity between sandstone and conglomerate beds, with overall trends of upwards-fining and a weaker trend of southward-fining away from the area of the southern strand of the Melinda Fault.

Palaeocurrent directions for the Mogalakwena Formation south of the Melinda Fault can be derived from trough cross-bedding foreset directions in the sand sheets. Palaeocurrent directions from the imbrication of clasts in the conglomeratic sheets could not be readily determined due to the general roundness of clasts. Palaeocurrent directions recorded for these strata are shown in Figure 4.55, which shows a unimodal palaeocurrent direction towards the S.W. (c.246°).

4.4.1.2: Western part of the study area:

The stratigraphic patterns described above for the Mogalakwena Formation in the eastern part of the study area are only partially applicable to the western area south of the southern strand of the Melinda Fault. The general sheet-like architecture with rare channels (elements CHS and CHR respectively; Miall, 1985; 1988; Table 3.1) is similar to that identified in the east (Figure 4.56), though there is a marked difference in the distribution of conglomerate-sized clasts. The fining-upwards pattern identified in the

Mogalakwena Formation conglomerates in the eastern part of the field area is still present in the west, although the cobble-sized clasts in the western conglomerates are generally found only in the basal 10 or 15m of the Mogalakwena strata above the Makgabeng Formation, and thus are restricted to a considerably smaller portion of the stratigraphy. Field observations suggest that the composition of the clasts is identical to those in the east (quartz and quartzite, with rare B.I.F. and fuchsitic quartz clasts). In the basal 10-15m of the Mogalakwena Formation, conglomerate sheets are 30-50cm thick, and are interbedded with coarse-grained sandstone sheets. Clasts have a maximum diameter of 10cm, which is smaller in size than those measured at this stratigraphic height in the east. Conglomerates are commonly located in channel elements (Figure 4.57) in this basal portion of the Mogalakwena stratigraphy. Upwards, the frequency and thickness of conglomeratic sheets decreases (sheets may only be one clast thick by about 20m height in the stratigraphy), and coarse granulestone and sandstone sheets become dominant.

Above this basal 15m, Mogalakwena strata only rarely contain pebble and cobble-sized clasts, and facies of coarse-, very coarse-grained sandstone and locally gravel-sized clasts are prevalent within each sheet-like architectural element. The presence of channel elements also decreases upwards with the increasing rarity of conglomerates.

Trough cross-bed set thickness in the sandstone sheets is generally smaller in these westerly outcrops of Mogalakwena strata, and is often between 10 and 15cm (Figure 4.58). Heavy mineral concentrations on foresets are diagnostic, and serve to enhance the appearance of foresets (Figure 4.58). This lithofacies is comparable with that of the Sandriviersberg Formation at the southern edge of the Main Waterberg basin, which grades laterally into the Mogalakwena Formation towards the N.E. (Figure 1.6). Figure 4.59 is taken at 24°20.00'S; 28°33.50'E at the south-eastern corner of the Main Waterberg basin, and shows many similarities with coarse sandstones of the co-eval Mogalakwena Formation in the eastern part of the study area.

The slight trend of southwards-fining from the Melinda Fault identified in the eastern part of the study area does not seem to be followed in the west. At 23°10.45'S; 28°39.05'E

(5km north-west of Glen Alpine dam), about 1.5km south of the projected line of the Melinda Fault, the Mogalakwena Formation consists of coarse sandstone and granulestone, and pebble- and cobble-sized clasts are conspicuously absent, despite the proximity of the Melinda Fault. In thin section, these westerly rocks of the Mogalakwena Formation appear to be poorly sorted with sub-angular grains of low sphericity (Figure 4.60).

Despite the fact that there appears to be a strong stratigraphic control over clast size and frequency (Figures 4.47, 4.49 and 4.51) and a weak trend of southwards-fining (Figures 4.48, 4.50 and 4.52) in the Mogalakwena conglomerate in the immediate vicinity of Blouberg Mountain in the eastern part of the study area, there appears to be less stratigraphic control and less lateral variation in coarseness of clasts in the western part of the study area.

Palaeocurrent directions for this western part of the field area, recorded from foreset directions in trough cross-bedded sandstones, are shown in Figure 4.61, and show a diagnostic unimodal direction towards the S.W., which corresponds to the palaeocurrent direction recorded in the eastern outcrops.

4.4.2: Mogalakwena strata north of the southern strand of the Melinda Fault:

The strata under investigation in this section occur north of the southern strand of the Melinda Fault under both the northern and southern foothills of Blouberg mountain. Outcrop in the southern foothills is restricted to numerous isolated outcrops underlying areas adjacent to the northern edge shear zone of the southern strand of the Melinda Fault, e.g. 23°07.30'S; 28°55.70'E on the farm Buffelshoek 261LR. Generally these strata have shallow dips (Appendix 1), in contrast to the steeply dipping and overturned Blouberg strata on the opposite side of the southern strand of the Melinda Fault.

The outcrops of Mogalakwena Formation which occur under the northern foothills of Blouberg mountain underlie the area around 23°06'S; 28°54'E on the farm Varedig

265LR, and also occur at isolated exposures at Sesuane Hill (23°04.40'S; 28°54.10'E), Mositone (23°03.02'S; 28°56.38'E) and Semaoko (23°02.70'S; 28°51.70'E). At these localities, a maximum of about 250m of sub-horizontal strata nonconformably overlie the basement and locally unconformably overlie the Blouberg Formation (Chapter 7) and are, in turn, locally unconformably overlain by the Wyllies Poort Formation of the Soutpansberg Group (Appendix 1) (Chapter 7).

The sedimentary rocks in all these locations, (underlying both the northern and southern foothills of Blouberg Mountain) are identical, and consist of sheet-like architectural elements (CHS) (Figure 4.62). Within these elements are facies of massive cobble conglomerate, locally trough cross-bedded pebble conglomerate, and trough cross-bedded coarse sandstone and granulestone.

Conglomeratic facies are only locally developed at the base of the sedimentary successions, and vary in thickness, reaching a maximum of about 10m, though they are more commonly 50cm–2m thick (Figure 4.63). Areas where the basal conglomerate is most thickly developed seem to occupy areas of low palaeotopography developed on the basement, such as at 23°05.57'S; 28°53.42'E, where clasts of up to 20cm seem to occupy a narrow (c.50m wide) N-S trending palaeovalley cut into the basement gneiss. Correspondingly, areas where basal conglomerates are thin, or even absent, seem to outcrop above localised palaeohighs in the basement. At 23°05.76'S; 28°53.47'E, a palaeotopography can clearly be seen developed on the angular unconformity between the sub-horizontal Mogalakwena Formation and the underlying, overturned Blouberg Formation. Here a post-Blouberg, pre-Mogalakwena fault (fault plane has a dip-direction of 57°→260°) with a displacement of 2m (probably with a reverse sense of movement, although there is evidence for some post-Mogalakwena normal reactivation too) appears to have created a small cliff in the palaeotopography, under which basal conglomerates of the Mogalakwena Formation have preferentially collected. Clasts within the basal conglomerate are generally vein quartz, quartzite, fuchsitic quartz, and B.I.F. (Figure 4.64), in common with Mogalakwena conglomerate developed to the south of the southern strand of the Melinda Fault.

The basal conglomerates, where developed, are interbedded with, and rapidly grade vertically into a thick (c.200m) succession of coarse- and very coarse-grained sandstone and granulestone, with well-developed trough cross-bedding (Figure 4.65). Sets are generally about 10cm thick, and commonly have heavy mineral concentrations on foresets and bedding planes (Figures 4.66 and 4.67).

Thin section data from these two areas show the similarity between the strata of these two areas. Point counting of 300 points from a thin section taken from the northern foothills of Blouberg (Fig 4.68) show that the rock is comprised of 35% quartz, 30% matrix (=clay), 21% lithic fragments (=quartzite) and 14% opaques. Point counting of 300 points from a thin section collected from Mogalakwena strata north of the southern strand of the Melinda fault in the southern foothills of Blouberg mountain (Figure 4.69) show that these rocks are composed of 50% quartz, 18% matrix (=clay), 24% lithic fragments (=quartzite) and 7% opaques. In both cases, the relatively high percentages of opaques are due to heavy mineral concentration on foresets.

Palaeocurrent analysis of the Mogalakwena strata north of the southern strand of the Melinda Fault, shown in a rose diagram in Figure 4.70, shows a unimodal current direction towards the S.W. This is parallel with palaeocurrent directions recorded in Mogalakwena sedimentary rocks to the south.

In terms of lithofacies, architectural elements and palaeocurrent directions, the sedimentary rocks discussed here are very similar to the more distal Mogalakwena lithologies in the western part of the main area of this formation in the study region (e.g. compare Figures 4.58 and 4.66). However these strata are reasonably dissimilar to the more conglomeratic Mogalakwena Formation sedimentary rocks underlying the immediately adjacent area south of the southern strand of the Melinda Fault (though palaeocurrent directions are parallel). Such dissimilarity of adjacent sedimentary rocks may account for varying opinions proposed by workers regarding the correlation of these lithologies. For example Meinster (1977) suggested that these northerly sedimentary

rocks predate the Blouberg (*sensu strictu*) lithologies to the south (Section 1.3.2), and Callaghan and Brandl (1991) suggested that these rocks correlate with the Soutpansberg Group (i.e. post-dating the Blouberg Formation) (Section 1.3.3). Significantly, Jansen (1976) also correlated the strata discussed here (his 'Varedig Formation') with the Mogalakwena Formation (Section 1.3.1).

It is considered unlikely that these strata to the north of the southern strand of the Melinda Fault can be correlated with any of the siliciclastic strata of the lower Soutpansberg Group (e.g. the Fundudzi Formation; Table 1.3) as proposed by Brandl (1991). There is generally a close match in lithofacies, architectural elements and palaeocurrent directions between the distal lithofacies of the Mogalakwena Formation and the strata described here. In contrast, the Fundudzi Formation is generally quartzitic, or composed of fine- to medium-grained sandstone and are pale in colour, and is only rarely conglomeratic (Brandl, 1987).

Figure 4.1: Trough cross-bedded coarse sandstone and granulestone in the Setlaole Formation at 23°09.67'S; 29°03.50'E. Hammer is 30cm long.

Figure 4.2: Detail of foliated clasts in Setlaole Formation at 23°09.67'S; 29°03.50'E. Note the general poorly-sorted, immature nature of the lithology. Pen is 15cm long.

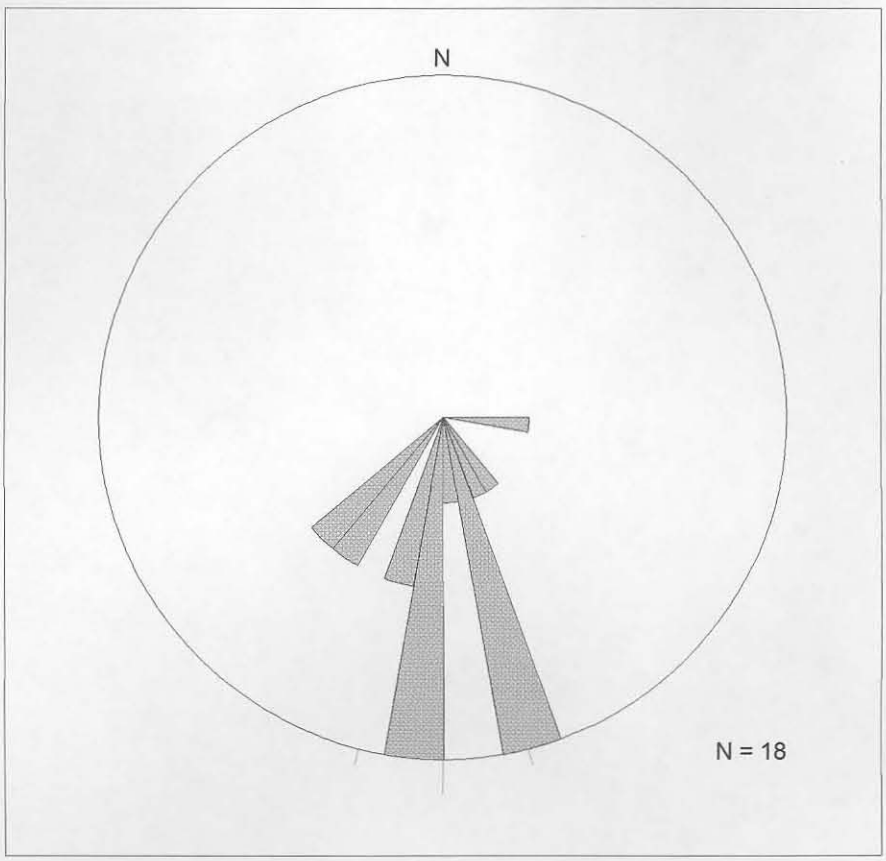

Figure 4.3: Rose diagram to show palaeocurrent directions recorded in the Setlaole Formation (in areas other than the type locality: see text). Principal direction (vector mean) is shown.

Figure 4.4: The lower nonconformity between the Setlaole Formation and the underlying basement. The basement consists of pink granitic material, with darker amphibolitic rocks locally juxtaposed by pre-Setlaole faulting. The Setlaole Formation is marked by a basal pebble conglomerate with quartz and granitic pebbles developed in hollows on the palaeosurface, and rapidly grades up into mudrock (dark upper layer). Recorded at 23°20.36'S; 28°58.00'E. Hammer is 30cm long.

Figure 4.5: Trough cross-bedded sets in coarse- to very coarse-grained sandstone of the Setlaole Formation at 23°20.36'S; 28°58.00'E. Lens cap is 5cm wide.

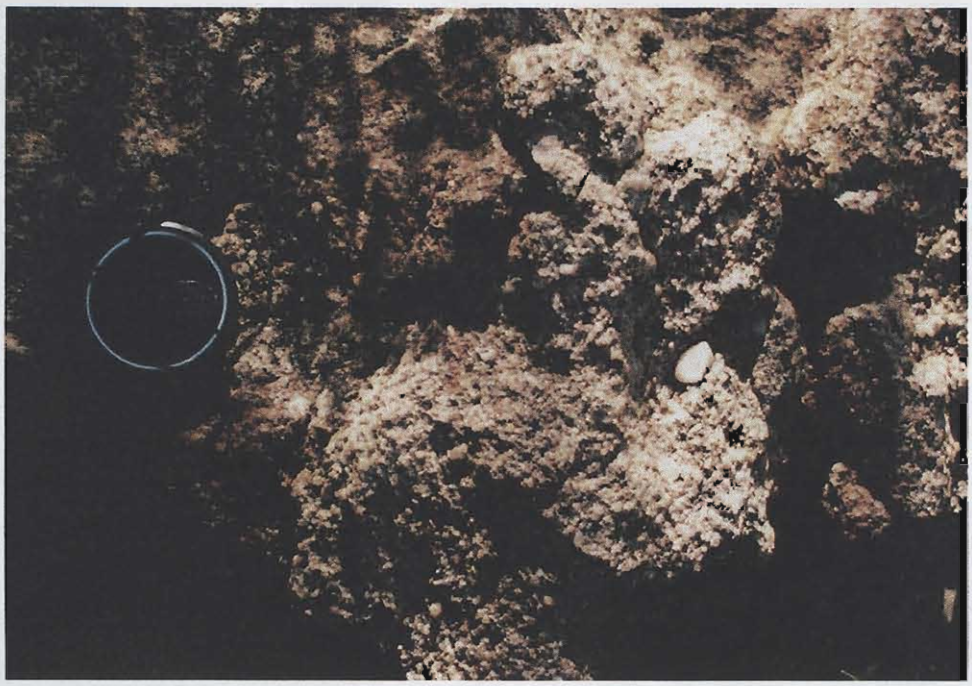

Figure 4.6: Pale-coloured pebbly granulestone facies in the Setlaole Formation at 23°20.90'S; 28°58.50'E. Lens cap is 5cm wide.

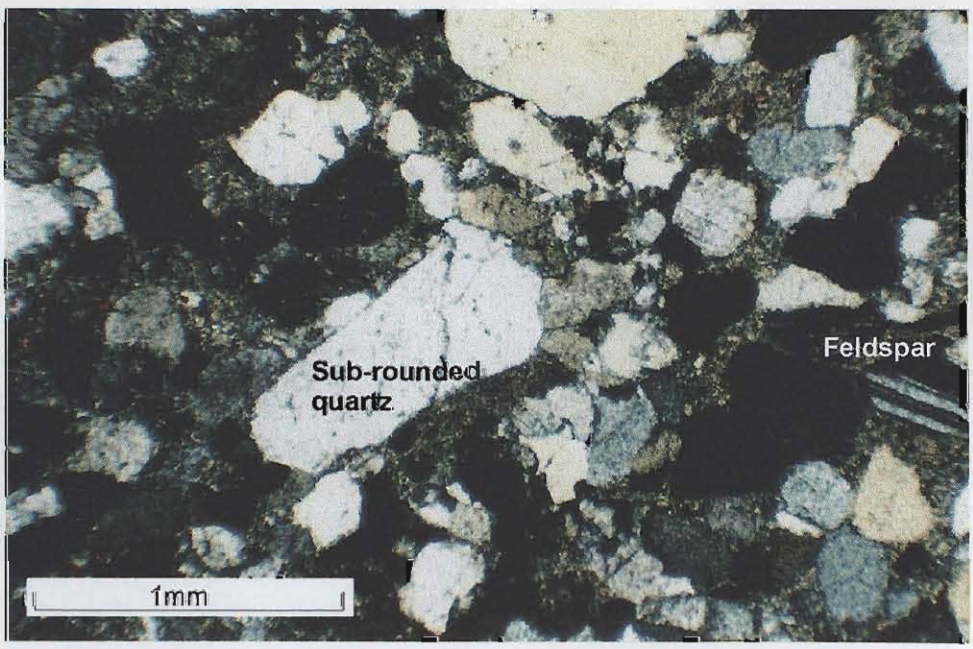

Figure 4.8: Photomicrograph from the Setlaole Formation, showing poor sorting and sub-angular to sub-rounded quartz grains and rare feldspar grains. Sample taken from 23°16.33'S; 28°59.94'E.

Figure 4.7: Rose diagram showing the palaeocurrent directions recorded from trough cross-beds in the Setlaole Formation at the type locality (23°20.90'S; 28°48.50'E). Principal direction (vector mean) is shown.

Figure 4.9: Strata which outcrops at 23°06.54'S; 28°49.38'E, comprised of pale-coloured pebbly granulestone. c.f. Figure 4.6. Lens cap is 5cm wide.

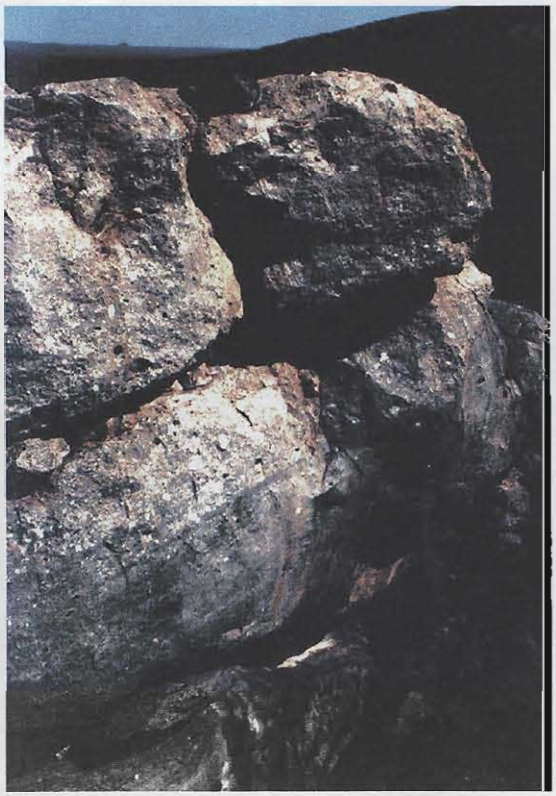

Figure 4.10: Pale coloured trough cross-bedded conglomerate and granulestone are interbedded with darker (purplish) horizontally laminated sandstone. Recorded at 23°06.54'S; 28°49.38'E. Rucksack at top of cliff for scale.

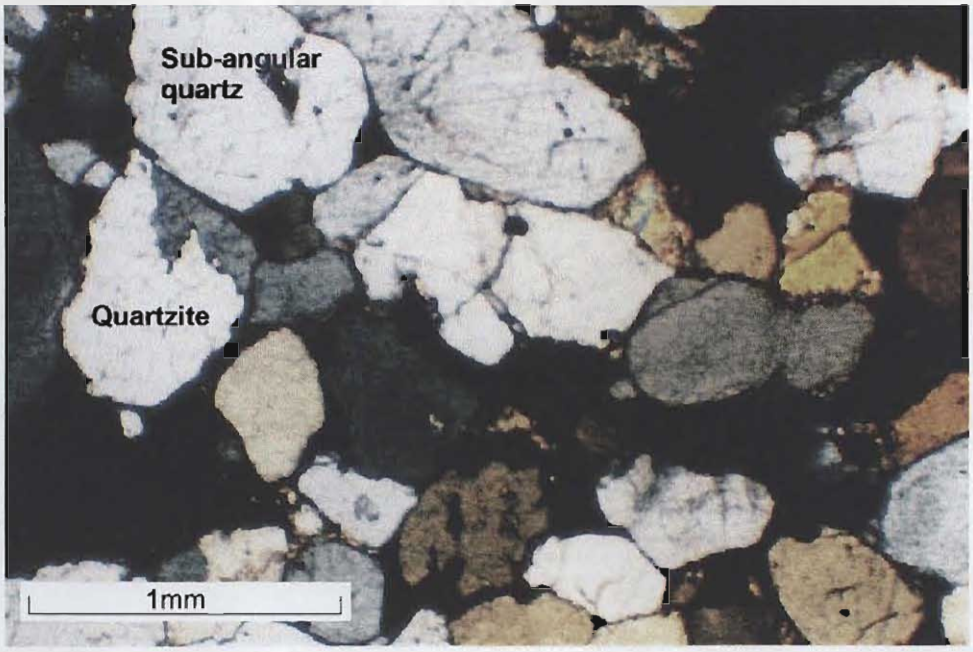

Figure 4.11: Photomicrograph from a sandstone clast from a conglomerate layer within the Setlaole Formation. Pebble is composed of sub-angular quartz grains, quartzitic lithic fragments and opaque minerals.

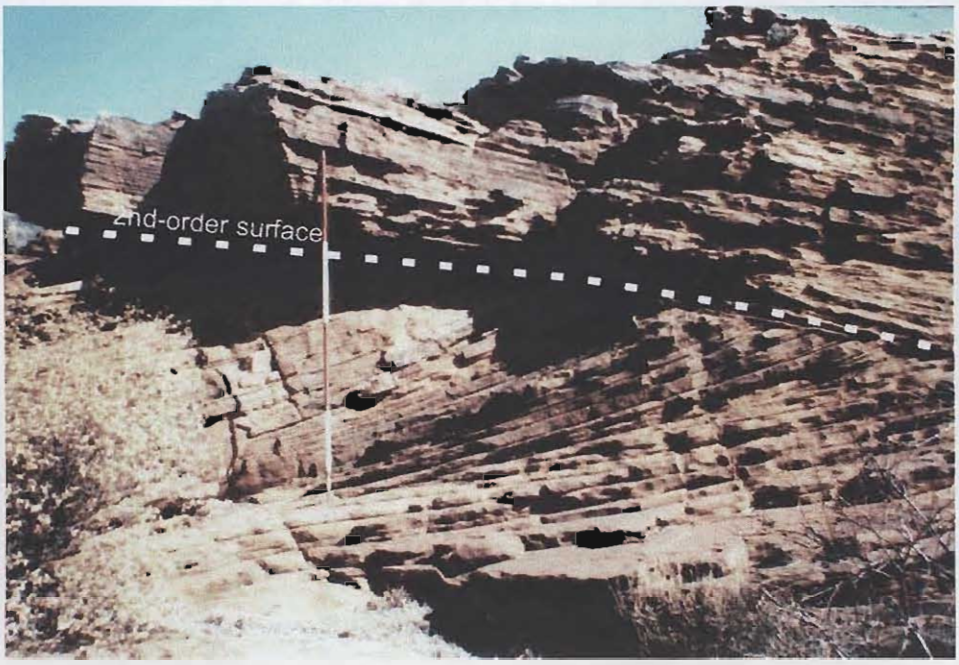

Figure 4.13: Second-order surface developed between two sets of large-scale trough cross-beds in the Makgabeng Formation. Recorded at 23°15.34'S; 28°48.70'E. Ranging pole is 2m long.

Depth		Lithology	Colour	Bed Thickness	Sorting	Comments
0						Mogolakwena Formation,
20		Cong			Poor	Makgabeng Formation at 29m
		M.sst.	Greyish red		Good	SSD: 29-31.5m, Mas:31.5-33m
		M.sst.			Good	Reduction marks up to 628m
40		M.sst.			Good	is frequent
		F.sst.	Pale Red	2mm	Good	Mas: 45-45.4m. SSD:49-50.48m
		F.sst.			Good	
60		F.sst.			Good	
		F.sst.			Good	
		F.sst.		2-20mm	Good	
80		F.sst.			Good	
		F.sst.		1-10mm	Good	
		F.sst.			Good	Interdune material + clay at 90m
100		F.sst.			Good	Interdune material + clay at 106m
		M.sst.	Moderate	2-10mm	Good	Mas: 107.7-111.2m; 112-114m
		M.sst.	red		Good	
120		M.sst.	Dusky Red		Good	Mas:120-122m
		M.sst.			Good	
		M.sst.			Good	
140		F.sst.			Good	
		F.sst.	Moderate		Good	
		F.sst.	red		Good	
160		F.sst.		2-5mm	Good	Mas: 164.7-165m; 170-175m
		F.sst.	Grey Red		Good	(massive with oblong,angular
		F.sst.			Good	clasts of silt/mud/sandstone)
180		F.sst.			Good	Mas:187.6-189m, 193-194m
		F.sst.		3mm	Good	
		F.sst.	Pinkish		Good	
200		F.sst.	grey		Good	Mas: 210-210.5m
		F.sst.		2-3mm	Good	
		F.sst.	Pale Red		Good	
220		F.sst.			Good	Mas: 236-240m
		F.sst.	Grey Red		Good	
		F.sst.		2-10mm	Good	
240		M.sst.			Good	Mas: 246-253m
		M.sst.	Dusky Red		Good	
		M.sst.			Good	
260		M.sst.	Grey red		Good	Mas: 266-266.2m, 267-276.4m;
		F.sst.		5mm	Good	268.4-269m; 272-272.4;
		F.sst.		2-5mm	Good	274-274.5m; 276.5-277.5m
280		F.sst.	Light Grey		Good	Mas: 282-282.4; 285-285.7m;
		M.sst		2-10mm	Good	288-288.7m
		M.sst			Good	
300		M.sst	Grey Red		Good	Mas: 306-306.6m;
		F.sst.		2-10mm	Good	
		F.sst.	Pale Red	5mm	Mod	

320	F.sst.	Dusky red		Mod	Mas: 327-327.7; 329-330.5
	M.sst.		2mm	Mod	
	M.sst.	Pinkish		Good	SSD at 338.8-339
340	M.sst.	grey		Good	Mas: 344-346.25m; 354-355.5m;
	C.sst.	Pale Red		Good	357-357.7; 358.3-358.9m
	C.sst.		2-5mm	Good	SSD at 346.25m
360	M.sst.			Good	360-360.4m -clay rich
	F.sst.			Good	361.3-361.7m-conglomerate in clay
	F.sst.			Good	Mas:374.5-382.7m (SSD)
380	F.sst.			Good	Mas: 384-384.4m; 395-
	F.sst.			Mod	400m (SSD structures present).
	F.sst.		2-10mm	Mod	
400	F.sst.		5mm	Mod	
	F.sst.			Good	
	F.sst.			Good	
420	F.sst.		2-10mm	Good	426-435m= red siltstone, with
	Silt			Good	interlayered sandstone
	M.sst.			Good	SSD at 433m
440	M.sst.			Good	
	M.sst.		1-3mm	Good	
	Diabase	Grey			
460	Diabase			Good	
	Diabase			Good	
	Diabase			Good	
480	Diabase			Good	
	Diabase			Good	
	F.sst.	Light	2mm	Mod	Altered Sandstone
500	F.sst.	brownish		Mod	
	F.sst.	grey	2-10mm	Mod	
	F.sst.			Mod	Mas: 517-519m
520	F.sst.			Mod	
	F.sst.	Grey red		Mod	
	M.sst.	Dusky red		Mod	
540	F.sst.			Good	Mas: 541.2-542.2m; 548-548.3m
	F.sst.	Greyish orange	1mm	Good	554.2 -554.8m; 556-556.4m
	F.sst.	Dusky red		Good	Interdune clay at 551m and 557m
560	F.sst.	Greyish orange		Good	Mas: 563-563.4m
	F.sst.	Pale Red	2-5mm	Good	
	F.sst.	Greyish orange	2-20mm	Good	
580	Silt	Moderate Red		Good	
	Shale		2-10mm	Good	
	Shale			Good	
600	F.sst.			Good	
	F.sst.	Pinkish grey		Good	
	F.sst.	Greyish Orange		Good	
620	F.sst.			Good	
	F.sst.			Mod	
	F.sst.		1-20mm	Mod	Mas: 638-638.3
640	M.sst.			Mod	Setlaole Formation, at 639m
	M.sst.		2mm	Mod	Distinct colour change from 'red'
	M.sst.	Pale red		Mod	to 'white' at 639m
660	F.sst.			Mod	

		F.sst.			Mod
		M.sst.	Pale brown		Mod
680		F.sst.			Mod
		F.sst.	Medium grey	2-10mm	Mod
		M.sst.	Dark yellowish		Mod
700		M.sst.	brown		Mod
		M.sst.	Medium grey		Mod
		F.sst.			Good
720		F.sst.	Pale brown		Good
		F.sst.	Dark yellowish		Good
		F.sst.	brown	2-5mm	Good
740		F.sst.	Light grey		Good
		F.sst.		2-10mm	Mod
		F.sst.	Pale brown		Mod
760		F.sst.			Mod
		M.sst.	Reddish brown		Mod
		Diabase	Grey		
780		F.sst.	Pale brown	2-4mm	Mod
		F.sst.			Mod
		Diabase	Grey		
800		F.sst.	Light grey	2-10mm	Mod
		F.sst.	Light brown		Mod
		Diabase	Grey		
820		F.sst.	Medium brown	2-10mm	Mod
		F.sst.			Mod
		F.sst.	Light brown	5-10mm	Mod
840		F.sst.			Mod
		Diabase	Grey		
		Diabase			
860		Diabase			
		Diabase			
		Diabase			
880		Diabase			
		Diabase			
		Diabase			
900		Diabase			
		Diabase			
		Diabase			
920		Diabase			
		Diabase			
		Diabase			
940		Diabase			
		Diabase			
		Diabase			
960		Diabase			
		Diabase			
		Diabase			
980		Diabase			
		Diabase			
		Diabase			
1000		Diabase			
		Diabase			

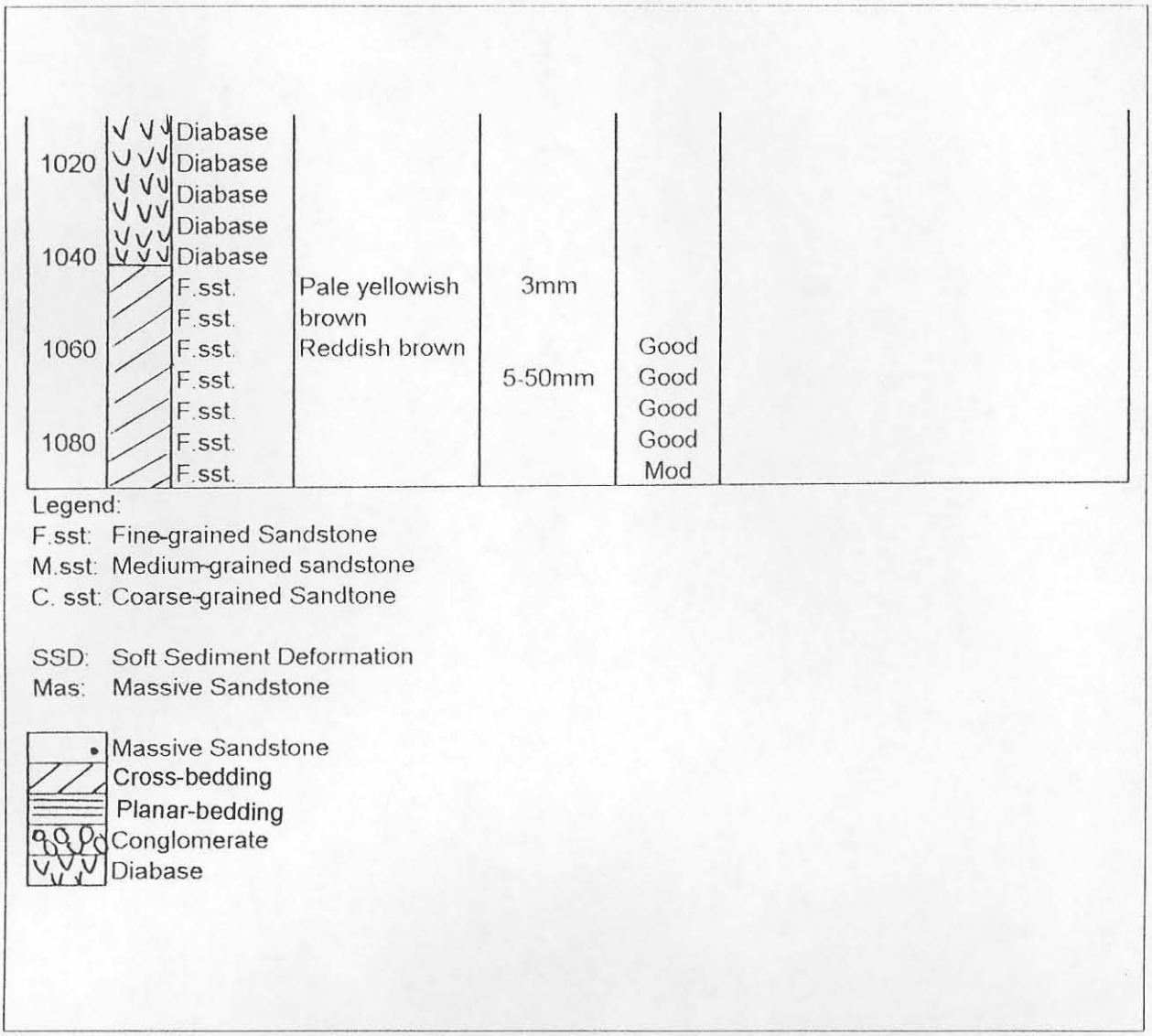

Figure 4.12: Borehole log from drill core through the Makgabeng Formation from farm Vleypan 411 (23° 28'S; 28° 37'E).

a.

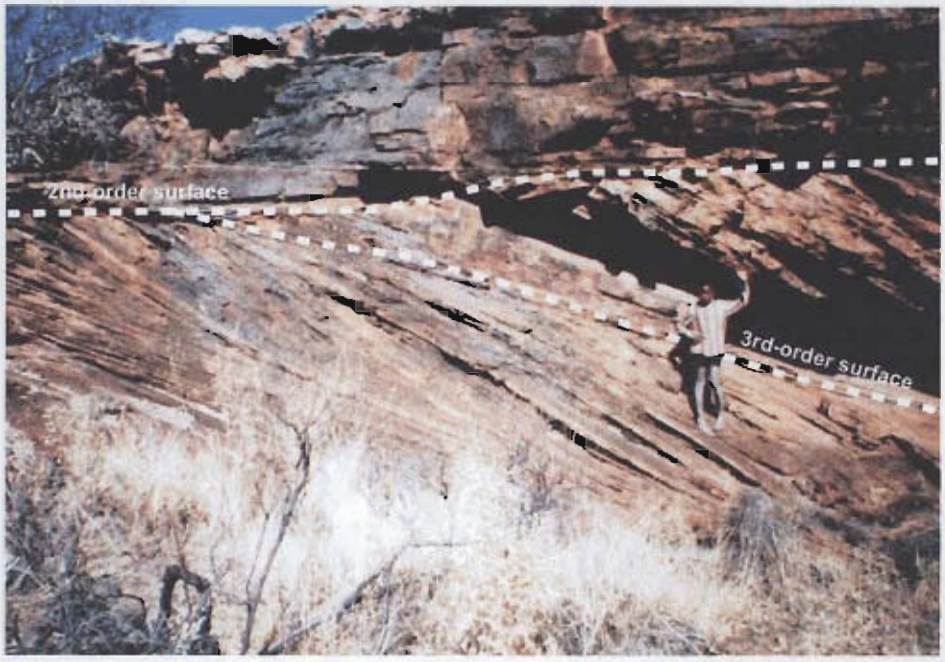

b.

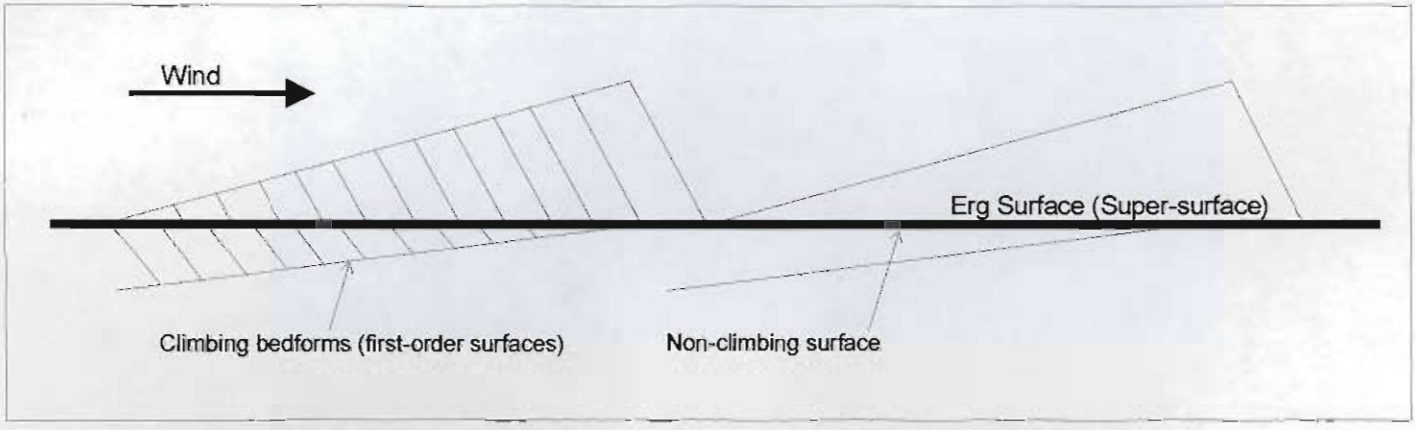

Figure 4.14a: Third-order (reactivation) surfaces developed within sets of large-scale trough cross-bedded sandstones in the Makgabeng Formation. Note the second-order surface which crosscuts them.

Figure 4.14b: Sketch illustrating climbing bedforms and horizontal nature of super-surfaces (e.g. erg surface) (after Brookfield, 1977).

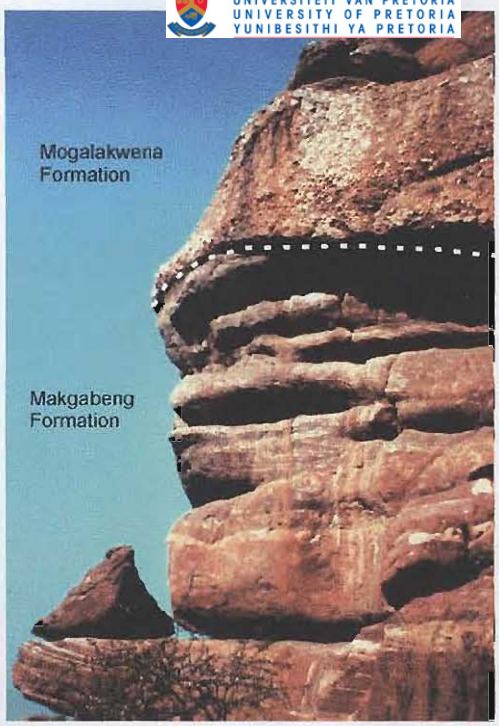

Figure 4.15: Super-surface developed between the Makgabeng Formation (bottom) and the Mogalakwena Formation (conglomeratic) at 23°11.47'S; 28°52.38'E. Cliff section is about 5m high.

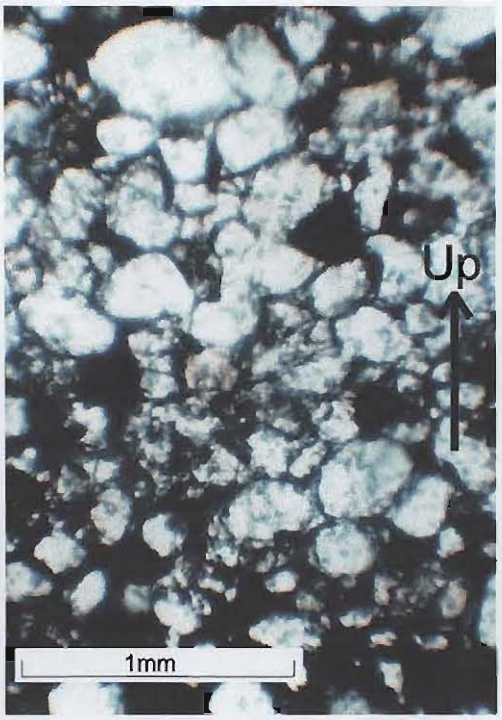

Figure 4.16: Photomicrograph from the large-scale cross-bedded sandstone facies association in the Makgabeng Formation, showing inverse-grading of sand grains within laminations. Quartz grains are generally well-sorted, rounded and have high sphericity.

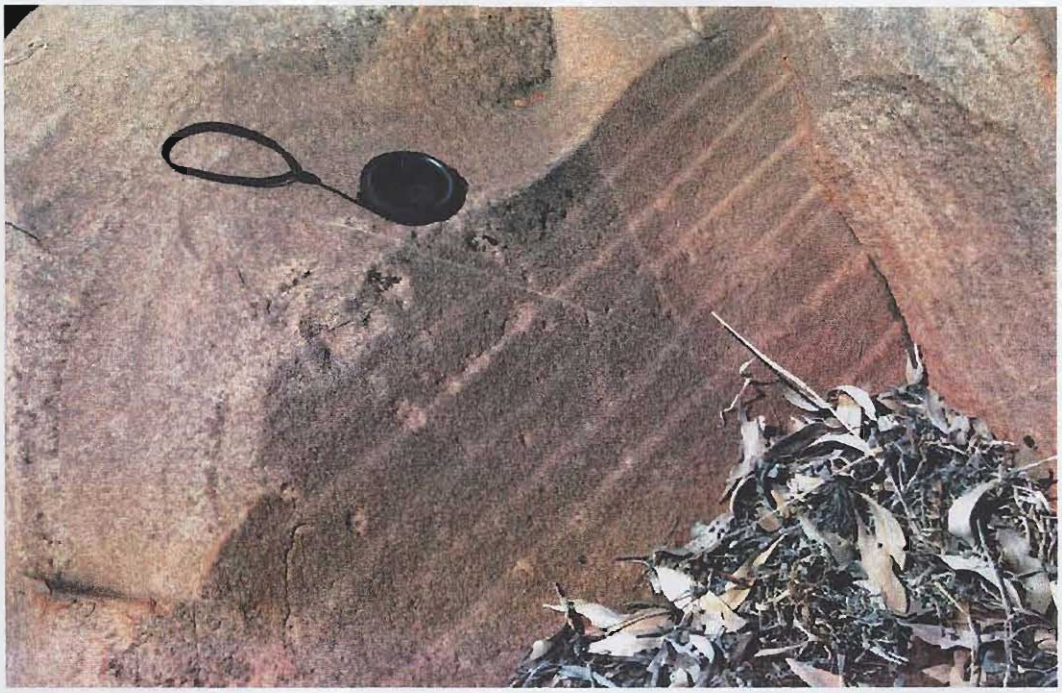

Figure 4.17: Asymmetric ripple marks in the Makgabeng Formation. Lens cap is 5cm wide.

Figure 4.18: Steeply-inclined (<30°) cross-beds comprising inversely-graded foresets in the Makgabeng Formation. View is perpendicular to the dip direction.

Figure 4.19: Wedge-shaped strata (pale-coloured rock) tapering in a down-dip direction.

Figure 4.21: Horizontally-bedded and rippled mudrocks with interbedded sandstone at 23°13.60'S; 28°52.80'E. Camera bag is 25cm high.

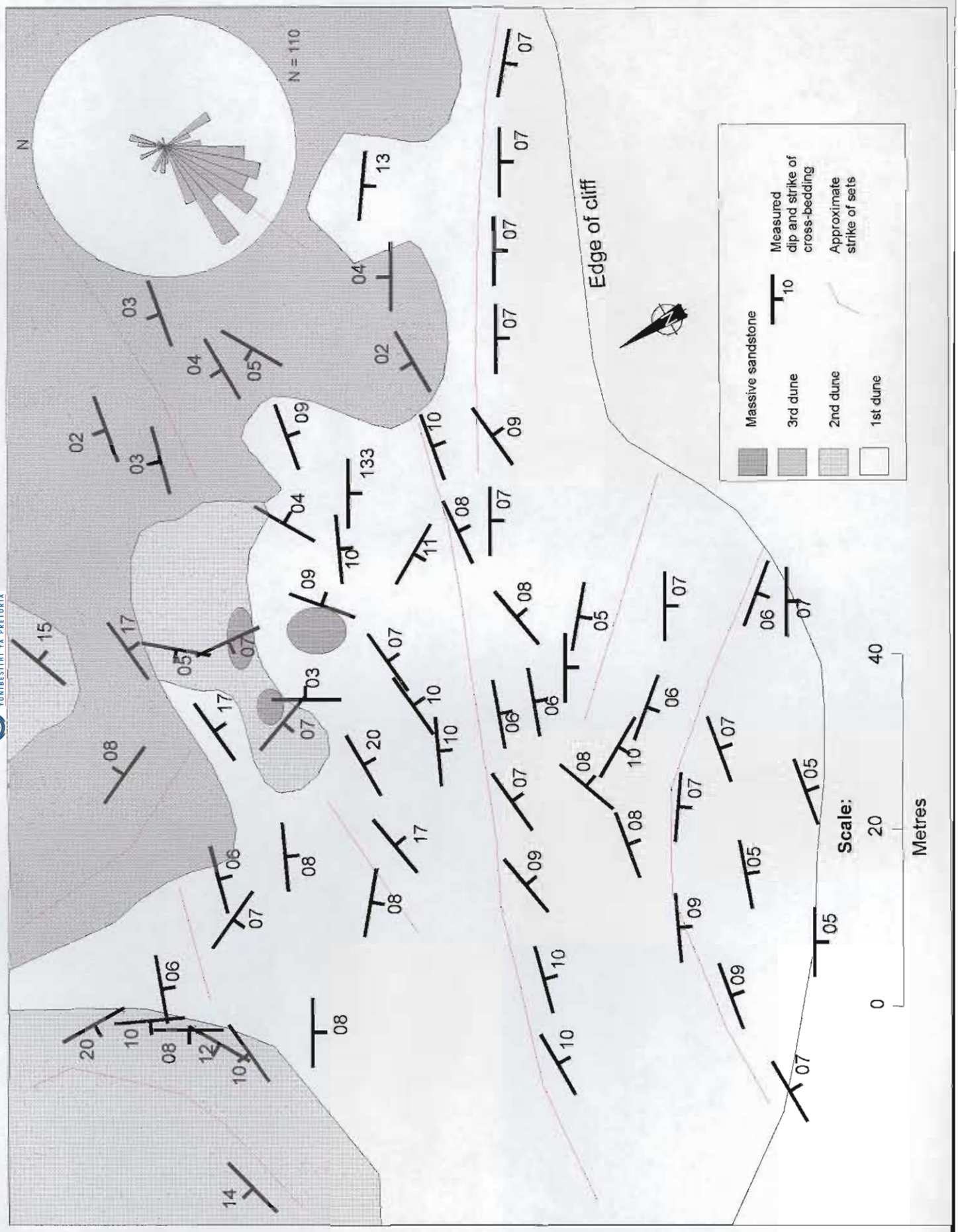

Figure 4.20: Map showing relationships between sets of large-scale trough cross-beds in the Makgabeng Formation at 23° 15.34'S; 28° 48.70'E. Rose diagram shows the orientation of foreset dip directionsfor foresets (planar and trough cross-beds) in the Makgabeng Formation. The principal direction (vector mean) is indicated.

Figure 4.22: Current ripples in mudrock in the Makgabeng Formation, with superimposed desiccation cracks. Pen is 15cm long.

Figure 4.23: Muddy roll-up structures in mudrock and sandstone in the Makgabeng Formation. Mud laminations contain of up to 720° of curvature, and "roll-ups" are orientated parallel to each other.

Figure 4.24: Muddy roll-up structures in mudrock and sandstone in the Makgabeng Formation.

Figure 4.25: Evaporite casts (possibly of gypsum crystals) developed in the rippled mudrock and sandstone facies association of the Makgabeng Formation.

Figure 4.26: Massive sandstone facies exposed in the top-most horizontal beds in this picture (about 5 beds between 30cm and 1m thick). Recorded at 23°15.34'S; 28°48.70'E.

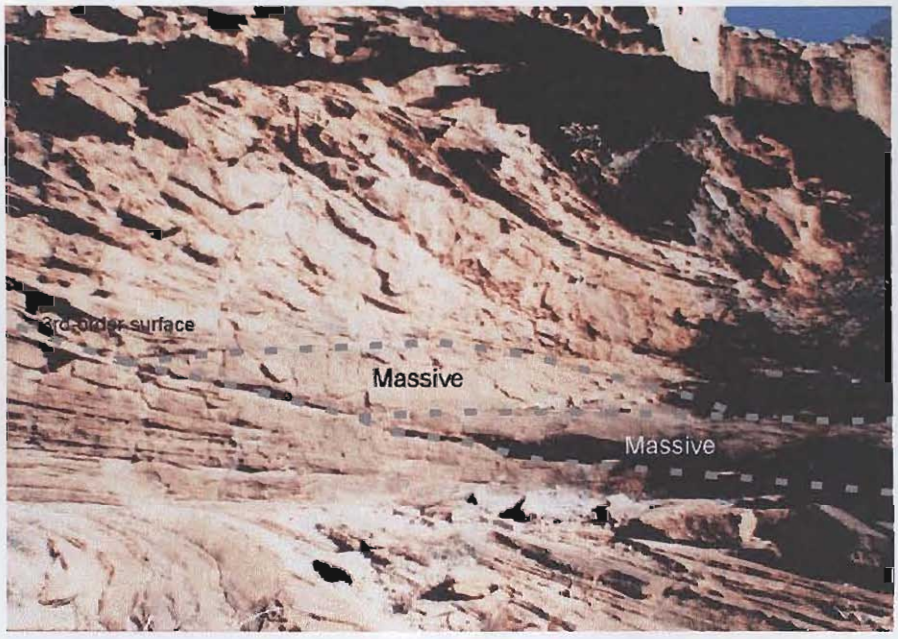

Figure 4.27: Two lens-shaped massive sandstone beds onlap to the left onto third-order surfaces. Massive beds are both about 40cm thick at their thickest point.

Figure 4.28: Channelised massive sandstone associated with more steeply-dipping inversely graded strata. View is in the down-dip direction.

Figure 4.29: The erosive nature of the massive sandstone is illustrated by the fact that the upper massive sandstone has cut down through the low-angled toeset cross-strata into more steeply-dipping cross-bedding of an older set. Pen is 15cm long.

Figure 4.30: Soft sediment deformation in the Makgabeng Formation. Laminations appear to have slumped, verging in a direction parallel to the dip-direction of the foreset. The preservation of laminae in the slumped strata suggests that they were cohesive, possibly due to the presence of water.

Figure 4.31: Channelised contact between inversely graded strata (bottom) and more massive strata of the pebbly sandstone facies association (top). Recorded at 23°16.01'S; 28°52.30'E. Hammer is 30cm long.

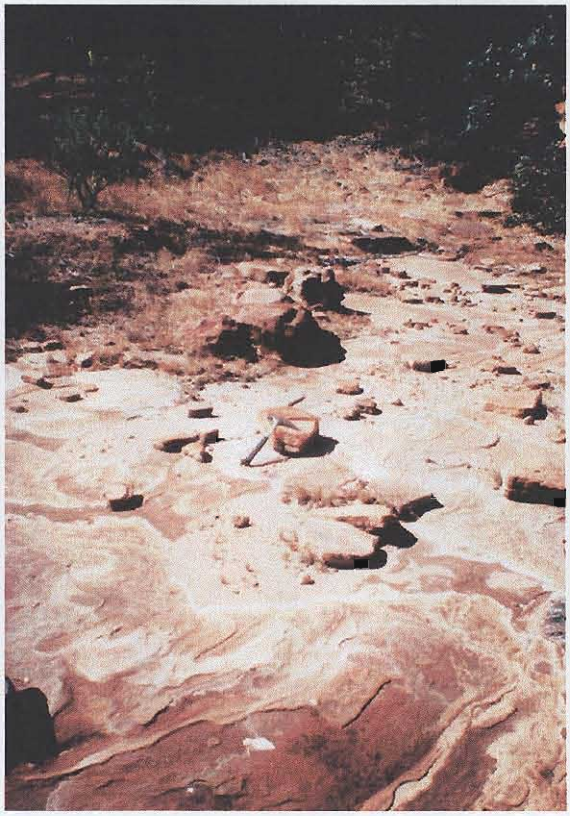

Figure 4.32: Planar laminated sandstone containing rare quartz pebbles. Recorded at 23°16.01'S; 28°52.30'E. Hammer is 30cm long.

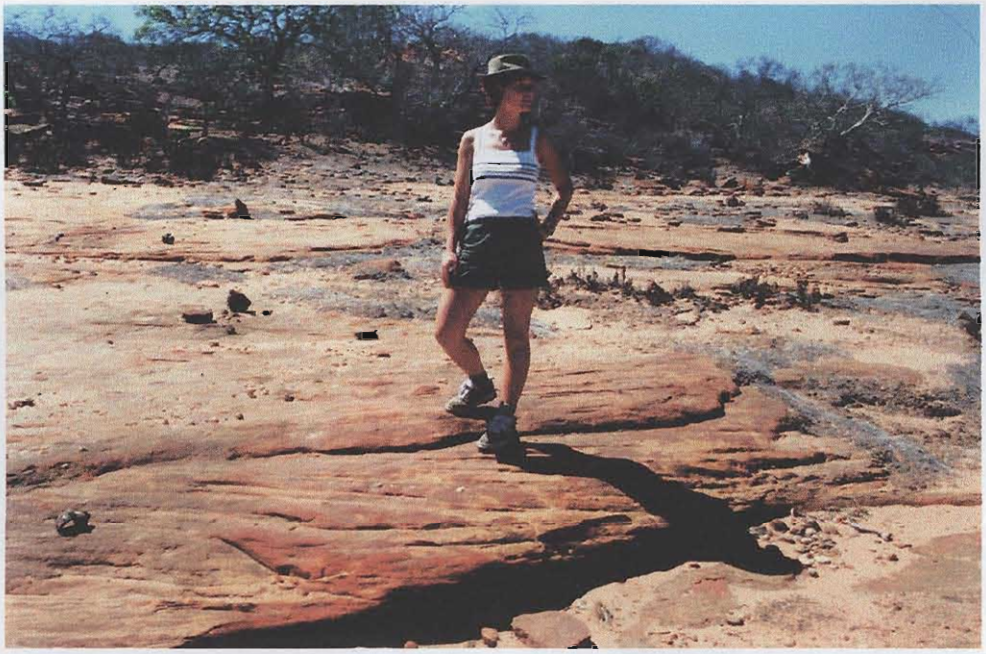

Figure 4.33: Relatively small (<50cm) set of planar cross-bedding, with quartz pebbles on foresets in the pebbly sandstone facies association. Recorded at 23°16.07'S; 28°52.42'E.

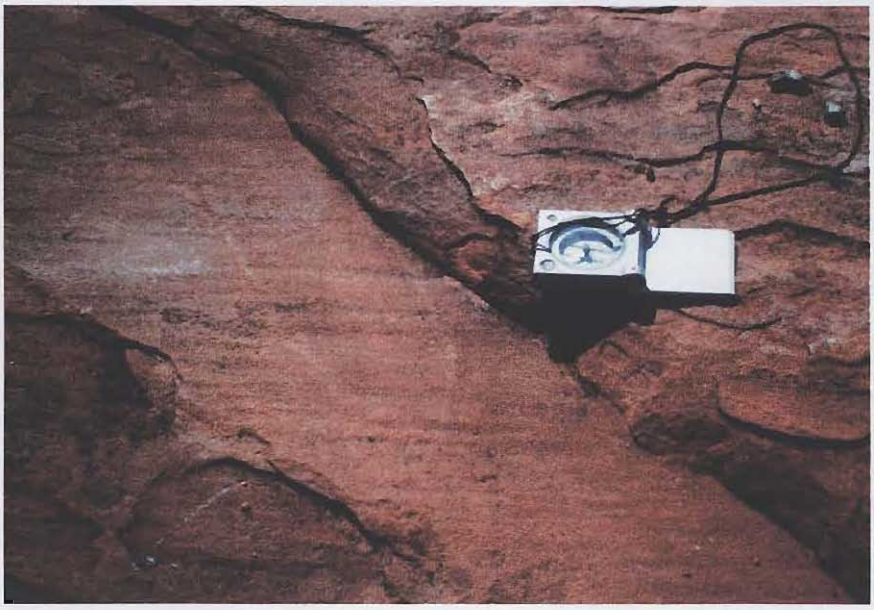

Figure 4.34: Parting lineation developed on planar-bedding surfaces in the pebbly sandstone facies association. Recorded at 23°16.07'S; 28°52.42'E. Compass is 8cm wide, and points north, indicating a north-south-trending current.

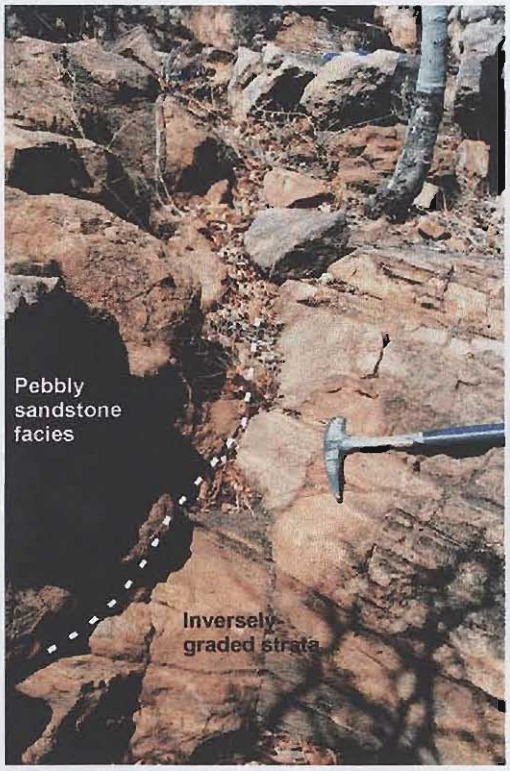

Figure 4.36: Steeply-inclined inversely-graded strata are overlain (and partly cut into by channels) by more massive sandstone of the pebbly sandstone facies association. Recorded at 23°16.01'S; 28°52.30'E. Hammer is 30cm long.

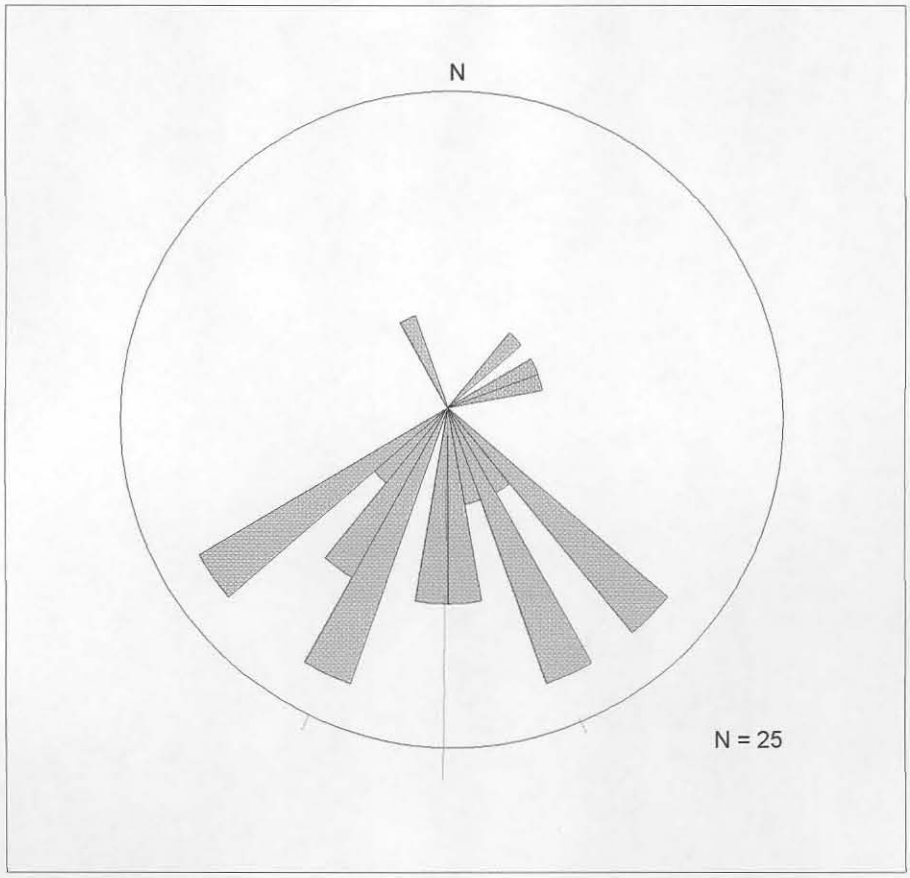

Figure 4.35: Rose diagram showing palaeocurrent directions recorded from trough cross-beds in the pebbly sandstone facies association. Principal direction (vector mean) is shown.

Figure 4.37: Interbedded conglomerate and sandstone sheet-like elements of the Mogalakwena Formation are exposed in steep-sided mesas at 23°16.25'S; 28°50.50'E. Cliffs are c.200m high.

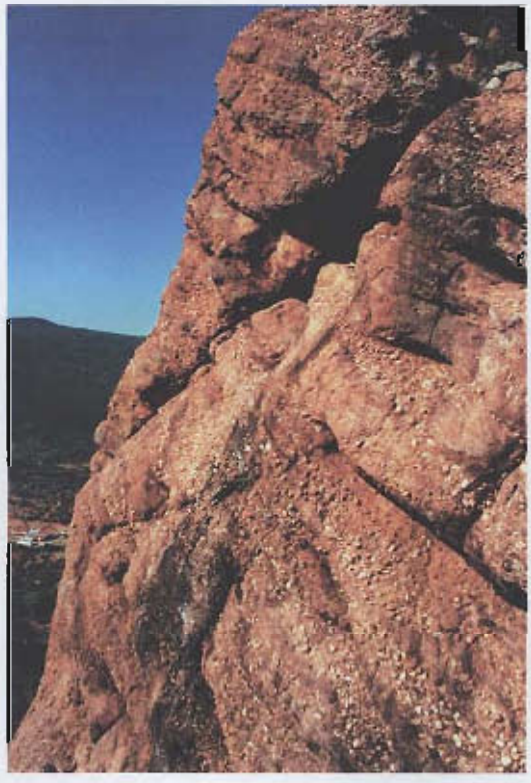

Figure 4.38: Interbedded sandstone and conglomerate sheets at 23°08.45'S; 28°54.15'E. Cliff is c. 10m high.

Figure 4.39: Large-scale conglomerate-filled channel forms (c. 5m deep, 50m wide) within sheet-like architectural elements in the Mogalakwena Formation, preserved at 23°08.21'S; 28°54.49'E.

Figure 4.40: Rare imbricated conglomerates are interbedded with cross-bedded sandstone sheets at 23°11.23'S; 28°52.44'E. Camera bag is 25cm high.

Figure 4.41: Well-rounded, massively bedded quartz and quartzite cobbles of high sphericity in conglomerate sheet of the Mogalakwena Formation at 23°11.23'S; 28°52.44'E. Note book is 20cm high.

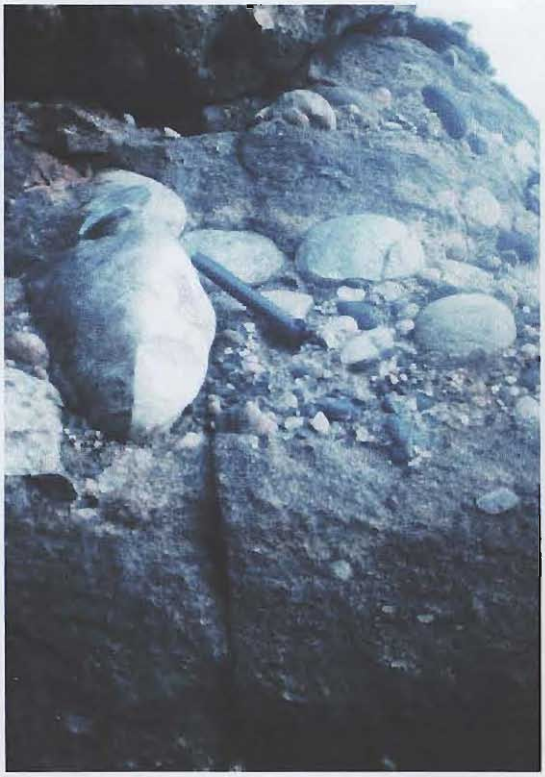

Figure 4.42: Cobbles of quartz, quartzite and B.I.F. in the Mogalakwena Formation at 23°06.69'S; 28°00.51'E.

Figure 4.43: Plan view of trough cross-bedding in sandy sheets in the Mogalakwena Formation. Recorded at 23°09.01'S; 28°42.01'E. Compass points north, indicating that palaeocurrent direction was to the S.W.

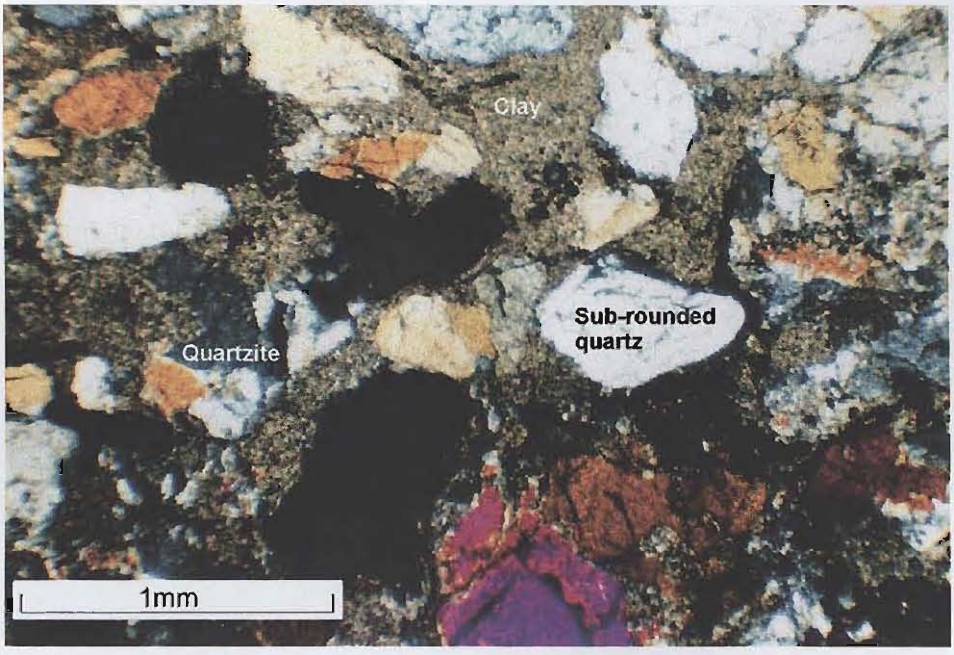

Figure 4.44: Photomicrograph of rock from sandy sheets, showing fairly well-sorted, sub-angular to sub-rounded quartz and quartzite grains (section is slightly too thick), with a high percentage of clay matrix.

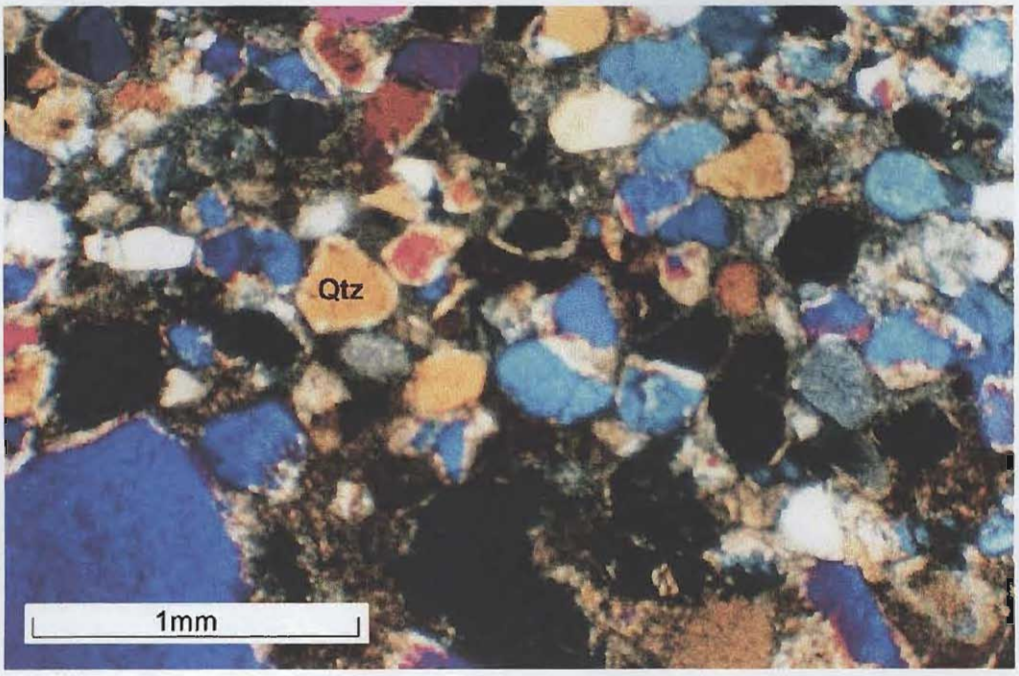

Figure 4.45: Photomicrograph of matrix from Mogalakwena granulestone, showing fairly well-sorted, sub-rounded quartz grains of medium sphericity. Section is slightly too thick.

Figure 4.46: Map showing the outcrop of the Mogalakwena Formation and the location of recording sites for pebble survey.

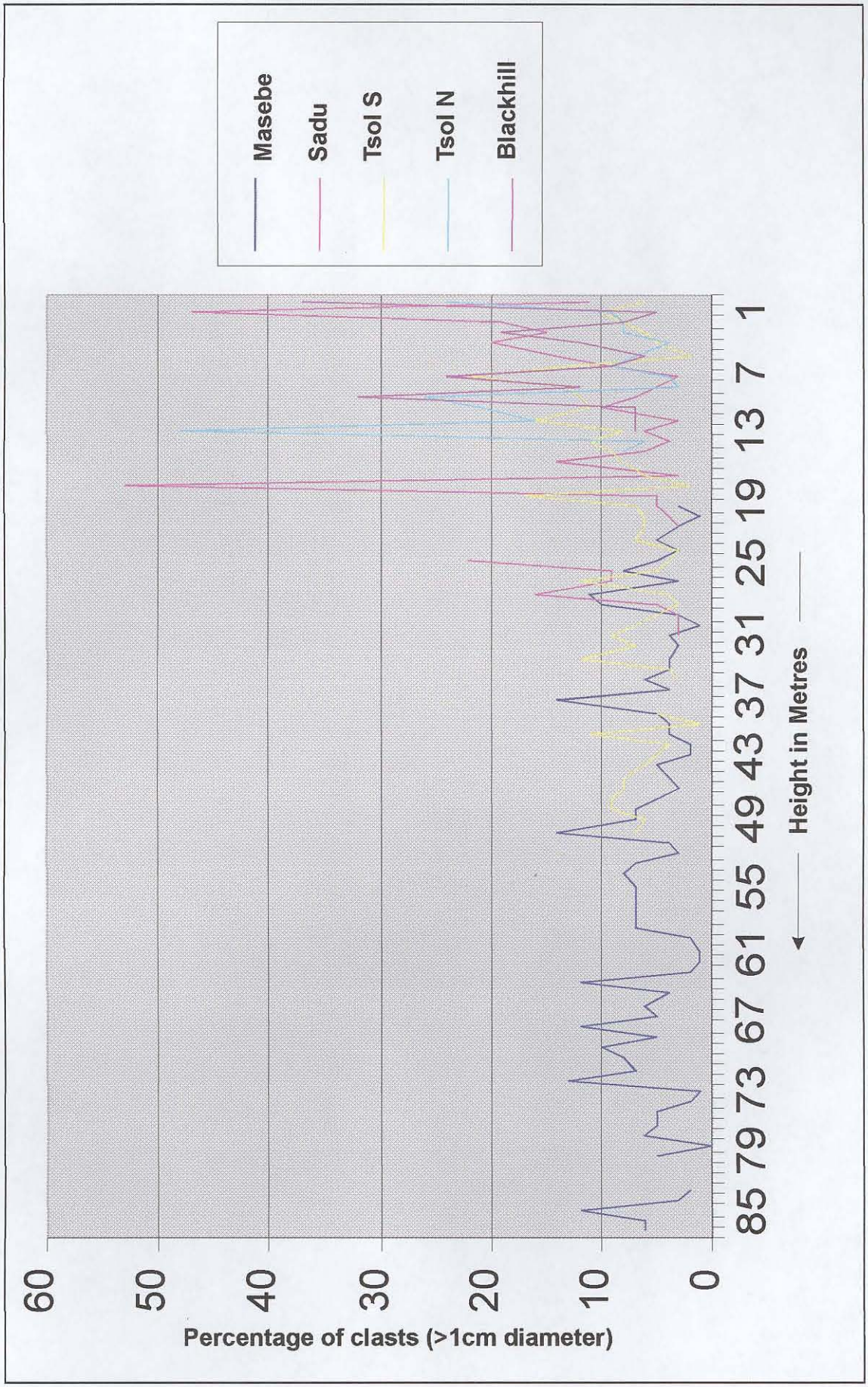

Figure 4.47: Graph to show the variance in the percentage of clasts >1cm diameter, with stratigraphic height in the Mogalakwena Formation.

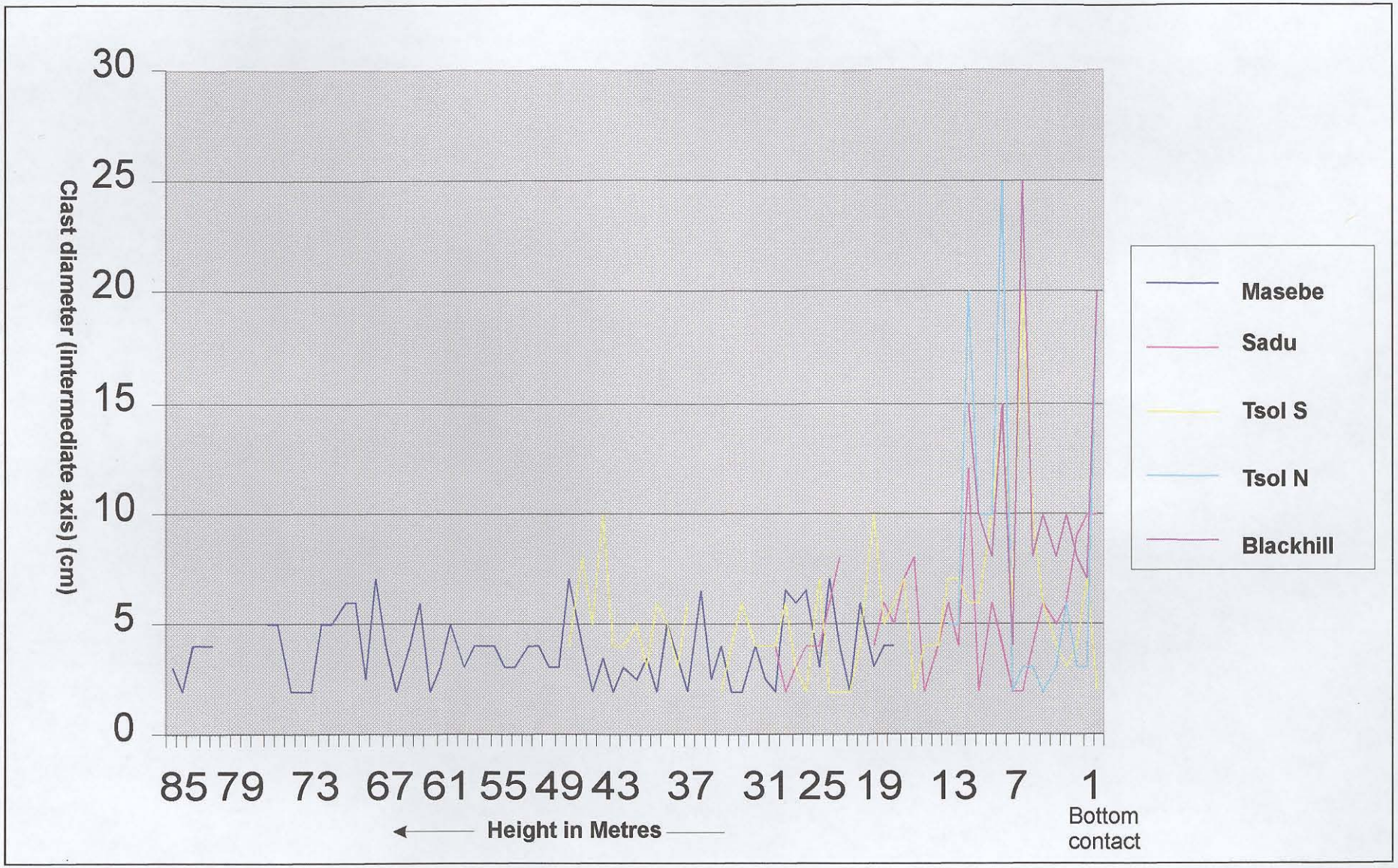

Figure 4.49: Graph to show variance in clast size (intermediate axis) with stratigraphic height in the Mogalakwena Formation.

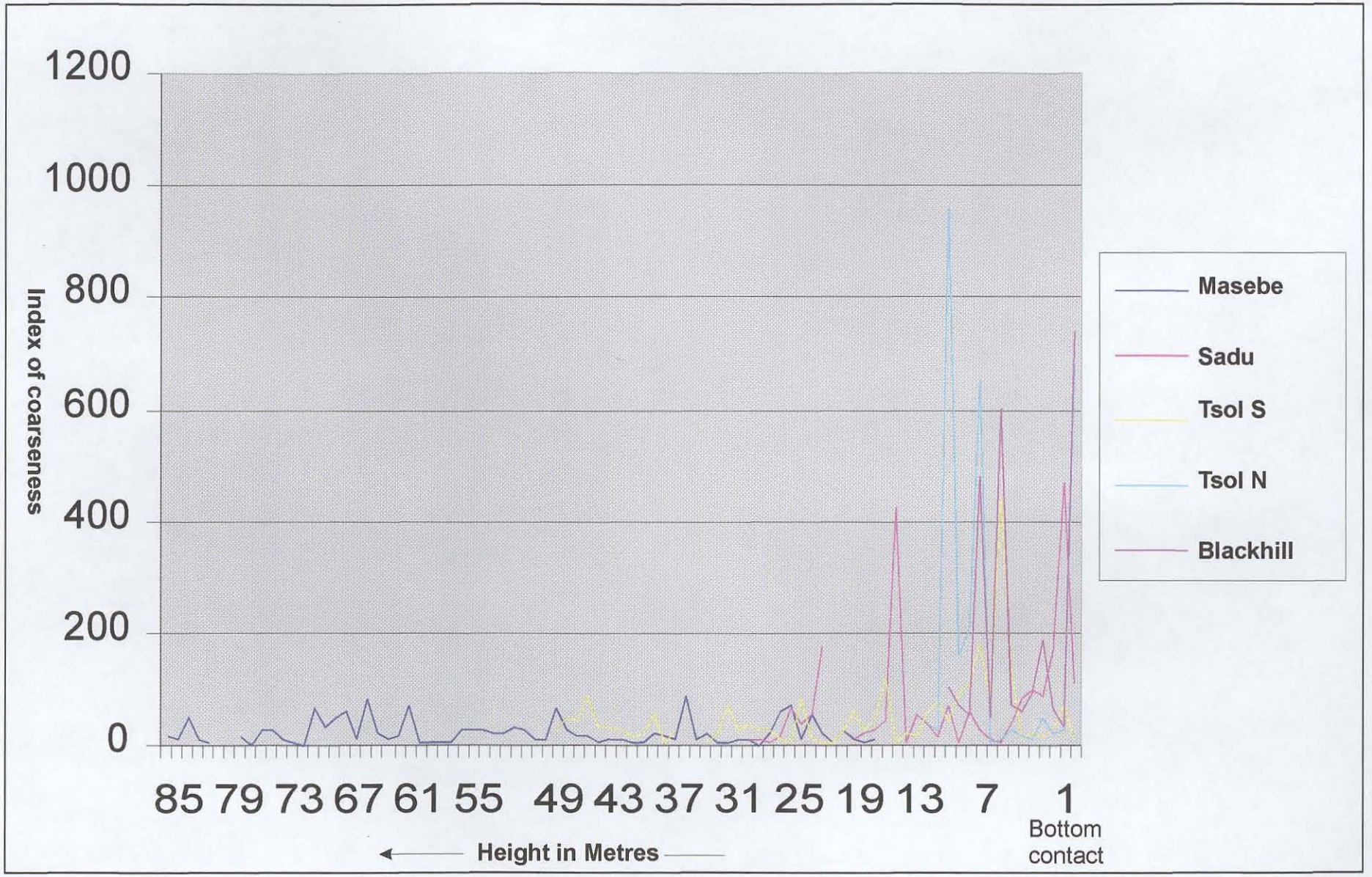

Figure 4.51: Graph to show variance of 'Index of Coarseness' (intermediate axis length x % of clasts) with stratigraphic height in the Mogalakwena Formation.

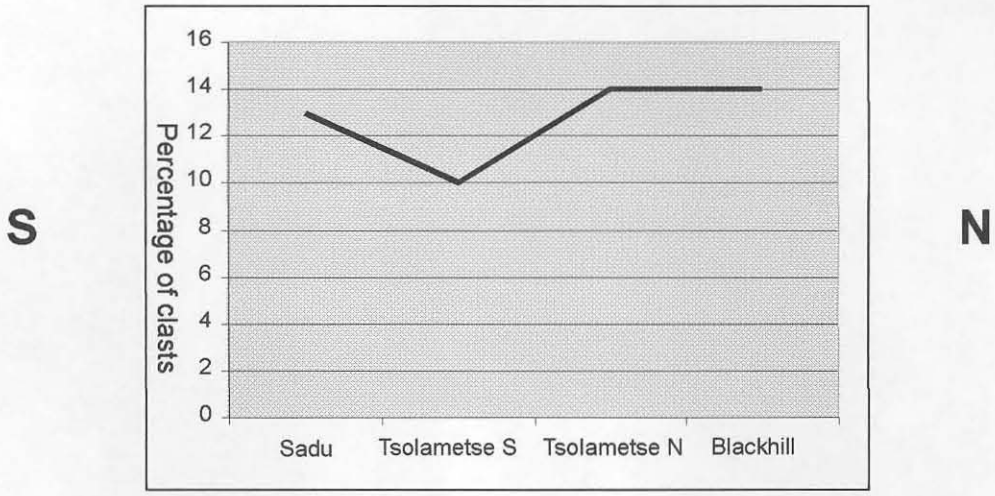

Figure 4.48: Graph showing variance in percentage of clasts from N to S.

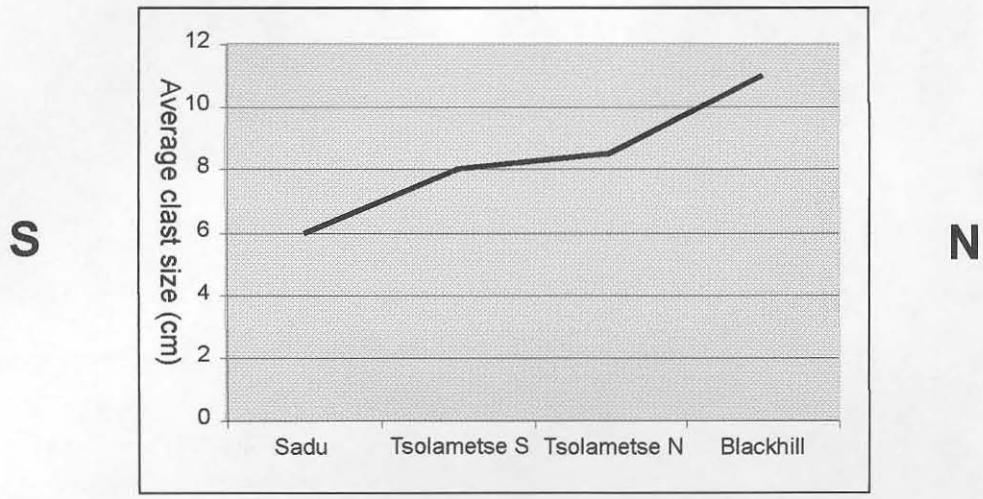

Figure 4.50: Graph showing variance in average size of clasts from N to S.

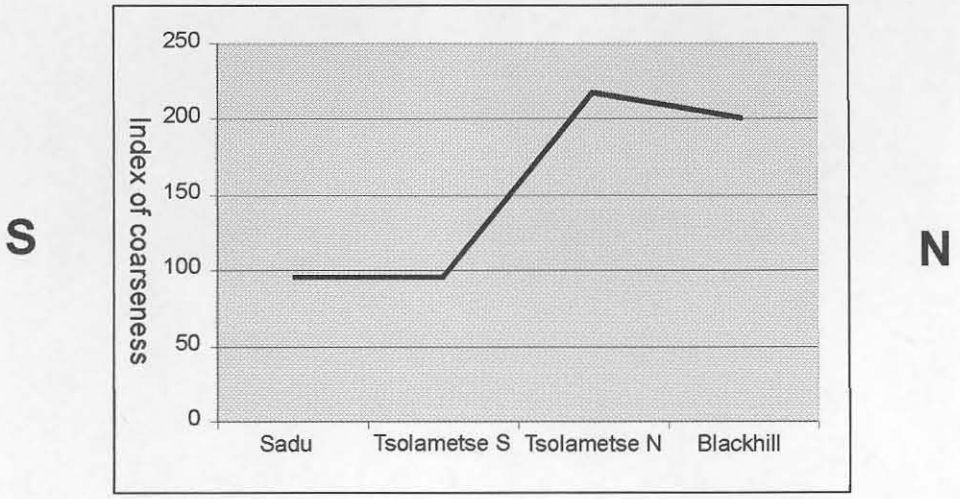

Figure 4.52: Graph to show the variance in the index of coarseness from N to S.

Figure 4.53: Graph to show variance in total percentages for each clast composition with stratigraphic height.

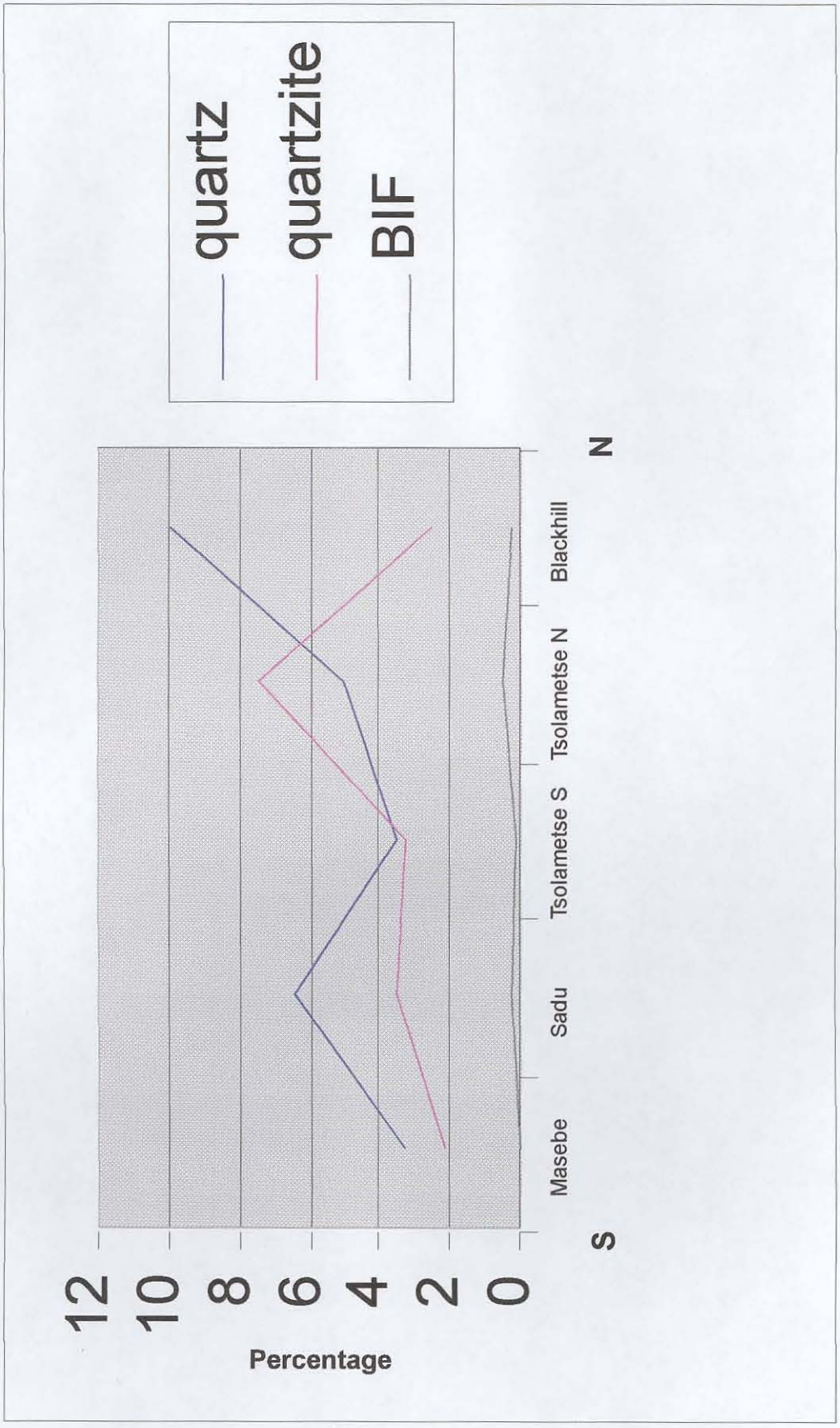

Figure 4.54: Graph to show N-S variance in quartz, quartzite and B.I.F. cobbles present in the Mogalakwena Formation.

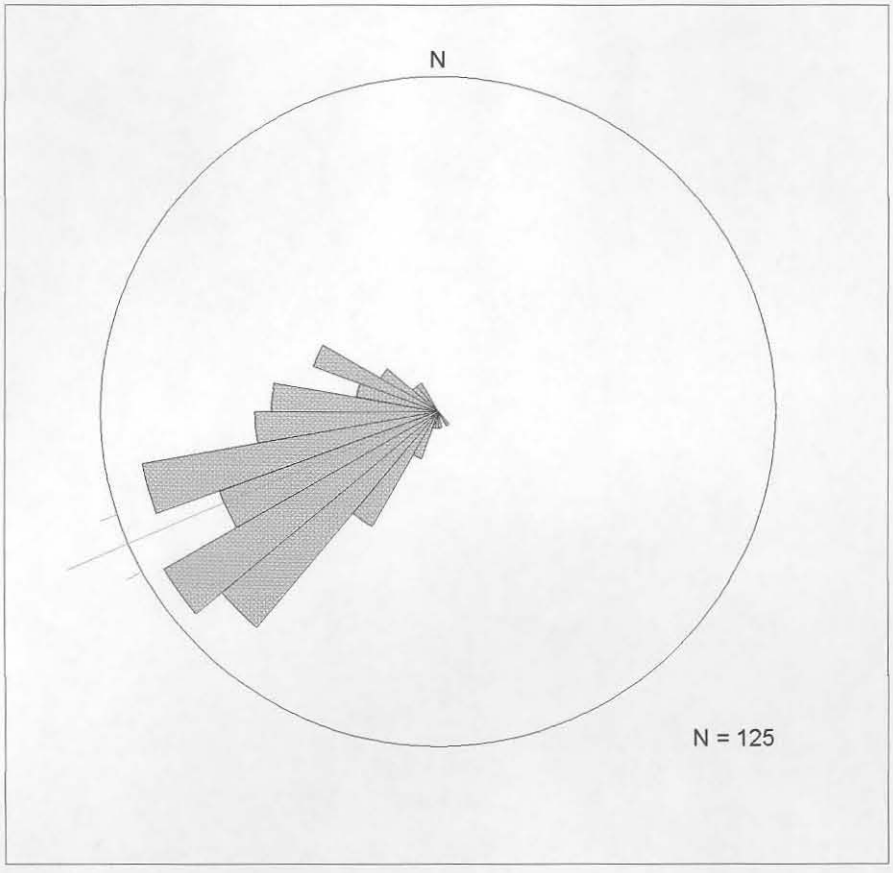

Figure 4.55: Rose diagram to show palaeocurrent directions recorded from trough cross-beds in the Mogalakwena Formation south of the southern strand of the Melinda Fault, in the eastern part of the study area. Principal direction (vector mean) is shown.

Figure 4.56: Sheet-like architectural elements developed at 23°09.36'S; 28°41.92'E. Note that the strata are considerably less conglomeratic than outcrops of Mogalakwena strata further to the east. Cliff is about 50m high.

Figure 4.57: Conglomerate-filled channel form in the Mogalakwena Formation at 23°15.38'S; 28°42.39'E. Strata are bedded parallel to the channel form. Note that pebble size is generally smaller than outcrops of Mogalakwena Formation in the eastern part of the study area (c.f. Figure 4.41). Hammer is 30 cm long.

Figure 4.58: Small (<10cm) trough cross beds with heavy mineral drapes on foresets, characteristic of sandy sheets in the Mogalakwena Formation in the western part of the study area. Recorded at 23°10.23'S; 28°44.18'E. Hammer is 30cm long.

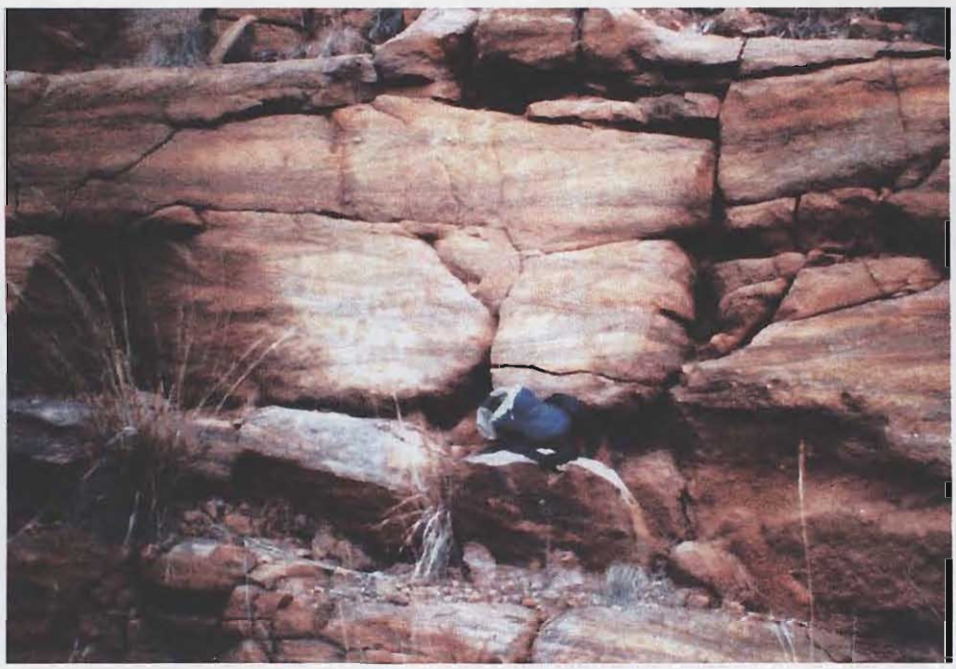

Figure 4.59: Small-scale trough cross-beds developed in the Sandriviersberg Formation (correlated with the Mogalakwena Formation) at 24°20.00'S; 28°33.50'E. Camera bag is 25cm high.

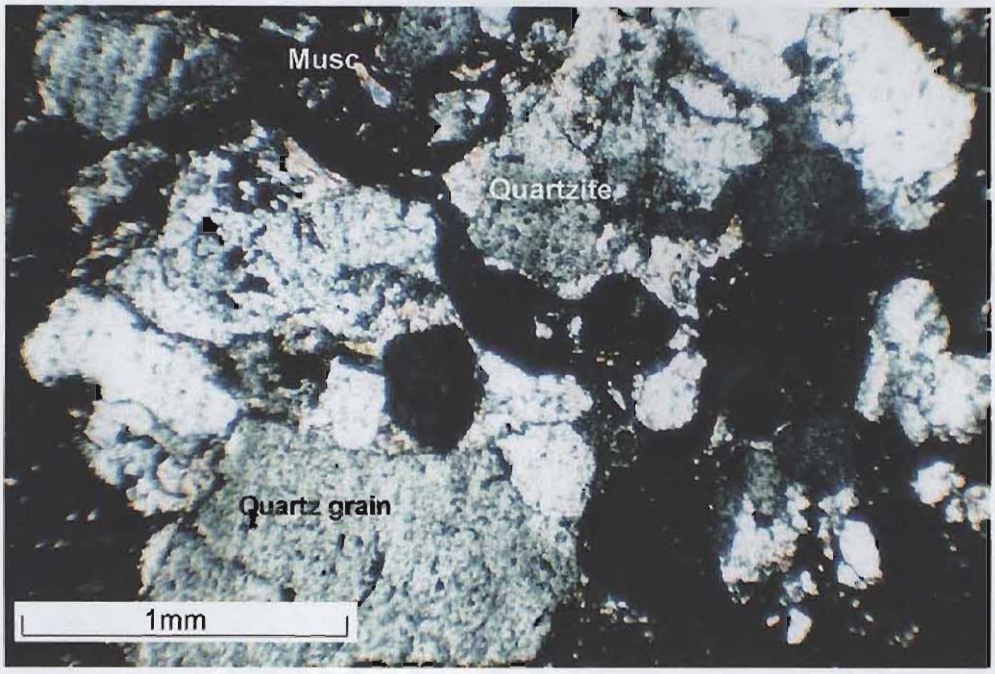

Figure 4.60: Photomicrograph of sandy sheets in the western part of the study area, showing poorly-sorted quartz grains and lithic fragments of quartzite with rare muscovite. Grains are sub-angular with low sphericity.

Figure 4.62: Sheet-like architectural elements of coarse sandstone and granulestone sheets in the Mogalakwena Formation at 23°06'S; 28°54'E. Cliffs are about 200m high.

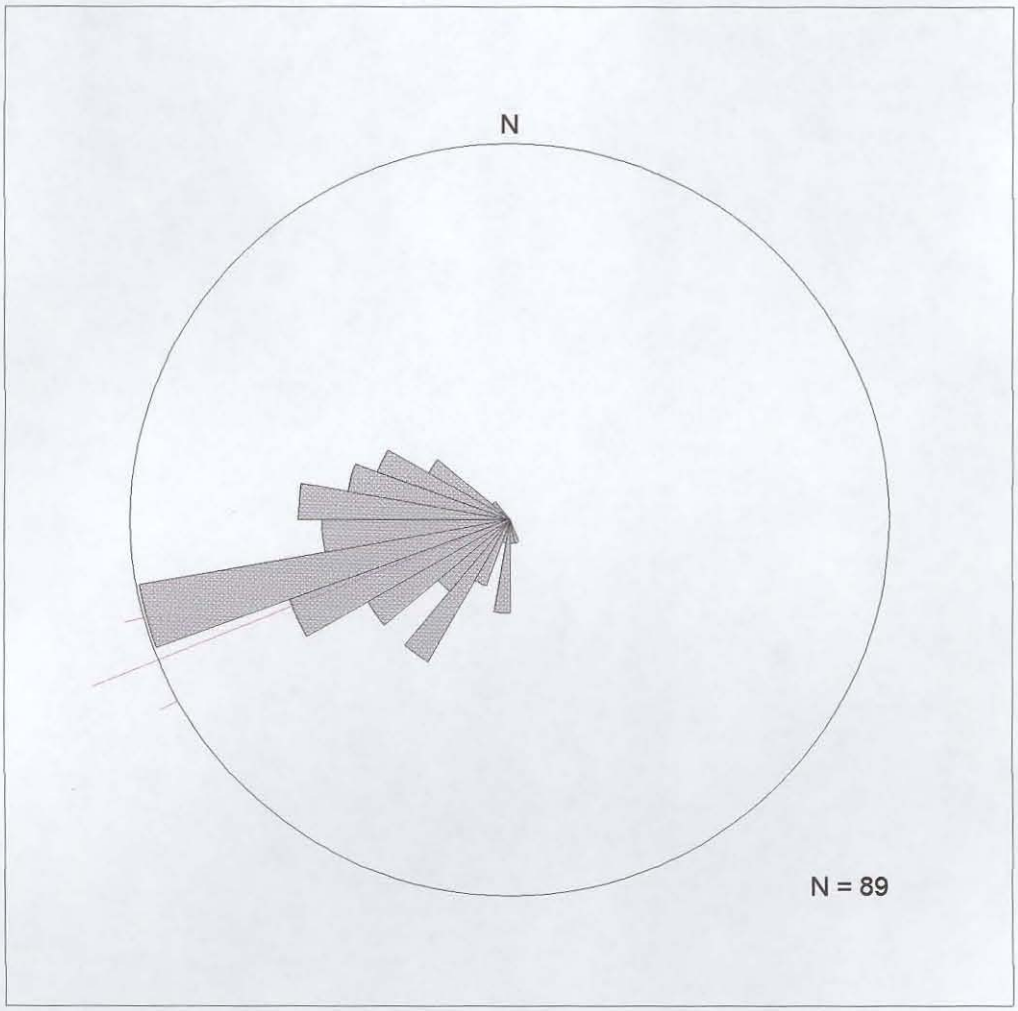

Figure 4.61: Rose diagram showing the palaeocurrent directions recorded from trough cross-beds in the western (distal) outcrops of the Mogalakwena Formation.

Figure 4.63: Thin basal conglomerates of the Mogalakwena Formation at 23°05.76'S; 28°53.47'E. Conglomerates unconformably overlie overturned rocks of the Blouberg Formation (see Chapter 7). Cliff section is 2m high.

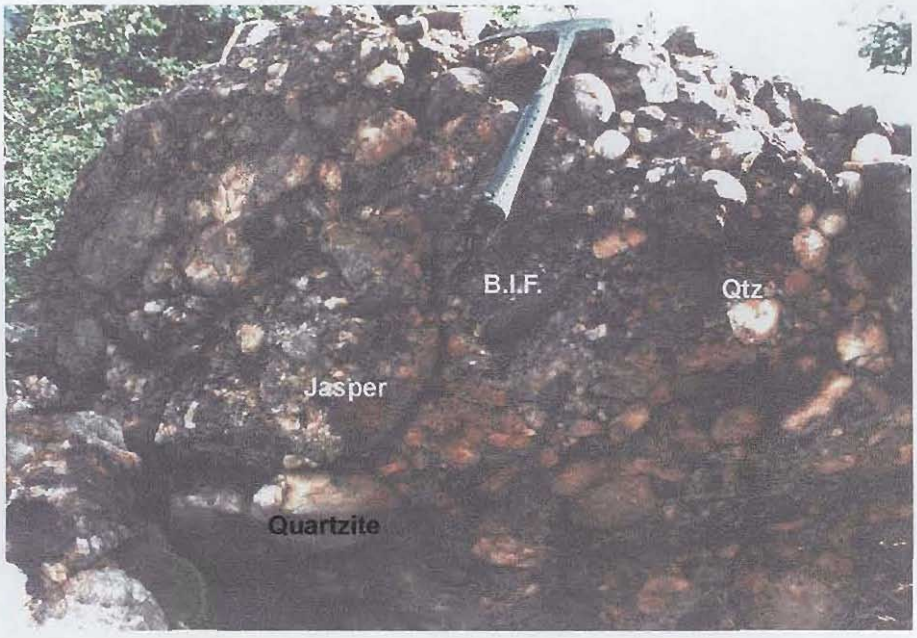

Figure 4.64: Detail of basal conglomerate in the Mogalakwena Formation at 23°05.74'S; 28°53.32'E. Note the presence of quartz, quartzite and B.I.F. clasts (c.f. Figure 4.42) and rare jasper clasts. Hammer is 30cm long.

Figure 4.65: Trough cross-bedded sandstone and granulestone at 23°05.74'S; 28°53.32'E. c.f. Figure 4.43. Pen is 15cm long.

Figure 4.66: Small-scale (<10cm) sets of trough cross-bedded sandstone with heavy mineral drapes developed on foresets. Recorded at 23°07.29'S; 28°57.40'E Note unimodal current direction (towards the W.S.W). c.f. Figure 4.58. Hammer is 30cm long.

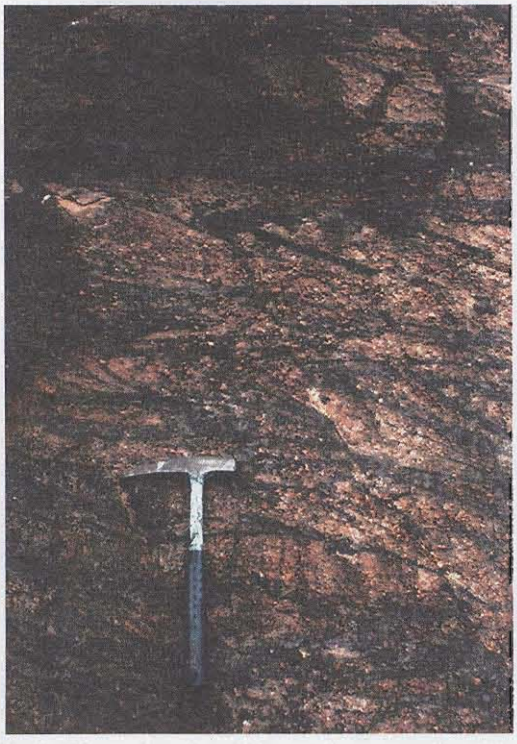

Figure 4.67: Small-scale (< 10cm) sets of trough cross-bedded sandstone with heavy mineral drapes developed on foresets. Recorded at 23° 05.76'S; 28°53.47'E. Hammer is 30cm long.

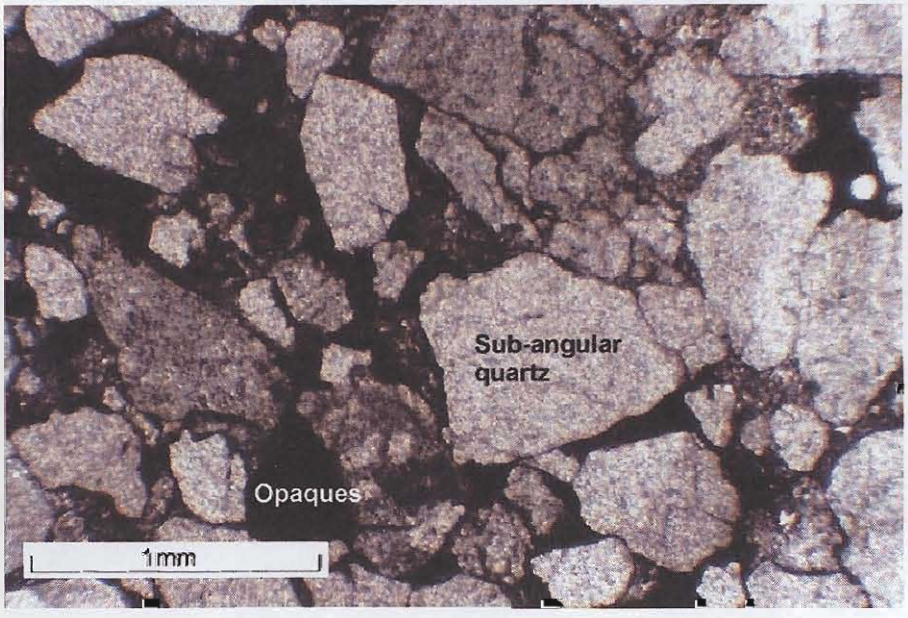

Figure 4.68: Photomicrograph of Mogalakwena strata from 23°05.76'S; 28°53.47'E with sub-angluar quartz grains and high percentage of opaque minerals. (Taken in plane polarised light.)

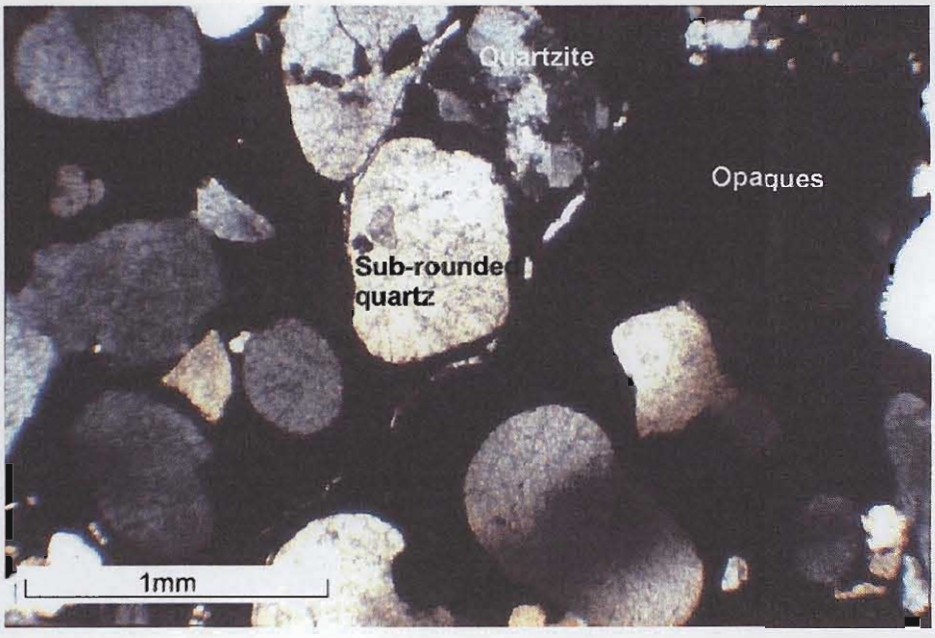

Figure 4.69: Photomicrograph of a thin section of Mogalakwena strata from 23°07.40'S; 28°56.87'E, with rounded to sub-rounded quartz and quartzite grains and opaque interstitial material.

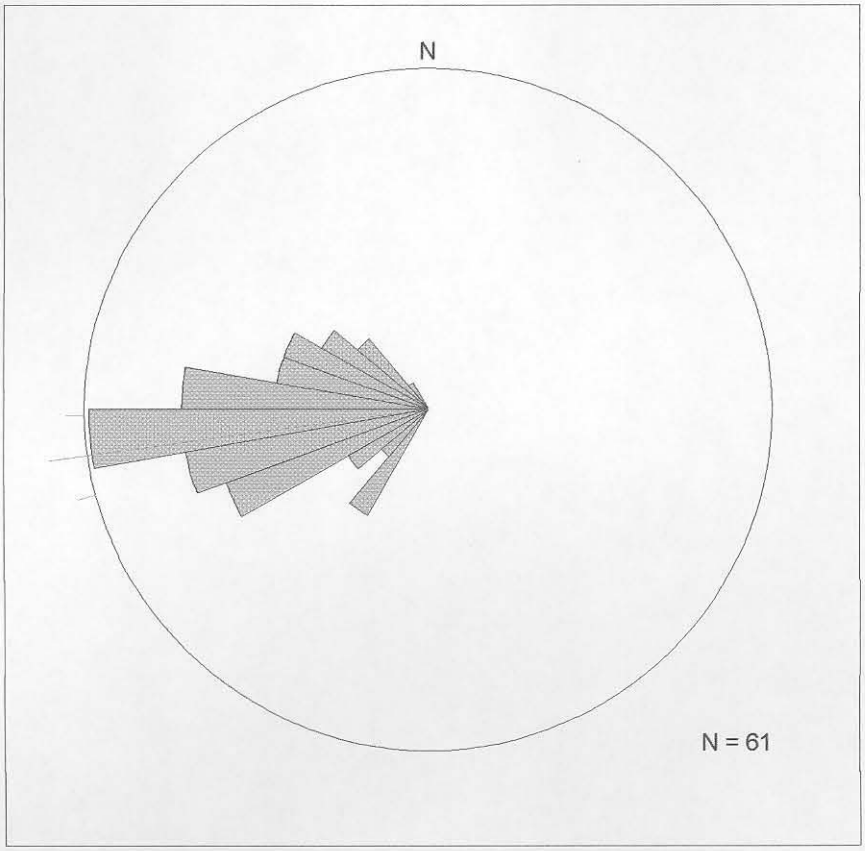

Figure 4.70: Rose diagram showing the palaeocurrent directions recorded from tough cross-beds in the Mogalakwena Formation north of the southern strand of the Melinda Fault. Principal direction (vector mean) is shown.

CHAPTER 5: THE SOUTPANSBERG GROUP.

Outcrops of the Soutpansberg Group within the study area can be classified within two formations: The Sibasa Formation and the Wyllies Poort Formation. The outcrop of the Sibasa Formation is limited to the western edge of Blouberg Mountain, and the Wyllies Poort Formation outcrops extensively in the northeastern part of the study area. Both formations only underlie areas to the north of the southern strand of the Melinda Fault. There is also an isolated outcrop of the Wyllies Poort Formation in the north western part of the study area, at around 23°06'S; 28°33'E (Appendix 1).

5.1: The Sibasa Formation:

Outcrops discussed in this section consist of an amygdaloidal rock that is usually highly weathered (Figures 5.1 and 5.2). The lithology is generally poorly exposed, though outcrops can be found on the lower slopes of Sesuane hill (23°07.5'S; 28°51.5'E) beneath the quartzites of the Wyllies Poort Formation, 6km west of this location, under the eastern slopes of Lebu hill, and also on the upper slopes of a deep valley at around 23°07.5'S; 28°54.50'E. Despite the poor outcrop and generally weathered nature of the rock, the presence of amygdales (Figure 5.1) and locally ropey texture (Figure 5.2), provides good evidence that the Sibasa Formation predominantly consists of lava flows. Three samples of lava were collected, one from each of these locations, and prepared for I.C.P.M.S. and X.R.F. analysis (both major and trace elements). The results from these analyses of the three lavas are shown in Table 5.1.

A plot of the weight percent of total alkalis ($Na_2O + K_2O$; Table 5.1) against silica of lavas from each of these three locations is shown in Figure 5.3, and shows that the lavas can be classified as basalt. Figure 5.3 also shows the plot of total alkalis against silica from previously published analyses (Crow and Condie, 1990) from Sibasa basalts outcropping in the Soutpansberg mountains to the east (Figure 1.7). Figure 5.3 demonstrates that lavas from the Blouberg area compare favourably with the composition of Sibasa basalts from elsewhere in the Soutpansberg basin. The basaltic/basaltic andesite

classification for the lavas is in contrast to the trachyandesitic composition for the same lithology, proposed by Jansen (1976) and Meinster (1977). They named the lavas as the "My Darling trachyandesitic Member" of the Blouberg Formation (Jansen, 1976) or the "My Darling lava Formation" of the pre-Blouberg Lebu Complex (Meinster, 1977). The basaltic composition presented here, and the fact that mapping shows that these basalts can only be seen to be overlain by the Wyllies Poort Formation (Appendix 1), agree with the proposal by Brandl (1986b) that the rocks rather correlate with the Sibasa Formation of the Soutpansberg Group. Even though elements K and Na are considered to be highly mobile, and may be of limited use in characterising ancient rocks, samples analysed were fresh, and such methods have been similarly successfully applied to other Precambrian volcanic rocks (e.g. Harmer and von Gruenewaldt, 1991).In thin section, these Sibasa basalts can be seen to be comprised of small phenocrysts of olivine (often replaced by serpentine), in a groundmass of plagioclase laths and augite (Figure 5.4).

Incompatible trace element data are also presented in Table 5.1. A plot of incompatible trace elements is shown in Figure 5.5, and shows relative enrichment of incompatible trace elements, with negative anomalies of Nb, P and Ti. Further discussion of the trace element chemistry of the Sibasa lavas will be given in Chapter 8, where these data will be compared with incompatible trace element data from dolerite dykes swarms intruding the Blouberg Formation and the Waterberg Group strata.

5.2: The Wyllies Poort Formation:

Strata of the Wyllies Poort Formation occupy the northern part of the study area, and underlie areas only to the north of the southern strand of the Melinda Fault (Appendix 1). Generally the Wyllies Poort Formation underlies the mountainous areas of Blouberg mountain and its foothills to the northeast, though the unit also outcrops in the north-western part of the study area (Appendix 1).

The strata are generally purple/brown quartzites, which locally contain thin pebble washes, about 3-10cm thick (Figure 5.6). Pebbles are composed of quartz, quartzite and,

rarely, coarse-grained sandstone, and are generally 1-2cm in diameter. Locally, the Wyllies Poort Formation is less recrystallised, and can be seen to be composed, generally, of medium- to coarse-grained sandstone, consisting of sub-angular to sub-rounded quartz and lithic (quartzite) grains with high sphericity. Locally these grains may reach up to 2mm in diameter (i.e small granules).

The mountainous terrain underlain by the Wyllies Poort Formation offers good topography over which architectural relationships can be easily traced from photographs. The Wyllies Poort Formation appears to be comprised of architectural elements of major sandstone sheets (element CHS; Table 3.1). Individual channel forms, so conspicuous in other clastic strata in the Blouberg area, are absent in the Wyllies Poort Formation (Figure 5.7).

The Wyllies Poort Formation has a maximum preserved thickness of about 700m, from its lower contact with the basement, Sibasa Formation or Mogalakwena Formation in the Blouberg mountain foothills, to the summit (Appendix 1). The generally steep nature of the topography around Blouberg mountain provides few accessible opportunities for recording vertical changes in facies characteristics throughout the succession. However, the line marked in Figure 5.8 follows a relatively safe footpath from the lower-most outcrops of the Wyllies Poort Formation to the summit. The following data describe the general vertical facies changes recorded from this area.

The lower-most 200m of the Wyllies Poort Formation are comprised of trough cross-bedded coarse sandstone facies (St; Table 3.1) with relatively small sets, consisting of moderately sorted, sub-rounded to sub-angular quartz grains and lithic clasts (quartzite). Quartz grains are commonly less than 1mm in diameter, though lithic clasts rarely reach more than 2mm in diameter (granules). Set thicknesses generally vary between 5 and 40cm (Figure 5.9). Soft-sedimentary deformation structures can be found locally (Figure 5.9). Cosets are up to 150cm in thickness. Pebbles are common in this lower-most portion of the Wyllies Poort strata, deposited either on bedding or foreset planes, and help define fining-upwards foreset laminae/beds.

Above the cross-bedded facies, strata consist of planar-bedded sandstone facies (Sh; Table 3.1), where beds are commonly 5-10cm thick. Again, patches which are less recrystallised appear to be composed of sub-angular to sub-rounded quartz grains up to 2mm in diameter, with similarly-sized lithic clasts (quartzitic). Parting lineation was not recorded on planar beds, though it may have been destroyed during recrystallisation if originally present. Locally, sets of very low-angled ($<10^0$) cross-bedding (facies Sl; Table 3.1) can be seen between the planar bedded facies. Bedding surfaces are locally ripplemarked (Facies Sr; Table 3.1), including symmetrical ripples (Figure 5.10), linguoid ripples (Figure 5.11) and asymmetric ripples (Figure 5.12). Together these three facies make up about 200m of the Wyllies Poort succession, and are devoid of pebbles.

Above this, about for about 300m vertically, a sandstone facies (composed of quartz grains and quartzitic lithic clasts) with large-scale trough cross-beds (St) is dominant. Again, pebble conglomerate interbeds are rare. Trough cross-bed sets are commonly between 1 and 2m in thickness; they are locally bound above and below by planar-bedded sandstone (Figure 5.13). Rarely, very low angled planar cross-bedding is also present, interbedded with the large scale trough cross-bedded facies (Figure 5.13). Locally, soft-sediment deformation is indicated by the presence of sand volcanoes (Figure 5.14). On the summit plateau of Blouberg mountain (the very top of the preserved section), there is a return to planar-bedded, ripplemarked sandstone facies (Sr; Table 3.1).

Thus the Wyllies Poort Formation can be considered to contain two dominant facies associations; (1.) small-and large-scale trough cross-bedded sandstones with interbedded pebble conglomerate, and (2.) planar-bedded sandstones with ripplemarks and low-angled (planar) cross-beds.

Wyllies Poort quartzite appears to have undergone intense pressure solution of grain boundaries, as shown by thin section in Figure 5.15, so that original textures are difficult to recognise. Areas which have undergone less pressure solution, and hence less recrystallisation, can be seen to be made up of sub-rounded to angular grains of quartz, with rare lithic clasts of quartzite (Figure 5.16), and grains appear to have quartz

overgrowths. Counting of 500 points from 1 section within the Wyllies Poort quartzites produced an average composition of 73% quartz grains and 27% lithic fragments, so they can be classified as lithic arenites (Pettijohn *et al.*, 1973). Recorded lithic fragments were quartzitic and, rarely, very fine sandstone.

Recorded pebbles within the Wyllies Poort Formation were generally quartz or quartzitic, though locally pebbles of coarse sandstone were found. A thin section of one of these sandstone pebbles is shown in Figure 5.17, and shows that interstitial red clays support the grains in the pebble. The composition of one of these sandstone pebbles was determined by point counting, and a survey of 500 points gave an average composition of 48% quartz grains, 25% lithic fragments (quartzite), and 27% interstitial matrix (red clay minerals). Thus, using the scheme of Pettijohn *et al.* (1973), ordinarily used to discriminate arenites, the sandstone pebbles can be characterised as having a lithic wacke composition. The thin section shown in Figure 5.18 is from a coarse-grained sandy sheet in the Mogalakwena Formation (Section 4.41) and closely resembles that of the coarse sandstone pebble shown in Figure 5.17. A point count from this Mogalakwena thin section showed an average composition (from 500 points) of 40% quartz, 39% matrix (=clays) and 21% lithic fragments (=quartzite), which compares favourably with the point count from the Wyllies Poort-hosted sandstone pebble.

Palaeocurrent directions recorded in the Wyllies Poort Formation are shown in Figure 5.19, and show that different facies recorded in the Wyllies Poort Formation generally show contrasting palaeocurrent directions. Large- and small-scale trough cross-bedded sandstones, recorded from the area shown on Figure 5.8, are given in Figure 5.19a. Ripplemarked sandstones (both asymmetric and symmetric) from the same area, associated with planar-bedded sandstone are shown in Figures 5.19b and 5.19c, respectively. Palaeocurrent directions measured from ripplemarked sandstones recorded in the north eastern foothills of Blouberg (at around 23°00'S; 29°07'E) are shown in Figure 5.19d.

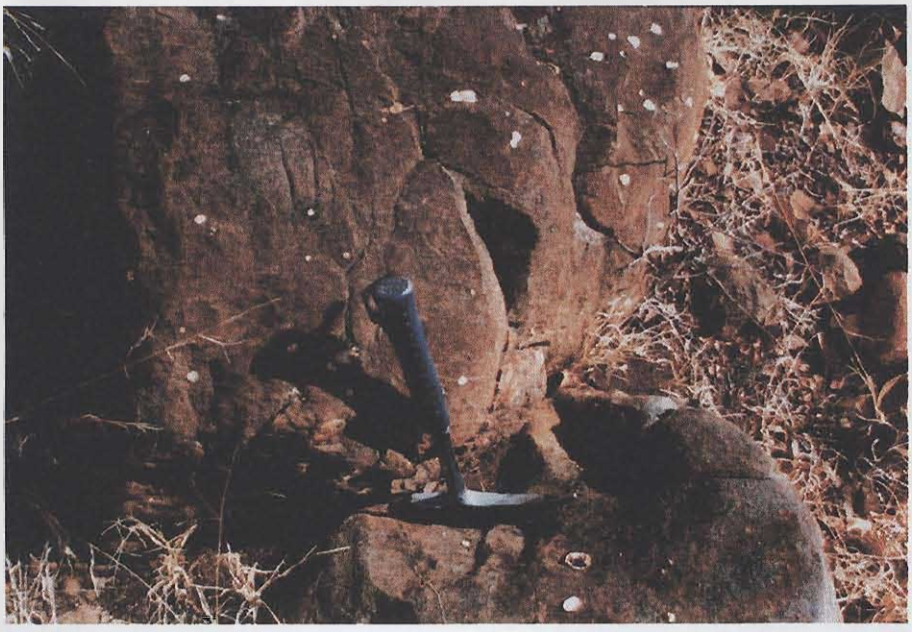

Figure 5.1: Amygdaloidal basalt of the Sibasa Formation at 23°06.68'S; 28°52.32'E. Hammer is 30cm long.

Figure 5.2: Ropey lava texture in basalt of the Sibasa Formation at 23°06.68'S; 28°52.32'E. Hammer is 30cm long.

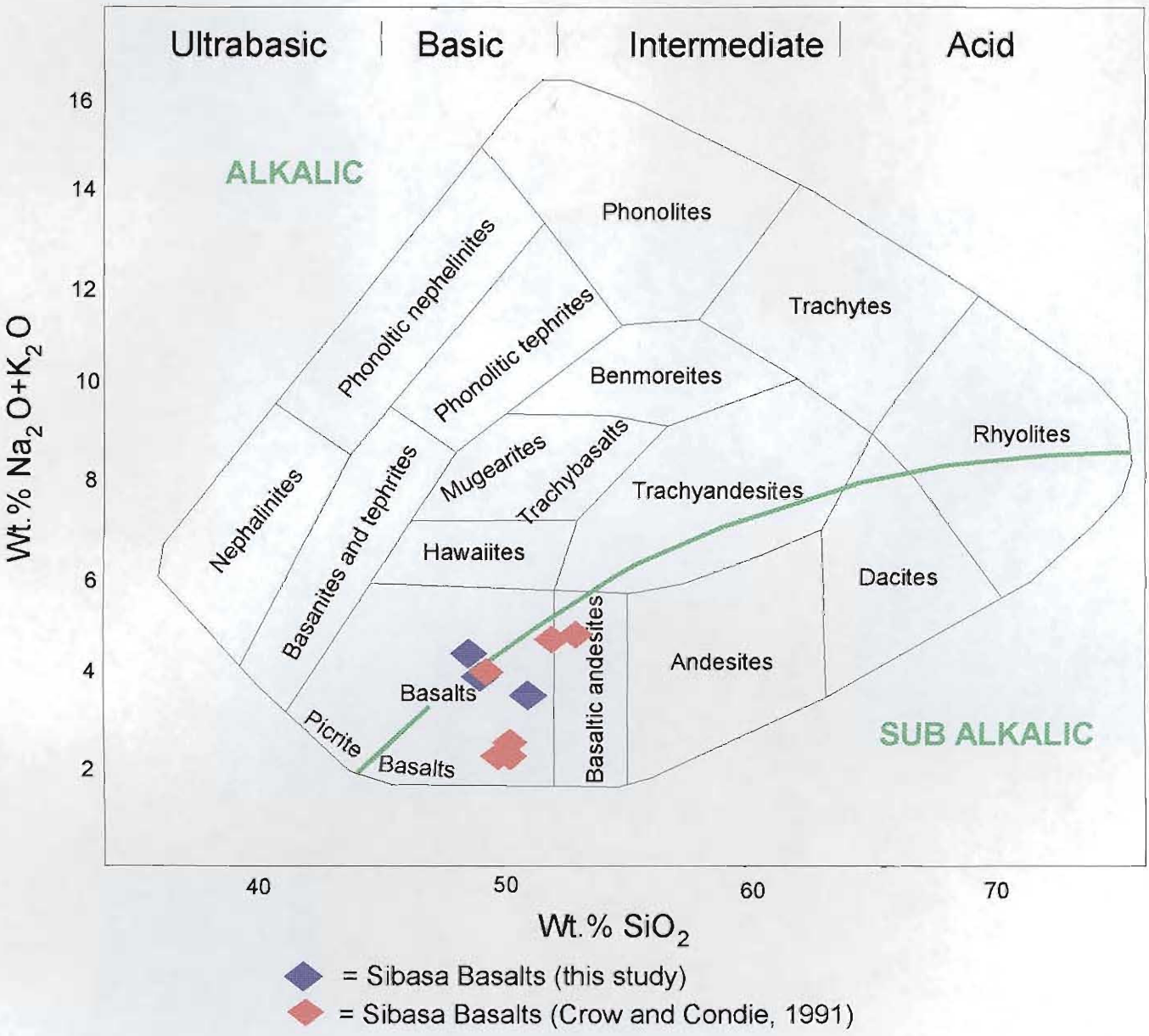

Figure 5.3: Total Alkali/Silica diagram (after Wilson, 1989) to show nomenclature of Sibasa basalts, and their comparison with Sibasa basalts analysed from elsewhere.

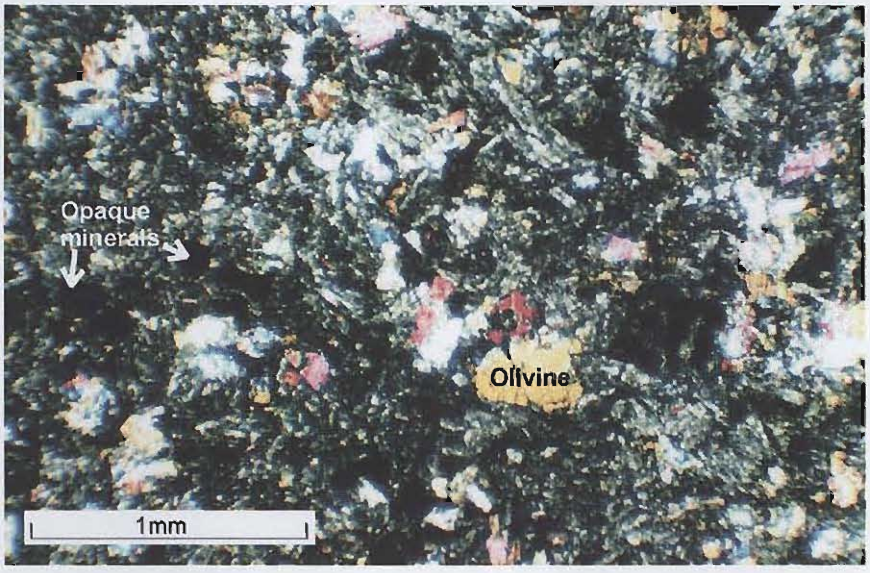

Figure 5.4: Photomicrograph of Sibasa basalt, showing olivine phenocrysts in a groundmass of plagioclase feldspar and augite. Several opaque minerals are also present.

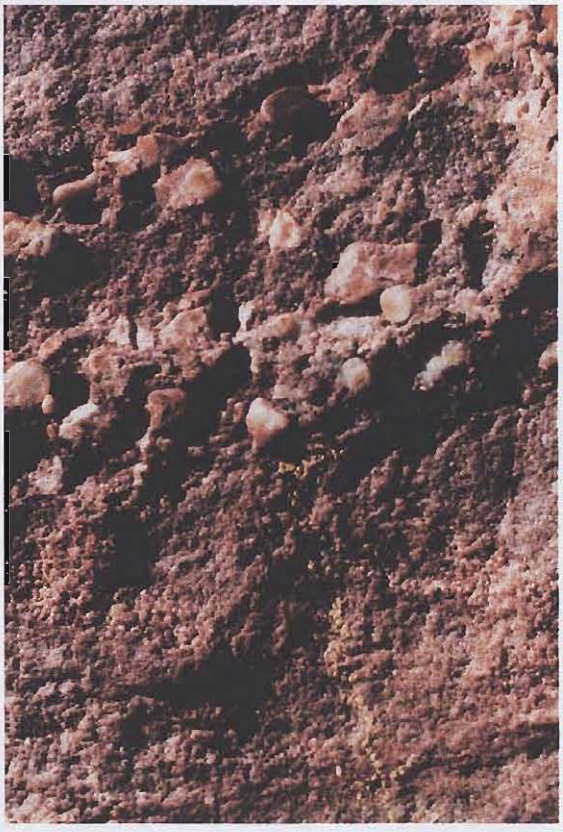

Figure 5.6: Thin layer of quartz pebbles in the Wyllies Poort Formation. Pebble layer is interbedded with brown/purple quartzite typical of the Wyllies Poort Formation. Section is 20cm high.

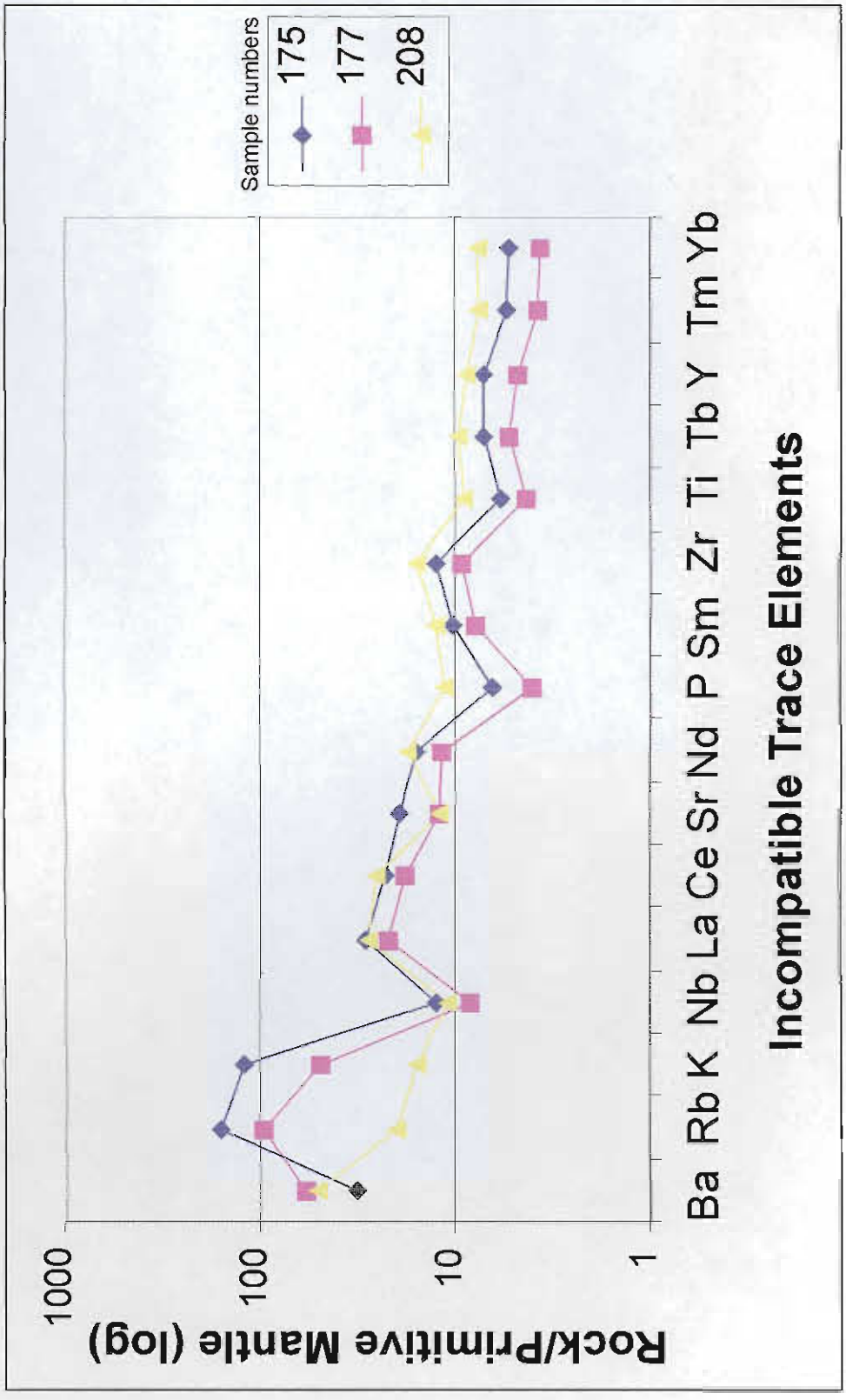

Figure 5.5: Spidergram to show values of normalised incompatible trace element values determined for the Sibasa Formation.

Figure 5.7: Oblique aerial photograph of the summit area of Blouberg mountain, showing relatively horizontally inclined sheet-like elements with no channel forms preserved.

Figure 5.9: Relatively small (20cm set thickness) trough cross-bedded sets in the lower part of the Wyllies Poort Formation. The indicated foresets have been overturned during soft sedimentary deformation, possibly caused by strong water currents during the deposition of subsequent beds.

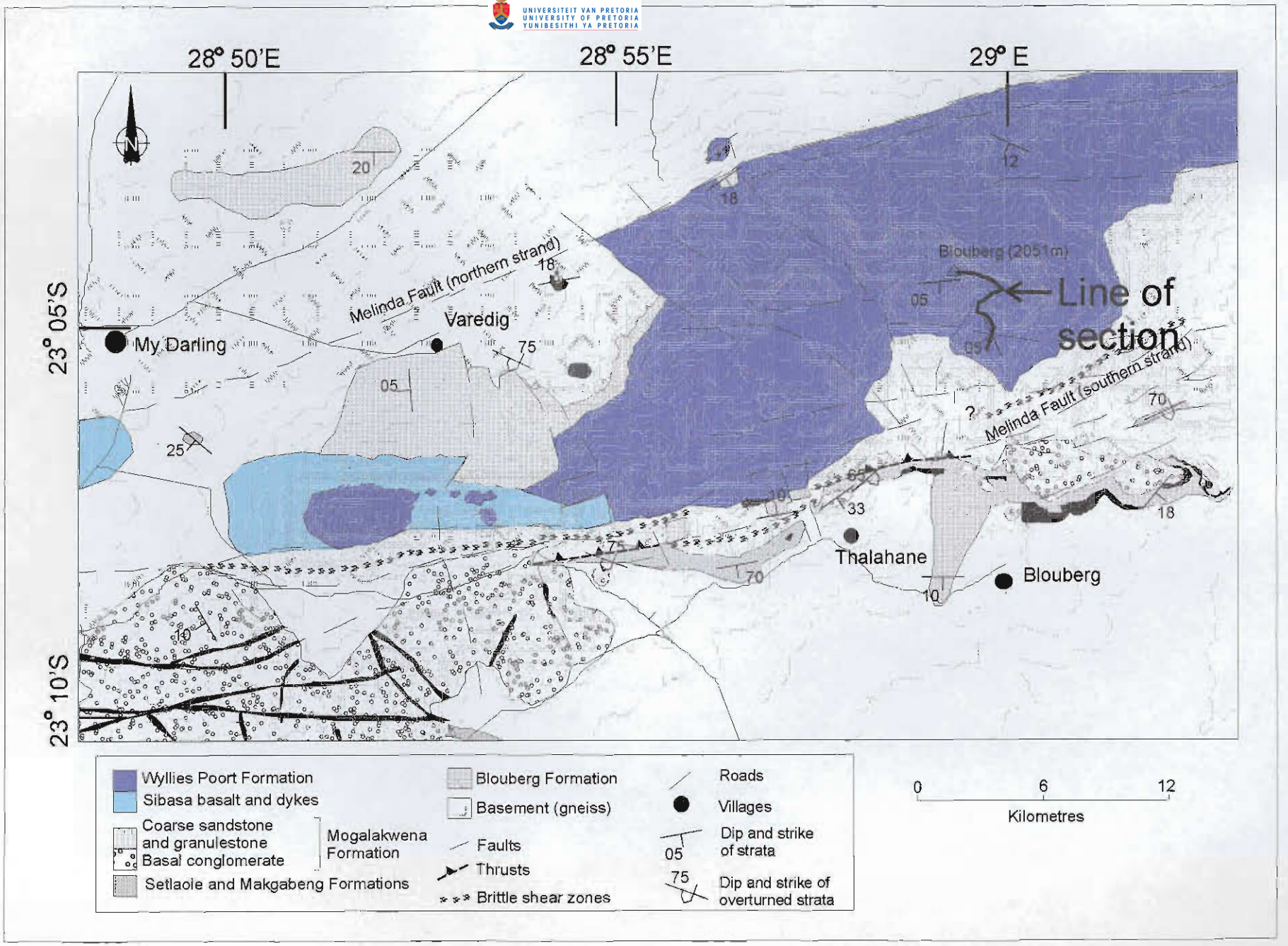

Figure 5.8: Location of stratigraphic section recorded in the Wyllies Poort Formation.

Figure 5.10: Large symmetric ripples in the mid-Wyllies Poort Formation at 23°04.57'S; 28°59.65'E. Hammer is 30cm long.

Figure 5.11: Linguoid ripples in the upper strata of the Wyllies Poort Formation. Recorded at 23°04.26'S; 28°59.19'E. Lens cap is 5cm wide.

Figure 5.12: Asymmetric ripplemarks in the Wyllies Poort Formation at 22°59.67'S; 29°09.58'E. Lens cap is 5cm wide.

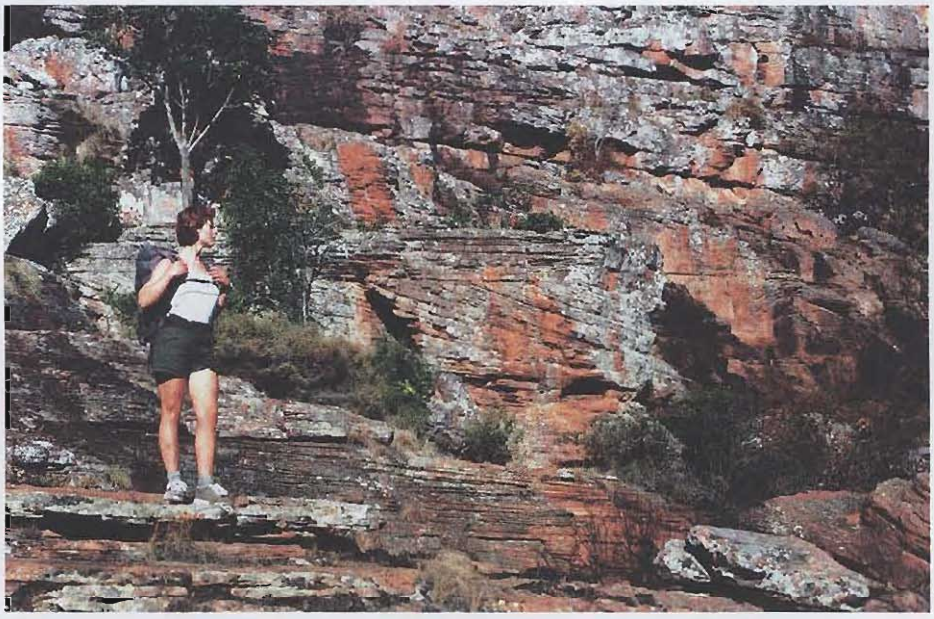

Figure 5.13: Large scale (>2m) trough cross-bedded sandstone (middle distance), interbedded with planar-bedded sandstone and rare very low angle (<10°) planar cross-bedded sandstone (foreground), in the mid-Wyllies Poort Formation. Recorded at 23°04.57'S; 28°59.65'E.

Figure 5.14: Plan section of a sand volcano, developed in the mid-Wyllies Poort Formation at 23°04.25'S; 28°59.52'E. Lens cap is 5cm wide.

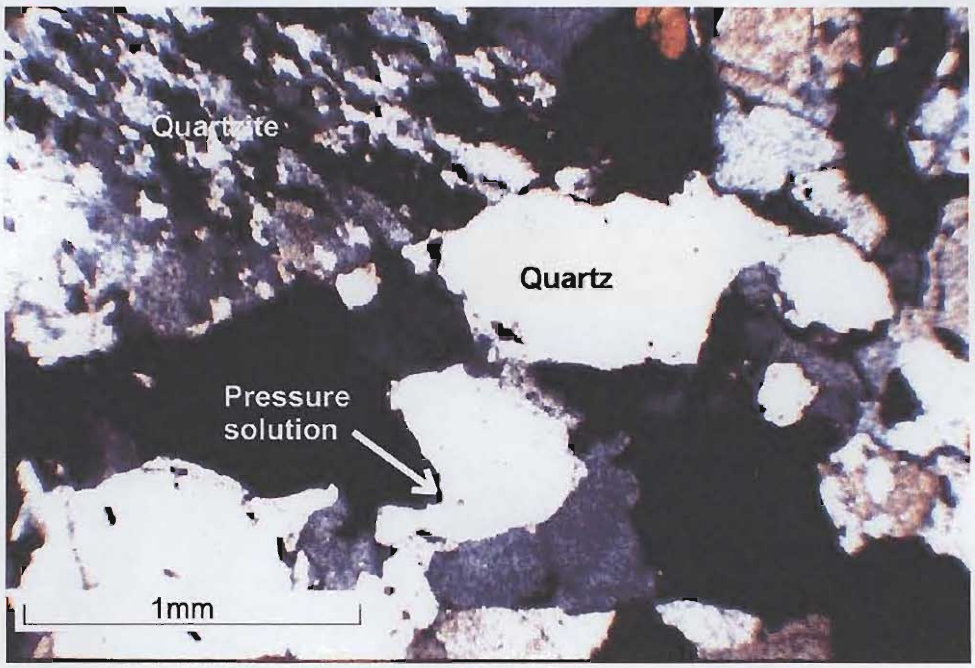

Figure 5.15: Photomicrograph of Wyllies Poort quartzite, showing pressure solution at boundaries of quartz and lithic grains (quartzite).

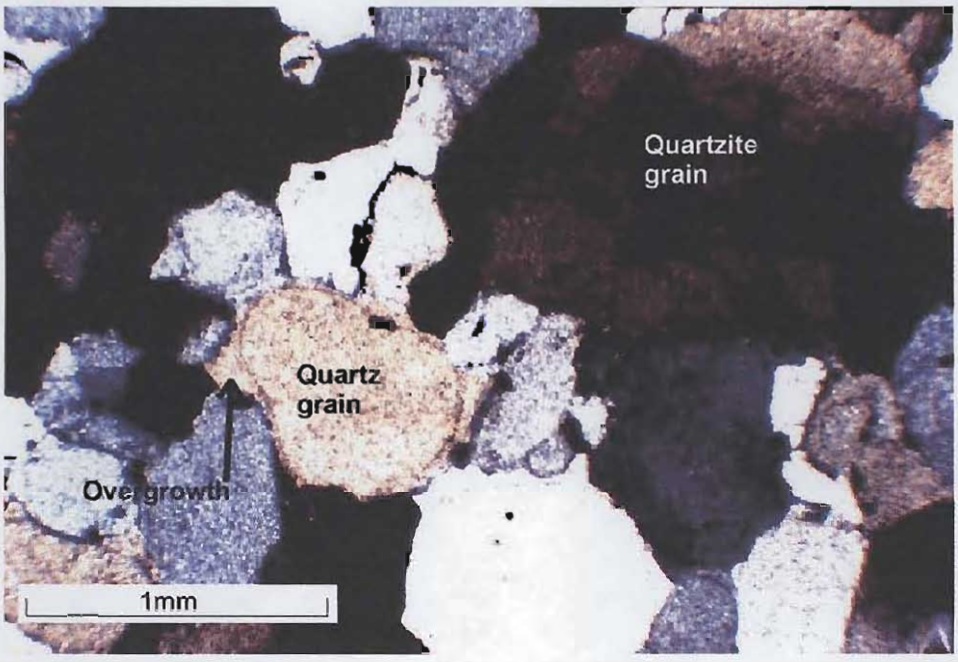

Figure 5.16: Photomicrograph of Wyllies Poort sandstone, showing sub-rounded to sub-angular grains with quartz overgrowths in optical continuity with parent grains of quartz and quartzite.

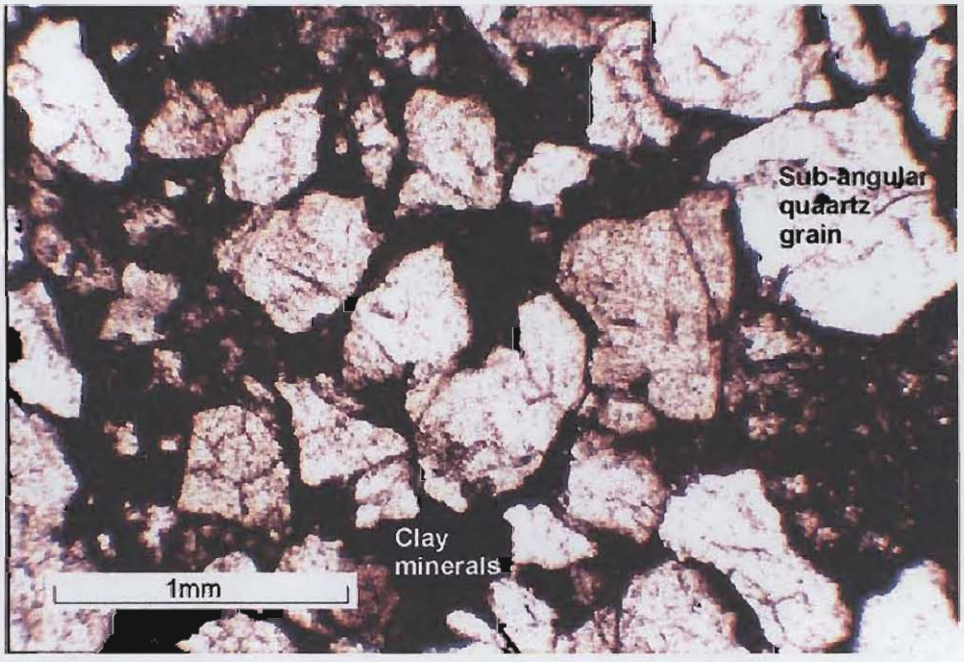

Figure 5.17: Photomicrograph from a sandstone pebble within the Wyllies Poort Formation. Sub-angular quartz grains are supported by interstitial red clay minerals.

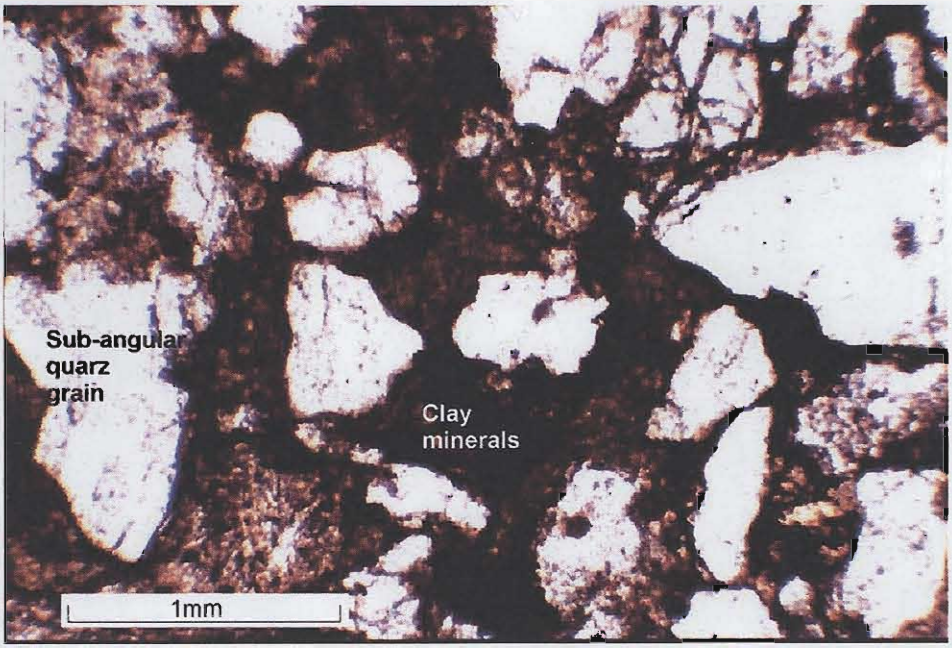

Figure 5.18: Photomicrograph of coarse sandstone from the Mogalakwena Formation, showing sub-angular quartz grains with interstitial red clay minerals. c.f. Figure 5.17.

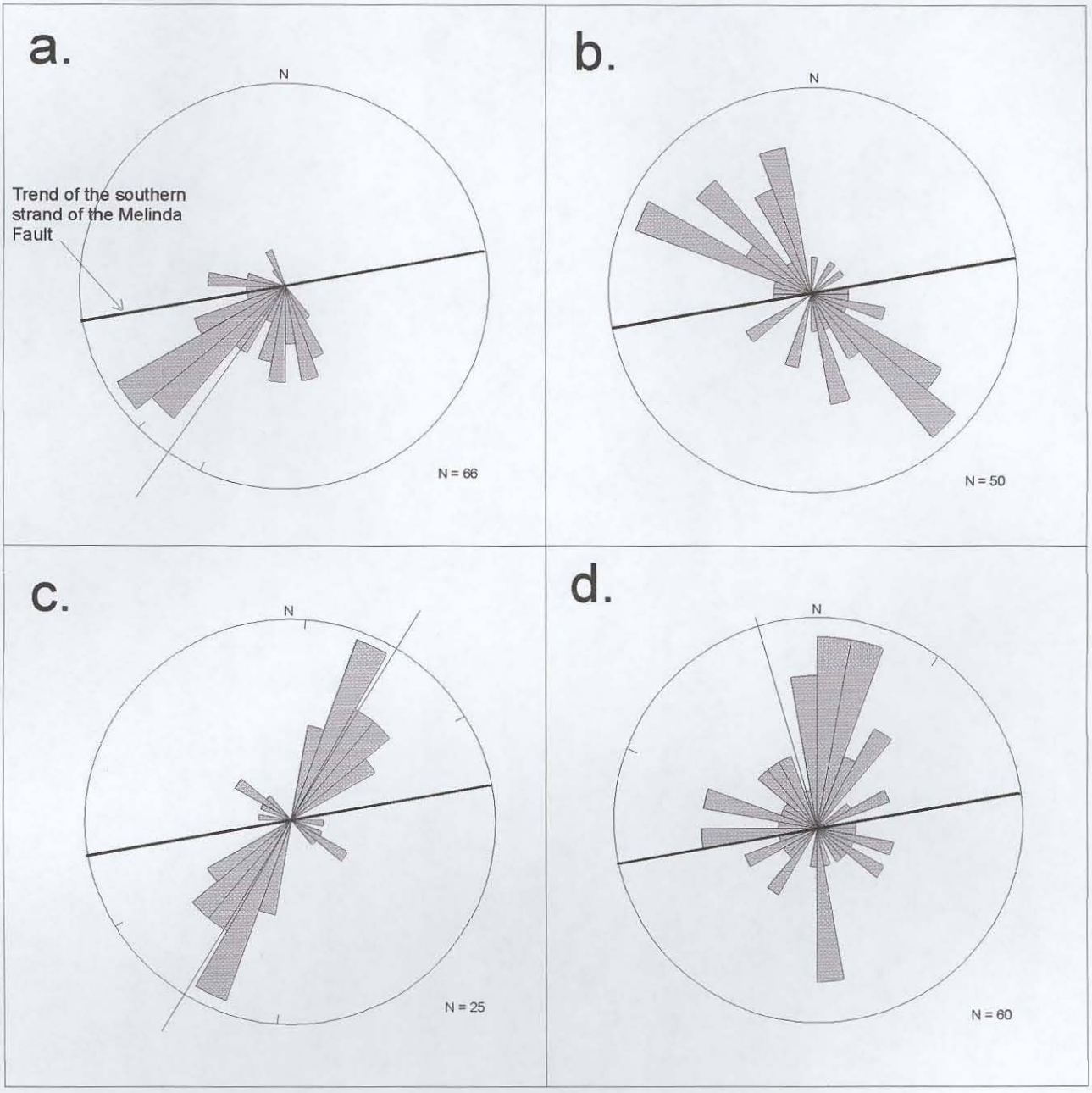

Figure 5.19: Rose diagrams showing the palaeocurrent directions recorded in different facies of the Wyllies Poort Formation: a.)Trough cross-bedded sandstone; b.) Asymmetric ripplemarks; c.) Symmetric ripplemarks (trend); d.) Asymmetric Ripplemarks in north-eastern foothills of Blouberg. Where appropriate, principal direction (vector mean) is indicated.

%	175	177	208
SiO2	49.05	50.84	48.56
TiO2	1.27	0.93	1.96
Al2O3	13.45	14.13	14
Fe2O3	13.8	11.83	16.31
MnO	0.18	0.18	0.21
MgO	3.59	6.25	5.42
CaO	12.12	9.33	6.92
Na2O	0.16	1.95	3.83
K2O	3.68	1.49	0.048
P2O5	0.14	0.09	0.25
Cr2O3	0	0.01	0.02
NiO	0.01	0.02	0.01
LOI	1.44	2	2.54
Total	98.97	99.12	100.62
Cu	98	101	249
Ga	27	17	20
Mo	2	<1	<1
Nb	9	6	8
Ni	80	141	82
Pb	5	3	2
Rb	101	62	13
Sr	412	255	260
Th	<5	<5	<5
U	<3	<3	<3
Y	33	22	40
Zn	81	84	137
Zr	142	104	177
Ba	223	404	358
Cl	32	<30	<30
Cr	27	60	130
%S	<0.01	<0.01	<0.01
Sc	38	31	35
V	312	230	384

Element	175	177	208
La	20.3	15.5	19.6
Ce	41.0	32.8	45.0
Pr	5.22	3.96	5.55
Nd	21.3	16.1	24.1
Sm	4.66	3.47	5.64
Eu	1.32	1.01	1.62
Gd	4.59	3.63	6.31
Tb	0.77	0.58	1.04
Dy	4.91	3.63	6.79
Ho	1.00	0.71	1.40
Er	2.91	1.97	4.02
Tm	0.41	0.28	0.57
Yb	2.63	1.81	3.75
Lu	0.38	0.27	0.57
Nb	9.0	6.0	8.0

Table 5.1: X.R.F and I.C.P.M.S. results for major (%) and trace (ppm) element abundances in the Sibasa Formation. Sample 175 is from 23° 06.73'S; 28° 47.61'E. Sample 177 is from 23° 07.10'S; 28° 50.10'E. Sample 208 is from 23° 07.30'S; 28° 54.70'E.

CHAPTER 6: INTRUSIVE ROCKS.

Intrusive igneous rocks occur only locally in the study area, and predominantly intrude in the area south of the southern strand of the Melinda Fault, where dykes locally cut the strata of the Waterberg Group, and locally rocks of the Blouberg Formation and the basement (Appendix 1). Other intrusive bodies, such as a sill cutting the Setlaole Formation (at 23°11.16'S; 29°01.17'E), and a granitic body, also cutting the Setlaole Formation (at 23°08.93'S; 29°03.75'E) were only encountered rarely.

Generally the intrusive rocks of the dyke swarms cutting the Waterberg, Blouberg and basement strata outcrop poorly, though the dykes can easily be identified from aerial photographs, on which the trend of dykes can be traced for several kilometres by contrasting vegetation patterns and by a slight negative relief caused by enhanced weathering of igneous rocks relative to the neighbouring sedimentary strata. Generally, these dykes seem to have a vertical dip, though rarely dykes with only gently-inclined dips were recorded cutting the Mogalakwena Formation (Figure 6.1). The trend of vertical dykes recorded south of the southern strand of the Melinda Fault is plotted in a rose diagram in Figure 6.2, and shows that the dykes have a dominant trend of E.N.E. to W.S.W.

Samples of three dykes from the field area were analysed by X.R.F and I.C.P.M.S for major and trace elements, respectively. The results of these analyses are shown in Table 6.1. Analysed samples were collected from a dyke cutting the basement at 23°04.52'S; 28°54.00'E (Sample no. 167), from a dyke cutting the Upper Member of the Blouberg Formation (Chapter 3) at 23°08.02'S; 28°55.18'E (Sample no. 227)(Figure 6.2), and from a dyke cutting the Mogalakwena Formation at 23°09.19'S; 28°41.09'E (Sample no. 197). A plot of the weight percent of $Na_2O + K_2O$ against total weight percent of SiO_2 (TAS diagram) for these three samples is shown in Figure 6.3, and shows that all three intrusive rocks are doleritic/dioritic. Incompatible trace element data were used to plot spidergrams (Figure 6.4) for these dolerites. They show relative enrichment in incompatible trace elements and negative anomalies in Nb, P and Ti.

In thin section, the dolerite dykes can be seen to be composed of plagioclase feldspar, augite and minor olivine, locally replaced by serpentine. Generally feldspar laths reach 1.5mm in length and augite crystals are about 1mm in diameter.

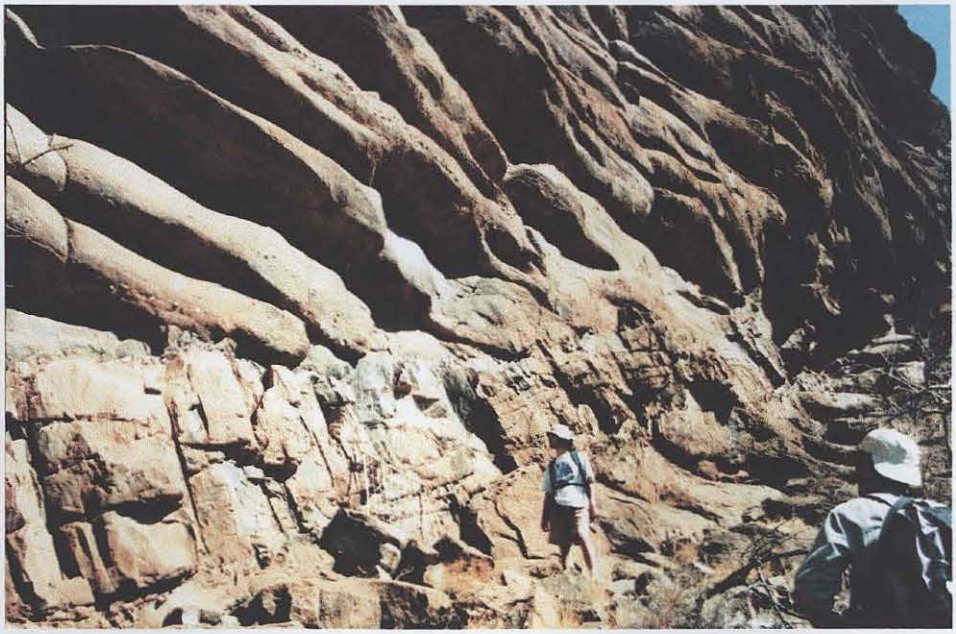

Figure 6.1: Gently dipping dyke cutting the Mogalakwena Formation at 23°16.05'S; 28°50.55'E.

Figure 6.3: Narrow (c. 20cm) E.N.E.-striking, vertically-dipping dyke cutting the Blouberg Formation at 23°09.05'S; 28°41.30'E. Hammer is 30cm long.

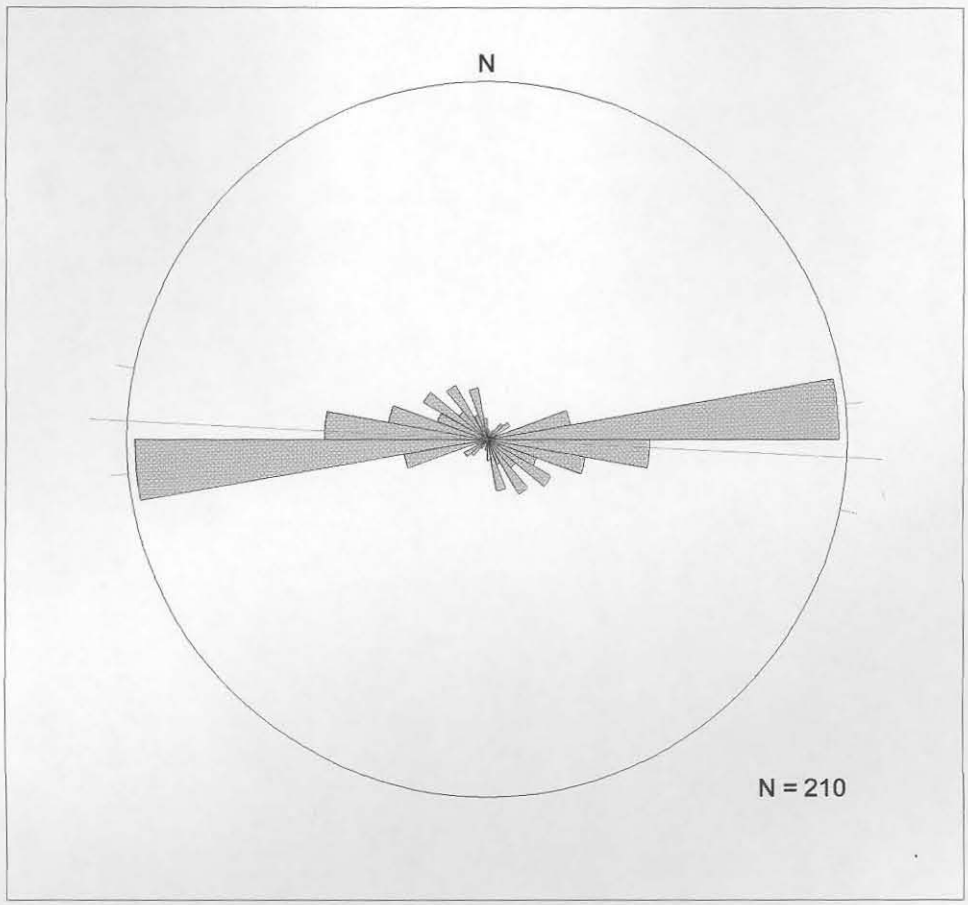

Figure 6.2: Rose diagram showing the orientation of dykes cutting the Waterberg Group strata. Principal trend is shown.

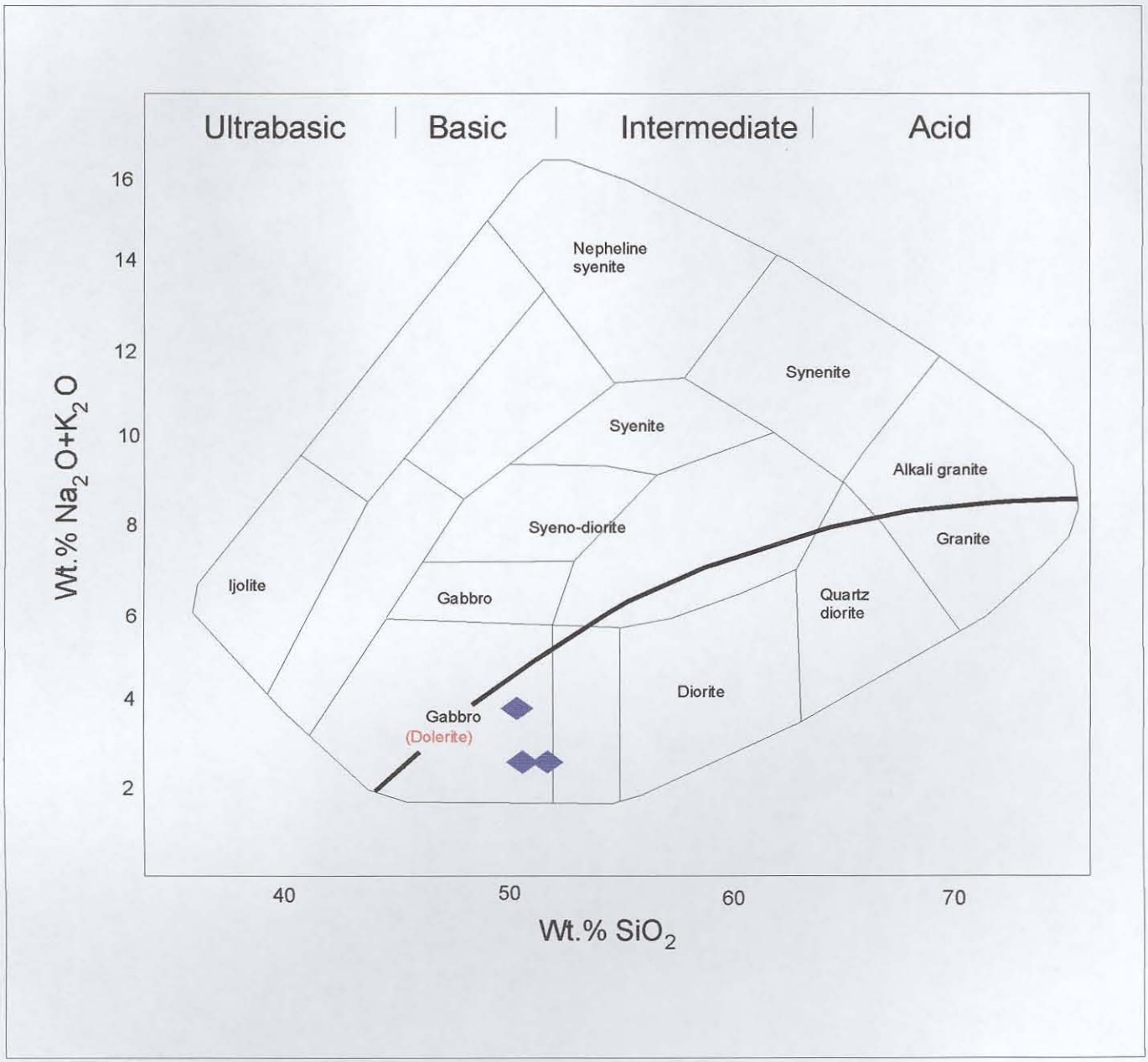

Figure 6.4: Total Alkali/Silica diagram (after Wilson, 1989) to show nomenclature for dykes intruding the basement, Blouberg Formation and Waterberg Group.

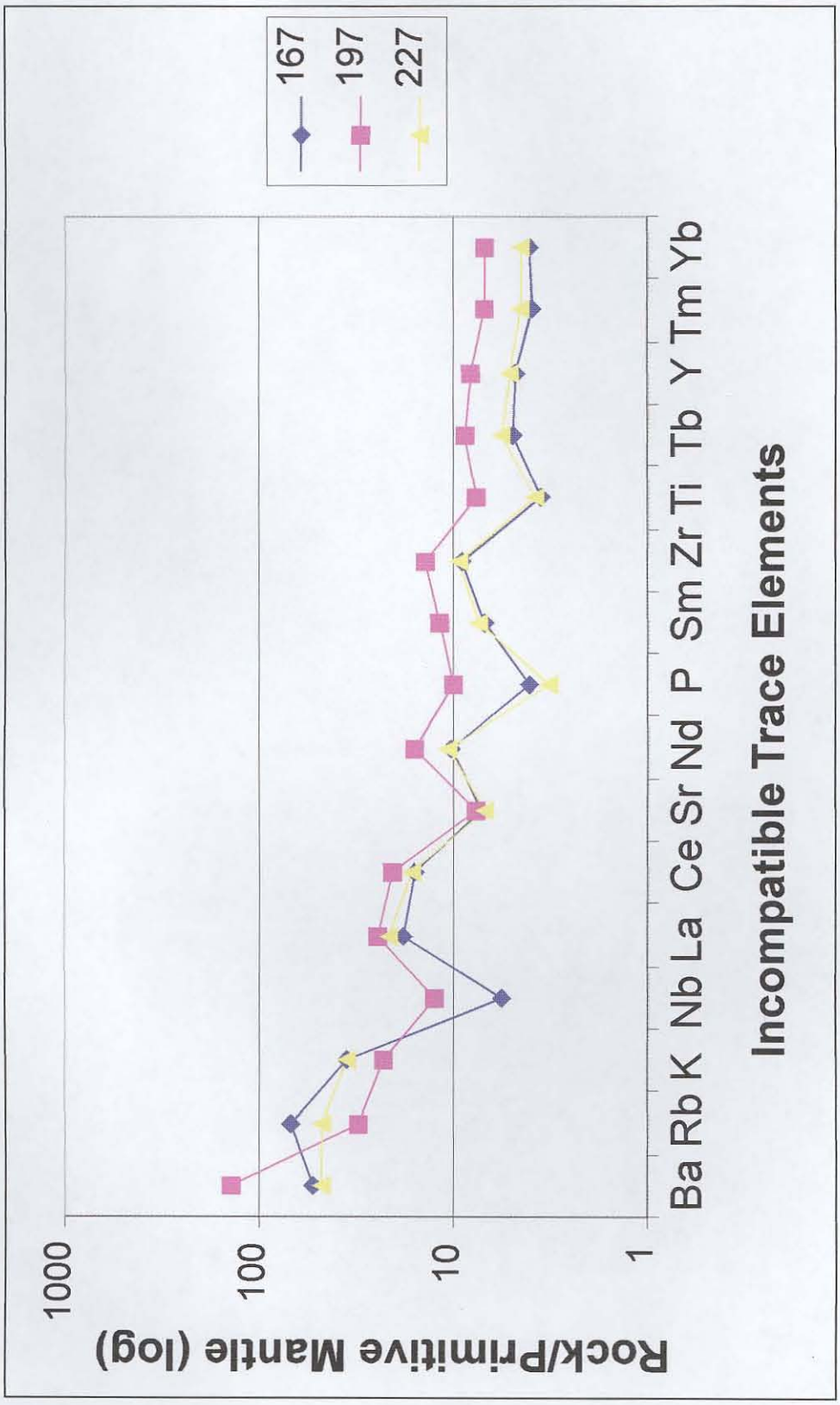

Figure 6.5: Spidergram to show values of normalised incompatible trace elements in the dykes cutting the basement, Blouberg Formation and Waterberg Group strata.

%	167	197	227
SiO2	52.09	51.03	50.82
TiO2	0.78	1.65	0.82
Al2O3	14.17	13.49	15.07
Fe2O3	10.17	14.18	12.02
MnO	0.15	0.21	0.34
MgO	5.53	5.82	5.63
CaO	9.61	10.02	5.63
Na2O	1.58	1.96	2.86
K2O	1.07	0.69	1.06
P2O5	0.09	0.22	0.07
Cr2O3	0.01	0.02	0.02
NiO	0.01	0.01	0.01
LOI	3.93	0.7	4.02
Total	99.23	99.98	98.15
Cu	16	221	71
Ga	14	20	16
Mo	<1	<1	<1
Nb	4	9	<2
Ni	78	77	91
Pb	<2	3	117
Rb	44	20	30
Sr	151	164	146
Th	<5	<5	<5
U	<3	<3	<3
Y	22	37	23
Zn	94	108	393
Zr	103	156	104
Ba	376	969	336
Cl	37	<30	<30
Cr	100	109	135
%S	<0.01	0.02	<0.01
Sc	42	38	40
V	256	325	246

Element	167	179	227
La	12.6	16.8	14.6
Ce	28.1	37.1	29.6
Pr	3.43	4.80	3.44
Nd	14.1	21.4	14.4
Sm	3.07	5.33	3.33
Eu	0.85	1.60	0.95
Gd	3.24	5.58	3.61
Tb	0.54	0.93	0.61
Dy	3.52	6.08	3.90
Ho	0.71	1.28	0.80
Er	2.05	3.70	2.37
Tm	0.29	0.52	0.33
Yb	1.97	3.42	2.18
Lu	0.30	0.51	0.32
Nb	4.0	9.0	2.0

Table 6.1: X.R.F. and I.C.P.M.S. results for major and trace element abundances in the dykes cutting the basement, Blouberg Formation and Waterberg Group.

CHAPTER 7: MAP RELATIONSHIPS AND STRUCTURAL GEOLOGY.

The map included as Appendix 1 shows the geological relationships recorded in the field. The following description considers the structural phenomenon within each stratigraphical unit in order, followed by a description of the structural relationships existing between each of the stratigraphical units and the structural description of intrusive rocks.

7.1: Structures present within the basement gneiss:

Many of the ductile deformational features in the basement gneiss have been described in Chapter 2. However in addition to these ductile structures, several structures were recorded that suggest deformation under more brittle conditions (Chapter 2).

Whilst the true gneiss in the field area is generally banded (the foliation plane is partially defined by alternating quartzo-feldspathic and amphibolite lenses), outcrops along the southern strand of the Melinda Fault, bear little resemblance to the banded gneiss. Discrete amphibolite lenses are not present in these rocks, and no clear foliation is visible (Figure 7.1). The rocks consist of small, angular fragments of quartz (Figure 7.2), and are generally intruded by thin (<3mm) quartz-filled veins, locally at closely spaced intervals (Figures 2.14 and 7.3), which may give the appearance of foliation, especially as the trend of the quartz veins is generally parallel to the strike of the foliation planes in the banded gneiss (approximately E.N.E-W.S.W.) (Chapter 2). Locally, however, the quartz veins are not present. The lithology, in the absence of densely intruding veins, closely resembles a crush micro-breccia (as defined by Roering *et al.*, 1989) (Figures 2.13 and 7.1). These brittle fault rocks are intimately associated with the inferred position of the southern strand of the Melinda Fault, and may represent brittle reactivation of ductile fabrics.

In addition to these fault rocks, other brittle faults can be found locally within the basement rocks. These are generally characterised by low-angle fault planes, with slickenside lineations developed rarely on the planar surfaces (Figures 7.4 and 7.5). The orientation of the recorded surfaces are shown in Figure 7.6, which additionally

shows the orientation of slickenside lineations which were recorded on some of these planes. Slickenside lineations plotted in Figure 7.6 suggest that vergence along these faults is approximately towards the north or south.

7.2: Structures present within the Blouberg Formation:

Generally the Blouberg Formation is characterised by steeply-dipping and overturned bedding. The strata along the southern edge of Blouberg mountain generally dip southwards, with angles of dip between 45° and 90° (e.g. Figure 3.19). Locally these beds are overturned, and dip northwards at angles up to 55°. The steeply-dipping beds in the Blouberg area consist of strata of the Lower Member of the Blouberg Formation (Chapter 3). However, rare outcrops of the Upper Member in the Blouberg area have only gently-dipping beds, which are in contrast to the steeply-dipping bedding geometry of the Lower Member. The orientation of bedding planes shown in Figure 7.7 define an approximately horizontal E-W trending fold-axis. Such folding is also visible in smaller-scale folds throughout the outcrops of the Blouberg Formation (e.g. Figures 3.24 and 7.8).

Bedding orientations shown in Figure 7.9 were recorded from an outcrop of Blouberg strata at 23°05.76'S; 28°53.47'E (Figure 7.8). This outcrop is significant in that it is the only outcrop of Blouberg strata which was recorded to the north of the southern strand of the Melinda Fault (Section 3.3; Appendix 1). Comparison of Figures 7.7 and 7.9 shows that both outcrops of Blouberg strata have a similarly orientated fold-axis and deformational characteristics.

In comparison to the general southward or northward dip-direction of the Blouberg Formation in the Blouberg area, dip-directions of Blouberg strata in the Kranskop area have contrasting geometry. Both the Lower and Upper Members of the Blouberg strata have very steep dips (80°-90°), though here the dip direction is consistently to the east or west, in contrast to the consistent north-south dip in the Blouberg area (Figure 7.7).

Faulting is recorded only locally in the Blouberg Formation. Southward-verging thrust faults and more steeply-dipping, southward-verging reverse faults displace the

Blouberg strata (Figure 7.10a). The sense of movement of the fault (Figure 7.10a) can be gained from the measurement of slickenside lineations, which plunge 52°, and have a trend of 004° (dip-slip movement), and which exhibit stepping indicative of a reverse sense of movement. This fault does not cut the Mogalakwena Formation which unconformably overlies the Blouberg Formation (Figure 7.10a)(Section 7.7).

Similarly, basement gneiss is locally thrust over the Blouberg Formation at 23°07.17'S; 29°02.66'E, where the thrust is marked by the presence of a brittle fault rock, exhibiting a weak sub-horizontal foliation, with a dip-direction of 10°→030° (Figure 7.4). The vergence of this thrust fault may have been towards the south. At around 23°06.93'S; 28°58.17'E, and 23°07.96'S; 28°55.25'E, the thrusting of the basement over the Blouberg Formation can be inferred by the presence of basement topographically above only gently-dipping Blouberg strata (Appendix 1), and similarly may have been thrust with a southward vergence. Slickenside lineations, which are only rarely recorded from within the Blouberg Formation, are shown in Figure 7.11, which shows that such lineations are generally orientated along a north-south trend (Figure 7.12).

The presence of steep, southward-dipping bedding and northward-dipping overturned bedding, and the presence of small-scale southward-vergent reverse- and thrust faults can best be explained by the inferred presence of large-scale southward-vergent reverse- or thrust faults above each section of overturned strata (Figure 7.10b). In the Dantzig area (23°06.50'S; 29°01.50'E; Appendix 1), relatively horizontally bedded Blouberg strata underlie the southern side of the valley, whilst steeply-dipping and overturned Blouberg strata outcrop on the northern flank. The southern outcrops are locally overlain by basement rocks, and they appear to be separated from each other by a southward-vergent thrust. The northern strata may represent a duplication of Blouberg strata (a duplex structure) bound above and below (in the floor of the valley) by the large-scale thrust faults. Though no other duplex-type structures were recorded in the Blouberg Formation, the continued presence of steeply-dipping and overturned bedding attests to the presence of large-scale southward-vergent thrust faults affecting the Lower Member of the Blouberg Formation and the basement rocks throughout the Blouberg mountain area. Despite the relatively intense folding, and the inferred

presence of large-scale faults necessary to produce overturned beds typical of the Blouberg Formation, large portions of the Blouberg strata, though steeply-dipping or overturned, show little evidence for micro-to mesoscopic deformation, and as a result sedimentary structures are generally well-preserved.

7.3: Structures present within the Setlaole Formation:

The paucity of outcrops that can be correlated with the Setlaole Formation within the study area does not allow for ready determination of structures characteristic of the Setlaole strata. However the outcrops which could be correlated with the Setlaole Formation in the south-eastern part of the study area are characterised by generally horizontal or shallow dipping bedding planes, and a general lack of deformation.

Previously, Jansen (1976) suggested that the Blouberg Formation and Setlaole Formation may correlate, though Meinster (1977) argued against this correlation. Although the Setlaole and Blouberg Formations locally have comparable lithofacies (Chapter 3 and Section 4.2) the strong disparity between generally steeply-dipping and overturned strata of the Blouberg strata, and the gently-dipping or horizontally-inclined Setlaole strata, can be used as a means of discrimination between these two formations. If they are indeed correlated, it is difficult to reconcile the presence of intense deformation within the strata of the Blouberg Formation, without these structures being at least partially propagated in the Setloale Formation. Other characteristics (palaeocurrent trend and comparison of lithofacies) were also used in addition to structural characteristics to discriminate between the Blouberg and Setlaole Formations during mapping (Appendix 1).

7.4: Structures present within the Makgabeng Formation:

The Makgabeng Formation is comprised generally of facies of large-scale trough and planar cross-bedded sandstones, and bedding planes are rarely preserved. However, facies consisting of planar-bedded mudstones and sandstones indicate that there is little deformation present in rocks of the Makgabeng Formation. Dips of bedding planes reach a maximum of only 5°. As described in Chapter 6, dyke swarms locally intrude the Makgabeng Formation, generally along an E.N.E- W.S.W. trend. Locally

it seems that some of these dykes have intruded along pre-existing fault planes, as locally there seems to be small displacement of strata across these dykes, visible in vertical sections. Though these displacements appear to relate to dip-slip faulting, the precise sense of movement has proved difficult to establish.

The Makgabeng Formation is not developed in close proximity to the southern strand of the Melinda Fault, and as a result deformation associated with this fault was not recorded.

7.5: Structures present within the Mogalakwena Formation:

The southern and western outcrops of the Mogalakwena Formation are similar to the outcrops of the Makgabeng Formation in that there is a lack of evidence for much tectonic disturbance of the strata. Dips of bedding planes only rarely exceed 5°, and there is little evidence for faulting, either recorded in the field or visible on aerial photographs. However, in common with the Makgabeng Formation, dyke swarms with a general E.N.E.-W.S.W trend are intrusive into the Moglakwena strata (Appendix 1).

In contrast to the southern and western outcrops of the Mogalakwena Formation, outcrops exposed to the north and east are more likely to contain evidence for tectonic disturbance, especially in outcrops adjacent to the southern strand of the Melinda Fault. Here, the dip of bedding planes may locally reach 30° towards the south (Appendix 1), though generally dips of bedding planes remain low-angled, typical of the remainder of the Mogalakwena Formation.

Along the southern strand of the Melinda Fault, such as at areas around 23°07.40'S; 28°56.87'E and 23°07.30'S; 28°57.60'E, there are outcrops of small sets of trough cross-bedded sandstones with heavy mineral accumulations on foresests (Figure 4.66), which correlate well with the more distal outcrops of the Mogalakwena Formation (Section 4.4). These outcrops lie within and to the north of the southern strand of the Melinda Fault zone, and at two locations (23°07.60'S; 28°55.70'E and 23°07.10'S; 28°57.49'E), are juxtaposed against the more proximal, conglomeratic

facies of the Mogalakwena Formation. The two contrasting facies associations are locally developed only about 20m away from each other at comparable topographic heights, and can likely be explained by juxtaposition of the distal facies against the proximal facies by faulting. Narrow intervening areas between these two facies can locally be seen to be occupied by crush breccia (Section 7.1), or to be intruded by dykes (Appendix 1).

Mogalakwena strata (distal facies) to the north of the southern strand of the Melinda Fault are generally horizontally inclined, or reach only relatively low angles of dip (Appendix 1), and only rarely show evidence for faulting.

7.6: Structures present within the Sibasa and Wyllies Poort Formations:

The Sibasa Formation does not generally outcrop sufficiently well to establish any structures present within it. However, it can be noted that the present extent of both the Sibasa Formation and the Wyllies Poort Formation above, is restricted to the northern side of the southern strand of the Melinda Fault within the study area. No outcrops of the Sibasa or Wyllies Poort Formation were identified south of this fault.

The outcrop of the Wyllies Poort Formation is good in areas of high relief on Blouberg mountain, and towards the far north-eastern corner of the field area. In the area around Blouberg mountain, including areas adjacent to the southern strand of the Melinda Fault, the Wyllies Poort Formation exhibits horizontal to low-angled bedding planes (e.g. Figure 5.6), though the strata are typically intensely jointed (Figures 7.13 and 7.14). At least two sets of joints were recorded in the upper slopes of Blouberg mountain. The two approximately vertical joint sets strike at 260-280°, and at 355-035° though, wherever these two joint sets intersect, they have a consistent angular difference of 70-80°.

Locally the Wyllies Poort Formation is also cut by approximately east-west trending major faults (Appendix 1), which can be traced easily on aerial photographs, and which apparently have a dextral displacement, though only rarely are they apparent in the field. Small-scale faults, which are of parallel strike to the major faults cutting the Wyllies Poort Formation, were recorded locally. Rarely, these exhibit a fabric, such as

that shown in Figure 7.15, and generally indicate dextral movement. At 23°04.69'S; 28°59.49'E, in the steep cliffs of Wyllies Poort strata about half way up the preserved section, evidence was gained for bedding-parallel thrust-faulting. Drag folded joints developed on the lower fault plane, with slickensides developed (possibly by flexural slip) on the folded joint surfaces, suggest that the upper portion was moved towards 315° (Figure 7.16).

In contrast to the generally horizontal bedding of the Wyllies Poort Formation in the area bound by the southern and northern strands of the Melinda Zault zone, the Wyllies Poort strata adjacent to the northern strand of the Melinda Fault is highly tectonised. In the far north-eastern corner of the study area, several splays from the northern strand of the Melinda Fault, with approximately parallel strike, displace the Wyllies Poort Formation. Appendix 1 shows that, generally, these splays of the northern strand of the Melinda Fault have an apparent dextral displacement. Dips of bedding planes of the Wyllies Poort strata within the Fault zone locally approach 90° (Figure 7.17).

Areas of Wyllies Poort strata adjacent to one of the splays of the northern strand of the Melinda Fault zone are commonly strongly recrystallised, so that primary sedimentary structures are only rarely preserved. Additionally, the strata in this area are locally pervasively intruded by quartz-filled veins. Figure 7.18 shows an area at 23° 00.93'S; 29° 02.88'E, where veins strike 100°. At the same location, quartz-filled veins can be seen to have intruded along earlier brittle faults, as shown in Figure 7.19. Similarly, in Figure 7.20, a dilatational vein, which strikes 140°, indicates approximately 2cm of sinistral displacement during intrusion. In other areas, such as at 23°00.51'S; 29°07.71'E and 23°02.08'S; 28°59.78'E, veins are parallel to the strike of the northern strand of the Melinda Fault, and may reach widths of several metres (Figure 7.21). The location of the northern strand of the Melinda Fault at 23°03.02'S; 28°56.38'E is marked by a small hill (Figure 7.22), which is underlain by white quartzite, which may reflect total recrystallisation, and the intrusion by quartz veins, of earlier brecciated Wyllies Poort strata.

Evidence for the type of initial fault rock, which existed prior to recrystallisation or veining, can be gained locally where patches of Wyllies Poort strata have escaped recrystallisation. Figures 7.23 and 7.24 show planes of fault breccia which have not recrystallised, and thus it seems likely that the northern strand of the Melinda Fault was initially characterised by the presence of fault breccia along the numerous splays of the Fault zone, prior to recrystallisation. Fabrics in the fault rocks are only rarely preserved: Figure 7.25 shows a fault plane with a dip-direction of 83°→190°, which has a weak S-C fabric developed, which suggests a dextral sense of movement. Slickensides recorded within the fault have a trend of 100°, and a plunge of 0°.

The strike of joint planes recorded from areas adjacent to the northern strand of the Melinda Fault are shown in a rose diagram in Figure 7.26, which shows that joints generally strike N.W.-S.E, though are rather variable. The strike of veins recorded from this area are shown in a rose diagram in Figure 7.27, which show much variation, though again strike dominantly N.W.-S.E. The orientation of small-scale fault planes in the Wyllies Poort Formation are shown in Figure 7.28, which shows that the fault planes generally strike E.N.E.-W.S.W., and are steeply-dipping. Rarely, fault planes with low angles of dip are also recorded. Slickenside lineations, locally recorded on some of these fault planes, are shown in Figure 7.29, and indicate both dip-slip and oblique-slip displacement on steeply dipping fault planes. Lineations recorded on low-angled fault planes generally trend towards the N.W. In addition, the orientation of quartz crystal growth in veins could also be recorded rarely. These vein quartz crystals were found to have long axes trending 202° and 210°.

7.7: Relationships present between stratigraphic units in the study area:

This section will consider the relationships between each of the stratigraphic units in the study area, examining whether contacts are conformable, disconformable, nonconformable or unconformable.

The rocks which are considered as basement gneiss can be demonstrated to be nonconformably overlain by all of the sedimentary rocks discussed in previous chapters. Although the nonconformable contact between the gneiss and the Blouberg Formation cannot be seen due to cover, the location of the nonconformity can be

estimated within about 10m at 23°09.01'S; 28°42.01'E, at the base of the Kranskop river section. At locations such as 23°05.76'S; 28°53.47'E, folded Blouberg strata are recorded in close proximity to basement rocks. It is interesting to note, however, that despite the east-west trending fold axis in the Blouberg Formation, the foliation of the gneiss, which crops out less than 100m away, shows little evidence for having being folded, as the E.N.E. strike and vertical dip of the foliation planes remain comparable to those recorded from other areas.

Other locations where the basal beds of the Blouberg Formation can be seen occur at 23°07.39'S; 28°57.46'E, where the lower contact of vertically dipping Blouberg strata is separated from a crush breccia by a 5m-wide zone of jasperitic hydrothermal alteration. As shown in Chapter 2 and Section 7.1, this is more likely to represent a faulted contact, rather than a nonconformable relationship with the basement.

Though the Setlaole Formation could not be directly demonstrated to nonconformably overlie the basement, gneiss was recorded outside the field area just to the east of outcrops of the Setlaole Formation. Here, the basement rocks outcrop at comparable altitudes to the generally horizontally inclined Setlaole strata, and no other strata has been recorded in intervening areas. This suggests that the Setlaole Formation nonconformably overlies the basement. The Makgabeng Formation seems to be developed nowhere above the basement gneiss. The basal beds of the Makgabeng Formation, on the eastern side of the Makgabeng plateau can only be demonstrated to rest conformably on the Setlaole Formation at 23°16.50'S; 28°59.50'E. The Mogalakwena Formation at 23°05.58'S; 28°53.42'E can be directly observed overlying the basement, where the contact is marked by a thin (<20m) conglomerate with well-rounded quartz, quartzite and banded iron formation cobbles, typical of all Mogalakwena conglomerates. Whilst the Wyllies Poort Formation cannot be directly observed to rest non-conformably on the basement, it is most likely to do so around the eastern edge of Blouberg mountain (c. 23°05'S; 29°01'E). Here gneiss underlies areas of relatively high altitude (<1400m), just beneath the Wyllies Poort Formation, and no other strata have been recorded cropping out between the two lithologies.

The Mogalakwena Formation, in addition to its nonconformable relationship with the basement gneiss, can be demonstrated to be developed on a pronounced angular unconformity with the Blouberg Formation beneath. This relationship is best developed at 23°07.35'S; 28°57.53'E (Figure 7.30), 23°06.80'S; 28°59.40'E (Figure 7.31), 23°05.76'S; 28°53.47'E (Figure 7.32) and also at 23°09.12'S; 28°41.22'E, at the top of the Kranskop section. The basal beds of the Mogalakwena Formation in all cases are conglomeratic, though in the case of the outcrops at Varedig (Figure 7.32) and Kranskop, the conglomeratic strata are thin (about 20m) compared to the Mogalakwena strata south of the southern strand of the Melinda Fault, where the basal conglomeratic beds may be at least 90m thick (Section 4.4.1.1).

The Mogalakwena is generally regarded as having a conformable relationship with the Makgabeng Formation beneath (e.g. Callaghan *et al.*, 1991). The strongly contrasting nature of the well-sorted, medium-grained arenaceous Makgabeng Formation and the coarse-grained sandy and conglomeratic Mogalakwena Formation allow for ready identification of the contact between these two formations (Figure 7.33). However, outcrops on the Makgabeng Plateau (e.g. 23°16.39'S; 28°52.57'E), where the contact between the Makgabeng and Mogalakwena formations is well-exposed, show clear joint sets developed in the underlying Makgabeng Formation which are not propagated in the Mogalakwena Formation above (Figure 7.34), and which can locally be observed to be exploited by the Mogalakwena Formation as basal channel margins (Figure 7.35). In addition, reduction spots which can be seen to be developed on the upper surface of the Makgabeng Formation do not continue into adjacent Mogalakwena rocks (Figure 7.36). This indicates that the Makgabeng Formation had lithified prior to deposition of the Mogalakwena Formation. It was shown in Section 4.3.3 that the massive sandstone facies was developed generally in the upper half of the Makgabeng Formation, and is absent from the lower half. Thus, the presence of this facies provides a coarse reference for the stratigraphic height of an outcrop within the Makgabeng Formation. Although both the Makgabeng and Mogalakwena Formations are generally horizontally-bedded, indicating a disconformable relationship, the Mogalakwena Formation can only be demonstrated to be deposited above Makgabeng outcrops frequently containing the massive sandstone facies in the south of the field area. The massive sandstone facies could not be recognised in the Makgabeng strata below the Mogalakwena Formation in the

outcrops towards the north. This suggests that the Mogalakwena Formation may be developed on successively older Makgabeng strata towards the north, and thus represent a slight angular unconformity between these two formations of the Waterberg Group.

Although it has generally been regarded (e.g. Jansen, 1976; Meinster 1977; Brandl, 1986b) that the Waterberg Group is nowhere developed either above or below the Soutpansberg Group, this work shows rather that the Mogalakwena Formation is developed beneath the Wyllies Poort Formation at around 23°05.76'S; 28°53.47'E. The contact between these two formations is shown in Figure 7.37 and in greater detail in Figure 7.38, These figures show that the Wyllies Poort Formation rests above the Mogalakwena Formation on a gentle angular unconformity.

The stratigraphic relationship between the Sibasa Formation and the Mogalakwena Formation could not, however, be established. As the map in Appendix 1 shows, these two Formations are developed together only in the western foothills of Blouberg. It is possible that the Mogalakwena Formation may dip westwards beneath the Sibasa basalt (Appendix 1), though it also possible that the contact between these two formations may be faulted here rather than sedimentary (Appendix 1). The relationship between the Sibasa Formation and the overlying Wyllies Poort Formation could not be established.

7.8: Relationships formed by intrusive rocks:

Appendix 1 shows that, whilst dyke swarms cut the basement, the Blouberg, Setlaole, Makgabeng and the Mogalakwena formations, they are undetected as cutting the Sibasa Formation, and were not recorded cutting the extensive outcrops of the Wyllies Poort Formation. There is also a pattern of spatial distribution, whereby the extent of outcrops of dykes is generally restricted to the area south of the southern strand of the Melinda Fault.

Figure 7.1: Crush breccia on the southern strand of the Melinda Fault at 23°07.39'S; 28°57.46'E. Note the lack of foliation or amphibolite lenses. Camera bag is 25cm high.

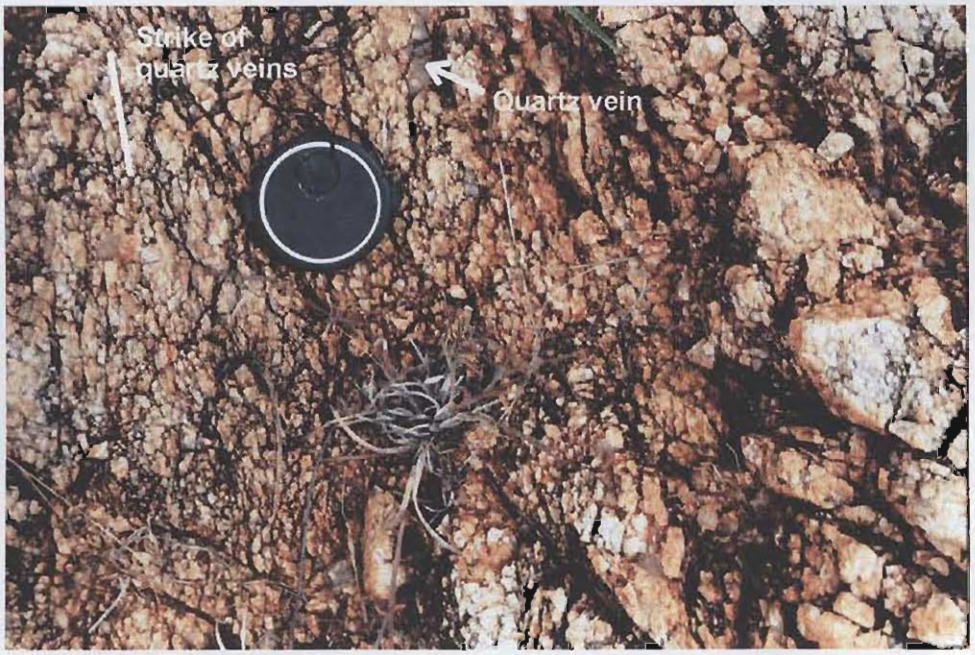

Figure 7.2: Detail of crush breccia at 23°07.39'S; 28°57.46'E. Note the lack of cohesion and presence of thin quartz veins. Lens cap is 5cm wide.

Figure 7.3: Crush breccia showing intense intrusion of quartz veins, which strike parallel to the strike of the southern strand of the Melinda Fault. Recorded at 23°07.39'S; 28°57.46'E. Lens cap is 5cm wide.

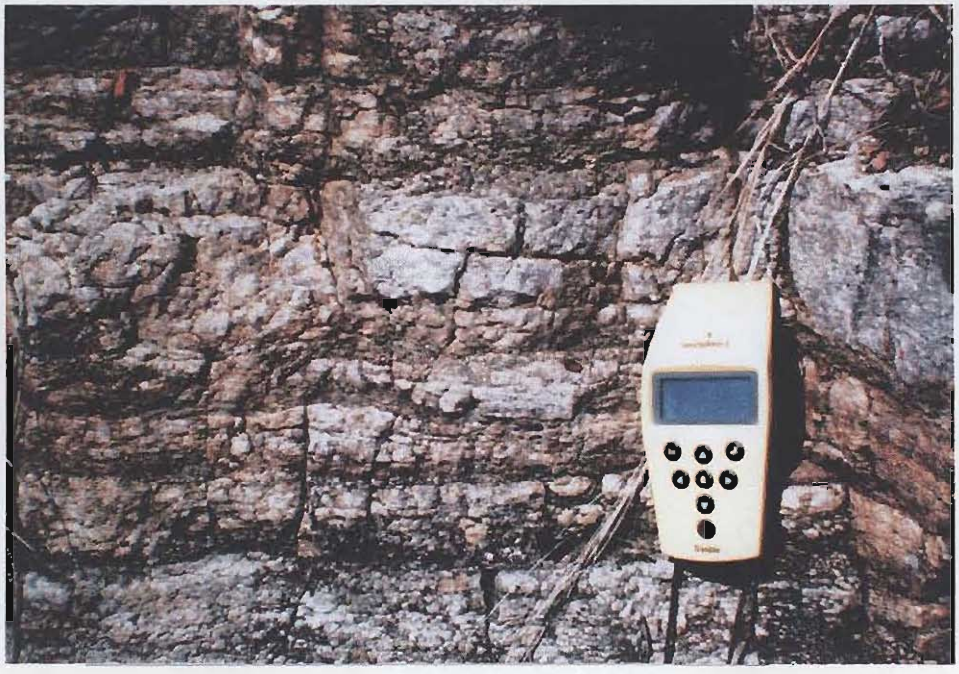

Figure 7.4: Low-angled foliation developed on a thrust fault at 23°07.17'S; 29°02.66'E. Dip-direction of thrust plane: 10°→030°. G.P.S. receiver is 15cm high.

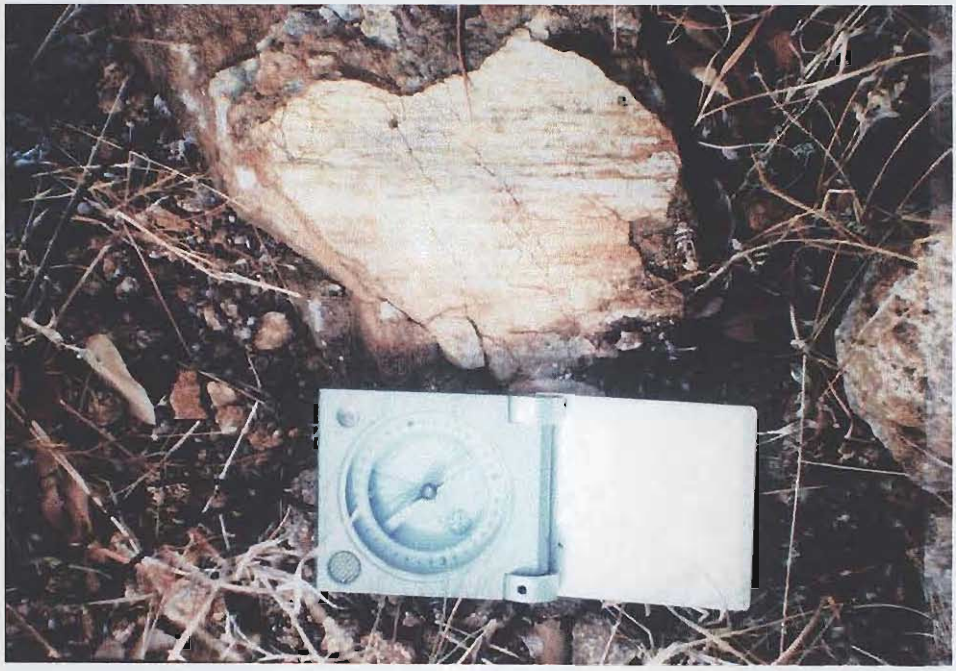

Figure 7.5: Horizontal slickensided surface caused by brittle reactivation in basement gneiss at 23°07.20'S; 29°02.92'E. The compass (7cm wide) is orientated parallel to the lineation, and shows a trend of 200°. Stepping on the surface suggests vergence towards the south.

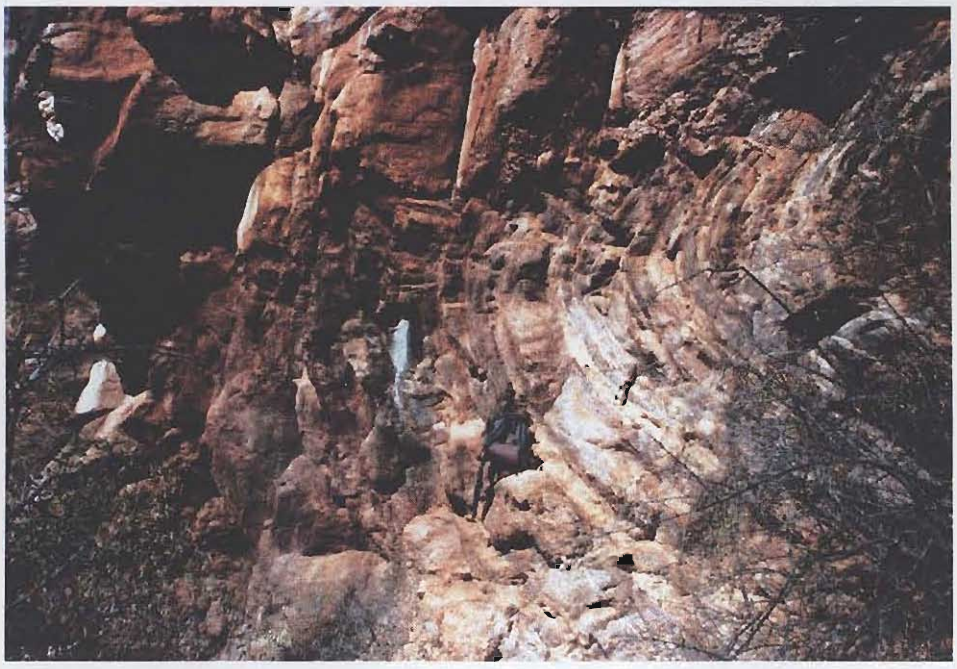

Figure 7.8: Folding developed in the Blouberg Formation at 23°05.76'S; 28°53.47'E. View is approximately eastwards, showing the east-west trending fold axis plotted in Figure 7.9. Rucksack is 50cm high.

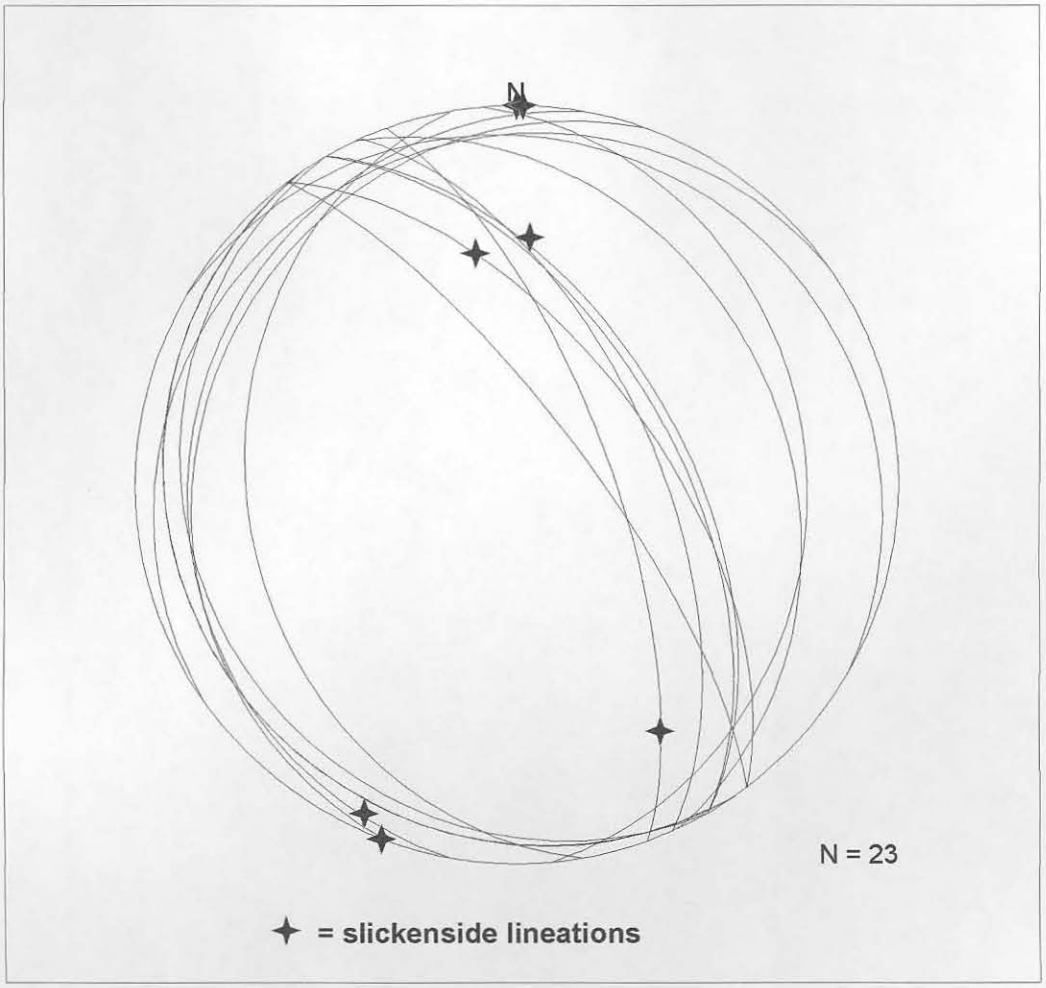

Figure 7.6: Stereographic projection showing orientation of low-angled thrust fault planes cuttingthe basement gneiss, and the orientation of slickenside lineations developed on some of those surfaces.

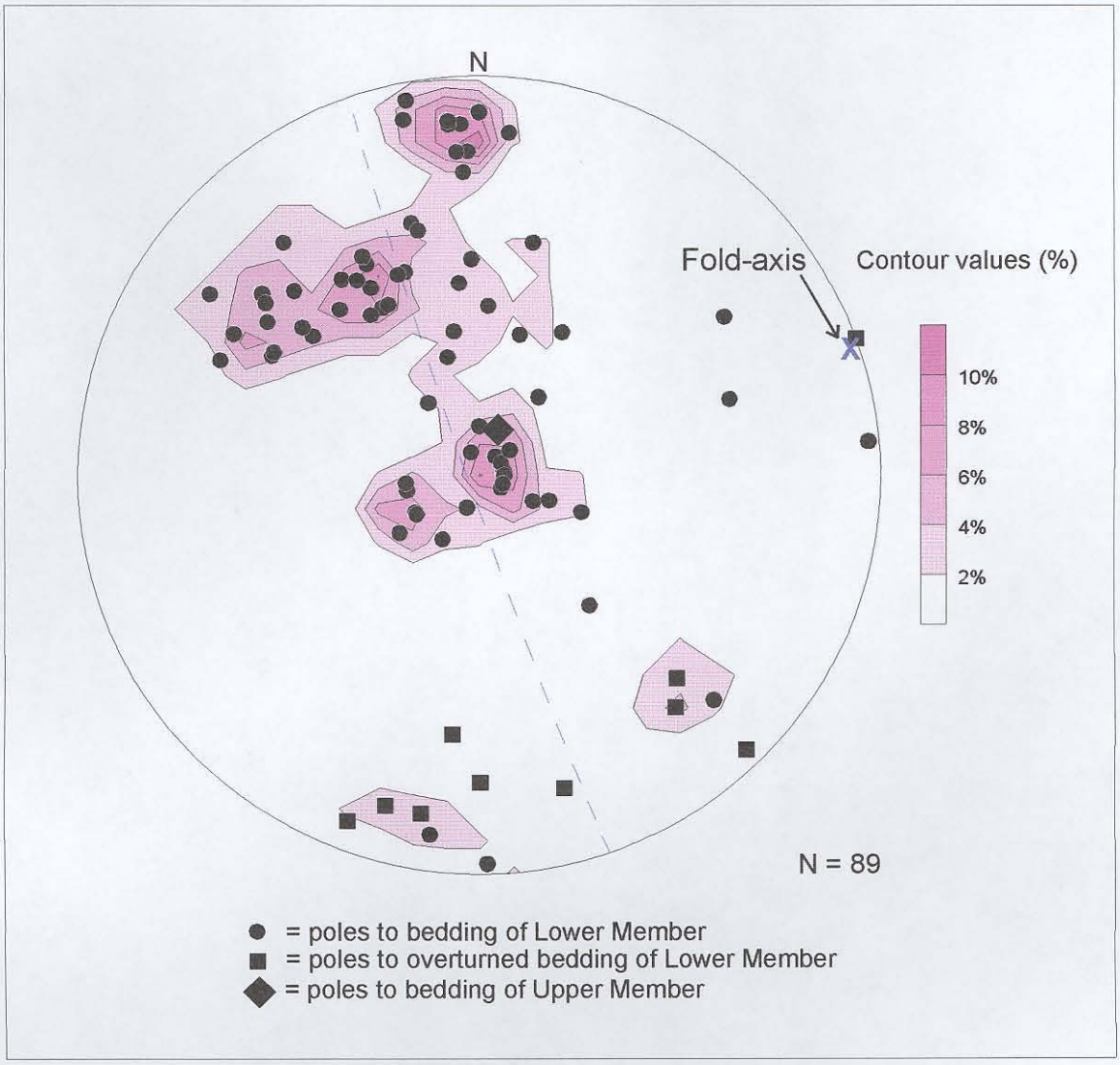

Figure 7.7: Stereographic projection showing poles to bedding planes recorded in the Blouberg Formation in the Blouberg mountain area.

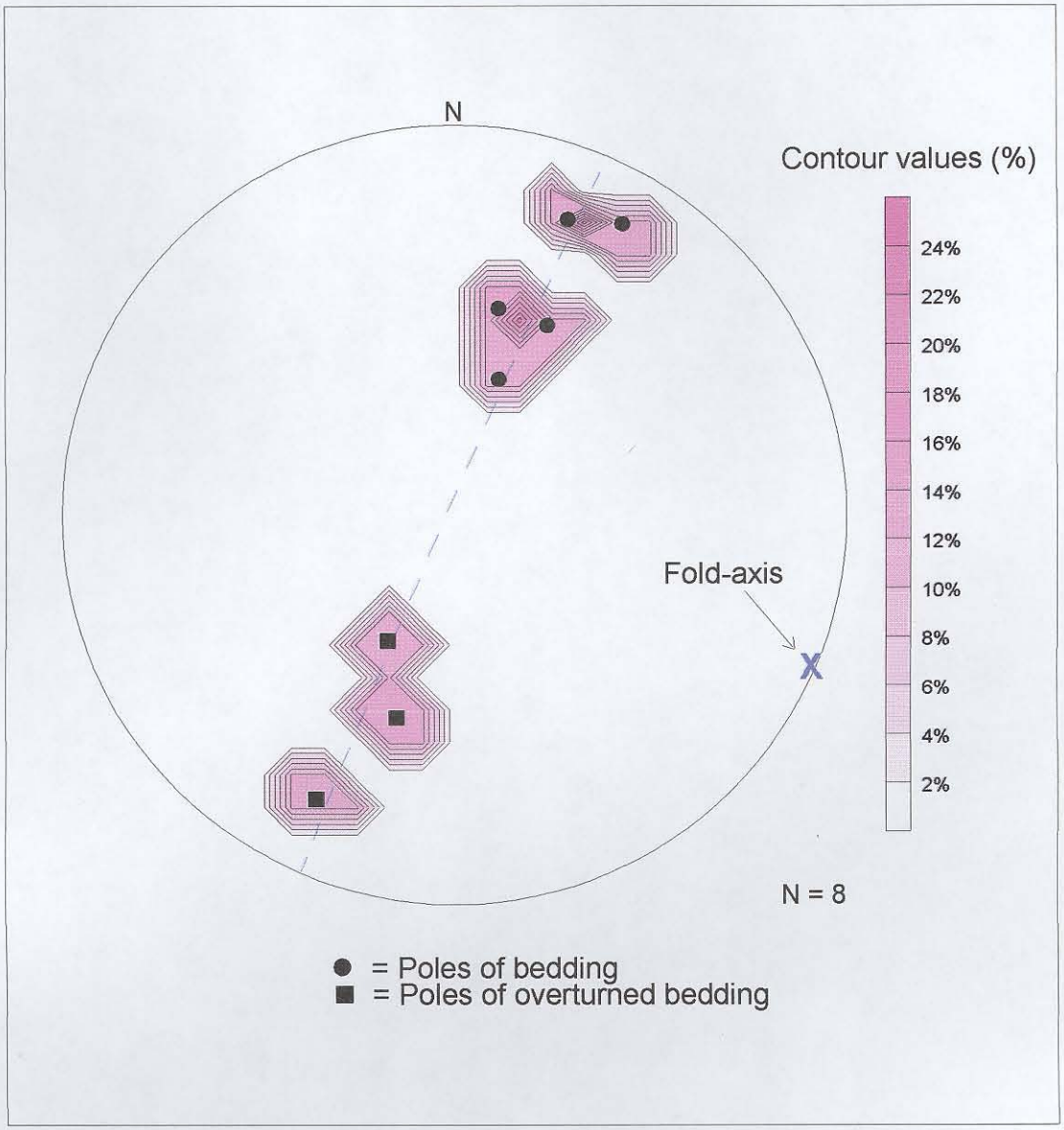

Figure 7.9: Stereographic projection showing poles to bedding planes of Blouberg strata at 23°05.76'S; 28°53.47'E.

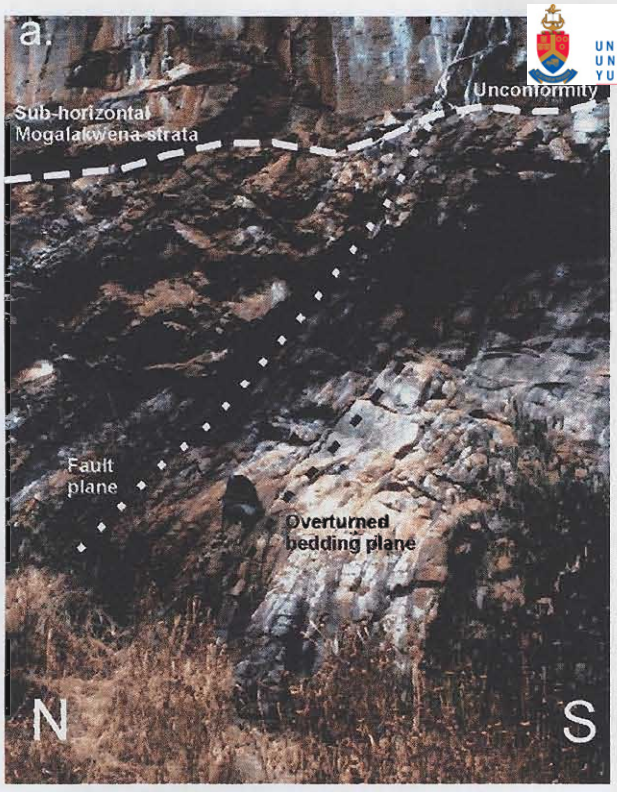

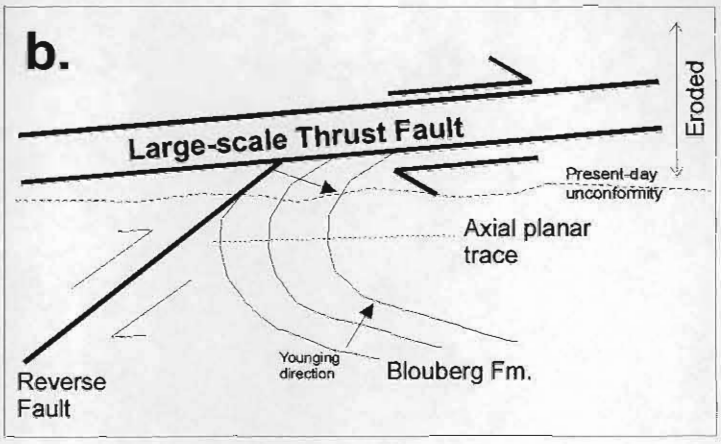

Figure 7.10a: Steeply-dipping reverse fault recorded at 23°06.70'S; 28°59.43'E, which cuts the Blouberg Formation. Fault plane has a dip-direction of 52°→004°, and slickenside lineations have an orientation of 52°→004° (i.e. dip-slip movement). Weak fabric and stepping on slickenside lineations suggest a vergence to the south. Rucksack is 50cm high.

Figure 7.10b: Folded and overturned bedding and reverse fault can be explained by the inferred presence of large-scale southwards-vergent thrust fault above ach portion of overturned bedding.

Figure 7.12: Slickenside lineations developed in the Blouberg Formation at 23°07.96'S; 28°55.25'E. Dip-direction of fault plane is 05°→228°, and slickenside lineations are orientated 0°→180°. Stepping suggests vergence towards the south. Compass (7cm wide) is orientated north.

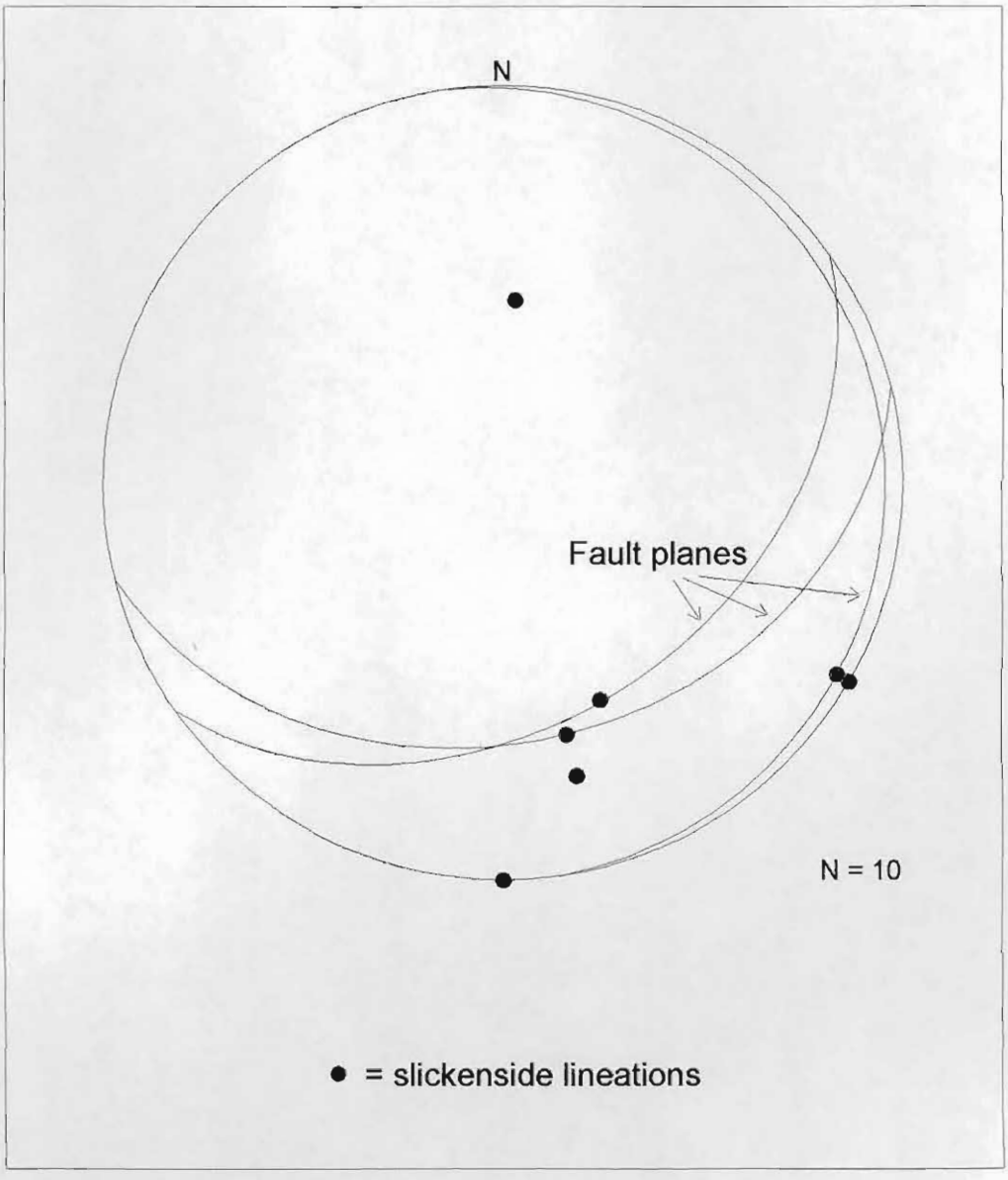

Figure 7.11: Stereographic projection showing the orientation of slickenside lineations and some associated fault planes in the Blouberg Formation.

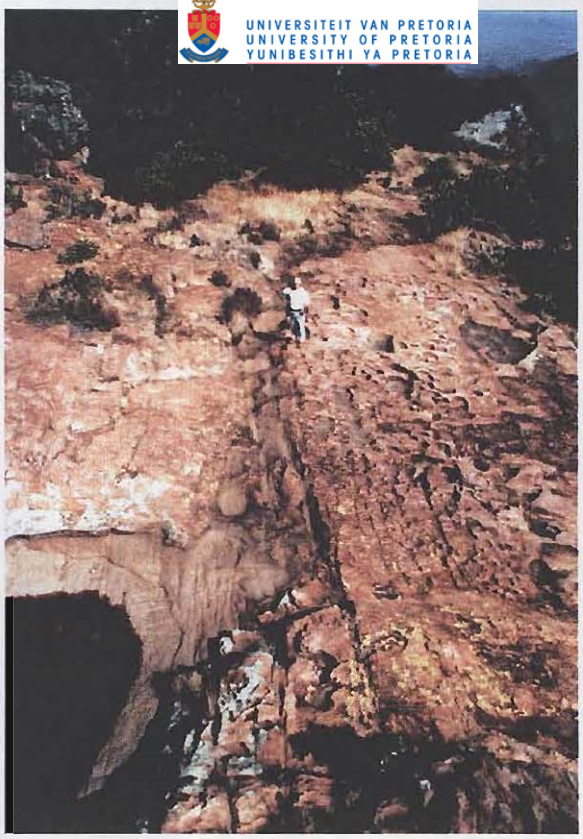

Figure 7.13: Intense jointing in the lower Wyllies Poort Formation at 23°04.99'S; 28°59.33'E. Joints strike 010°. View looking south.

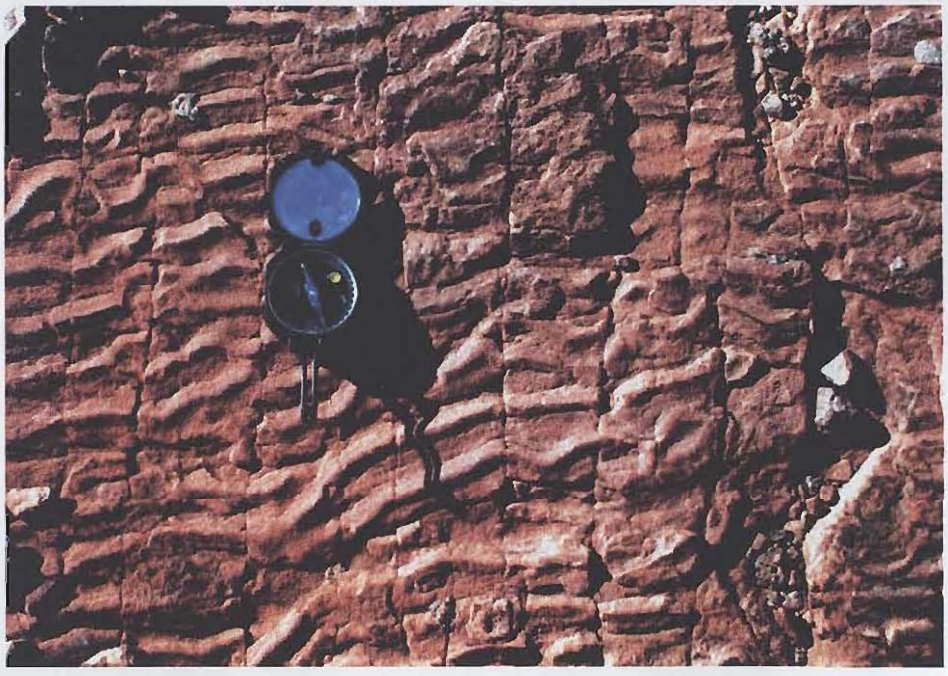

Figure 7.14: 010°-striking joint planes developed in the asymmetric rippled planar bedding of the upper Wyllies Poort Formation at 23°04.22'S; 28°59.38'E (summit of Blouberg mountain). Compass is 6cm wide.

Figure 7.15: Fault developed in the lower strata of the Wyllies Poort Formation at 23°04.99'S; 28°59.33'E. Fault plane strikes 285°, and fabric suggests dextral strike-slip displacement. Needle of compass (7cm wide) points to north.

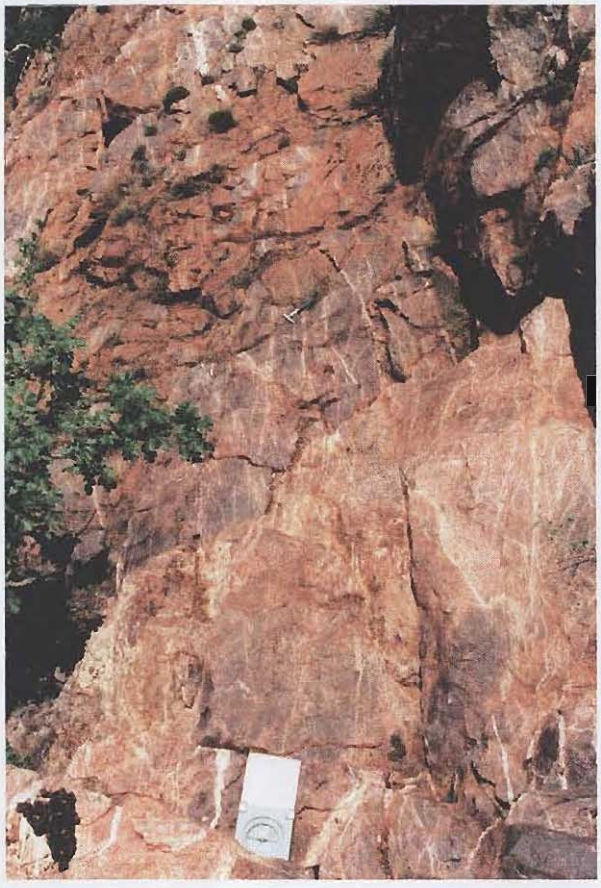

Figure 7.18: Quartz-filled veins intruding the Wyllies Poort Formation at 23°00.93'S; 28°02.88'E. Veins strike 100°. Needle of compass (7cm wide) points north, and hammer (in middle ground) is 30cm long.

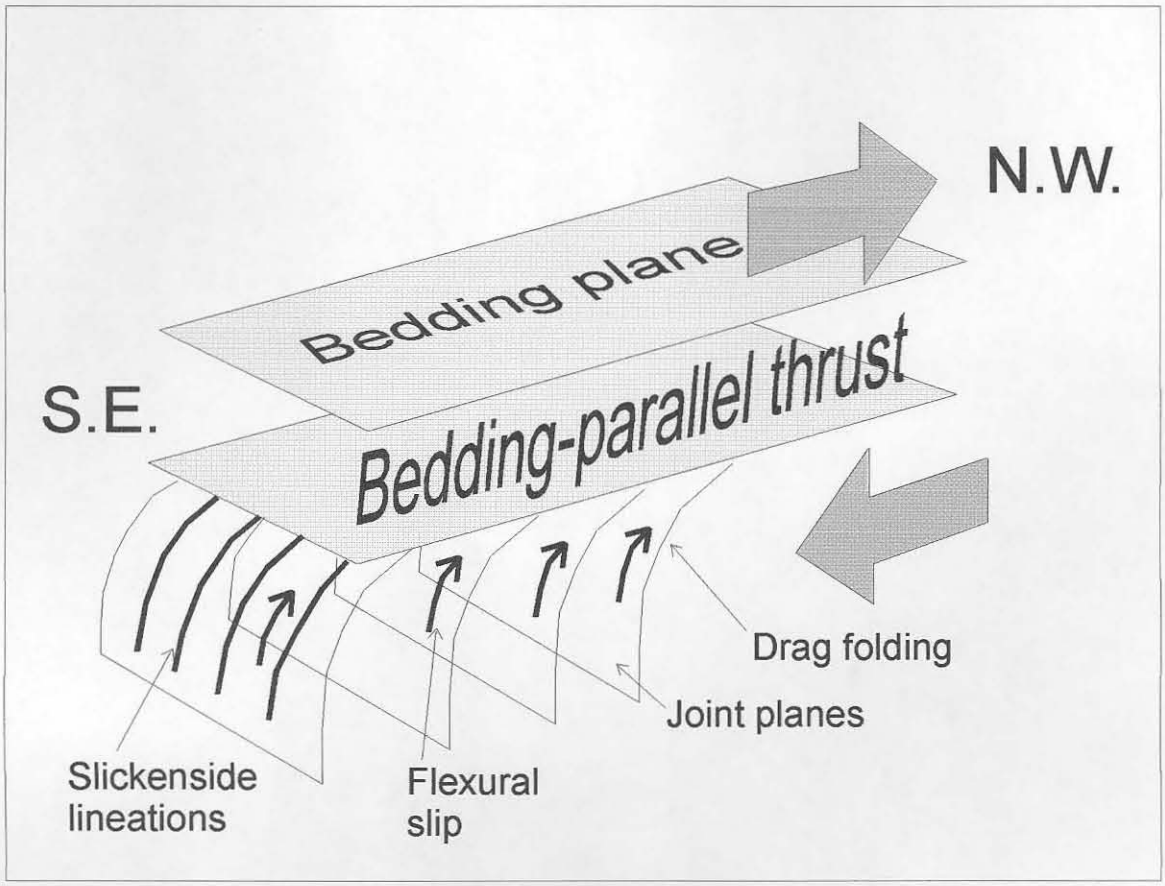

Figure 7.16: Sketch showing relationship between bedding-parallel thrust, folded joint planes, and slickenside lineations recorded at 23° 04.69'S; 28° 59.49'E.

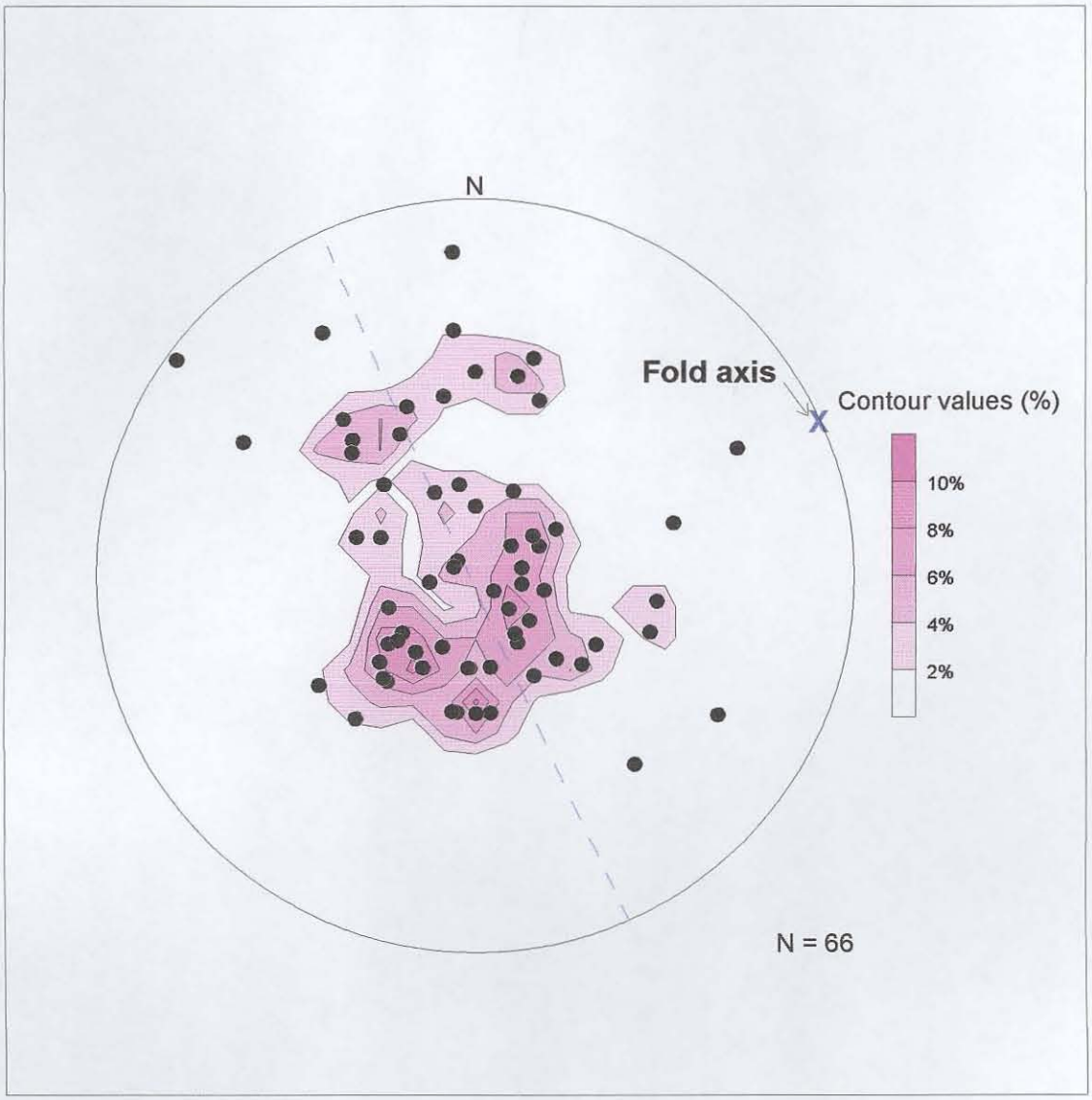

Figure 7.17: Stereographic projection showing the poles to bedding planes in the Wyllies Poort Formation in the vicinity of the northern strand of the Melinda Fault. Fold axis (01°→ 066°) is shown.

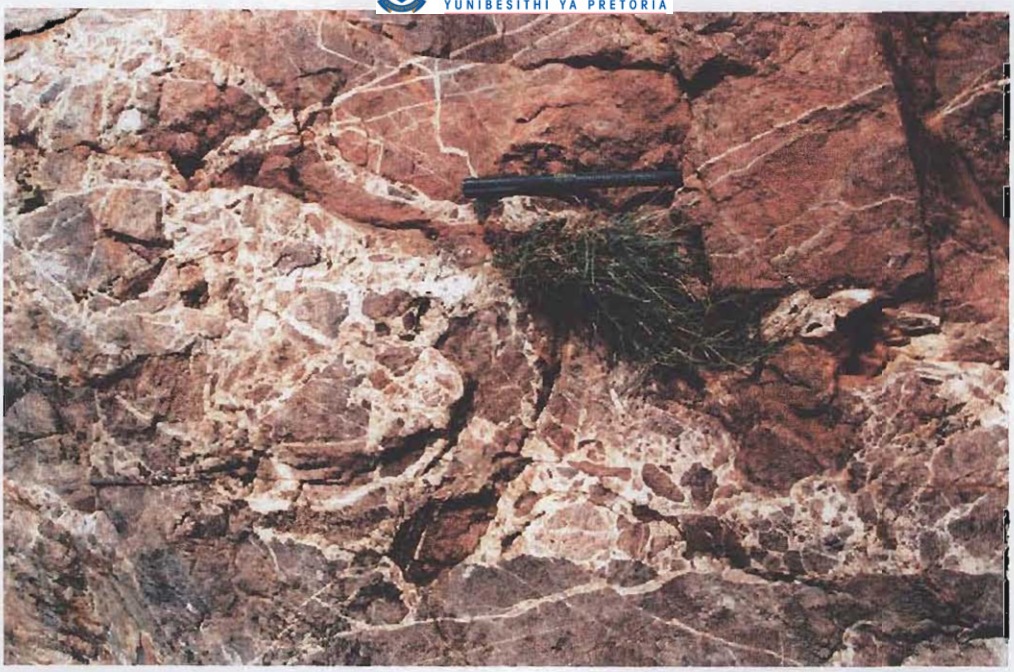

Figure 7.19: Quartz-filled veins intruding an early brittle fault in the Wyllies Poort Formation at 23°00.93'S; 28°02.88'E. Pen is 15cm long.

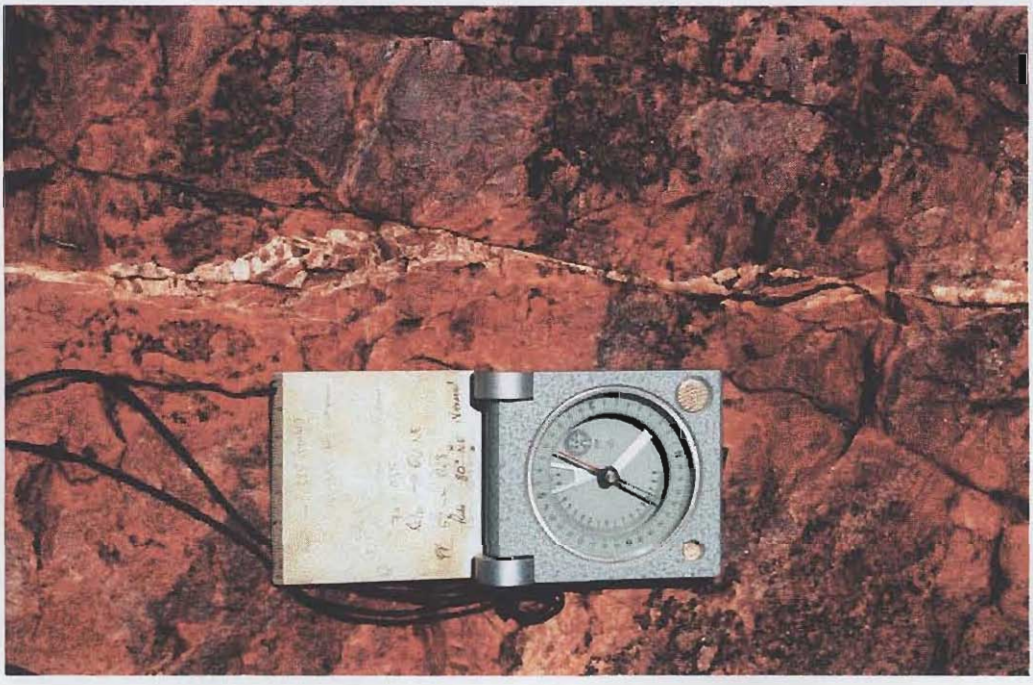

Figure 7.20: 140°-striking sinistral dilatational vein (displacement c. 2cm) at 23°01.34'S; 28°04.45'E. Needle of compass (7cm wide) points north.

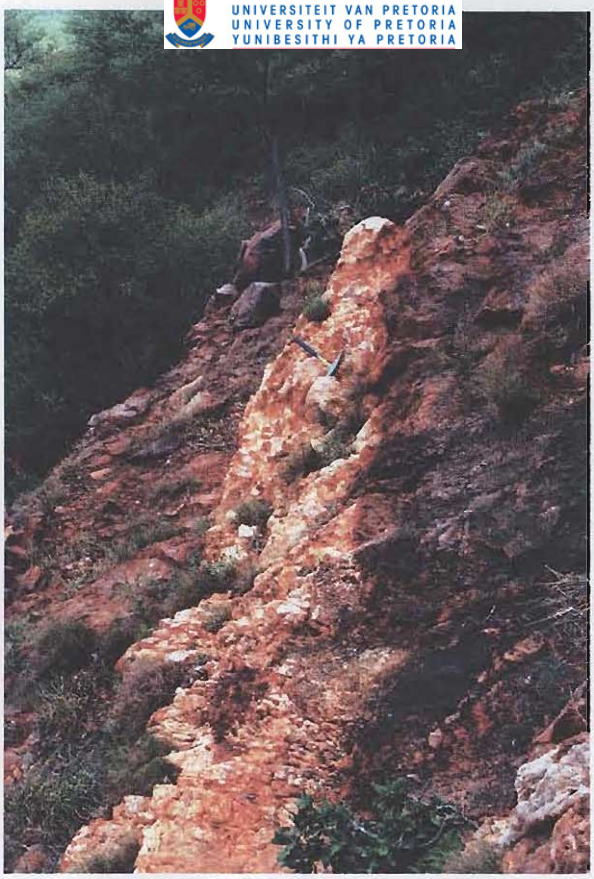

Figure 7.21: 1.5m wide quartz-filled vein cutting the Wyllies Poort Formation at 23°00.51'S; 28°07.71'E. Hammer is 30cm long.

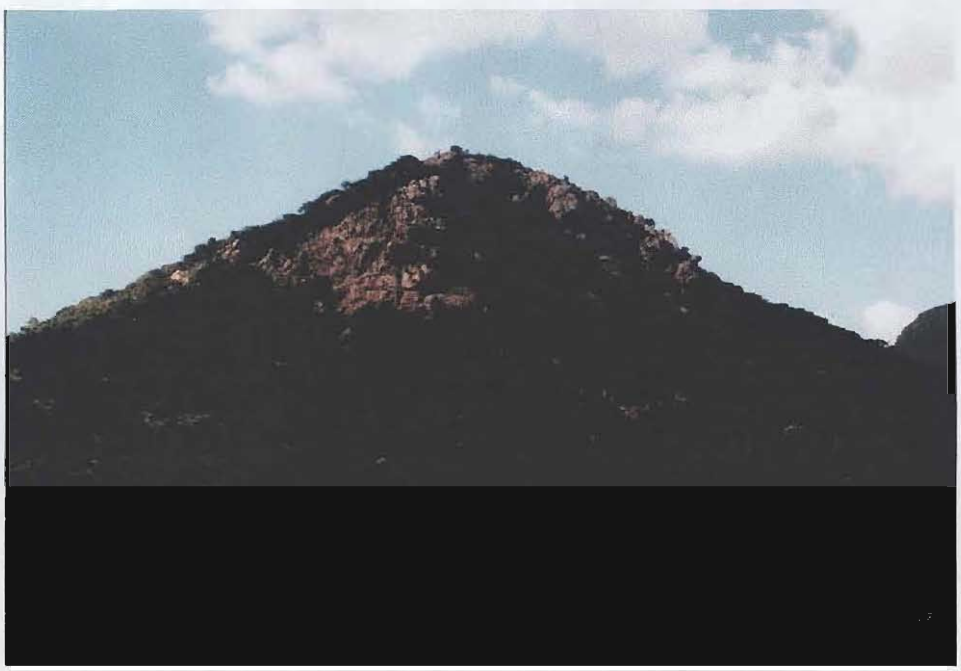

Figure 7.22: Small hill at 23°03.02'S; 28°56.38'E composed of white quartzite. The northern strand of the Melinda Fault is thought to underlie this area (Appendix 1).

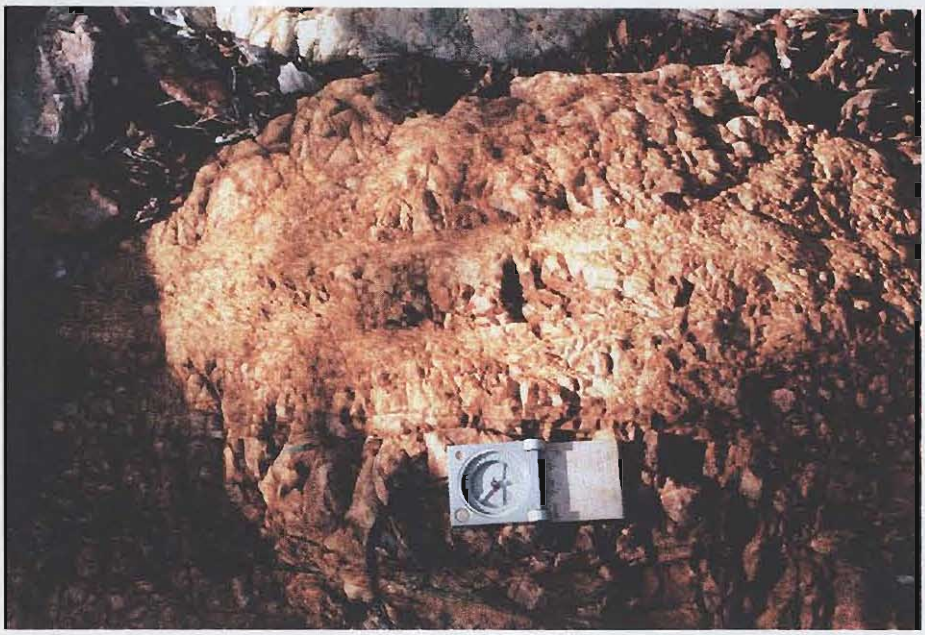

Figure 7.23: East-west striking fault breccia cutting the Wyllies Poort Formation at 23°02.50'S; 29°04.10'E. Needle of Compass (7cm wide) points north.

Figure 7.24: Fault plane with a dip-direction of 74°→033° at 23°01.23'S; 28°02.07'E, with fault breccia preserved on the fault plane. Pen is 15cm long.

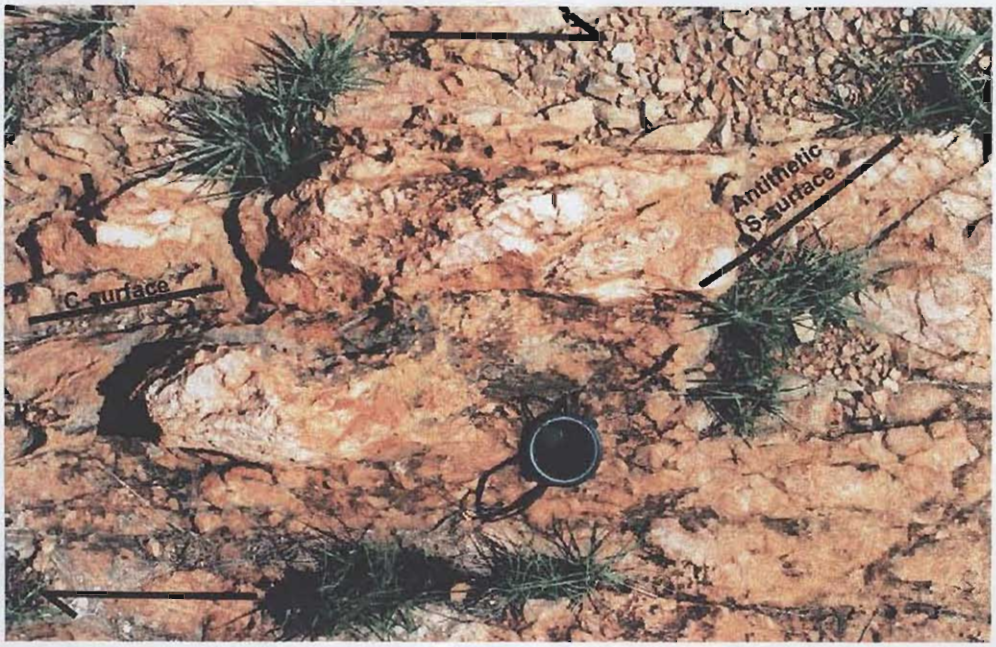

Figure 7.25: Fault breccia at 23°01.31'S; 28°04.65'E, with a weak S-C fabric which suggests dextral displacement. Lens cap is 5cm wide.

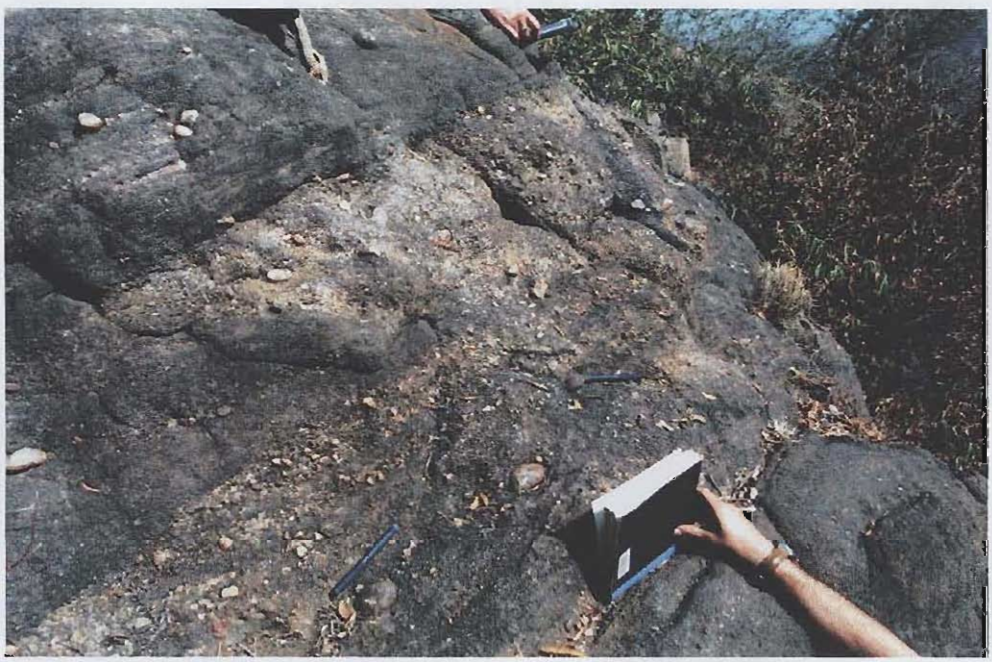

Figure 7.30: Pronounced angular unconformity between the overturned Blouberg Formation (bedding plane indicated by lower notebook) and the Mogalakwena Formation above (bedding plane indicated by upper notebook). Recorded at 23°07.35'S; 28°57.53'E.

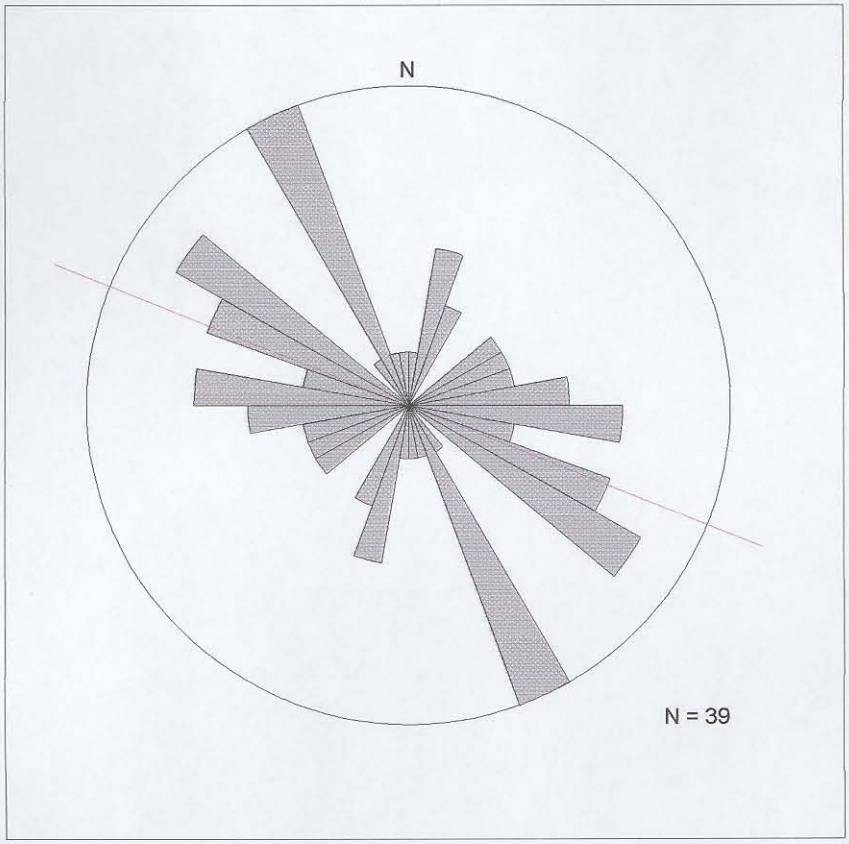

Figure 7.26: Rose diagram showing the strike of joints in the Wyllies Poort Formation. Principal trend is shown.

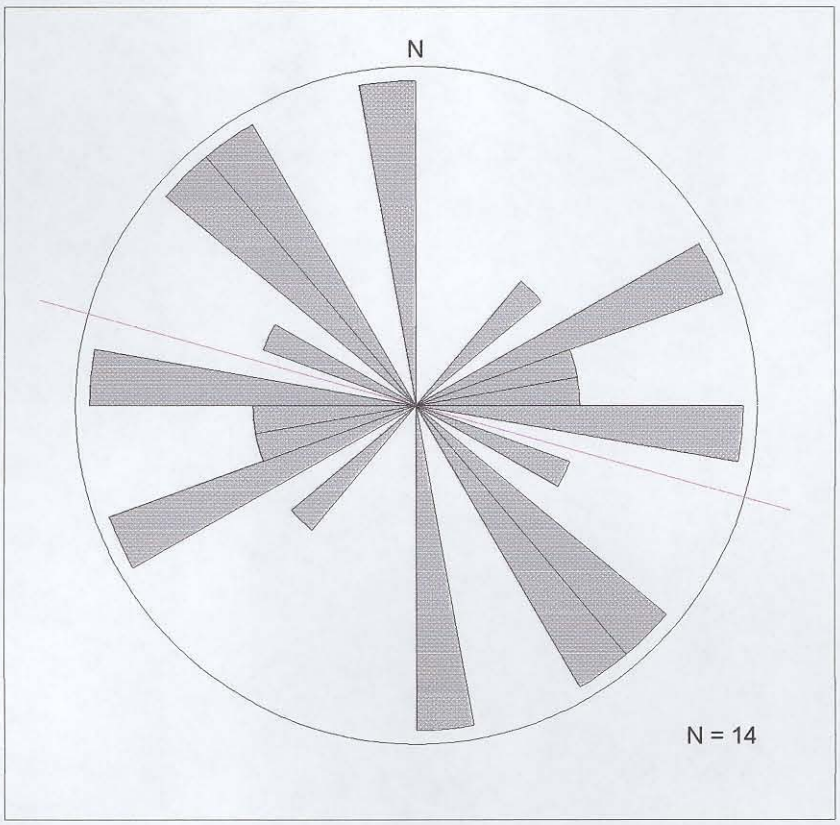

Figure 7.27: Rose diagram to show the strike of veins cutting the Wyllies Poort Formation. Principal trend is shown.

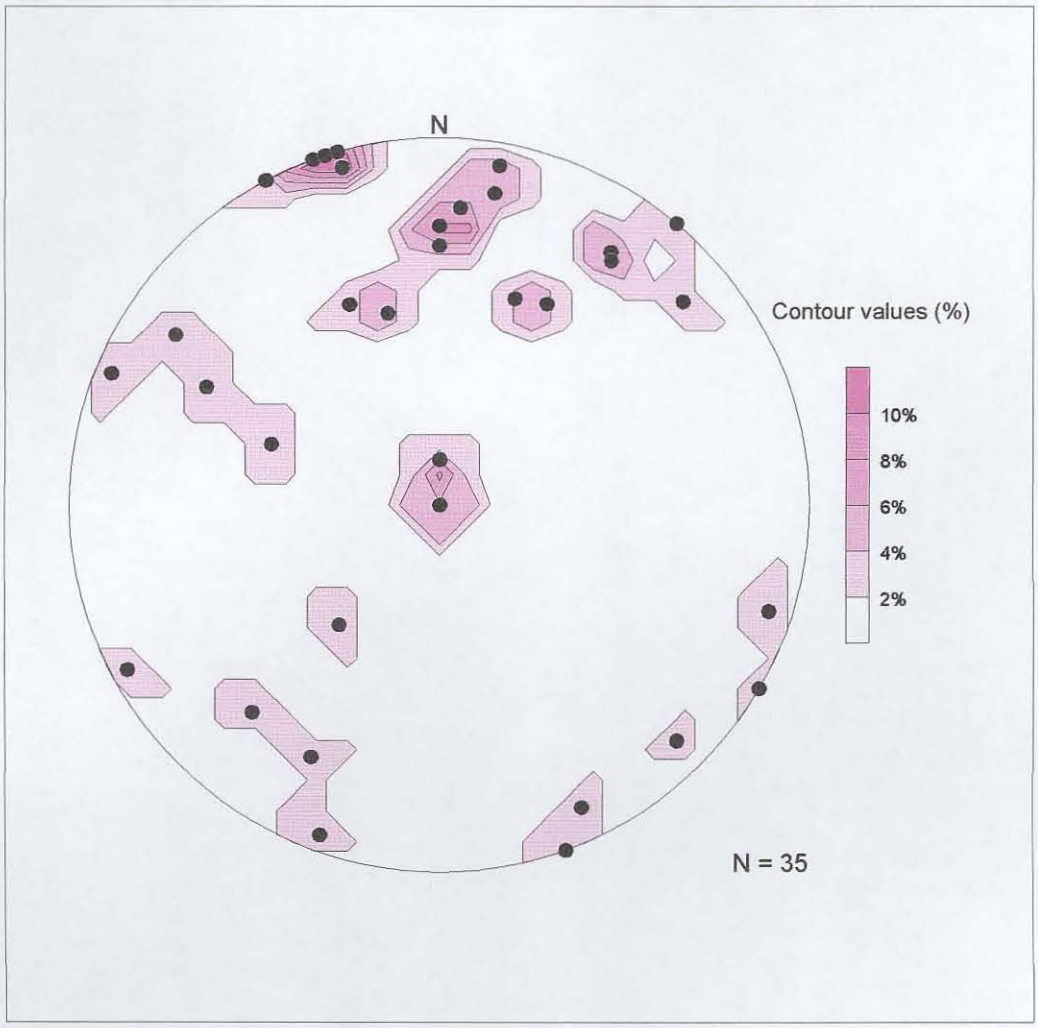

Figure 7.28: Stereographic projection of poles to fault planes in the Wyllies Poort Formation (associated slickensides are potted in Figure 7.29).

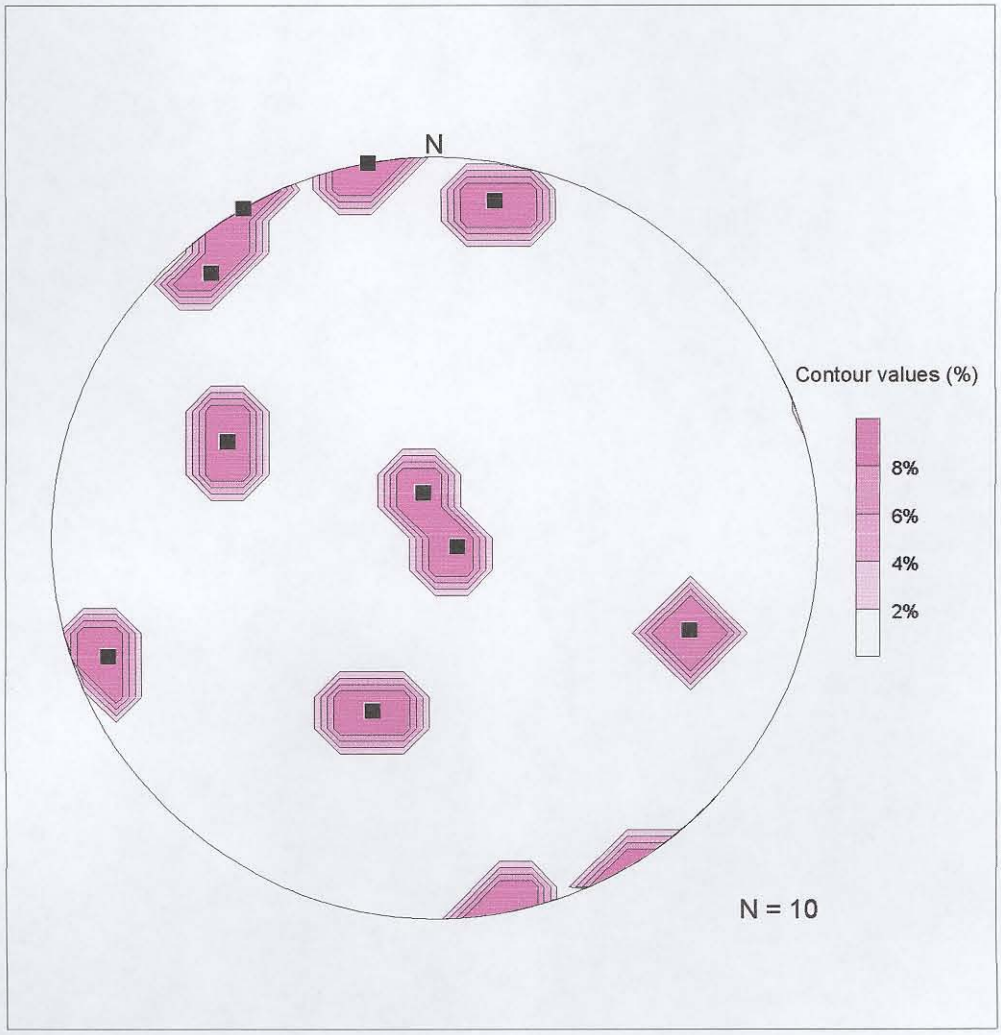

Figure 7.29: Stereographic projection showing the orientation of slickenside lineations (associated with fault planes in Figure 7.28) in the Wyllies Poort Formation.

Figure 7.31: Pronounced angular unconformity between the folded and locally overturned Blouberg Formation and the Mogalakwena Formation above. Recorded at 23°06.80'S; 28°59.40.'E. Note the 1m deep channel developed on the upper surface of the Blouberg Formation to the left of the hammer (30cm long). View taken looking east.

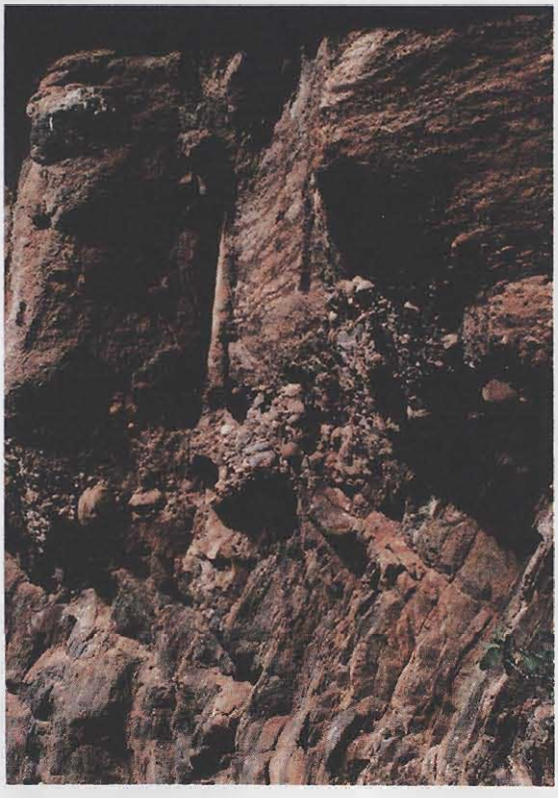

Figure 7.32: Pronounced angular unconformity between the overturned Blouberg Formation and the Mogalakwena Formation above, marked by thin basal conglomerate. Recorded at 23°05.76'S; 28°53.47'E. Cliff section is c. 2m high.

Figure 7.33: Disconformity (or slight angular unconformity) developed between the Makgabeng Formation (laminated medium-grained sandstone) and the Mogalakwena Formation (cobbles and coarse sandstone). Recorded at 23°11.23'S; 28°52.44'E. Lens cap is 5cm wide.

Figure 7.34: Disconformity (or unconformity) between the Makgabeng Formation (with well-developed joint planes) and the Mogalakwena Formation (with no joint planes). Recorded at 23°16.39'S; 28°52.57'E. Large pebble in Mogalakwena Formation is 6cm long.

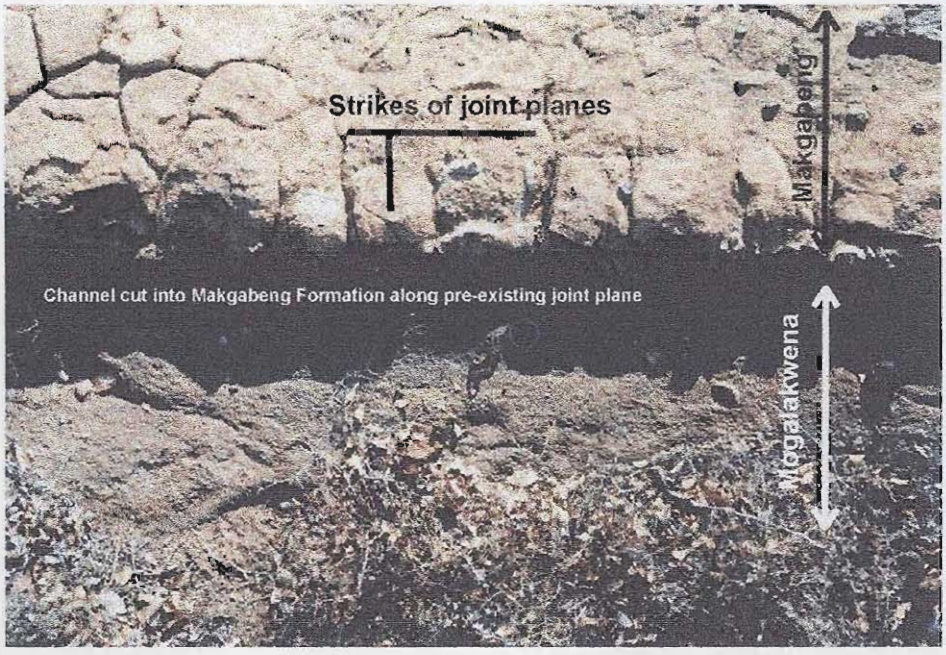

Figure 7.35: Joint plane in the Makgabeng Formation is exploited as a channel during deposition of the Mogalakwena Formation. Note that joint planes in the Makgabeng Formation are not continuous in the Mogalakwena Formation. Recorded at 23°16.39'S; 28°52.57'E. View is vertical. Lens cap is 5cm wide.

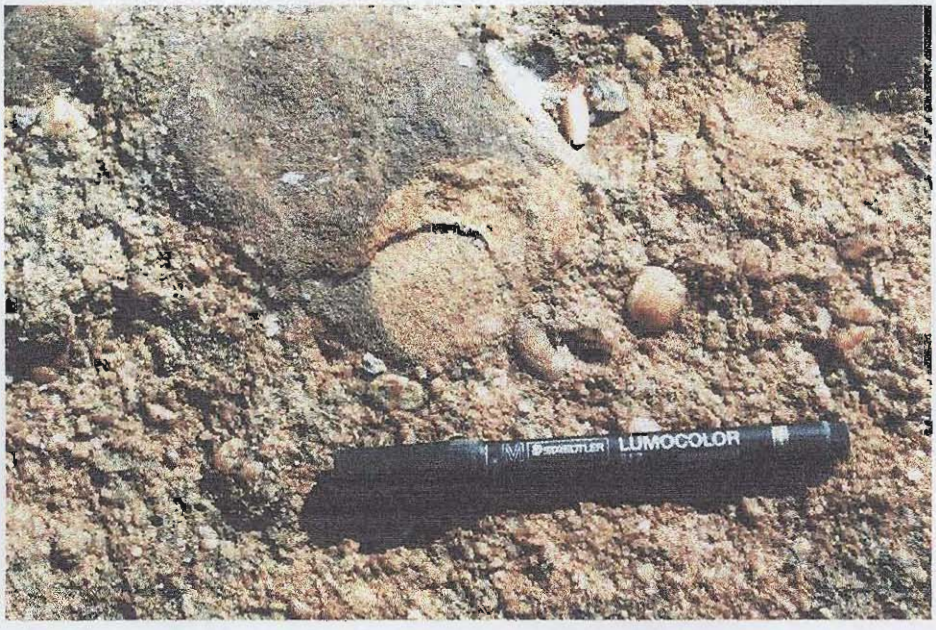

Figure 7.36: Reduction spot in the upper surface of a small inlier of the Makgabeng Formation is not continuous into coarse grained strata of the Mogalakwena Formation, indicating the onset of diagenetic processes prior to deposition of the Mogalakwena Formation. Recorded at 23°16.39'S; 28°52.57'E. Pen is 15 cm long.

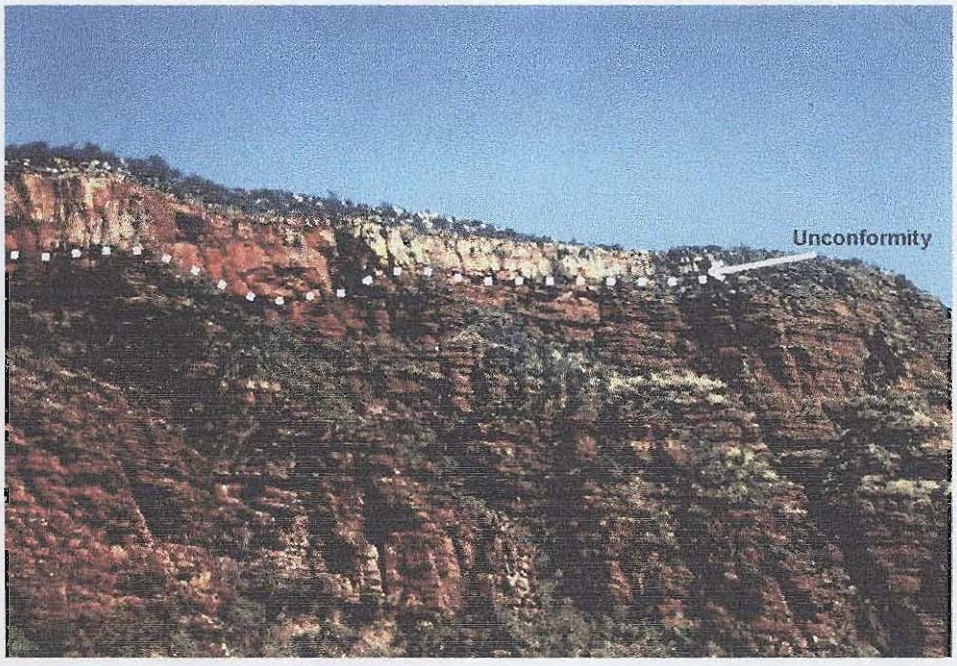

Figure 7.37: Gentle angular unconformity developed between the Mogalakwena Formation and the Wyllies Poort Formation above. Recorded at 23°05.76'S; 28°53.47'E. Cliff section is 100m high.

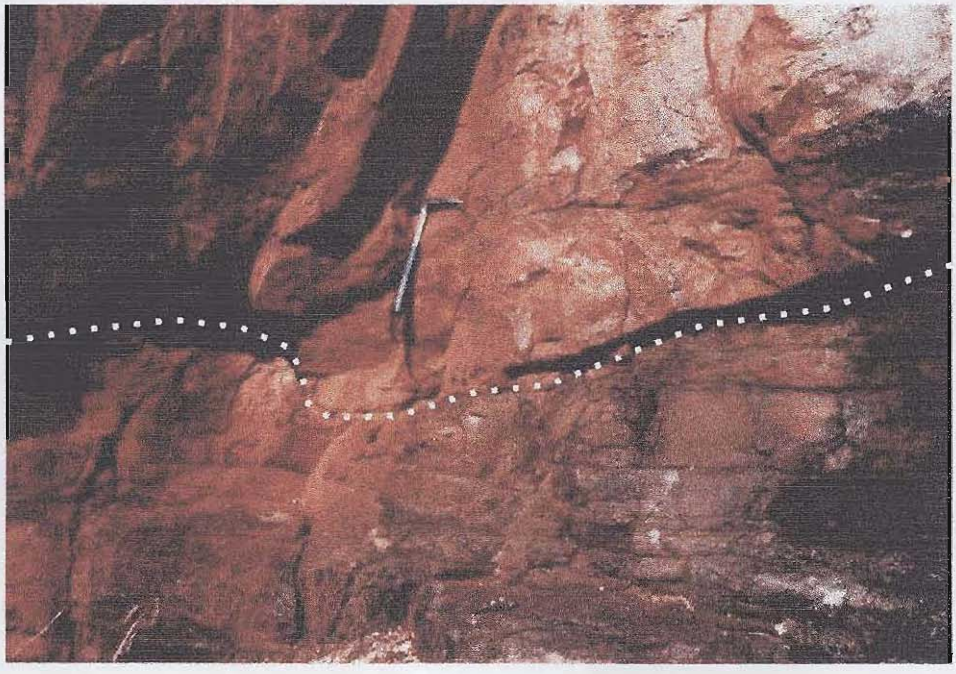

Figure 7.38: Detail of the gentle angular unconformity between the Mogalakwena Formation and the Wyllies Poort Formation above. Recorded at 23°05.76'S; 28°53.47'E. Hammer is 30cm long.

CHAPTER 8: GEOLOGICAL HISTORY.

In this chapter, the geological history for the area in the vicinity of Blouberg mountain will be considered. The data from each of the stratigraphic units presented in Chapters 2-6, and the structural data from Chapter 7 will be combined and analysed to produce a provisional model of basin evolution for the study area.

8.1: Tectonic setting:

8.1.1: Tectonic interpretation of basement rocks:

The foliated rocks of the basement are positioned along the projected extension of the E.N.E.-W.S.W. Palala Shear Zone. In the Palala area (23°20'S; 28°05'E), these rocks consist principally of mylonitic and ultra-mylonitic rocks (McCourt and Vearncombe, 1992). The foliation planes in the banded gneiss recorded in the study area are generally parallel to the foliation in the mylonite at the Palala Shear Zone. The higher-grade gneiss recorded in the study area suggests, however, that deeper crustal levels in the Shear Zone are represented at Blouberg. The general sinistral sense of movement recorded in the banded gneiss at Blouberg compares favourably with the sinistral sense of movement recorded at the Palala Shear Zone (e.g. McCourt and Vearncombe, 1992; Broekhuizen, 1998).

The map of foliations in the gneiss shown in Figure 2.10 shows foliations with at least two contrasting strikes. From Figure 2.10 an earlier foliation can be identified, which strikes N.E.-S.W., and is cut by a secondary foliation, which strikes W.N.W-E.S.E. This secondary foliation may be related to the Sunnyside Shear Zone, which is thought to merge with the Palala Shear Zone in this area (Figure 1.3; Kröner *et al.*, 1999). Broekhuizen (1998) also reported a secondary mylonitic (dextral) foliation with an E.S.E strike in the Palala area.

The Palala Shear Zone is generally regarded as representing the suture between the northern edge of the Kaapvaal Craton (Southern Marginal Zone) and the Central Zone

of the Limpopo Mobile Belt (McCourt and Vearncombe, 1992). The Central Zone is regarded as having docked with the Kaapvaal Craton during c. 2.7 Ga (McCourt *et al.*, 1995; McCourt and Armstrong, 1998) or c. 2.0 Ga (Kröner *et al.*, 1999) transpressional collision. The structural data exhibited by rocks of the Palala Shear Zone provide evidence for the kinematics of this event (i.e. they indicate sinistral-reverse oblique slip). Having identified the rocks beneath Blouberg mountain as representing a continuation of the Palala Shear Zone, this suggests that the strata in the northern part of the study area are located on the suture on the northern edge of the Kaapvaal Craton. Any model for basin evolution constructed for strata in the study area should consider this fundamental structure as a possible tectonic control.

8.1.2: Tectonic interpretation of the Blouberg Formation:

The oldest of the sedimentary strata developed nonconformably on the basement gneiss are the rocks of the Blouberg Formation, which is subdivided into two contrasting members (Lower and Upper; Chapter 3). The extent of the outcrop of both of these members is restricted to a narrow zone across the study area (Appendix 1). If the c.10km-wide Palala Shear Zone is projected eastwards through the Blouberg area, it can be seen that the extent of the preserved Blouberg strata is restricted to the area likely to be underlain by the Shear Zone.

Of the two members of the Blouberg Formation, only the Lower Member was found to outcrop over a reasonably large area. The dip-directions of bedding planes of the Lower Member in the vicinity of Blouberg mountain, shown in Figure 7.7, and especially the presence of northward-dipping overturned beds in the Lower Member of the Blouberg Formation, suggest that southward-vergent thrusts have affected the Blouberg and older rocks (Section 7.2). This is corroborated by the presence of low-angled, southward-vergent thrust faults (e.g. Figures 7.4, 7.5 and 7.6), which have locally thrust basement rocks over Blouberg strata, and by the presence of southward-vergent reverse faults cutting the Lower Member of the Blouberg Formation (e.g. Figures 7.10, 7.11 and 7.12). Such high-angled reverse faults could also, however, be interpreted as being related to positive flower structures, caused by transpressional

movement along the Palala Shear Zone. Additionally, geophysical evidence from the Melinda Fault outside the field area suggests that the Melinda Fault is vertically dipping (G. Brandl, pers. com.). However, it generally appears that the Lower Member of the Blouberg Formation has been subjected to a positive basin inversion, resulting from a stress field with an approximately north-south orientated compression.

The contrast in lithofacies between the generally sandy Lower Member and generally conglomeratic Upper Member of the Blouberg Formation, represents a clear coarsening-upwards succession for the Formation as a whole (Figure 3.1). The conglomeratic Upper Member consists of large, angular cobbles of quartz, quartzite and feldspathic, foliated rocks which are likely to have been derived from a proximal source of basement gneiss. As shown in Figure 3.1, the contact between the Lower and Upper Members is sharp, and can be interpreted to reflect depositional changes as a response to sudden tectonic uplift of a source area nearby; a single coarsening-upward succession as suggested above is thus not pertinent.

In contrast to the steeply-dipping Lower Member, rare outcrops of Upper Member strata around Blouberg mountain have bedding planes with only low angles of dip (Figure 7.7; Appendix 1). Thus the Upper Member appears to be unaffected by the tectonic event which was responsible for the southward-vergent thrusting and overturning of the older Blouberg strata. It is possible that the southward-vergent event, and the event responsible for the tectonic uplift of the Blouberg Upper Member source area were the same, as both events post-date the Lower Member, but pre-date the deposition of the Upper Member.

In contrast, the 1400m of Blouberg strata recorded in the Kranskop section appear to be unaffected by any southward-vergent tectonic event. Instead, bedding planes dip consistently and steeply to the west, which is difficult to reconcile with the tectonic model proposed above. However, the considerable distance (c. 25km westwards) between the Kranskop strata and the outcrops in the area of Blouberg mountain, and the fact that the Kranskop strata lie adjacent to the Melinda Fault (where the northern

and southern strands have merged), suggest that the tectonic history in this area may have been different. It seems that Kranskop strata were only overturned *after* the deposition of the Upper Member of the Blouberg Formation, as both Lower and Upper members exhibit comparable deformation. Although difficult to interpret, this may represent a continuation of syn-Blouberg deformation into post-Blouberg times. The change in dip direction between the Blouberg mountain strata (which dip to the south or are overturned and dip to the north) and the Kranskop strata (which dip steeply towards the west) may be due to localised rotation or drag folding alongside the Melinda Fault. As Blouberg strata in both areas are unconformably overlain by gently-dipping Mogalakwena strata, this suggests that the age of all the events proposed above can be constrained to at least pre-dating deposition of the Mogalakwena Formation.

8.1.3: Tectonic interpretation of the Waterberg Group (Setlaole, Makgabeng and Mogalakwena formations):

Generally these strata are not particularly deformed in the southern part of the study area. However it is important to note the fact that the Makgabeng Formation does not appear to be preserved less than 4km south of the southern strand of the Melinda Fault. This may have been due to the presence of an elevated palaeotopography to the north in the immediate vicinity of the southern strand of the Melinda Fault, so that erosion rather than deposition prevailed there during Makgabeng times. The earlier, syn-Blouberg basin inversion (southward-vergent thrusts) may have produced such high relief northwards of the southern strand of the Melinda Fault, and implies a small time gap between Blouberg and Setlaole / Makgabeng sedimentation.

Outcrops of the younger Mogalakwena Formation, however, underlie areas much further north than the Makgabeng Formation. Adjacent to the southern strand of the Melinda Fault, bedding begins to dip more steeply (Appendix 1), and contrasting facies of the Mogalakwena Formation are juxtaposed against each other, separated from each other by brittle faults (Figures 2.14, 2.15, 7.1, 7.2 and 7.3). Though no

foliation exists in the crush breccia fault rocks, the following evidence suggests that these faults are extensional (normal) dip-slip faults.

The presence of reverse fault planes dipping steeply to the north in the Blouberg Formation (Figure 7.10) suggest that a northward-dipping fault plane was already established beneath the Mogalakwena rocks. The E.N.E.-W.S.W striking veins throughout the fault rocks, and the generally E.N.E-W.S.W.-striking post-Mogalakwena, syn-Sibasa dyke swarm cutting the Waterberg Group (Figure 6.2; see Section 8.1.4 below), suggest that the syn-Blouberg reverse faults may have reactivated during syn-Sibasa times under a stress field with approximately N-S orientated extension. Thus the faults are likely to be northward-dipping normal faults, which were active prior to the deposition of the Soutpansberg Group in the area. These normal faults are envisaged to have juxtaposed the upper (sandstone and granulestone) Mogalakwena in the hanging wall to the north, against the lower (conglomeratic) Mogalakwena strata in the footwall.

An alternative model for the juxtaposition of distal facies of the Mogalakwena Formation against inferred proximal facies is that dextral strike-slip movement occurred along the southern strand of the Melinda Fault. However, in order to juxtapose these sediments, a displacement of around 25km is necessary in order to juxtapose such relatively mature sediments from distal parts of the basin with more proximal rocks. Such a large dextral displacement is considered unlikely in view of the narrow, localised extent of the crush breccia.

The southern strand of the Melinda Fault therefore appears to comprise northward-dipping faults which were active as reverse faults in syn-Blouberg times, and as normal faults in post-Mogalakwena / syn-Sibasa times. Generally it appears that the later event must have occurred as a reactivation along the older fault planes. Locally, however, field relationships suggest that the reverse faults failed to reactivate, e.g. in the vicinity of Dantzig, at the eastern end of the southern foothills of Blouberg mountain (23°06.5'S; 29°01.5'E). Here, it seems that the normal, syn-Mogalakwena component is only poorly developed, as basement rocks occupy areas of relatively

high topography in the hanging wall to the north, compared with gneiss north of the southern strand of the Melinda Fault further to the west, which outcrops only at low altitudes. This indicates that little or no syn-Sibasa normal displacement has occurred in the hanging wall in the Dantzig area, and evidence for only the syn-Blouberg reverse faults was recorded (Section 7.2).

8.1.4: Tectonic interpretation of the Soutpansberg Group:

The lack of outcrops of the Sibasa Formation with any significant preserved structures has not allowed for any direct tectonic inferences to be made. However, a comparison between the incompatible trace element pattern shown in Figure 5.5 (Sibasa basalt) and Figure 6.4 (dykes cutting the Waterberg Group), shows that both igneous rocks have comparable geochemistry (Figure 8.1). In particular, Figure 8.1 shows that relative ratios of incompatible trace elements (Nb to Yb) for the six samples (3 dolerite dykes, 3 basaltic Sibasa lavas) remain constant, throughout varying degrees of fractional crystallisation. This indicates a common parental magma for both the dykes and the Sibasa lavas. Similarly, a plot of Zr against Y, shown in Figure 8.2, suggests that all six samples likely had the same parental magma, as these highly incompatible elements maintain the same ratios relative to each other throughout successive episodes of fractional crystallisation. Thus it seems that the dyke swarm cutting the Blouberg Formation and Waterberg Group to the south of the southern strand of the Melinda Fault was a feeder to the lavas of the Sibasa Formation above. Such an interpretation strengthens the hypothesis that the Soutpansberg Group post-dates the Waterberg Group, as Soutpansberg-aged rocks appear to intrude the Waterberg strata. Additionally, it must be borne in mind that the dyke swarm, which intrudes the Waterberg Group so intensely, cannot be demonstrated to cut the Wyllies Poort Formation (Appendix 1). Reliable age-dating of Sibasa basalts and dolerite from the dykes may confirm the suggestion that the dykes cutting the Waterberg Group acted as feeders to the Sibasa Formation, and in addition provide age constraints for the minimum age for the deposition of the Waterberg Group (Mogalakwena and older formations).

Trace element signatures from basalts of the Sibasa formation and inferred feeder dykes to the lavas suggest a subduction-related, calc-alkaline signature. However, it must be bourne in mind that many igneous rocks throughout the Kaapvaal Craton (e.g. volcanics of the Transvaal Supergroup and mafic intrusives of the Bushveld Complex) also possess a subduction-related geochemical signature (e.g. Harmer and von Gruenewaldt, 1991). Such signatures are thought to be inherited form lithospheric source rocks, which had been generated through subduction-related processes at the time of Archaean crustal development, rather than indicating the actual tectonic regime under which the magmas were generated (Harmer and von Gruenewaldt, 1991).

The orientation of the strike of dykes developed in the Blouberg and Waterberg strata is generally E.N.E-W.S.W (Figure 6.2). This suggests that, at the time of dyke intrusion and eruption of the Sibasa basalts, an extensional stress field prevailed and the extension direction was orientated perpendicular to the plane defined by the dyke swarm (i.e. approximately north-south extension; Section 8.1.3).

It is important to note that neither the Sibasa Formation nor the Wyllies Poort Formation can be demonstrated to outcrop south of the southern strand of the Melinda Fault in the study area. Similarly, no Soutpansberg strata have been recorded southwards of the projected line of the Palala Shear Zone anywhere else along the Soutpansberg basin (Cheney *et al.*, 1990). However, outcrops have been recorded further to the north, including xenoliths that have been correlated with the Soutpansberg Group within the Venetia Kimberlite pipe near Messina (Barton and Pretorius, 1996).

The structural data from the northern strand of the Melinda Fault, where it cuts the Wyllies Poort Formation, suggest that the northern strand may be a dextral strike-slip fault, though with a considerable dip-slip component developed locally. This can be inferred from the rose diagrams shown in Figures 7.26 and 7.27, and stereographic projections shown in Figures 7.28 and 7.29. Figure 7.26 shows that joint planes in the Wyllies Poort Formation have a dominant strike towards the N.W, suggesting

maximum extension towards the N.E. and S.W., with the direction of maximum compression from the north-west and south-east. Similarly the strike of veins (Figure 7.27) suggest compression from the N.W. and S.E. Figure 7.28 show that the dominant planes of small-scale faults match the geometry of the northern strand of the Melinda Fault (a steeply-dipping E.N.E-W.S.W-striking fault), and Figure 7.29 shows that slickenside lineations recorded from these fault planes dominantly show an azimuth directed E.N.E.-W.S.W, with generally shallow plunges. However many of these lineations (those with a steep plunge) also demonstrate a considerable dip-slip component developed on many of the fault planes. Bedding orientations from outcrops of the Wyllies Poort Formation in the vicinity of the northern strand of the Melinda Fault, plotted in Figure 7.17, suggest that the Wyllies Poort Formation is locally folded, with a horizontal fold-axis with a N.E.-S.W. trend.

Together this evidence suggests that a N.W. to S.E. -directed compression was responsible for general dextral (though also oblique) displacement along the northern strand of the Melinda Fault (Figure 8.3) at a time which post-dates the deposition of the Wyllies Poort Formation. The regional pattern of displacement of the Wyllies Poort Formation by the northern strand of the Melinda Fault, especially where the projected line of the Fault displaces the Soutpansberg strata north east of Vivo (c. 22°58'S; 29°21'E), by up to 17km, appears to confirm the dextral sense of movement proposed here.

8.1.5: Conclusions regarding the age relationships and tectonic setting in the study area:

The age-relationships between the stratigraphic units that can be inferred from this work are shown in Table 8.1, where they are compared with the existing stratigraphic subdivision, as proposed and debated by Jansen (1976) and Meinster (1977). The map in Figure 8.4 shows the location of an idealised cross-section from north to south through Blouberg mountain, which is shown in Figure 8.5. This sketch cross-section illustrates the structural geology and is constructed with regard to the proposed tectonic history of the study area described above. Similarly, cross-sections through

the Blouberg mountain area, constructed from the map in Appendix 1, are provided in Appendix 3.

8.2: Depositional Palaeoenvironments:

In this section, the depositional setting of each of the sedimentary units recorded in the study area will be extrapolated from the data presented in earlier Chapters.

8.2.1: Depositional setting of the Blouberg Formation:

The Lower Member of the Blouberg Formation is characterised by relatively small sets of trough cross-bedded purplish sandstone with gravel-filled channel forms developed locally (Sections 3.2 and 3.3). The purple colour in areas which have not been reduced indicates the presence of syn-diagenetic oxygen, which may also have been present in the atmosphere at the time of deposition, although a considerable time period may elapse between deposition and final lithification of sedimentary rocks. The content of carbon dioxide in the Precambrian palaeo-atmosphere decreased in a complex manner over geological time, as illustrated by palaeosol data (Holland et al., 1986; Rye and Holland, 1998). Detrital pyrite and uraninite deposits, which are unstable under oxidising conditions, are restricted to deposits older than c. 2.0 Ga, and BIF, with few exceptions, pre-date 1.85 Ga (Kasting, 1991; Condie, 1997). Red beds *sensu stricto* (i.e., those with clasts partially covered by iron-stained clays rather than just having red pigmented intergranular material) were virtually absent prior to c. 2.0 Ga (e.g. Eriksson and Cheney, 1992). The appearance of red beds thereafter suggests a substantial increase in atmospheric oxygen levels (Kasting, 1993; Rye and Holland, 1986), as also supported by palaeosol compositions which support a rapid rise in atmospheric oxygen close to c. 1.9 Ga (Holland, 1994). Thus the presence of red beds throughout the entirety of the siliciclastic successions in the study area suggests that none of the sediments is older than c. 1.9-2.0 Ga.

The sedimentary facies associations in the Lower Member of the Blouberg Formation are composed of facies of planar and trough cross-bedded sandstone (Sp and St),

together with trough cross-bedded pebble conglomerate (Gt). Although it was impossible to establish architectural elements within the Blouberg Formation, which can be used in order to discriminate fluvial styles (Miall, 1992) the facies comprising the Blouberg Formation can be interpreted, instead of architectural elements, in order to infer a depositional setting for the Blouberg Formation. Facies St can be interpreted to have formed due to the migration of aqueous dunes under lower flow regime conditions, using the scheme of Miall (1977) (Table 8.2a). Similarly, facies Sp (planar cross-bedded sandstone) can be interpreted to reflect deposition from linguoid bars or sand waves, and stratified gravel channels (Gt) can be interpreted as having being deposited as minor channel fills (Table 8.2a). These interpretations can be applied throughout the Lower Member of the Blouberg Formation, which is comprised of associations of these three facies. These interpretations, when considered together with the fact that the Blouberg strata are red beds (and therefore most likely of continental origin), have relatively unimodal palaeocurrent directions (in the Blouberg mountain area; Figure 3.33) and the predominance of bedload material over suspended sediment in the preserved rocks (muddy sandstones are rare in the Blouberg Formation) suggest a fluvial depositional palaeoenvironment that closely resembled that of low-sinuosity distal braided sheetflood systems (Miall, 1992). Models for Blouberg rivers being meandering or having anastomosing channel systems, which require resistant river banks in order to form, are considered unlikely in view of the lack of vegetation and soil producing biota in the Palaeoproterozoic. The paucity of preserved argillaceous rocks in the Blouberg Formation would seem to qualify this argument. In the general absence of terrestrial vegetation, and with enhanced mechanical and chemical weathering processes inferred for the Precambrian (Condie, 1997; Corcoran *et al.*, 1998), it is thought that Precambrian rivers had a high bedload and low bank stability (e.g. Mueller and Corcoran, 1998; Van der Neut and Eriksson, 1999). Therefore braided river patterns are generally accepted for pre-vegetative Precambrian rivers (Schumm, 1968b; Cotter, 1978; Long, 1978; Eriksson et al., 1998).

It should again be stressed that palaeohydraulic data, presented in Section 3.5, cannot be used as an indicator of absolute values of calculated parameters, but can rather be

used to compare parameters as they vary across an individual basin, or even between basins. The palaeohydraulic data presented in Figures 3.36, 3.37 and 3.38 show how calculated parameters vary from east to west, along the inferred axis of the Blouberg basin. Parameters calculated using clast sizes within channels (Figure 3.36) show reasonable systematic variation across the basin. Stream power (W) seems to increase towards the west. This is compatible with westerly-increasing discharge (Q) values (Figure 3.36) which correlate well with an approximately westward palaeocurrent direction (Figures 3.33 and 3.35). As discharge values essentially reflect the size of the catchment area (e.g., Van der Neut and Eriksson, 1999), it is inferred that more braided channels on an increasingly broad fluvial system developed towards the west; stream power would have increased along with an enhanced volume of water derived from the larger catchment area. The fact that estimations calculated for water velocity (v) appear to decrease towards the west, whereas palaeoslope (s) values increase in the same general direction (Figure 3.36), serve to illustrate the inherently large potential errors in calculations of palaeohydraulic parameters (e.g., Van der Neut and Eriksson, 1999).

Palaeohydrological parameters that were calculated from cross-stratification set heights within the Blouberg Formation show little systematic E-W variation along the probable axis of the Blouberg basin. Discharge (Q) and bankfull water discharge (Qb) appear to increase towards the centre of the basin (Location B in Figure 3.35; Figures 3.37 and 3.38). Drainage area (Ad and Ad(1))and stream length also appear to be greatest at the centre of the basin (Figure 3.38), whilst palaeoslope (s and s(1))appears to be steepest at the margin of the preserved basin (Locations A and F in Figure 3.35; Figure 3.37), all of which are logical general conclusions for most basins. Channel depth (db) and width (wb) show little variation (Figure 3.37).

The general increase in discharge, drainage area, and stream length towards the centre of the preserved Blouberg basin (Location B in Figure 3.35), and the concomitant lowering of palaeoslope, are compatible with braided fluvial deposition within a pull-apart basin, as also envisaged by Brandl (1986b). Pull-apart basins typically form within active strike-slip fault zones (see Section 8.1.2), have their margins bound by

fault scarps (i.e. steep palaeoslopes at the margins of the basin) and are characterised by current directions which flow towards the centre of the basin (Crowell, 1974). Rapid lateral facies changes and rapid subsidence are also characteristics of pull-apart basins (Miall, 1996). The Blouberg Formation appears to contain many of these features, especially the characteristic of rapid subsidence (e.g. 1400m of immature sediment in the Kranskop area; Section 3.2). The localised extent of the outcrop, restricted to areas overlying the Palala Shear Zone, shows that the Blouberg Formation has been deposited within an active fault zone. Assuming that the area around locations B and D (Figure 3.35) is the approximate centre of the Blouberg basin, the paucity of reliable palaeocurrent directions from the Lower Member in the western half of the Blouberg basin mean that a centrally-flowing pattern of palaeocurrent directions cannot be established. However, palaeocurrents from the Lower Member in the east of the basin are generally more systematic, and would seem to reflect transport along a basin axis. The lack of thickly developed Blouberg successions in the east, compared to the Kranskop strata, may indicate that the basin deepened westwards.

The facies present in the Upper Member of the Blouberg Formation contrast with the generally sandy-bedload braided river palaeoenvironment which is thought to have prevailed at the time of deposition of the Lower Member. The change of facies between the Lower and Upper Members is rapid; although the exact facies change is not exposed in the Kranskop section, the upper-most beds of the Lower Member, and the lower-most beds of the Upper Member are developed within 5m of each other. This suggests that palaeoclimatic conditions, which tend to be more gradual, are unlikely to have been responsible for the change in sedimentation regime. The sudden change to more immature sediment for the Upper Member can rather be interpreted as a response to tectonic activity in the source area for the Blouberg sediments (Section 8.1.2).

Within the Upper Member of the Blouberg Formation poorly stratified, matrix-supported, sub-angular to sub-rounded cobbles imply that debris flows were now the predominant depositional process (Miall, 1996). Planar-bedded and cross-bedded

coarse sandstone and granulestone red-beds can be identified locally, and trough cross-beds can be seen to be developed within channel-fills, which were erosive into the matrix-supported conglomerate. This suggests that aqueous dunes, linguoid bars and sand waves were migrating across the basin of the Upper Member, and again, considering the Precambrian conditions, would suggest a braided, fluvial palaeoenvironment between periods of debris flow. The general upwards-fining, cyclical nature of the conglomerates, which pass vertically into sandstones (where each cycle is generally less than 1m thick) suggests a fairly rapid cyclicity in discharge, perhaps due to fluctuating precipitation. Flood events generating debris flow deposits within a vegetation-free and soil-poor palaeoenvironment were followed by traction current deposition of more sandy detritus as floods abated.

8.2.2: Depositional setting of the Setlaole Formation:

The facies recorded from the few outcrops of the Setlaole Formation, which are generally similar to those found in the Blouberg Formation, suggest a fluvial setting. The presence of trough cross-bedded sandstones as a dominant facies, reflecting migrating dunes, a relatively unimodal southerly palaeocurrent data (Figure 4.3) support this interpretation. The disparity between palaeocurrent directions of the Blouberg Formation and Setlaole Formation is one of the few criteria that could be to discriminate between these two very similar strata. As with the Blouberg model, the Precambrian age would have favoured braided systems rather than anastomosing or meandering. Again, the lack of argillaceous sediment preserved within the Setlaole Formation concurs with a braided fluvial environment.

8.2.3: Depositional setting of the Makgabeng Formation:

The five facies associations identified within the Makgabeng Formation (Chapter 4) are: a.) Large-scale trough and planar cross-bedded sandstone; b.) Horizontally-bedded and rippled mudstone and sandstone; c.) Rippled and cross-bedded sandstone; d.) Massive sandstone, and e.) Pebbly sandstone. Of these, the large-scale trough and planar cross-bedded sandstone is the most abundant. The inverse-grading of sand

grains in laminations is diagnostic of wind-ripple strata deposited during aeolian sedimentation (Hunter, 1977, 1981; Kocurek and Dott, 1981), indicating that the Makgabeng Formation was generally lain down as aeolian dunes in a palaeodesert. Ripple indices recorded from ripplemarks developed on foresets are consistent with aeolian transport (McKee, 1945, 1979). Planar cross-bedded strata with steep angles of inclination are likely to represent straight-crested, transverse aeolian dunes, whereas the large-scale trough cross-bedded strata are likely to represent sedimentation in either sinuous-crested (aklé) or barchanoid sand dunes (McKee, 1979). The wedge-shaped strata present amongst the wind-ripple strata most likely represent grain flow strata, where tongue-shaped dry avalanches of sand fell from an over-steepened dune crest (Hunter, 1977,1981; Kocurek, 1981).

The horizontally-bedded and rippled mudstone and sandstone facies, is generally found overlying very low-angled or horizontal dune foresets (i.e they were deposited at the base of the sand dunes). This facies association can be interpreted to reflect a drying-up sequence. Lower-most massive sandstone, stratified sandstone and current-rippled sandstone in this facies association may reflect deposition sheetflows during periods of heavy precipitation (Eriksson *et al.*, 2000). Upper wave and combined flow ripples with subordinate wind-rippled sandstone, adhesion warts, desiccation cracks, evaporite casts and roll-up structures appear to represent ponding of the sheetfloods, followed by gradual drying. The fact that this facies association overlies horizontally inclined foresets of dune deposits suggest that this facies association was deposited in flat-lying interdune areas, which may be prone to flooding during periods of heavy, periodic precipitation events (Eriksson *et al.*, 2000). The muddy roll-up structures recorded in the upper beds of this facies are of interest, as usually desiccating mud polygons attain a maximum curl of 90-120°, before disintegrating (Schieber, 1998). These roll-up structures, which attain a maximum curl of 720°, are most likely to represent the growth, desiccation and subsequent resedimentation of algal mats over the upper surface of the drying lake muds (Eriksson *et al.*, 2000). The growth of cells of cyanobacteria over the surface of the mud is thought to have added sufficient cohesion to the substrate to prevent disintegration upon desiccation. The parallel orientation of the roll-up structures may reflect their subsequent transport by flowing

water, so that the roll-ups are now orientated parallel to a palaeocurrent direction. Significantly these roll-up structures from the Makgabeng palaeodesert may represent the earliest recorded colonisation of a wholly terrestrial (and harsh desert) environment by microbial organisms (Eriksson *et al.*, 2000).

The various facies incorporated within the rippled and cross-bedded sandstone facies association can be interpreted to reflect the following depositional processes: strongly asymmetric ripples = aqueous current ripple migration; slightly asymmetric ripples = aqueous combined flow ripple migration; inversely-graded laminations = aeolian wind ripple strata; symmetrical ripples = wave ripple migration; massive sandstone = suspension (Simpson *et al.*, under review). These facies are consistent with an interpretation of the deposits accumulating in a playa lake setting, as all the facies described above have also been identified together in both modern and ancient playa deposits (Lowenstein and Hardie, 1985; Renaut and Last, 1994; Wedge et al., 1994; Demicco and Hardie, 1994; Turner and Smith, 1997; Sweet 1999; Irmen and Vodra, 2000). The small pits recorded in these inferred playa lake deposits, filled by sandstone, mudstone or siltstone and characterised by preferential cementation, are typical of features associated with thin salt crusts (Smoot and Castens-Seidell, 1994), where wind-borne clay particles aggrade on hydroscopic films on salt crystals (Simpson *et al.*, under review). Intercalated facies of wind-ripple strata are thought to reflect the local encroachment of aeolian dunes over the margins of the dried-up playa lakes during times of low precipitation or during sandstorms, during which sand flux may fill a playa lake within hours (Wedge *et al.*, 1994).

The great thickness attained by this facies association (30m) indicates that such playa lake deposits were relatively long-lived within the Makgabeng palaeodesert, and their stratigraphic relationship with the underlying interdune deposits (Section 4.3.3.2) may indicate progressively higher rates of seasonal (or longer interval) precipitation during deposition of the Makgabeng sand sea.

The genesis of the massive sandstone facies association is more enigmatic. The presence of dewatering structures, desiccation structures and parting lineations on the

upper surface of the massive beds, and the close association with soft-sedimentary deformation of steeply-dipping aeolian foresets (which is inconsistent with the failure of dry sand), suggest that the massive sand was wet during its deposition (Simpson *et al.*, under review). Third–order (reactivation) surfaces (McKee, 1966; Brookfield, 1977) have been related to a temporary change in wind direction, and may also record a hiatus in aeolian sedimentation (Brookfield, 1977). The local onlap of massive beds onto third-order surfaces indicates that massive beds are deposited whilst aeolian deposition had been interrupted. The geometry of the massive sandstone beds, which are lenticular at the bottom of aeolian palaeodunes and channelised higher up the preserved dune face, suggests that water-saturated sand slumped down the lee face of sand dunes and became channelised, perhaps due to the funnel-shaped nature of barchan sand dunes (Simpson *et al.*, under review). The erosive nature of the massive channel-fills suggests that flow was turbulent in these channels. As the angle of repose decreased, the channels are thought to have spread out into lobe-shaped deposits over the dune plinth. The decrease in flow depth, which would have accompanied the transition from channelised to lobate geometry, would have led rather to a short-lived and localised increase in flow energy, as evinced by rare occurrences of lobate massive sandstone eroding the underlying wind-ripple strata (Simpson *et al.*, under review). Thereafter, reduced gradients led to laminar flow conditions for the massive sandstone lobes.

The triggering mechanism behind the slope failure of sand dunes, considering the fact that the massive deposits are likely to have been transported as water-saturated flows, is likely to have been periodic torrential rainfall (e.g. Loope *et al.*, 1999). The presence of interdune deposits (with rainspots locally preserved on muddy beds) grading upwards into large playa lake deposits, indicates that intermittent rainfall was significant in the Makgabeng desert's palaeoclimate. It is thought that during periods of rain, steeply-dipping foresets close to the crest of the dune and which were stable under dry conditions, became saturated with percolating meteoric water. As the maximum angle of repose of dry sand is greater than that of its wet counterpart, as the rainstorm continued failure of the top part of the dune could have occurred. Rainfall must have fallen at a rate that exceeded the rate at which water could have percolated

through the aeolian dune sand, otherwise meteoric water would have drained down to the water table, and the sand could not have become sufficiently saturated to lead to slope failure. Loope *et al.* (1999) suggest that such rainfall rate may be of the order of 250mm in 6 hours. Such a model is consistent with modern events reported from Sandhills in Nebraska, where stable, vegetated dunes collapsed after a period of heavy rainfall (Loope *et al.*, 1999). It is also possible that microbial organisms played a role in stabilising some dune crests before saturation and failure occurred.

The fact that the massive sandstone facies are absent in the lower part of the Makgabeng Formation, and can generally be seen to become more common towards the top, is evidence for long-term climatic change throughout syn-Makgabeng times, and suggests that the desert became steadily wetter through time. The increase in the presence of massive sandstones towards the top of the Makgabeng Formation is also recorded in the borehole log (Figure 4.12), where massive sandstones are only recorded in the top-most 570m of Makgabeng strata, and are absent from the lower-most 280m. This overall increase in precipitation towards the top of the Makgabeng formation is also recorded in the increasingly common transition from inferred interdune deposits to playa lake deposits (discussed above). At this period in geological history, where land plants were generally absent, even high rates of periodic precipitation might not necessarily lead to the cessation of aeolian sedimentation. Increasingly wet weather might also explain the gradual dominance of barchan dunes over transverse dunes towards the top of the Makgabeng Formation. Barchan dunes generally form rather than transverse dunes under dwindling sediment supply (McKee, 1979). If rainfall rates increased, more sand might have been removed from source areas by fluvial action which bypassed the erg, rather than being retained as aeolian bedforms.

The facies present within the pebbly sandstone facies association are difficult to reconcile with any aeolian process. The relatively large quartz pebbles were not recorded in any other facies association in the Makgabeng Formation, though quartz grains included in the generally massive sandstone of this facies association are identical to those associated with the dune deposits. This suggests that dune sand has

been reworked into this facies, and that quartz pebbles were transported into the erg. The presence of small-scale trough and planar cross-bedding, preserved channel forms and parting lineations on planar-bedded and laminated sandstone surfaces indicate the migration of sub-aqueous dune and bar bedforms, channel scouring, and upper flow regime plane-bed flow. Thus, the features of this facies association are consistent with those of ephemeral rivers (Miall, 1996), which may have flowed across the Makgabeng desert. In particular, the presence of plane-bed laminated sand with parting lineations is indicative of high-velocity, flashy discharge which is a characteristic of ephemeral streams (Miall, 1996). Quartz and quartzite pebbles could not have been brought into the desert by aeolian processes, and thus fluvial processes are considered likely. The trend of parting lineations and channels, and the dip-direction of foresets suggest that these ephemeral rivers flowed southwards. This palaeocurrent direction matches those from the Setlaole Formation beneath, and it seems that both these formations were deposited when there was an area of higher relief to the north from which rivers drained.

The widespread evidence for an increasingly wet palaeoclimate recorded in the upper strata of the Makgabeng Formation also provides evidence for the cessation of aeolian conditions. Increasing precipitation may initially have caused the transition from transverse to barchan dunes, and increasingly common ephemeral rivers may have removed material away from aeolian source areas altogether, thus ending deposition in the Makgabeng sand sea.

8.2.4: Depositional setting of the Mogalakwena Formation:

The conglomerates and interbedded trough cross-bedded sandstones and granulestones of the Mogalakwena Formation (Facies Gmm, and St) are grouped together in sheet-like architectural elements (CHS; Miall, 1992; Table 3.1), and locally, conglomerate filled channels occur (architectural element CHR; Miall, 1992; Table 3.1; Section 4.4.1.1). Trough cross-bedding, preserved in the sandstone and granulestone of the Mogalakwena Formation implies migrating aqueous dunes (Table 8.2a) and the ubiquitous presence of architectural element CHS is compatible with the

migration of braided fluvial channels (Miall, 1992; Table 8.2b). Unimodal palaeocurrent directions recorded from the Mogalakwena Formation (Figures 4.55, 4.61, 4.70) suggest that rivers were flowing from the N.E. and E.N.E, and this palaeocurrent direction is reflected by a facies change towards the S.W.: The dominant conglomeratic lithofacies in the vicinity of the southern strand of the Melinda Fault (Section 4.4.1.1) become subordinate towards the S.W., and more distal outcrops in the southwestern portion of the study area are dominanted by trough cross-bedded sandstone and granulestone, locally with heavy mineral concentrations developed on foresets (Section 4.4.1.2). The conglomerate-dominated facies in the east can therefore be regarded as proximal, and the trough cross-bedded sandstone and granulestone in the west can be regarded as distal facies equivalents.

The Mogalakwena Formation is developed considerably farther northwards than any of the older formations of the Waterberg Group (Section 4.4.2). The basal pebble and cobble conglomerates are generally compositionally (quartz, quartzite and banded iron formation cobbles and pebbles) and texturally mature, suggesting that the sediment had travelled some distance. The conglomerates appear to be most fully developed at the base and close to the southern strand of the Melinda Fault in the southern foothills of Blouberg mountain, so it is likely that this fault exerted a controlling factor over the deposition of the conglomerates. Conglomerates to the north of the southern strand of the Melinda Fault are relatively thin (max 10m)(Section 4.4.2), similar to those developed in distal areas in the S.W. of the study area. The dominant trough cross-bedded sandstones north of the southern strand of the Fault, characterised by heavy mineral concentrations on foresets, are also identical with the facies from the distal outcrops of the Mogalakwena Formation in the S.W. This suggests that basal conglomerates of the Mogalakwena Formation thin northwards, and younger, distal facies equivalents are more fully developed in this area to the north of the southern strand of the Melinda Fault. This implies that the Mogalakwena Formation onlapped northwards over the southern strand of the Melinda Fault. The brittle northwards-dipping normal faults identified along the southern strand of the Melinda Fault (Section 8.1.3) appear to have juxtaposed the distal facies from the top part of the Mogalakwena strata in the hanging wall against

the basal conglomeratic facies in the footwall to the south after the end of Mogalakwena deposition.

Considered as a whole, the strata of the Waterberg Group can be seen to gradually encroach northwards over time, as successive formations appear generally to have their preserved margins established progressively further to the north, ultimately onlapping over the southern strand of the Melinda Fault. This would suggest that an area of high topography established to the north, approximately over the Central Zone of the Limpopo Mobile Belt, was gradually being peneplaned throughout the Waterberg deposition. Such a model is qualified by the general veering of fluvial palaeocurrent directions from southwards (Setlaole and Makgabeng Formations), i.e. directly away from the inferred palaeohigh, to southeastwards (Mogalakwena Formation), i.e. obliquely away from a less developed topography.

8.2.5: Depositional setting of the Wyllies Poort Formation:

The Wyllies Poort Formation appears to be comprised of two dominant facies associations; trough cross-bedded sandstones with pebble washes developed locally, and planar bedded sandstones with ripplemarks and very low-angled cross bedding developed locally. Both these facies associations are developed in sheet-like architectural elements, and are inferred to have developed in braided fluvial conditions (Miall, 1992; Table 8.2b). However, these two different facies associations contain evidence for contrasting palaeocurrent directions. Palaeocurrent directions recorded from trough cross-bedded sandstone generally suggest flow towards the S.W. (sub-parallel to the trend of the southern strand of the Melinda Fault and the Palala Shear Zone). Asymmetric ripplemarks, in contrast, suggest that weak currents flowed from the N.W and S.E. Similarly, symmetric ripplemarks suggest small -scale wave action from the N.W or S.E. Ripplemarks recorded from the northeastern foothills of Blouberg mountain suggest a main flow from the south, with a minor flow from the north.

The fact that no outcrops of any Soutpansberg strata have been identified south of the projected line of the Melinda Fault, whilst outcrops are common to the north, suggests that the Soutpansberg strata may have been deposited in a half-graben environment, with the hanging wall to the north. Leeder and Gawthorpe (1987) state that one of the criteria for recognising sedimentation in a half-graben environment is that contrasting facies contain contrasting palaeocurrent directions. It is possible that the approximately southwards-flowing palaeocurrents (Figure 5.19) (the planar-bedded sandstones with ripplemarks and locally developed low-angled cross-beds) represent fast-flowing water under upper flow regime conditions, down the gently-dipping hanging wall side of the half-graben. Large- and small-scale trough cross-beds are likely to represent reworking of sediment by aqueous dunes along low-sinuosity, longitudinally-flowing trunk rivers, which flowed parallel to the half-graben axis.

Graben-type models have been proposed earlier for the Soutpansberg Group (e.g. Jansen, 1975; Barker, 1976), though they were refuted by Cheney *et al.*, (1990), who interpreted the Soutpansberg Group as representing a remnant of a once craton-wide cover sequence (i.e. the Soutpansberg Group was *preserved in*, rather than *deposited in* the Soutpansberg trough). One of the arguments against a Soutpansberg depository developed along the Palala Shear Zone put forward by Cheney *et al.* (1990), was that no fault had been identified to the south of the Soutpansberg mountains which could have acted as a southern graben margin. Additionally, several outcrops of Soutpansberg strata had been identified further north than Jansen's (1975) proposed northern margin to the Soutpansberg graben.

Evidence presented here from the Blouberg area suggests that the southern margin of the Soutpansberg Group may be bound by the northward-dipping normal faults along the southern strand of the Melinda Fault, as demonstrated in Sections 8.1.3 and 8.2.4. This normal fault is thought to have displaced the Mogalakwena strata as a response to approximately north-south orientated extension that accompanied the intrusion of the Sibasa feeder dyke swarm, and may have acted as a southern-bounding fault to the Soutpansberg half-graben.

8.3: Provisional basin evolution model for the study area:

During this section, the interpretations of the structural setting and the sedimentary palaeoenvironments which have been described above, will be considered together to produce a provisional model for basin evolution over time of the study area around Blouberg mountain.

The Palala Shear Zone appears to be a factor affecting both the structure and the sedimentation of the study area. Faults (e.g. the Melinda Fault Zone and other reverse faults or thrusts) appear to have formed above the Palala Shear Zone, and have a parallel strike. The extent of all of the sedimentary units discussed in this work appears to be at least partially controlled by structures developed along the Palala line. Palaeocurrent directions in the sedimentary strata are often either parallel to (e.g. the Mogalakwena Formation and the trough cross-bedded facies of the Wyllies Poort Formation) or perpendicular to (e.g. the Setlaole Formation and the ephemeral river facies of the Makgabeng Formation) the Palala line. Therefore it is likely that the geological evolution of the study area has been mainly controlled by periodic reactivation along the suture between the Kaapvaal Craton and the Central Zone of the Limpopo Mobile Belt.

The generally sinistral strike-slip sense of movement recorded in the banded gneiss in the basement is likely to have formed in the collision between the Kaapvaal Craton and the Central Zone of the Limpopo Mobile Belt. The highly ductile deformation of this transpressional event is in contrast to all the younger, brittle deformation, which has affected the generally unmetamorphosed sedimentary rocks in the overlying strata. The fact that sedimentary strata were deposited over such high-grade metamorphic rocks in the field area, indicates that a considerable period of time had elapsed between collision and the onset of Blouberg sedimentation, for such deep crustal rocks to have been exhumed prior to sedimentation. The following paragraphs consider the basin evolution and tectonic history of the Blouberg area following the exhumation of the basement gneiss. This history is also shown schematically in Figure 8.6.

The extent of the Blouberg Formation appears to be restricted to basins developed only above the Palala Shear Zone, and evidence from the Kranskop area suggests that, whilst limited in aerial extent, the basin may have subsided rapidly (at least 1400m of immature sedimentary rocks are preserved) prior to basin inversion and subsequent erosion. The general immaturity, varying palaeocurrent directions and apparently variable palaeohydraulic inferences, and the fact that these rocks are developed over a major transpressional shear zone, show that the strata of the Blouberg basin have many characteristics in common with those associated with pull-apart basins (Figure 8.6a). No strike-slip faults were identified which may have bounded a Blouberg pull-apart basin, though it is likely that any such faults would have been reactivated several times in the subsequent deformational history, and kinematic indicators were likely to have been destroyed. It is therefore not possible to identify whether such a postulated pull-apart basin may have formed as a response to dextral or sinistral strike-slip movement.

The southwards-vergent basin inversion affecting the Lower Member of the Blouberg Formation indicates that a compressional regime, orientated approximately perpendicular to the previously transpressional Palala Shear Zone (Figure 8.6b), affected the area. This had the effect of overturning the Lower Member of the Blouberg Formation, locally thrusting basement over the lower Blouberg strata, and uplifting the basement source area to the north, leading to vigorous erosion and sedimentation of the Upper Member of the Blouberg Formation, in small localised depositories.

A corollary of southwards-vergent thrusting is that the crust to the north is likely to have been uplifted and thickened, so it is probable that this event produced a highland area north of the Palala Shear Zone in the area occupied by rocks of the Central Zone ('Limpopo mountains' in Figure 8.6c). The evidence for the presence of such a highland area is reflected in the sedimentary record; the Setlaole and Makgabeng Formations do not appear to have been deposited to the north, and southerly directed fluvial palaeocurrent directions in these strata suggest that rivers flowed off these

mountains. The palaeowind direction recorded from cross-bedding in the Makgabeng palaeo-erg generally blew towards the S.W. and W.S.W., suggesting that winds may have been funnelled along the Limpopo mountain ridge. Of the Waterberg strata, only the upper part of the Mogalakwena Formation encroached northwards over the denuding Limpopo mountains. This onlap relationship is exhibited by thin basal conglomerates which are generally restricted to north-south trending palaeovalleys, and which are overlain by distal coarse sandstone and granulestone, indicating that the source area of the Limpopo mountains had retreated northwards and eastwards as Mogalakwena sedimentation progressed. The lack of coarse clastic material in the upper and distal parts of the Mogalakwena strata is indicative of peneplation of the source area to the north and east. It is difficult to reconcile the unimodal westwards and southwestwards palaeocurrent directions recorded in the Mogalakwena Formation with the apparent northwards onlap of the Mogalakwena strata over the southern strand of the Melinda Fault, and the rarely inferred presence of north-south trending palaeovalleys. It seems likely that the Mogalakwena rivers may have flowed obliquely (and sub-parallel) to the edge of the mountains to the north, with the edge of the mountain land defined by the southern strand of the Melinda Fault (Figure 8.6c).

Together, the Blouberg and Mogalakwena Formation can be thought of as representing a flysch (syn-tectonic) and molasse (post–tectonic) sequence, respectively, developed as a result of orogenic reactivation within the Limpopo Mobile Belt, which created the Limpopo mountains (Figure 8.6c). Such a model, however, must be reconciled with the fact that no basement-derived gneiss clasts have been reported in the conglomerates of the Mogalakwena Formation. In contrast, however, clasts of gneiss have been reported in the basal Tshifhefhe Formation of the Soutpansberg Group (Brandl, 1987). This can be explained by considering different sediment maturity between these two stratigraphic units. Clasts within the Waterberg Group are likely to have been transported a considerable distance, so that foliated gneiss clasts derived from a Limpopo source are unlikely to have survived transport. Clasts within the basal Soutpansberg strata are likely to have been transported only a short distance, possibly from proximal fault scarps bounding a half-graben, and so remain intact within conglomeratic beds.

The Soutpansberg Group can be interpreted to have been deposited as a response to renewed tectonism, though in a generally extensional setting, in contrast to the earlier, syn-Blouberg, compressional regime (Figure 8.6d). The orientation of feeder dykes to the Sibasa Formation suggests a generally north-south orientated extensional regime, and it is likely that the previously imposed, northward-dipping, syn-Blouberg reverse faults located along the southern strand of the Melinda Fault, were reactivated as normal faults. These normal faults locally juxtaposed the upper, distal strata of the Mogalakwena Formation in the hanging wall against the basal conglomeratic strata in the footwall of the southern strand of the Melinda Fault (Figure 8.6d).

In order to accomplish this juxtaposition of the contrasting facies of the Mogalakwena strata, a considerable displacement is inferred along the Melinda Fault. Downward displacement of the hanging wall is thought to have created a depository above, which was fault bound only to the south (i.e. a half-graben). It is this depository in which the Soutpansberg Group is thought to have been laid down, initially with the only locally developed lava of the Sibasa Formation, and subsequently with the sandstones of the Wyllies Poort Formation (Figure 8.6d). The general maturity of the Wyllies Poort Formation may be a reflection of the considerable distance of transport across the low-angled palaeotopography in the hanging wall. The changes in facies and palaeocurrent directions recorded in the Wyllies Poort Formation are thought to represent transverse and longitudinal fluvial regimes within the half-graben environment.

Evidence for the most recent reactivation above the Palala Shear Zone was recorded from the post-Wyllies Poort northern strand of the Melinda Fault, which may be a dextral strike-slip fault (Figure 8.6e). It proved impossible to further constrain the timing of this reactivation, though in other areas the Melinda Fault is thought to cut the strata of the Karoo Supergroup (Brandl, 1986). Therefore a Phanerozoic timing for this reactivation may be appropriate.

Overall, the sedimentary basins in the area around Blouberg mountain can be considered to have been created as a response to a three-stage tectonic sequence, of

north-south orientated compression (Blouberg Formation), tectonic quiescence and denudation (Waterberg Group), and north-south orientated extension (Soutpansberg Group). Age constraints available from the literature which have bearing on this proposed tectonic history are not very precise. Cheney *et al.* (1991) suggest an age of 1.8 Ga - 1.9 Ga for the Sibasa basalt (whole rock analysis). A corollary of this is that all the Waterberg-aged rocks, generally regarded as being about 1.6 Ga-1.7 Ga (Callaghan *et al.*, 1991), may be several hundred million years older, as they have been shown to pre-date the Soutpansberg rocks. The fact that all sedimentary strata discussed in this work are red beds, indicates that they were all deposited and lithified after c. 1.9 - 2.0 Ga (Eriksson and Cheney, 1992).

The minimum age of ductile movement along the Palala Shear Zone was gained from the age of a cross-cutting pseudotachylite vein, which showed that movement ceased at c. 2042 Ma (Brandl and Reimold, 1990). It therefore seems that the events proposed in this chapter may have occurred between about 2.0 Ga and 1.8 Ga. Such a time constraint is difficult to reconcile with the age of ~1700Ma for the middle Waterberg Group (Makgabeng Formation) proposed by Jansen (1976), which was based on the fact that the Abbotspoort Fault in the Palala area, which does not displace the Makgabeng Formation, *does* displace Palala granite, dated at 1770±30 Ma. A similar age of 1725±245 Ma for the Palala granite was reported by Barton and McCourt (1983), though they indicate that this may be a reset age. Walraven *et al.* (1990) suggest that the Palala granite is most likely of Bushveld age (~2050 Ma), thus only constraining the deposition of the Waterberg strata to a post 2050 Ma age.

The outcome of current opposing opinions regarding the age of the Limpopo collisional event (whether it occurred at 2.65 Ga or 2.0 Ga) is of obvious relevance to this work. If a c. 2.0 Ga date for collision along the Palala Shear Zone is considered (Kröner *et al.*, 1999), there appears to be little time for exhumation of the banded gneiss, the subsequent deposition of the various sedimentary units, and the intervening tectonic events. However, an older (2.65 Ga) age for the collision allows sufficient time for exhumation, and on this basis it may be postulated that the brittle, syn-Blouberg basin inversion and flysch deposition may be related to the c. 2.0 Ga

(Limpopo reactivation) event itself. Thus the history proposed here would tend to favour a model with 2.65 Ga collision, and a 2.0 Ga reactivation (such as that proposed by McCourt and Armstrong, 1995), where reactivation at 2.0 Ga occurs possibly as a result of the Magondi Orogeny (part of the Africa-wide Eburnean event), or the Vredefort structure, or the emplacement of the Bushveld Complex (McCourt and Armstrong, 1998).

Figure 8.1: Spidergram to compare values of normalised incompatible trace elements for dykes (D) and the Sibasa Formation (S).

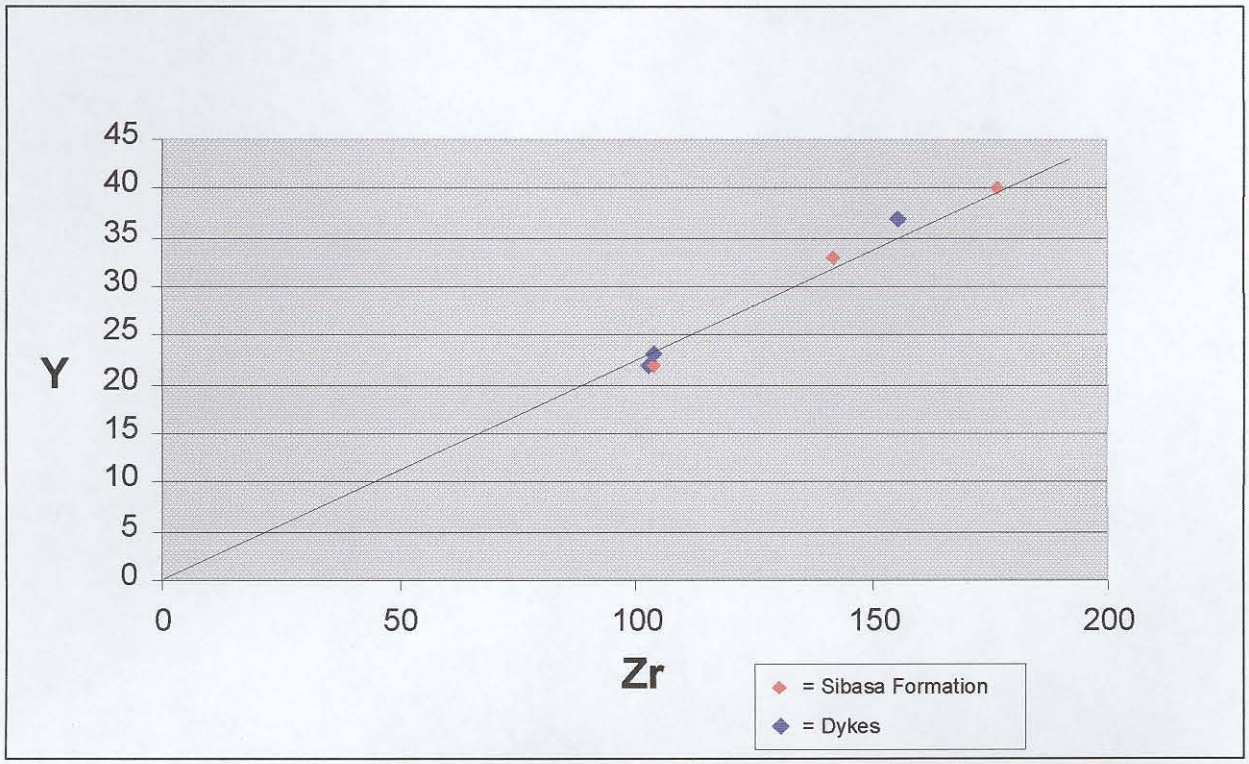

Figure 8.2: Variation diagram between Zr and Y for the Sibasa basalts and dykes intruding the study area, suggesting a common parental magma.

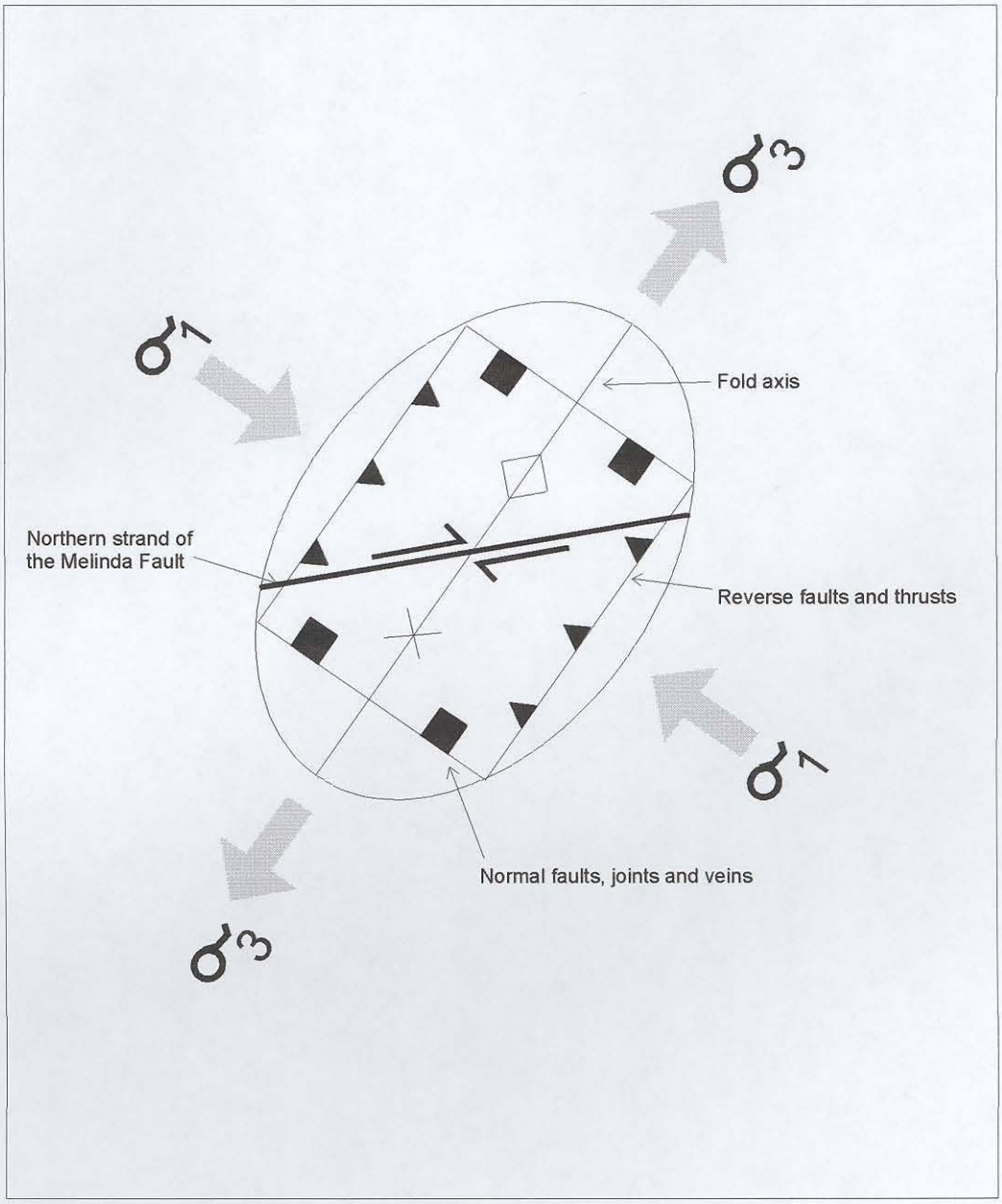

Figure 8.3: Strain ellipse which accounts for the structures recorded in the Wyllies Poort Formation adjacent to the northern strand of the Melinda Fault and its splays.

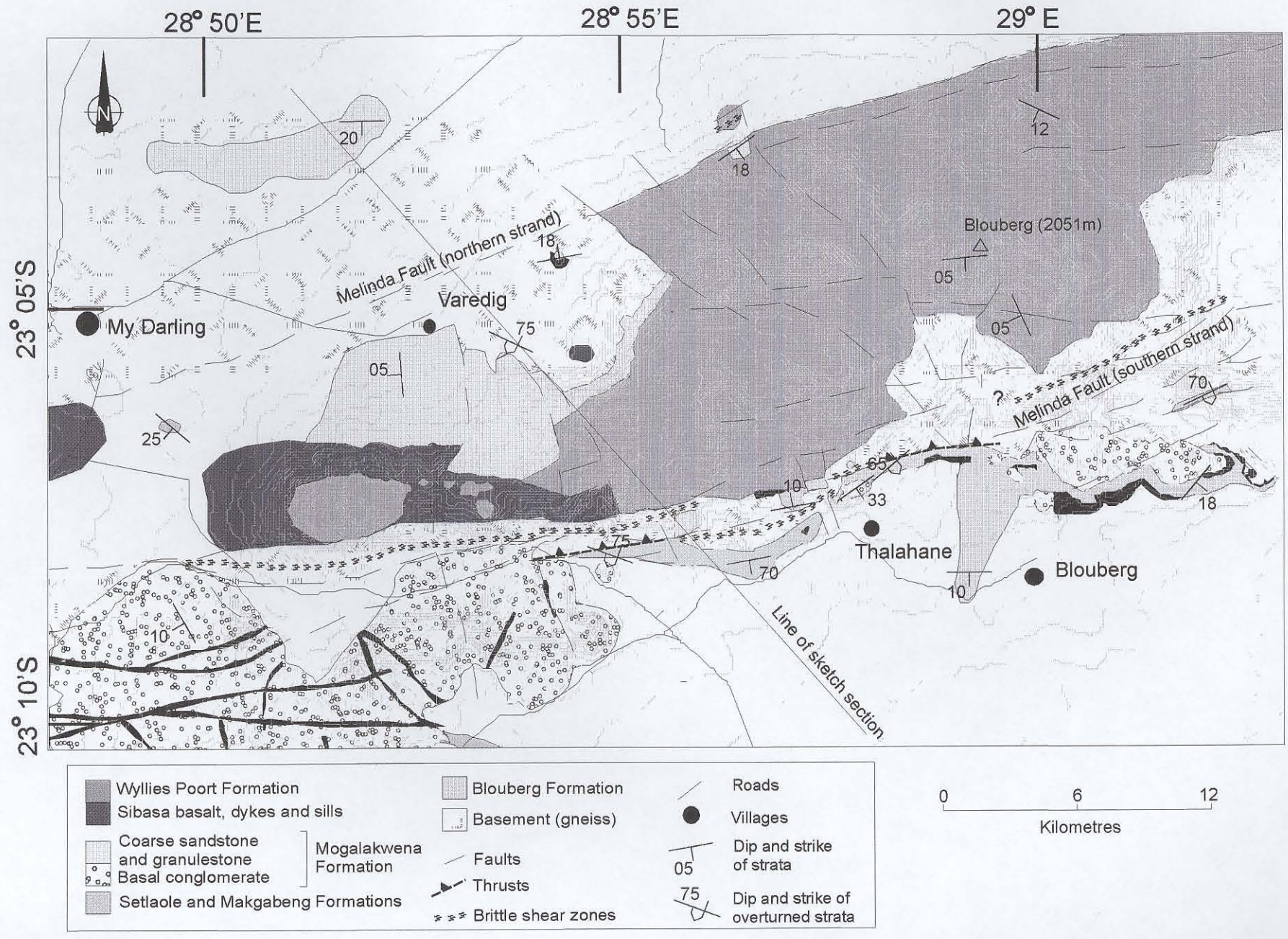

Figure 8.4: Map showing approximate line of idealised cross-section shown in Figure 8.5.

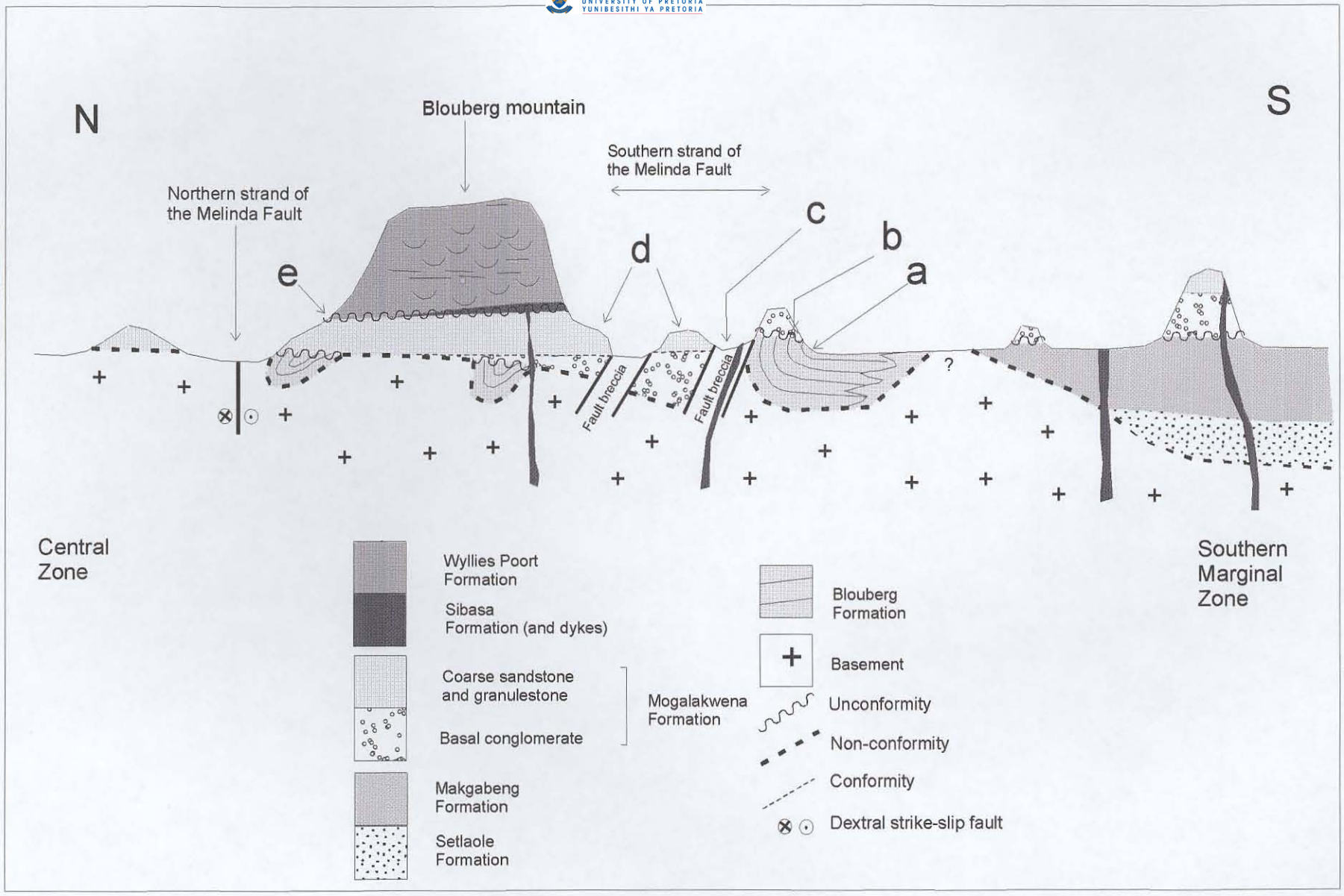

Figure 8.5: Idealised cross-section through Blouberg mountain, showing the structural relationships proposed in Chapter 8.

a.

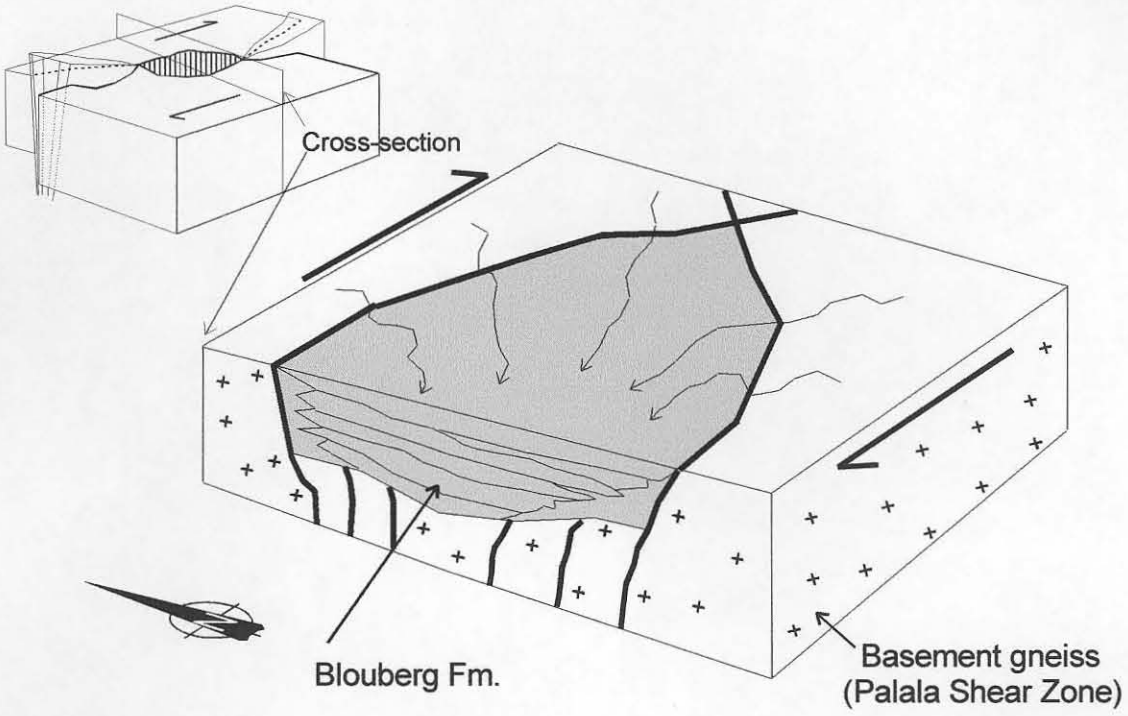

Blouberg Formation (Lower Member) sedimentation in deep, localised depositories, possibly reflecting pull-apart basins, caused by strike-slip reactivation along the Palala Shear Zone.

b.

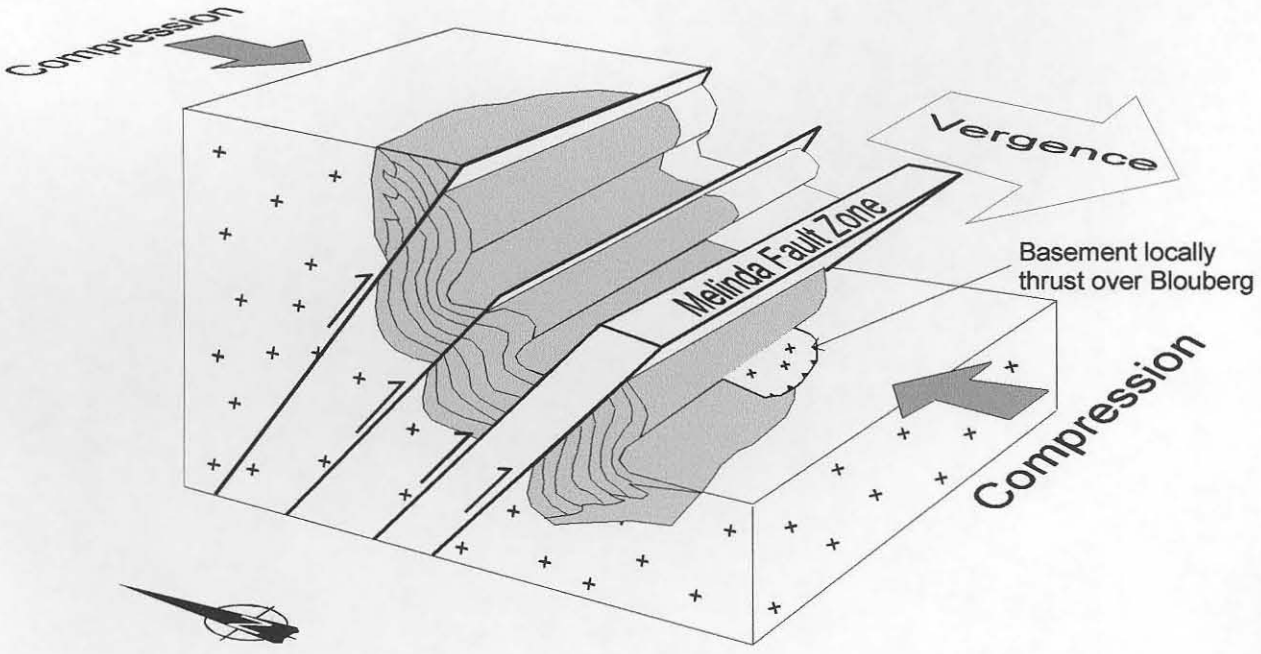

Lower Member of Blouberg Formation is folded, locally overturned and faulted during southwards-vergent, N-S orientated compression. Reverse faults dip to the north. Upper Member is deposited locally thereafter.

c.

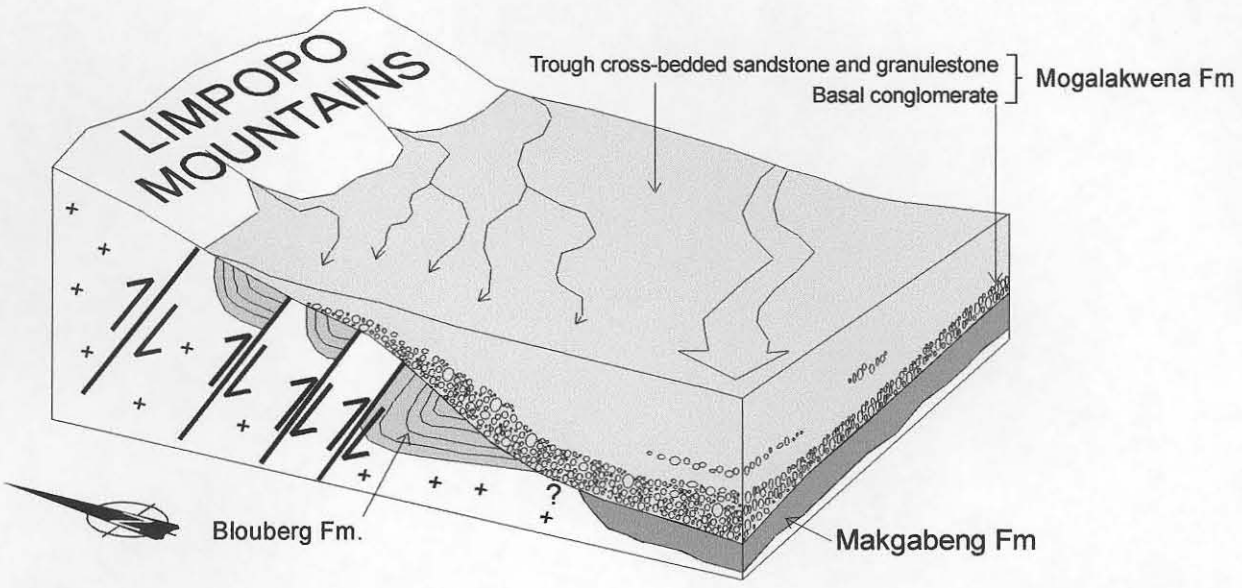

Mogalakwena conglomerates, granulestones and sandstones lain unconformably on the Blouberg Formation and nonconformably on the basement.

d.

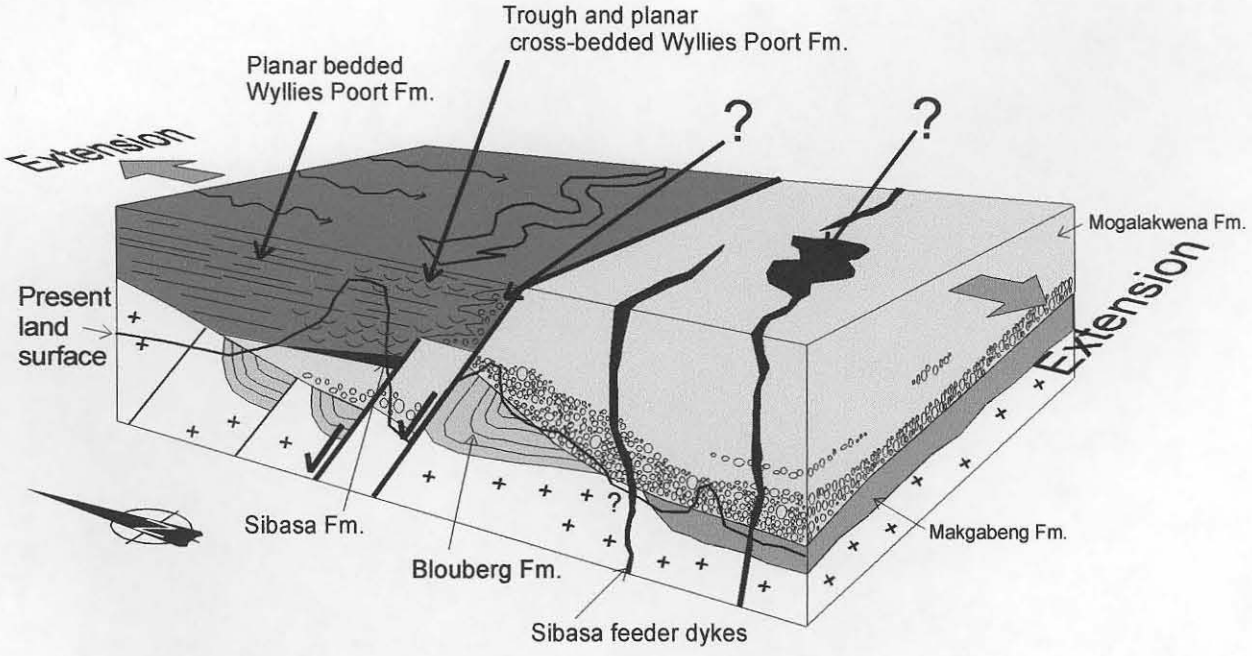

Melinda Fault reactivated as normal faults in an extensional regime, creating a half-graben for the Soutpansberg Group depository. The laterally extensive Wyllies Poort Formation is deposited unconformably over the Mogalakwena Formation, and nonconformably over the basement.

e.

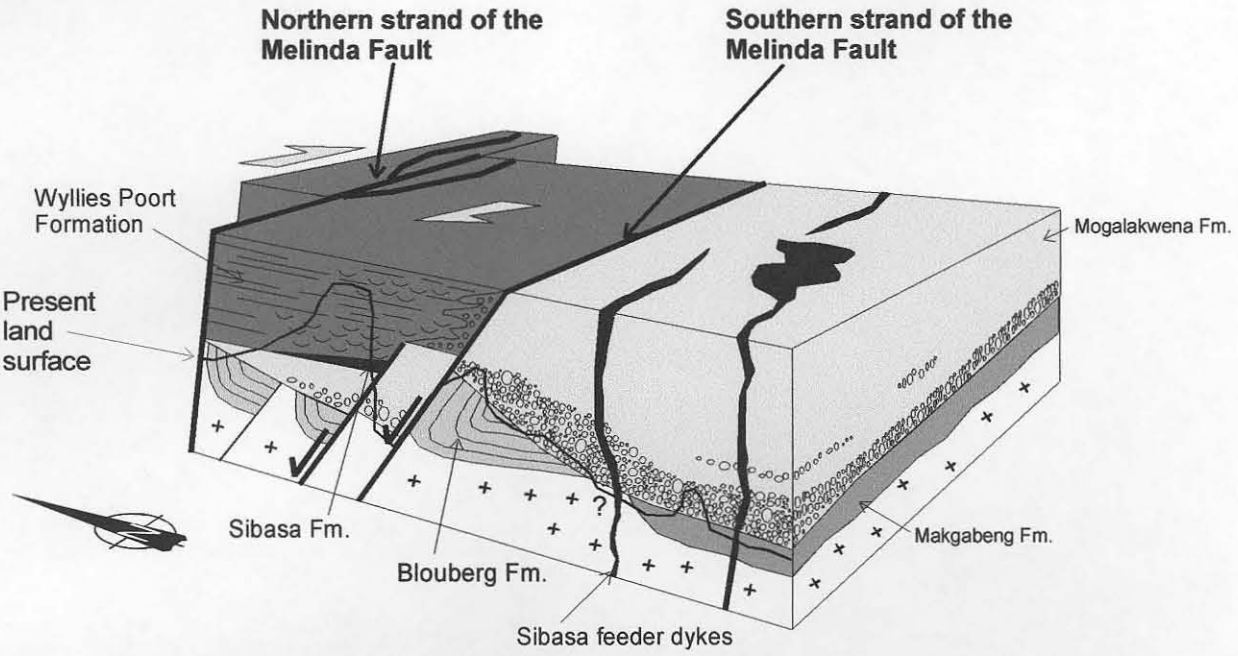

Northern strand of the Melinda Fault activates as a dextral strike-slip fault, and displaces the Soutpansberg strata, probably during the Phanerozoic.

Figure 8.6: Block diagrams illustrating the proposed model for the tectonic and sedimentary evolution of the Blouberg area.

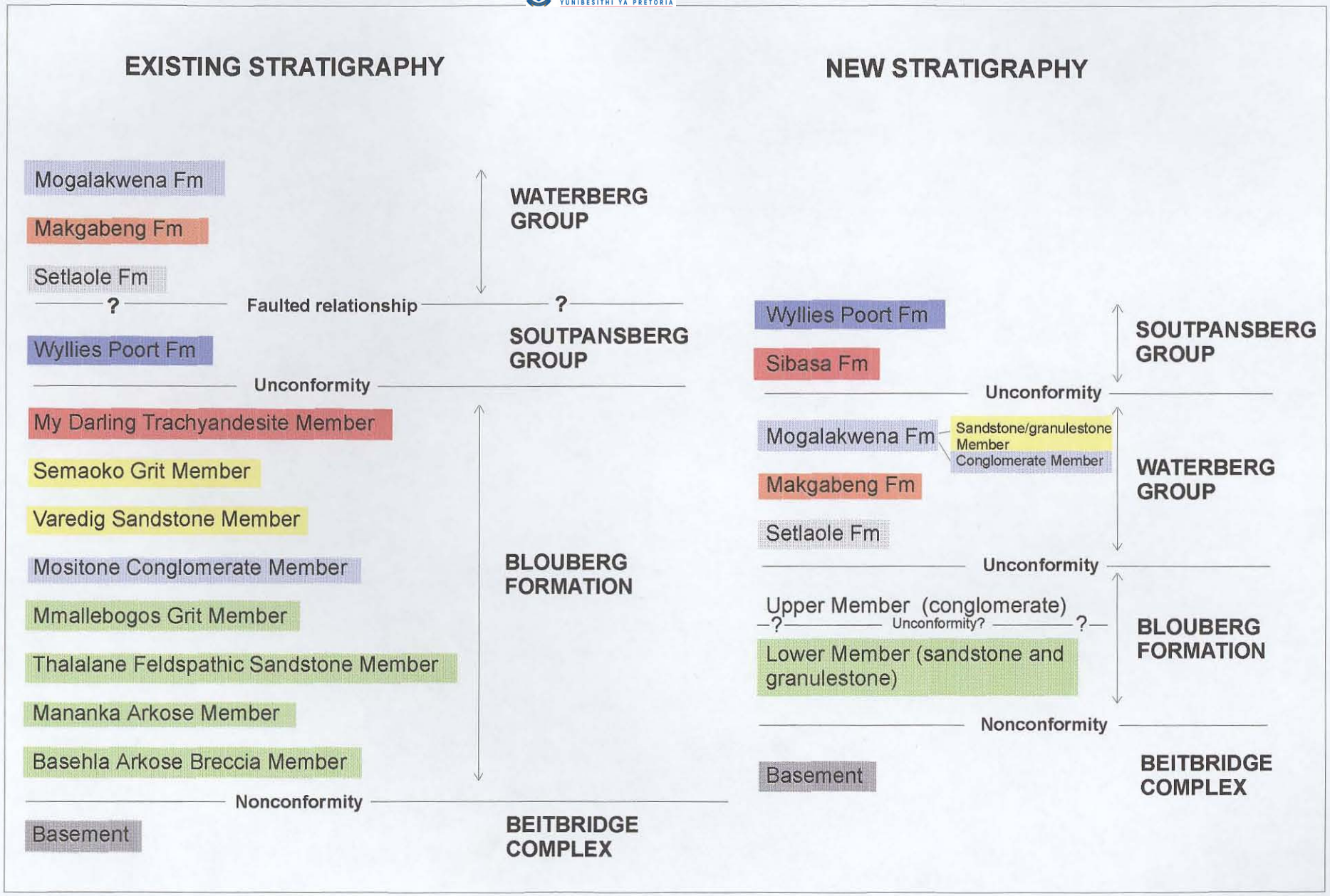

Table 8.1: Proposed new stratigraphic subdivision of the study area. Coloured boxes illustrate correspondence between the existing (Jansen, 1976; Meinster, 1977) stratigraphy and the proposed new stratigraphy.

a.

Facies Code	Facies	Sedimentary structures	Interpretation
Gmm	Matrix-supported, massive gravel	Weak grading	Plastic debris-flow (High stregth, viscous)
Gmg	Matrix-supported gravel	Inverse to normal grading	Pseudoplastic debris flow (Low strength, viscous)
Gci	Clast-supported gravel	Inverse grading	Clast-rich debris flow (high strength) or pseudoplastic debris flow (low strength)
Gcm	Clast-supported massive gravel	-	Pseudoplastic debris flow (inertial bedload, turbulent flow)
Gh	Clast-supported, crudely bedded gravel	Horizontal bedding, imbrication	Longitudinal bedforms, lag deposits, sieve deposits
Gt	Gravel, stratified	Trough cross-beds	Minor channel fills
Gp	Gravel, stratified	Planar cross-beds	Transverse bedforms, deltaic growths from older bar remnants
St	Sand, fine to very coarse may be pebbley	Solitary or grouped trough cross-beds	Sinuous-crested and linguoid (3D) dunes
Sp	Sand, fine to very coarse may be pebbley	Solitary or grouped planar cross-beds	Transverse and linguoid bedforms (2D dunes)
Sr	Sand, fine to very coarse	Ripple cross-lamination	Ripples (Lower flow regime)
Sh	Sand, fine to very coarse, may be pebbley	Horizontal lamination parting or streaming lineation	Plane-bed flow (Critical flow)
Sl	Sand, fine to very coarse, may be pebbley	Low-angle(<15°) cross-beds	Scour-fills, humpback or washed-out dunes, antidunes
Ss	Sand, fine to very coarse, may be pebbley	Broad, shallow scours	Scour fill
Sm	Sand, fine to coarse	Massive or faint lamination	Sediment gravity flow deposits
Fl	Sand, silt, mud	Fine lamination very small ripples	Overbank, abandoned channel, or waning flood deposits
Fsm	Silt, mud	Massive	Backswamp or abandoned channel deposits
Fm	Mud, silt	Massive desiccation cracks	Overbank, abandoned channel or drape deposits
Fr	Mud, silt	Massive, roots, bioturbation	Rootbed, incipient soil
C	Coal, carbon-aceous mud	Plant, mud films	Vegetated swamp deposit
P	Palaeosol carbonate (Calcite, siderite)	Pedogenic features; nodules, filaments	Soil with chemical precipitation

b.

Element	Symbol	Lithology	Interpretation
Major sandstone sheet	CHS	Gm, Se, St, Sh, Sl, rare Sp	Braided fluvial channel
Major sandstone ribbon	CHR	Gm, Se, St, Sh, Sl, rare Sp	Anastomosed fluvial channel
Minor sandstone sheet	CS	Se, Sh, Sl, rare St, Sr	Sheet splay
Minor sandstone lens	CRS	Se, St, Sl, Sh, Sr	Minor crevasse channel

Table 8.2a.: Interpretation of facies classifications (after Miall, 1996). b.: Interpretation of architectural elements (based on those of the Cutler Formation, New Mexico) (after Miall, 1996).

CHAPTER 9: ECONOMIC POTENTIAL.

A small, abandoned mine is situated at 23°08.30'S; 29°42.70'E. The mine is located approximately where the northern and southern strands of the Melinda Fault merge at the western side of Blouberg mountain. The host rock consists of foliated granitic and locally amphibolitic material that now resembles mylonite. The foliation planes generally have a dip-direction of 75°→053°, which is consistent with the regional (Palala parallel) trend. The foliation planes are locally exploited by wide (50cm-1m) veins containing quartz, baryte and small amounts of galena. The baryte content is between 35 and 50% (Willemse, *et al.*, 1944). The mine was considered uneconomic for either lead or baryte mining, and has closed.

Several rocks in the study area were sampled for hydrothermal or placer gold mineralisation. Sampling including the wide quartz veins associated with the northern strand of the Melinda Fault, where it cuts the Wyllies Poort Formation at 23°02.08'S; 28°59.78'E, and hydrothermally altered jasperitic patches developed between the base of the Blouberg Formation and the breccia of the southern strand of the Melinda Fault at 23°07.39'S; 28°57.46'E and 23°07.81'S; 28°56.74'E. Conglomerates from the Blouberg, Mogalakwena and Wyllies Poort formations were sampled for placer gold deposits by fire assay. Only one pebble conglomerate showed any traces of gold (0.9g/tonne), which was collected from the base of the Mogalakwena Formation at the unconformity with the Blouberg Formation at 23°07.35'S; 28°57.53'E. Other samples of basal Mogalakwena conglomerate were collected from this unconformity in other areas of the study area, but did not indicate further mineralisation. The location of the gold mineralisation (on an angular unconformity adjacent to the southern strand of the Melinda Fault) may rather reflect hydrothermal mineralisation associated with the Fault rather than placer deposition.

The continental, fluvial environment proposed here for the Blouberg Formation suggests that it holds no potential as a target for Sedex-type massive sulphide exploration. No other data of economic importance were encountered during this work.

CHAPTER 10: CONCLUSIONS.

In the preceeding chapters, the geology of the Blouberg Formation, Waterberg and Soutpansberg Groups in the area of Blouberg mountain, Northern Province, South Africa, has been described. From this data, a provisional model for the sedimentary and tectonic evolution of the strata in this area has been proposed.

Of importance to the geology of the Blouberg mountain area is the fact that it appears to straddle the suture between the Southern Marginal Zone (reworked Kaapvaal Craton) and the exotic terrane of the Central Zone of the Limpopo Mobile Belt. This suture is generally regarded as being marked by the Palala Shear Zone, which outcrops 50km W.S.W. of the study area, and it seems that the ductile deformation recorded in the banded gneiss in the basement lithologies of the study area represent a higher-grade (i.e. deeper crustal) equivalent to the rocks of the Palala Shear Zone. Thus the underlying crust of the Blouberg mountain area can be considered to have been assembled during the collisional tectonics of the Limpopo event, which took place at either 2.7Ga (with subsequent reactivation at 2.0; McCourt and Armstrong, 1998) or only at 2.0 Ga (e.g. Kröner *et al.*, 1999).

The oldest basin preserved along this cratonic suture is that of the Blouberg Formation. This work has generally simplified the earlier model proposed by Jansen (1976) for the sedimentation of the Blouberg Formation. Jansen (1976) accounted for the varying sedimentary rocks that he included in the Blouberg Formation as having been laid within an active block-faulted terrain, thus allowing for a range of sediments to have been deposited within small, localised fault-bounded basins at different times. This work has shown that all strata outcropping to the north of the southern strand of the Melinda Fault, which Jansen (1976) had included within the Blouberg Formation (i.e. the Mositone Conglomerate Member, the Semaoko Member and the Varedig Member), correlate well with distal facies of the Mogalakwena Formation (Waterberg Group) and, as such, should not be considered within the stratigraphy of the Blouberg Formation. Similarly the My Darling Trachyandesite Member (Blouberg Formation according to Jansen, 1976), which

has been demonstrated to be basaltic, should rather be considered as representing a western eruptive centre of the Sibasa Formation (Soutpansberg Group).

Having motivated for the removal of the upper-most four of Jansen's (1976) Blouberg Members from the Blouberg Stratigraphy, the remaining, lowermost four members of Jansen's stratigraphy can be considered to represent the Blouberg Formation (*sensu stricto*). Using the facies identified within a 1400m-thick provisional type section of the Blouberg Formation as a stratigraphic model, all other outcrops of the Blouberg Formation (*sensu stricto*) appeared to compare at least reasonably well with this Kranskop section. Thus Jansen's (1976) model involving short-lived sedimentation in isolated block-faulted basins need not be applied, and the Blouberg Formation can rather be considered to represent a two-fold cycle of sedimentation (Lower and Upper Members), separated by a period of proximal uplift and tectonism. The same tectonism was likely also responsible for the southward-vergent basin inversion of the Lower Member of the Blouberg Formation. The generally restricted, rapidly deepening nature of the Blouberg basin (indicated by outcrops of the Lower Member), situated along a major fault zone, is consistent with its formation as a pull-apart basin.

The fluvial and aeolian-derived strata of the Waterberg Group in the study area (Setlaole, Makgabeng and Mogalakwena formations), have previously been considered to outcrop only to the south of the southern strand of the Melinda Fault (e.g. Jansen, 1976; Meinster, 1977). This work has shown that this distribution holds only for the Makgabeng Formation. The Setlaole Formation may outcrop 2km S.E. of My Darling, indicating a slight encroachment northwards over the Fault Zone. More convincingly, all strata to the north of the southern strand of the Melinda Fault, formerly mapped as the Blouberg Formation (Jansen, 1976; Meinster, 1977) are interpreted here as Mogalakwena strata, albeit distal facies, related to relatively proximal conglomeratic Moglalakwena strata in adjacent areas immediately to the south. The presence of Mogalakwena strata underlying these more northerly regions suggests that the Waterberg basin onlapped northwards over the cratonic suture, now active as a brittle displacement zone along the southern strand of the Melinda Fault.

The presence of distal (sandstone and granulestone) facies alongside proximal (conglomeratic) facies of the Mogalakwena Formation, separated by crush breccia along the southern strand of the Melinda Fault, suggests that they were juxtaposed by faulting. This was most likely accomplished by a northward-dipping normal fault, as a reactivation of fault planes imposed earlier during the inversion of the lower Blouberg basin. The N-S orientated extensional regime necessary to produce such faulting was likely accompanied by intrusion of dyke swarms into pre-existing basement, Blouberg and Waterberg strata. Upon reaching the surface, the dykes appear to have fed the basaltic lavas of the Sibasa Formation (Soutpansberg Group).

Normal displacement along the southern strand of the Melinda Fault, with the hanging wall to the north, not only juxtaposed contrasting facies of the Mogalakwena Formation, but is also interpreted to have created a southern boundary to a half-graben type basin. Such a basin is envisaged to have acted as a depository for the Soutpansberg Group, as the preserved outcrops of both the Sibasa Formation and the Wyllies Poort Formation are restricted only to the north of the southern strand of the Melinda Fault. Facies characteristics and palaeocurrent directions recorded in the Wyllies Poort Formation are compatible with a fluvial half-graben type depositional setting.

Post-Soutpansberg deformation is represented by the activation of the northern strand of the Melinda Fault, which appears to have displaced the Wyllies Poort Formation by dextral strike-slip movement. Displacement appears to have been accommodated along numerous E.N.E-W.S.W striking splays (flower structure), which occur throughout the northern part of the study area. In the area N.E. of Vivo (in the northeastern part of the study area), these splays appear to have merged and approximately 17km of displacement is indicated here. There is no evidence that this post-Wyllies Poort dextral displacement in any way reactivated the adjacent southern strand of the Melinda Fault.

Thus the sedimentary and tectonic history of the Blouberg Formation, Waterberg and Soutpansberg Groups in the area of Blouberg mountain can be considered in terms of

continued reactivation along a cratonic suture. A sedimentary basin appears to have formed as a result of pull-apart tectonics (Lower Member of the Blouberg Formation) caused by strike-slip reactivation along the suture, only to be inverted during a reorientation of the stress field to approximately N-S. Such tectonism lead to renewed, rapid sedimentation during these syn-tectonic times (Upper Member), and restricted the extent of the successor Waterberg basin (Setlaole and Makgabeng Formations) to the south. General tectonic quiescence, following this N-S oriented compression, allowed for the denudation of the uplifted area to the north and, and deposition of the (upper Waterberg) Mogalakwena Formation, derived from now denuding sources to the north and east. As Mogalakwena fluvial sedimentation continued, these deposits onlapped over the southern strand of the Melinda Fault. The deposition of the Blouberg and Waterberg strata can thus be considered as representing flysch (syn-tectonic) and molasse (post-tectonic) style sedimentation, respectively.

After the end of Waterberg deposition, when the uplifted area to the north had been greatly denuded, renewed reactivation along the southern strand of the Melinda Fault appears again to have controlled sedimentation, during a period of N-S orientated extension, which can be considered to be a reversal of the syn-Blouberg tectonic regime. This led to the creation of the Soutpansberg depository in a half-graben environment.

Subsequent, late-stage reactivation along the suture did not reactivate the southern strand of the Melinda Fault, but instead displaced strata further north, but still parallel to the suture, creating the northern strand of the Melinda Fault.

Thus the geology of the Blouberg mountain area can be considered as a model for basin development and inversion within the realm of a zone of any linear fundamental tectonic weakness, such as a suture zone. Along such zones, it is likely that overlying and adjacent areas are prone to reactivation during any subsequent tectonic episodes, leading to complex structural and sedimentological relationships as basins are created, inverted and superimposed along a long-lived zone of tectonic weakness.

ACKNOWLEDGEMENTS.

I am grateful to several people who helped during the course of this work. Geo Steyn, Kobus Brummer, Charl van Jarsveld, Celine Ravault, Blaise Videt and Pierre Lebrun acted as field assistants during part of the winters of 1998 and 1999, and Wulf Mueller, Patricia Corcoran, Subir Sarkar, visited during field work, and offered advice on field methodology. Ed Simpson and Ken Eriksson spent several weeks with me, during our survey of the Makgabeng Formation. Their tutoring in aeolian sedimentation and handling of data was invaluable. Reneé Greyvensteyn is thanked for her assistance with ArcView during the compilation of the maps, and Wolf Maier is thanked for his advice on the igneous petrology.

The Northern Province Department of Environmental Affairs and Tourism kindly offered accommodation at Blouberg Nature Reserve, and Peter and Janine Snyman of Blouberg Conservation Project provided a home, a family and friendship during the field work.

Gold Fields of South Africa (Pty) Limited funded this project, and this is gratefully acknowledged. In particular, thanks must go to Pat Vickers, Phil Lambert and Steve Ellis who showed much interest in the work.

Finally, I would like to thank Prof. Pat Eriksson and Dr. Roelof van der Merwe, who acted as supervisor and co-supervisor respectively. It has been a pleasure to work with them both.

REFERENCES.

Allen, J.R.L. (1968): Current Ripples. North Holland, Amsterdam.

Anderson, W. (1910): Notes on the general geology of a little known portion of the Waterberg district, between Nylstroom and the Limpopo River to the north west: Trans. geol. Soc. S. Afr., **13**. 17-25.

Anhaeusser, C.R., Mason, R., Viljoen, M.J. and Viljoen, R.P. (1969): A reappraisal of some aspects of Precambrian shield geology. Bull. geol. Soc. Am., **80**. 2175-2200.

Bagnold, R.A. (1954): The physics of blown sand and desert dunes. Methuen, London.

Bahnemann, K.P. (1971): in: E.R. Morrison and J.F. Wilson (Eds.), Symposium on the Granites, Gneisses and related rocks. Excursion guidebook, Geol. Soc. S. Afr., Johannesburg. 44p.

Barker, O.B. (1976): Discussion: H. Jansen: "The Soutpansberg trough (northern Transvaal)-an aulacogen". Trans. geol. Soc. S. Afr., **78**. 146-148.

Barker, O.B. (1979): A contribution to the geology of the Soutpansberg Group, Waterberg Supergroup, northern Transvaal. M.Sc thesis, University of the Witwatersrand, Johannesburg. 116p. (Unpubl.).

Barker, O.B. (1983): A proposed geotectonic model for the Soutpansberg Group within the Limpopo Mobile Belt, southern Africa. In: W.J. van Biljon and J.H. Legg (Eds.), The Limpopo Belt. Spec. Publ. Geol. Soc. S. Afr, **8**. 181-190.

Barker, O.B., Eriksson, P.G. and van der Neut, M. (in press): The Soutpansberg, Waterberg Groups and Blouberg Formation. In: R.J. Thomas, S. McCourt and M.R. Johnson (Eds.), Geology of South Africa. Geol. Soc. S. Afr., Johannesburg

Barton, J.M., Jr., (1979a): The chemical composition, Rb-Sr isotopic systematics and tectonic setting of certain post-kinematic mafic igneous rocks, Limpopo Mobile Belt, southern Africa. Precamb. Res., **9**. 57-80.

Barton, J.M., Jr., (1979b): Crustal evolution clues. Nuclear Active, **21**. 16-19.

Barton, J.M., Jr. (1980): The pattern of Archaean crustal evolution in southern Africa as deduced from the evolution of the Limpopo Mobile Belt and the Barberton Granite-Greenstone Terrane. Sec. Int. Archaean Symp. Perth, 1980, Extended Abstracts. 80-82.

Barton, J.M., Jr. (1981a): The status of isotopic investigations of the Limpopo Mobile Belt. Geocongress '81 Abstracts, Geol. Soc. S. Afr. 14-17.

Barton, J.M., Jr. (1981b): The pattern of crustal evolution in southern Africa as deduced from the evolution of the Limpopo Mobile Belt and the Barberton Granite-Greenstone Terrane. Spec. Publ. geol. Soc. Australia, 7. 21-31.

Barton, J.M., Jr., (1981c): (Ed.), Limpopo Excursion Guidebook, Geol. Soc. S. Afr. 134p.

Barton, J.M., Jr. (1983a): Introduction to Limpopo Belt: In: W.J. van Biljon and J.H. Legg (Eds.), The Limpopo Belt. Spec. Publ. Geol. Soc. S. Afr, **8**. 1-3.

Barton, J.M., Jr. (1983b): Pb-isotopic evidence for the age of the Messina Layered Intrusion, Central Zone, Limpopo Mobile Belt. In: W.J. van Biljon and J.H. Legg (Eds.), The Limpopo Belt. Spec. Publ. Geol. Soc. S. Afr, **8**. 39-42.

Barton, J.M., Jr. (1983c): Pb- isotopic studies of banded iron-formation, Central Zone, Limpopo Mobile Belt. In: W.J. van Biljon and J.H. Legg (Eds.), The Limpopo Belt. Spec. Publ. Geol. Soc. S. Afr, **8**. 43-44.

Barton, J.M., Jr. (1996): The Messina layered intrusion, Limpopo belt, South Africa: and example of in-situ contamination of an Archaean anorthosite complex by continental crust. Precambrian Res., **78**. 139-150

Barton, J.M., Jr. and Key, R.M. (1981): The tectonic development of the Limpopo Mobile Belt and the evolution of the Archaean cratons of southern Africa, 185-212. In: A. Kröner (Ed.), Precambrian plate tectonics. Elsevier, Amsterdam.

Barton, J.M. Jr. and Key, R.M. (1983): Rb-Sr ages and geological setting of certain rock units from the Central Zone of the Limpopo Mobile Belt, near Zanzibar, eastern Botswana. In: W.J. van Biljon and J.H. Legg (Eds.), The Limpopo Belt. Spec. Publ. Geol. Soc. S. Afr, **8**. 19-26.

Barton, J.M., Jr. and McCourt, S. (1983): Rb-Sr age for the Palala Granite, Limpopo Mobile Belt. In: W.J. van Biljon and J.H. Legg (Eds.), The Limpopo Belt. Spec. Publ. Geol. Soc. S. Afr, **8**. 45-46.

Barton, J.M., Jr. and Pretorius, W. (1997): Soutpansberg age (1.85 Ga) magmatism and metallogenesis in southern Africa: a result of regional rifting. International symposium on Plumes, Plates and Mineralisation, Abstracts. University of Pretoria, Pretoria, South Africa.

Barton, J.M., Jr and Ryan, B. (1977): A review of the geochronologic framework of the Limpopo Mobile Belt. Bull. Geol. Surv. Botswana, **12**, 183-200.

Barton, J.M., Jr. and Sergeev, S. (1997): High precision, U-Pb analyses of single grains of zircon from quartzite in the Beitbridge Group yields a discordia. S. Afr. J. Geol., **100**. 37-41.

Barton, J.M., Jr. and van Reenen, D.D. (1992a): When was the Limpopo Orogeny? Precambrian Res., **55**. 7-16.

Barton, J.M., Jr. and van Reenen, D.D. (1992b): The significance of Rb-Sr ages of biotite and phlogopite for the thermal history of the Central and Southern marginal zones of the Limpopo Belt of southern Africa and the adjacent portions of the Kaapvaal craton. Precambrian Res., **55**. 17-31.

Barton, J.M., Jr., Fripp, R.E.P. and Ryan, B. (1977): Rb/Sr ages and geological setting of ancient dykes in the Sand River Area, Limpopo Mobile Belt, southern Africa. Nature, **267**. 487-490.

Barton, J.M., Jr., Ryan, B. and Fripp, R.E.P. (1978): The relationship between Rb-Sr and U-Th-Pb whole rock and zircon systems in the greater than 3790 m.y.old Sand River Gneisses, Limpopo Mobile Belt, southern Africa. U.S. geol. Surv. Open File Rept., **78-701**. 27-28.

Barton, J.M., Jr., Fripp, R.E.P. and Horrocks, P. (1979a): Effects of metamorphism on the Rb-Sr and U-Pb systematics of the Singelele and Bulai gneisses, Limpopo Mobile Belt. Trans. geol. Soc. S., Afr. **82**. 259-269.

Barton, J.M., Jr., Fripp, R.E.P., Horrocks, P. and McLean, N. (1979b): The geology, age and tectonic setting of the Messina Layered Intrusion, Limpopo Mobile Belt, southern Africa. Am. J. Sci, **279**. 1108-1134.

Barton, J.M., Jr., Ryan, B. and Fripp, R.E.P.(1983a): Rb-Sr and U-Th-Pb isotopic studies of the Sand River Gneisses, Central Zone, Limpopo Mobile Belt. In: W.J. van Biljon and J.H. Legg (Eds.), The Limpopo Belt. Spec. Publ. Geol. Soc. S. Afr, **8**. 9-18.

Barton, J.M., Jr., Fripp, R.E.P. and Horrocks, P.C. (1983b): Rb-Sr ages and chemical composition of some deformed Archaean mafic dykes, Central Zone, Limpopo Mobile Belt, southern Africa. In: W.J. van Biljon and J.H. Legg (Eds.), The Limpopo Belt. Spec. Publ. Geol. Soc. S. Afr, **8**. 27-38.

Barton, J.M., Jr., Du Toit, M.C., van Reenen, D.D. and Ryan, B. (1983c): Geochronologic studies in the southern marginal zone of the Limpopo Mobile Belt, southern Africa. In: W.J. van Biljon and J.H. Legg (Eds.), The Limpopo Belt. Spec. Publ. Geol. Soc. S. Afr., **8**. 55-64.

Barton, J.M., Jr., van Reenen, D.D. and Roering, C. (1990): The significance of the 3000Ma granulite facies mafic dykes in the Central Zone of the Limpopo belt, southern Africa. Precambrian Res., **48**. 299-308.

Barton, J.M., Jr., Holzer, L., Kamber, B., Doig, R., Kramers, J.D. and Nyfeler, D. (1994): Discrete metamorphic events in the Limpopo belt, southern Africa: implications for the application of P-T paths in complex metamorphic terrains. Geology, **22**. 1035-1038.

Barton, J.M., Jr., Barton, E.S. and Smith C.B. (1996): Petrography, age and origin of the Scheil alkaline complex, northern Transvaal, South Africa. J. Afr. Earth. Sci., **22**. 133-145.

Berger, M., Kramers, J.D. and Nägler, T.F. (1995): Geochemistry and geochronology of charnoenderbites in the Northern Marginal Zone of the Limpopo belt, southern Africa, and genetic models. Schweiz. Mineral. Petrogr. Mitt., **75**. 17-42.

Blakey, R.C., Havholm, K.G. and Jones, L.S. (1996): Stratigraphic analysis of eolian interactions with marine and fluvial deposits, middle Jurassic Page Sandstone and Carmel Formation, Colorado Plateau, U.S.A. J. Sed. Res., **66**. 324-342.

Blenkinsop, T.G. and Frei, R. (1996): Archaean and Proterozoic mineralisation and tectonics at the Renco Mine (Northern Marginal Zone, Limpopo Belt, Zimbabwe). Econ. Geol., **91**. 1225-1238.

Boryta, M and Condie, K.C. (1990): Geochemistry and origin of the Archaean Beitbridge complex, Limpopo belt, South Africa. J. Geol. Soc. London, **147**. 229-239.

Brandl, G. (1983): Geology and geochemistry of various supracrustal rocks of the Beitbridge Complex east of Messina. In: W.J. van Biljon and J.H. Legg (Eds.), The Limpopo Belt. Spec. Publ. Geol. Soc. S. Afr, **8**. 103-112.

Brandl, G. (1986): The geology of the Pietersburg area: explanation of Sheet 2328 (1:250000), Geological Survey of South Africa, Pretoria, 43p.

Brandl, G. (1987): The geology of the Tzaneen area: explanation of Sheet 2330 (1:250000), Geological Survey of South Africa, Pretoria, 55p.

Brandl, G. (1988): The central zone of the Limpopo metamorphic province: its geological setting and the significance of its southern boundary. Extended Abstracts, Geocongress 88, Geol. Soc. S. Afr. 39-42.

Brandl, G. (1990): Geological setting, petrography and geochemistry of the Alldays Gneiss and associated mafic dykes, Limpopo Belt, South Africa. In: J.M. Barton, Jr. (Ed.), The Limpopo Mobile Belt: A Field Workshop on Granulites and Deep Crustal Tectonics. Department of Geology, Rand Afrikaans University, Johannesburg. 22-25.

Brandl, G. (1991): The early Proterozoic Blouberg Formation: its geological setting and stratigraphic position. Precambrian sedimentary basins of southern Africa: Terra Nova abstract supplement **3**.

Brandl, G. and Reimold, W.U. (1990): The structural setting and deformation associated with pseudotachylite occurrences in the Palala shear belt and Sand river gneiss, Northern Transvaal. Tectonophysics, **171**. 201-220.

Broekhuizen, A. (1998): The geology of the Koedoesrand Formation, north-western Transvaal, and its relationship to the Palala Shear Zone. M.Sc. thesis, University of Pretoria. (Unpubl.).

Brookfield, M.E. (1977): The origin of bounding surfaces in ancient aeolian sandstone. Sedimentology, **24**. 303-332.

Callaghan, C.C. (1987a): The geology of the Waterberg group in the Southern portion of the Waterberg Basin. M.Sc. thesis, University of Pretoria, 164p. (Unpubl.).

Callaghan, C.C. (1987b): The geology of the Waterberg Group in the southern portion of the Waterberg Basin. Bull. geol. Surv. S. Afr., 104. 83p.

Callaghan, C.C. and Brandl, G. (1991): Conference on Precambrian sedimentary basins of southern Africa: Excursion guide to the Waterberg Group and Blouberg Formation. Geol. Soc.S. Afr. 51p.

Callaghan, C.C., Eriksson, P.G. and Snyman, C.P. (1991): The sedimentology of the Waterberg Group in the Transvaal, South Africa: An overview. J. Afr. Earth Sci. Spec Publ.

Chavagnac, V., Nägler, T.F. and Holzer, L. (1997): Nd systematics in migmatites: examples of "too old" leucosomes from the Limpopo belt. Terra Nova 9 Abstract Supplement (1). 366.

Cheney, E.S. and Twist, D. (1986): The Waterberg 'basin' – a reappraisal, Trans. geol. Soc. S. Afr., **89**. 353-360.

Cheney, E.S., Barton, J.M., Jr, and Brandl, G. (1990): Extent and age of the Soutpansberg sequences of southern Africa. S. Afr. J. Geol., **93**. 664-675.

Coertze, F.J., Jansen, H. and Walraven, F. (1977): The transition from the Transvaal sequence to the Waterberg Group. Trans. geol. Soc. S. Afr., **80**. 145-156.

Condie, K.C. (1997): Plate Tectonics and Crustal Evolution. 4th edition, Butterworth-Heinman, Oxford.

Corcoran, P.L., Mueller, W.U. and Chown, E.H. (1998): Climatic and tectonic influences on fan deltas and wave- to tide controlled shoreface deposits: evidence from the Archaean Keskarrah Formation, Slave Province, Canada. Sediment. Geol., **120**. 125-152.

Costa, J.E. (1983): Paleohydraulic reconstruction of flash-flood peaks from boulder deposits in the Colorado Front Range. Bull. Geol. Soc. Amer., **94**. 986-1004.

Cotter, E. (1978): The evolution of fluvial style, with special reference to the central Appalachian Palaeozoic. In: A.D. Miall (Ed.), Fluvial sedimentology. Mem. Can. Soc. Petrol. Geol., Calgary, **5**. 361-383.

Coward, M.P. (1983): Some thoughts on the Tectonics of the Limpopo Belt: In: W.J. van Biljon and J.H. Legg (Eds.), The Limpopo Belt. Spec. Publ. Geol. Soc. S. Afr, **8**. 175-180.

Coward, M.P., Graham, R.H., James, P.R. and Wakefield, J. (1973): A structural interpretation of the northern margin of the Limpopo Orogenic belt, southern Africa. Phil. Trans. R. Soc. Lond., **A273**. 487-492.

Cox, K.G., Johnson, R.L., Monkman, C.J., Stilman, C.J., Vail, J.R. and Wood, D.N. (1965): The geology of the Nuanetsi igneous province. Phil. Trans. R. Soc. Lond., **A257.** 71-218.

Crow, C. and Condie, K.E. (1990): Geochemistry and origin of early Proterozoic volcanic rocks from the Transvaal and Soutpansberg successions, South Africa. Precambrian Res., **47**. 17-26.

Crowell, J.C., (1974): Sedimentation along the San Andreas Fault, California. In: R.H. Dott and R.H. Shaver (Eds.), Modern and ancient geosynclinal sedimentation. Soc. Econ. Paleontol. Mineral. Spec. Publ., **19**. 292-303.

Cullen, D.J. (1960): A note on the distribution of the Waterberg and Loskop Formations in the southern Bechuanaland Protectorate. Trans geol. Soc S. Afr., **63**. 161-174.

Daly, R.A. and Molengraaf, G.A.F. (1924): Structural relations of the Bushveld Igneous Complex, Transvaal. J. Geol., **32(1)**. 1-35.

De Bruiyn, H. (1971a): The geology of the central portion of the Waterberg Basin around Vaalwater, northern Transvaal: Rep. geol. Surv. S. Afr., **1971-0045**. 11p. (Unpubl.).

De Bruiyn, H. (1971b): The geology of the eastern portion of the Waterberg Basin between Mokamole and the Blouberg (Sheet 2328): Rep. geol Surv. S. Afr., **1971-0045**. 11p. (Unpubl.).

De Bruiyn, H. (1972a): Folded cross-bedding in the Waterberg System. Ann. geol. Surv. S. Afr. **9**. 91-93.

De Bruiyn, H. (1972b): Report on the Nooitgedacht lead mine, north east of Vaalwater, northern Transvaal: Rep. geol. Surv. S. Afr., **1972-0041**. 5p. (Unpubl.).

De Villiers, S.B. (1963): Die Geologie van die noordewestelike gedeelte van gebied 2428B: Int. Rep. geol. Surv. S. Afr., **1963-0065**. 31p. (Unpubl.).

De Villiers, S.B. (1966): Voorkoms van ilmaniet-sirkoonhoudende sandsteen in die distrikte Waterberg en Potgietersrus: Rep. geol. Surv. S. Afr., **1966-0013**. (Unpubl.).

De Villiers, S.B. (1967): Aanvoerrigtings van sedimente van die Sisteme Loskop en waterberg in Noorde-Transvaal soos weer-spieël deur kruisgelaagdheid: Ann. geol. Surv. S. Afr., **6**. 63-68.

De Vries, W.C.P. (1969): Stratigraphy of the Waterberg System in the Southern Waterberg area, north western Transvaal. Ann. geol. Surv. S. Afr., 7. 43-56.

De Vries, W.C.P. (1970): The geology of the southern portion of the Waterberg area, north eastern Transvaal. Rep. geol. Surv. S. Afr., **1970-0062**. (Unpubl.).

De Vries, W.C.P. (1973): Sedimentary structures in the southern and central portions of the Waterberg area, north-western Transvaal: Ann. geol. Surv. S. Afr., 7. 56-73.

Demicco, R.V. and Hardie, L.A. (1994): Sedimentary structures and early diagenetic features of shallow marine carbonate deposits. S.E.P.M. Atlas Ser., **1**. 265p.

Du Plessis, C.P. (1987): New perspectives on early Waterberg Group sedimentation from the Gatkop area, northwestern Transvaal. S. Afr. J. Geol., **90**. 395-408.

Du Plessis, M.D. (1972a): The relationship between the Bushveld Complex and the Waterberg System in the area between Loubad and Warmbad. Ann. geol. Surv. S. Afr., **9**. 85-88.

Du Plessis, M.D. (1972b): The geology of the area north west of Warmbaths, Transvaal: Sheet 2428C. Rep. geol. Surv. S. Afr. **1972-0043**. (Unpubl.).

Du Preez, J.W. (1944): The structural geology of the area east of Thabazimbi and the genesis of the associated iron ores: Ann. Univ. Stellenbosch, **22A**. 263-360.

Du Toit, M.C. (1979): Die geologie en struktuur van die gebiede Levubu en Bandelierkop in Noord Transvaal. Ph.D. thesis, Rand Afrikaans Univeristy, Johannesburg. 241p. (Unpubl.).

Du Toit, M.C. and van Reenen, D.D. (1977): The southern margin of the Limpopo Mobile Belt, northern Transvaal, with special reference to metamorphism and structure. Bull. Geol. Surv. Botswana, **12**. 83-97.

Du Toit, M.C., van Reenen, D.D. and Roering, C. (1983): Some aspects of the geology, structure and metamorphism of the Southern Marginal Zone of the Limpopo Metamorphic Complex. In: W.J. van Biljon and J.H. Legg (Eds.), The Limpopo Belt. Spec. Publ. Geol. Soc. S. Afr, **8**. 121-142.

Eriksson, K.A. and Simpson, E.L. (1998): Controls on spatial and temporal distribution of Precambrian aeolianites. Sedimentary geology, **120**. 5-53.

Eriksson, K.A. and Vos, R.G. (1979): A fluvial fan depositional model for middle Proterozoic red beds from the Waterberg Group, South Africa. Precambrian Res. **9**, 169-188.

Eriksson, P.G. and Cheney, E. S. (1992): Evidence for the transition to an oxygen-rich atmosphere during the evolution of red beds in the Lower Proterozoic sequences of southern Africa. Precambrian Res., 54. 257-269.

Eriksson, P.G., Reczko, B.F.F., Boschoff, A.J., Schreiber, U.M., van der Neut, M. and Snyman, C.P. (1995): Architectural elements from Lower Proterozoic braid-delta and high-energy tidal flat deposits in the Magaliesberg Formation, Transvaal Supergroup, South Africa. Sediment. Geol., **97**. 99-117.

Eriksson, P.G., Condie, K.C., Tirsgaard, H., Mueller, W.U., Altermann, W., Miall, A.D., Aspler, L.B., Catuneanu, O and Chiarenzelli, J.R. (1998): Precambrian clastic sedimentation systems. Sed. Geol., **120**. 5-53.

Eriksson, P.G., Simpson, E.L., Eriksson, K.A., Bumby, A.J., Steyn, G.L. and Sarker, S. (2000): Muddy roll-up structures in siliciclastic interdune beds of the c. 1.8 Ga Waterberg Group, South Africa. Palaios, **15**. 177-183.

Ethridge, F.G. and Schumm, S.A. (1978): Reconstructing paleochannel morphologic and flow characteristics: methodology, limitations and assessment. In: A.D.Miall (Ed.). Fluvial Sedimentology. Mem. Can. Soc. Petrol, Geol., Calgary, **5**. 703-721.

Fripp, R.E.P. (1981): The ancient Sand River Gneisses, Limpopo Mobile Belt, South Africa. Spec. Publ. geol. Soc. Australia, **7**. 329-335.

Fripp, R.E.P. (1982): The Precambrian geology of the area around the Sand River near Messina, northern Transvaal. Ph.D. thesis. University of the Witwatersrand, Johannesburg. 251p. (Unpubl.).

Fripp, R.E.P. (1983): The Precambrian geology of the area around the Sand River near Messina, Central Zone, Limpopo Mobile Belt. In: W.J. van Biljon and J.H. Legg (Eds.), The Limpopo Belt. Spec. Publ. Geol. Soc. S. Afr, **8**. 89-102.

Fripp, R.E.P., Lilly, P.A. and Barton, J.M., Jr. (1979): The structure and origin of the Singelele gneisses at the type locality near Messina, Limpopo Mobile Belt. Trans, geol, Soc. S. Afr. **82**. 161-167.

Fripp, R.E.P., Van Nierop, D.A., Callow, M.J., Lilly, P.A. and Du Plessis, L.U. (1980): Deformation in part of the Archaean Kaapvaal Craton, South Africa. Precambrian Res., **13**. 241-251.

Frick, A. (1970): Sedimentological aspects of a portion of the southeastern Waterberg area: Ann. geol. Surv. S. Afr., **8**. 69-74.

Frick, A. (1971): Sedimentological aspects of a portion of the southeastern Waterberg area: Rep. geol. Surv. S. Afr., **1971-0050**. 12p. (Unpubl.).

Frick, A. (1972a): The possibility of heavy mineral deposits in the Waterberg System: Ann. geol. Surv. S. Afr., **9**. 93-95.

Frick, A. (1972b): Geological and geochemical investigations of a portion of the southeastern Waterberg basin. Rep. geol. Surv. S. Afr., **1972-0002**. 23p. (Unpubl.).

Frick, A. (1972c): Heavy mineral deposits in the sediments of the Waterberg System. Rep. geol. Surv. S.Afr., **1972-0021**. 6p. (Unpubl.).

Geological Survey of South Africa (1985): Sheet 2328 (Pieterburg, 1: 250 000). Geol. Surv. S. Afr. Govt. printer, Pretoria.

Glatthaar, C.W. (1965): Die verysterde piroklasteen 'n na-Waterbergse graneit, suid-oos van die dam Rust de Winter: M.Sc. thesis, University of Pretoria. 80p. (Unpubl.).

Harger, H.S. (1897): On the occurrence of red sandstone in the Pretoria district. Trans. geol. Soc. S. Afr., **3(9)**. 107-108.

Harmer, R.E. and von Gruenewaldt, G. (1991): A review of magmatism associated with the Transvaal Basin-Implications for its tectonic setting. S. Afr.J.Geol., **94**. 104-122.

Hall, A.L. (1932): The Bushveld Igneous Complex of the central Transvaal. Mem. Geol. Surv. S. Afr. **28**.

Hatch, F. and Corstorphine, G. (1905): The geology of South Africa. 2nd edition, MacMillan and Co., London. 394p.

Hepworth, J.V. (1977): The Limpopo Mobile Belt, some questions. Bull. Geol. Surv. Botswana, **12**. 28-38.

Hofmann, A., Kröner, A. and Brandl. G. (1998): Field relationships of mid- to late-Archaean high-grade gneisses of igneous and sedimentary parentage in the Sand River, Central Zone of the Limpopo belt, South Africa. S. Afr. J. Geol., **101**. 185-200.

Holland, H.D. (1994): Early Proterozoic atmospheric change. In: S. Bengston (Ed.), Early Life on Earth. Columbia University Press, New York. 237-244 p.

Holland, H.D., Lazar, B., McGaffrey, M. (1986): Evolution of the atmosphere and oceans. Nature, **320**. 27-33.

Holmes, A. and Cohen, L. (1957): Geochronologie africains 1956, resultats acquis au ler juillet 1956. Mem. Acad. R. Sci. Colon. Belg., 1-169.

Holmes, G.G. (1904): Some notes on the geology of the northern Transvaal. Trans. geol. Soc. S. Afr., **7**. 51-56.

Holzer, L. (1995): The magmatic petrology of the Bulai Pluton and the Tectono-metamorphic overprint at 2.0 Ga in the Central Zone of the Limpopo belt. (Messina-Beitbridge area, southern Africa). Diploma thesis, Unversity of Berne, Switzerland. (Unpubl.).

Holzer, L., Kamber, B.S., Kramers, J.D. and Frei, R. (1996): The tectono-metamorphic event at 2 Ga in the Limpopo belt and the resetting behaviour of chronometers at high temperature. Commun. geol. Surv. Namibia, **10**. 129-140.

Holzer, L., Kramers, J.D. and Blenkinsop, T.G. (1997): Granulite facies metamorphism in the Limpopo Central Zone (southern Africa): evidence for a Proterozoic continental collision between the Kaapvaal and Zimbabwe cratons. Terra Nova **9** Abstract Supplement (1), 365.

Holzer, L., Frei, R., Barton, J.M., Jr. and Kramers, J.D. (1998): Unravelling the record of successive high grade events in the Central Zone of the Limpopo belt using Pb single phase dating of metamorphic minerals. Precambrian Res., **87**. 87-115.

Horrocks, P.C. (1980): Ancient Archaean supracrustal rocks from the Limpopo Mobile Belt. Nature, **286**. 596-599.

Horrocks, P.C. (1981): The Precambrian geology of the area between Messina and Tshipise, Limpopo Mobile Belt. Ph.D. Thesis, University of the Witwatersrand, Johannesburg. 205p. (Unpubl.).

Horrocks, P.C. (1983): The Precambrian geology of an area between Messina and Tshipise, Limpopo Mobile Belt. In: W.J. van Biljon and J.H. Legg (Eds.), The Limpopo Belt. Spec. Publ. Geol. Soc. S. Afr, **8**. 81-88.

Hunter, R.E. (1977): Basic types of stratification in small aeolian dunes. Sedimentology, **24**. 361-387.

Hunter, R.E. (1981): Stratification styles in eolian sandstones: Some Pennsylvanian to Jurassic examples from the western interior U.S.A. In: F.G. Etheridge and R.M. Flores (Eds.), Recent and Ancient Nonmarine Depositional Environments: Models for Exploration: SEPM Spec. Publ., **31**. 315-329.

Ichihashi, T. and Miyano, T. (1995): A unique P-T trajectory of the Limpopo Central Zone with Tectonic setting deeper to the marginal zones, northeast Beitbridge, Zimbabwe. Centennial Congress. Geol. Soc. S. Afr., Extended abstracts **II**. 178-180.

Irmen, A.P. and Vondra, C.F. (2000): Aeolian sediments in the lower to middle (?) Triassic rocks of central Wyoming. Sediment. Geol., **132**. 69-88.

Jaeckel, P., Kröner A., Kamo, S.L., Brandl, G. and Wendt, J.I. (1997): Late Archaean to early Proterozoic granitoid magmatism and high-grade metamorphism in the central Limpopo belt, South Africa. J. Geol. Soc. London, **154**. 25-44.

Janisch, E.P. (1932): Notes on the Central Part of the Zoutpansberg Range and the Origin of Lake Funduzi. Trans. geol. Soc. S. Afr., **34**.

Jansen, H. (1969): The structural evolution of the southern part of the Waterberg Basin. Ann. geol. Surv. S. Afr., **7**. 57-62.

Jansen, H. (1970a): Volcanic rocks and associated sediments in the southern portion of the Waterberg Basin. Ann. geol. Surv. S. Afr., **8**. 53-61.

Jansen, H. (1970b): The geology of the area around Nylstroom: Rep. geol. Surv. S. Afr., **1970-0057**. 25p. (Unpubl.).

Jansen, H. (1975a): Precambrian basins on the Transvaal Craton and their sedimentological and structural features. Trans. geol. Soc. S. Afr., **78**. 25-33.

Jansen, H. (1975b): The Soutpansberg trough (northern Transvaal) –an aulacogen. Trans. geol. Soc. S. Afr., **78**. 129-136.

Jansen, H. (1976): The Waterberg and Soutpansberg Groups in the Blouberg area, northern Transvaal. Trans. geol. Soc. S. Afr., **79**. 281-291.

Jansen, H. (1977): Authors reply to discussion by B. Meinster. The Waterberg and Soutpansberg Groups in the Blouberg area, northern Transvaal. Trans. geol, Soc. S. Afr., **80**, 296-298.

Jansen, H. (1982): The geology of the Waterberg basins in the Transvaal, Republic of South Africa. Mem. Geol. Surv. S. Afr., **71**, 98p.

Jansen, H., Meinster, B. and de Vries, W.C.P. (1970): The geology of the area between Thabazimbi and Rankins Pass. Rep. geol. Surv. S. Afr., **1970-0061**. 40p. (Unpubl.).

Jansen, H., Meinster, B., de Bruiyn, H. and du Plessis, H. (1972): Modern concepts of Waterberg tectonics and sedimentation. Rep. geol. Surv. S. Afr., **1972-0046**. 28p. (Unpubl.).

Jorrisen, E. (1904): On the occurrence of dolomite and chert series in the north eastern part of the Rustenburg district. Trans geol. Soc. S. Afr., 7. 30-38.

Kamber, B.S. and Biino, G.G. (1995): The evolution of high T-low P granulites in the Northern Marginal Zone sensu stricto, Limpopo Belt, Zimbabwe-the case for petrography. Schweiz. Mineral. Petrogr. Mitt., **75**. 427-454.

Kamber, B.S., Kramers, J.D., Napier, R., Cliff, R.A. and Rollinson, H.R. (1995a): The triangle shear zone, Zimbabwe, revisited; new data document an important date at 2.0 Ga in the Limpopo Belt. Precambrian Res., **70**. 191-213.

Kamber, B.S., Blenkinsop, T.G., Villa, I.M., Dahl, P.S. (1995b): Proterozoic transpressive deformation in the Northern Marginal Zone, Limpopo belt, Zimbabwe. J.Geol., **103**. 493-508.

Kasting, J.F. (1991): Box models for the evolution of atmospheric oxygen: An update. Palaeogeogr., Palaeoclimatol., Palaeoecol., **97**. 125-131.

Kent, L.E. (1939): A copper occurrence in the Zoutpansberg (Bosch Farm). Trans. geol. Soc. S. Afr. **62**.

Key, R.M., Ermanovics, I.F. and Skinner, A.C. (1983): The evolution of the Southern Margin of the Limpopo Mobile Belt in Botswana. In: W.J. van Biljon and J.H. Legg (Eds.), The Limpopo Belt. Spec. Publ. Geol. Soc. S. Afr, **8**. 169-174.

Knyaston, H. and Mellor, E.T. (1912): The geology of the country around Warmbaths and including the Rooiberg tin field: Expl. Sheet **10** (Nylstroom), geol. Surv. S. Afr. 52p.

Kocurek, G. (1988): First-order and super bounding surfaces in eolian sequences – Bounding surfaces revisited. Sediment. Geol. 56. 193-306.

Kocurek, G. and Dott, R.H., Jr. (1981): Distinction and uses of stratification type in the interpretation of eolian sand: J. Sed. Pet., **51**. 579-595.

Kröner, A., Nemchin, A.A., Jaeckel, P., Hofmann, A., Brandl, G. and Pidgeon, R.T. (1998): Field relationships and age of supracrustal Beitbridge Complex and associated granitoid gneisses in the Central Zone of the Limpopo Belt, South Africa. S. Afr. J. Geol., **101**. 201-213.

Kröner, A., Jaeckel, P., Brandl, G., Nechin, A.A. and Pidgeon, R.T. (1999): Single zircon ages for granitoid gneisses in the Central Zone of the Limpopo Belt, southern Africa and geodynamic significance. Precambrian Res., **93**. 299-337.

Layer, P.W., Kröner, A and Jaeckel, P. (1996): Cooling history in the Central Zone of the Limpopo belt, South Africa, as revealed by U-Pb, Pb-Pb and $^{40}Ar/^{39}Ar$ mineral ages. EOS, Trans. Am. Geophys. Union. 77. Supplement, F820.

Le Roux, H.D. (1942): The geology of a portion of the north-eastern section of the New Belgium block of farms. Sheet 31, Potgeitersrust district. Rep. geol. Surv. S. Afr., **1942-0052**. (Unpubl.).

Leeder, M.R. (1973): Fluviatile fining-upwards cycles and the magnitude of palaeochannels. Geol. Mag., **110**, 265-276.

Leeder, M.R. and Gawthorpe, R.L. (1987): Sedimentary models for extensional tilt-block/ half-graben basins. In: M.P. Coward, J.F. Dewey and P.F. Hancock (Eds.), Continental Extension Tectonics. Geol. Soc. Lond. Spec. Publ., 28. 139-152.

Leopold, L.B., Wolman, G.M. and Miller, J.P. (1964): Fluvial processes in Fluvial Geomorphology. Freeman, San Francisco.

Light, M.P.R., 1982: The Limpopo Belt: a result of continental collision. Tectonics **1**, 325-342.

Long, D.G.F. (1978): Proterozoic stream deposits: some problems of recognition and interpretation of ancient sandy fluvial systems. In: Miall, A.D. (Ed.), Fluvial sedimentology. Mem. Can. Soc. petrol. Geol., Calgary, **5**. 313-342.

Loope, D.B., Mason, J.A. and Dingus, L. (1999): Lethal landslides from aeolian dunes. J.Geol.

Lowestein, T.M. and Hardie, L.W. (1985): Criteria for the recognition of salt-pan evaporites. Sedimentology, **32**. 627-644.

MacGregor, A.M. (1953): Precambrian formations of tropical southern Africa. Int. Geol. Cong. Algiers, 1952, **19**. 39-50.

Mason, R. (1973): The Limpopo Mobile Belt-southern Africa. Phil. Trans. R. Soc. Lond., A273. 463-485.

McCourt, S. (1983): Archaean lithologies of the Koedoesrand area, north-west Transvaal, South Africa. In: W.J. van Biljon and J.H. Legg (Eds.), The Limpopo Belt. Spec. Publ. Geol. Soc. S. Afr, **8.** 113-120.

McCourt, S. (1995): The crustal architecture of the Kaapvaal crustal block, South Africa, between 3.5 Ga and 2.0 Ga. Min.Dep. **30**. 86-89.

McCourt, S. and Armstrong, R.A. (1998): SHRIMP U-Pb zircon chronology of granites from the Central Zone, Limpopo Belt, southern Africa: Implications for the age of the Limpopo Orogeny. S. Afr. J. Geol., **101**. 329-337.

McCourt, S. and Vearncombe, J.R. (1987): Shear zones bounding the Central Zone of the Limpopo belt, and adjacent granitoid-greenstone terranes: implications for late Archaean collision tectonics in southern Africa. Precambrian Res., **55**. 553-570.

McCourt, S. and Vearncombe, J.R. (1992): Shear zones of the Limpopo Belt and adjacent granitoid-greenstone terranes: implications for late Archaean collision tectonics in southern Africa. Precambrian Res. **55**. 553-570.

McKee E.D. (1945): Small-scale structures in the Coconino sandstone of northern Arizona: J.Geol., **53**. 313-325.

McKee, E.D. (1979): Ancient sandstones considered to be eolian. In: E.D. McKee (Ed.), A study of global sand seas: U.S. geol. Surv. Prof. Pap., **1052**. 187-238.

McKee, E.D. (1966): Structures of dunes at White Sands National Monument, New Mexico (and a comparison with structures of dunes from other selected areas) Sedimentology, **7**. 1-69.

Meinster, B. (1969): Bedding or cross-bedding? Ann. geol. Surv. S. Afr., 7. 63-67.

Meinster, B. (1970a): Deformed cross-bedding in the Swaershoek stage, Waterberg System. Ann. geol. Soc. S. Afr., 2. 63-68.

Meinster, B. (1970b): The geology of the area between Matlabas and Buffelsdrif, north-western Transvaal (Sheet 2326; Ellisras, 2426; Thabazimbi). Rep. geol. Surv. S. Afr., **1970-0143**. 34p. (Unpubl.).

Meinster, B. (1971): The geology of the south eastern portion of the Waterberg basin between Heuningfontein and the Makapansberge (Sheet 2428). Rep. geol. Surv. S. Afr., **1971**. 38p. (Unpubl.).

Meinster, B. (1972): The geology of the area around Gatkop, east of Thabazimbi, Transvaal. Rep. geol. Surv. S. Afr., **1972-0040**. 35p. (Unpubl.).

Meinster, B. (1975): Thrusting and block faulting around Gatkop, east of Thabazimbi, Transvaal. Ann. geol. Surv. S. Afr., **10**. 57-72.

Meinster, B. (1977): Discussion on H. Jansen: The Waterberg and Soutpansberg groups in the Blouberg area, northern Transvaal. Trans. geol. Soc. S. Afr., **80**. 289-296.

Meinster, B. and Tickell, S.J. (1975): Precambrian aeolian deposits in the Waterberg Supergroup. Trans. geol. Soc. S. Afr., **78**. 191-200.

Mellor, E.T. (1904): The Waterberg Formation and its relation to other Formation in the Transvaal. Trans.geol. Soc. S. Afr., 7. 39-50.

Mellor, E.T. (1905a): The geology of a portion of Springbok Flats and the adjacent areas. Ann. Rep. geol. Surv.Tvl., **1904**, Tvl. Mines Dept. 27-36.

Mellor, E.T. (1905b): The geology of the neighbourhood of Rhenosterkop. Ann. Rep. geol. Soc. Tvl., **1904**, Tvl. Mines. 45-55.

Mellor, E.T. (1907): The geology of the central portion of the Middelberg district, including the town of Middelberg. Ann. Rep. geol. Surv. Tvl., 1906. Tvl. Mines Dept. 53-71.

Mellor, E.T. (1908): Discussion on paper by H. Merensky: The rocks belonging to the area of the Bushveld Granite Complex. Proc. Geol. Soc. S. Afr.,11. 35-36.

Mellor, E.T. (1909a): On a portion of the Waterberg district west of Potgietersrus. Ann. Rep. geol. Surv. Tvl., 1908. Tvl. Mines Dept. 25-50.

Mellor, E.T. (1909b): The geology of Hoekbergen in the Waterberg district, including Gatkop. Ann. Rep. geol. Surv. Tvl. 1908. Tvl. Mines Dept. 51-60.

Mellor, E.T. (1910): The geology of a portion of the Waterberg district to the north of Nylstrrom including Zwagershoek. Ann. Rep. geol. Surv. Tvl. 1908. Tvl. Mines Dept. 41-51.

Mellor, E.T. and Trevor, T.G. (1908): Report on the reconnaissance of the north western Zoutpansberg district. Spec. Publ. geol. Surv. Tvl. **1908**.

Merensky, H. (1908): The rocks belonging to the area of the Bushveld Granite Complex in which tin may be expected with descriptions of the deposits actually found. Trans. geol. Soc. S. Afr., **11**. 25-42.

Miall, A.D. (1977): A review of the braided river depositional environment. Earth. Sci. Rev., **13**. 1-62.

Miall, A.D. (1978): Lithofacies and vertical profiles in modern braided river deposits: A summary. Fluvial sedimentology, Memoir **5**. Canadian Society of Petroleum geologists, Calgary. 668p. 597-604.

Miall, A.D., (1985): Architectural element analysis: a new method of facies analysis applied to fluvial deposits. Earth Sci. Rev., **22**. 261-308.

Miall, A.D. (1988): Facies architecture in clastic sedimentary basins. In: K. Kleinspehn and C. Paola (Eds.), New perspectives in basin analysis. Springler, Berlin, Heidelburg, New York. P. 67-81.

Miall, A.D. (1992): Alluvial deposits. In: R.G. Walker and N.P. James (Eds.), Facies models: response to sea level change. Geological association of Canada, St. John's Newfoundland. 119-142.

Miall, A.D. (1996): The geology of fluvial deposits. Springer-Verlag, Berlin, Heidelburg, New York.

Mkweli, S., Kamber, B. and Berger, M. (1994): Westward continuation of the craton-Limpopo belt tectonic break in Zimbabwe and new age constraints on the timing of thrusting. J. geol. Soc. Lond. **152**. 77-83.

Molengraaff, G.A.F. (1898a): Geological sketch of the Waterberg district. Ann. Rep. geol. Surv. Tvl., **1898**. 18-26.

Molengraaf, G.A.F. (1898b): Rapport over het jaar 1898 van den Staats-geo-loog. Ann. Rep. geol. Surv. Tvl., **1898**, 58.

Molengraaf, G.A.F. (1901): Geologie de la Republique Sud-Africaine du Transvaal. Bull. Geol. Soc. France, **4 (1)**. 13-92.

Molengraaf, G.A.F. (1904): Geology of the Transvaal. Esson and Perkins, Johannesberg. 90p.

Moodie, G.P. (1872): Map of the South African Republic (Transvaal). In: Callaghan (1987b).

Mueller, W.U. and Corcoran, P.L. (1998): Characteristics of pre-vegetational, late orogenic basins: examples from the Archean Superior Province, Canada. Sediment. Geol., **120**. 177-203.

Osterkamp, W.R. and Hedman, E.R. (1982): Perennial streamflow characteristics related to channel geometry and sediment in the Missouri River basin. Prof. Pap. U.S. geol. Surv., **1242**. 37p.

Passchier, C.W. and Trouw, R.A.J.: (1998): Micro-tectonics. Springer-Verlag, Berlin, Heidelburg, New York. 289p.

Pettijohn, F.J., Potter, P.E., Siever, R. (1972): Sand and sandstone. Springer, Berlin, Heidelburg, NewYork. 618p.

Renault, R.W. and Last, W.M. (Eds.) (1994): Sedimentology and geochemistry of modern and ancient saline lakes. SEPM (Soc. Sediment. Geol.) Spec. Publ., **50**. 334 p.

Retief, E.A., Compston, W., Armstrong, R.A. and Williams, I.S. (1990): Characteristics and preliminary U-Pb ages of Zircons from Limpopo belt lithologies. Extended abstracts, Limpopo Workshop, Rand Afrikaans University, Johannesburg. 95-99.

Robertson, I.D.M and Du Toit, M.C. (1982): The Limpopo Belt. In: D.R. Hunter (Ed.), The Precambrian of the southern hemisphere. Elsevier, Amsterdam. p. 641-671.

Roering, C., Berlenbach, J. and Schweitzer, J.K. (1989): Guidelines for the classification of Fault Rocks. Comro, Johannesburg. 22p.

Roering, C., van Reenen, D.D., Smit, C.A., Barton, J.M., Jr., De Beer, J.H., De Wit, M.J., Stettler, E.H., Van Schalkwyk, J.F., Stevens, G. and Pretorius, S. (1992): Tectonic model for the evolution of the Limpopo Mobile belt. Precambrian Res., **55**. 539-552.

Rogers, A.W. (1925): Notes on the north-eastern part of the Zoutpansberg district. Trans. geol. Soc. S. Afr., **28**.

Rollinson, H.R. (1993): A terrane interpretation of the Archaean Limpopo belt. Geol. Mag., **130**. 755-765.

Rollinson, H. and Blenkinsop, T. (1995): The magmatic, metamorphic and tectonic evolution of the Northern Marginal Zone of the Limpopo belt, in Zimbabwe. J. Geol. Soc. Lond., 152. 65-75.

Ryan, B., Kramers, J.D., Stacey, J.S., Delevaux, M., Barton, J.M., Jr. and Fripp, R.E.P. (1983): Sr and Pb isotopic studies and K/Rb ratio measurements relating to the origin and emplacement of copper deposits near Messina, South Africa. In: W.J. van Biljon and J.H. Legg (Eds.), The Limpopo Belt. Spec. Publ. Geol. Soc. S. Afr, **8**. 47-54.

Rye, R. and Holland, H.D. (1998): Paleosols and the evolution of atmospheric oxygen: a critical review. Amer. J. Sci., **298**. 621-672.

S.A.C.S. (South African Committee for Stratigraphy) (1980): Stratigraphy of South Africa. Part 1 (Comp L.E. Kent). Lithostratigraphy of of the Republic of South Africa, South West Africa/Namibia abd the Republics of Boputhatswana, Transkei and Venda: Handbook of the Geological Survey of South Africa, **8**. 690p.

Schieber, J. (1998): Possible indicators of microbial mat deposits in shales and sandstones: examples from the mid-Proterozoic Belt Supergroup, Montana, U.S.A. Sed. Geol., **120**. 105-124.

Schumm, S.A. (1968a): River adjustment to altered hydrologic regimen-Murrumbidgee River and palaeochannels, Australia. Prof. Pap. U.S. geol. Surv., **598**, 65p.

Schumm, S.A. (1968b): Speculations concerning palaeohydrologic controls of terrestrial sedimentation. Bull. Geol. Soc. Am., **79**. 1573-1588.

Schumm, S.A. (1972): Fluvial palaeochannels. In: J.K. Rigby and W.K. Hamblin (Eds.), Recognition of ancient sedimentary environments. Spec. Publ. Soc. Econ. Paleont. Miner., Tulsa, **16**. 98-107.

Simpson, E.L. Kuklis, C.A., Eriksson, K.A., Eriksson, P.G. and Bumby, A.J. (1999): Interbedded eolian dune, interdune and playa deposits, ~1.8 Ga Makgabeng Formation, Waterberg Group, South Africa: climate implications. Geol. Soc. Am. Abstracts with programs, **31 (7)**. 284-285.

Simpson, E.L., Eriksson, K.A., Eriksson, P.G. and Bumby, A.J. (under review): Eolian dune degradation and generation of Massive Sandstones in the Paleoproterozoic Makgabeng Formation, Waterberg Group, South Africa. J. Sed. Res.

Smoot, J.P. and Castens-Seidell, B. (1994): Sedimentary features produces by efflorescent crusts, Saline Valley and Death Valley, California. In: (W. Renaut and W.M. Last (Eds.), Sedimentology and geochemistry of modern and ancient Saline lakes. Spec. Publ. S.E.P.M. (Soc. Sediment. Geol.), Tulsa, **50**. 73-90.

Söhnge, P.G. (1945): The geology of the Messina Copper Mines and surrounding country. Mem. Geol.Surv. S. Afr., **40**.

Söhnge, P.G., Le Roux, H.D. and Nel, H.J. (1948): The geology of the country around Messina. Expl. Sheet **46**, geol. Surv. S. Afr.

Sweet, M.L. (1999): Interaction between aeolian, fluvial and playa environments in the Permian Upper Rotliegend Group, U.K., southern North Sea. Sediment., **46**. 171-187.

Stettler, E.H., (1991): The present thickness of sediments in the main Waterberg basin as derived from Geophysical data. Precambrian sedimentary basins of southern Africa. Absracts, 58. Terra Nova **3**.

Stevens, G. and van Reenen, D.D. (1992): Partial melting and the origin of metapelitic granites in the Southern Marginal Zone of the Limpopo belt, South Africa. Precambrian Res., **55**. 303-319.

Strauss, C.A. (1942): The geology of the north eastern portion of the New Belgium block, Potgietersrust. Rep. geol. Surv. S. Afr., 1942-0053. (Unpubl.).

Strauss, C.A. (1948): The petrology of a small dolerite and granophyre complex in the New Belgium block, Potgietersrust district. Trans. geol. Soc. S. Afr., **50**. 73-101.

Taljaard, M.S. (1938): On the Physiography of an area in the north-eastern Transvaal (a) and an area in northern South-West Africa (b). Ann. Univ. Stellenbosch, **16**.

Tickel, S.J. (1975): Braided river deposits in the Waterberg Supergroup. Trans. geol. Soc. S. Afr., **78**. 83-88.

Therriault,A.M., Reimold, W.U. and Reid, A.M. (1997): Geochemistry and impact origin of the Vredefort Granophyre. S. Afr. J. geol,. **100**, 115-122.

Tirsgaard, H. (1993): The architecture of Precambrian high energy tidal channel deposits: an example from the Lyell Land Group (Eleonore Bay Supergroup), north east Greenland. Sediment. Geol. **88**. 137-152.

Treloar, P.J. and Blenkinsop, T.G. (1995): Archaean deformation patterns in Zimbabwe: true indicators of Tibetan-style crustal extension or not? In: P.P. Coward and A.C. Ries (Eds.) Early Precambrian Processes. Geol. Soc. Spec. Publ. **95**. 87-108.

Treloar, P.J., Coward, M.P. and Harris, N.B.W. (1992): Himalayan-Tibetan analogies for the evolution of the Zimbabwe craton and Limpopo Belt. Precambrian Res., **55**. 571-587.
Tsunogae, T. and Yurimoto, H. (1995): Single zircon U-Pb geochronology of the Limpopo belt by secondary ion mass spectrometry. Geochem. J., **29**. 197-205.

Turner, B.R. (1980): Palaeohydraulics of an upper braided river system in the main Karoo Basin, South Africa. Trans. geol. Soc. S. Afr., **83**. 425-431.

Turner, B.R. and Smith, D.B. (1997): A playa deposit of pre-Yellow Sands age (Upper Rotliegend/Weissliegend) in the Permian of Northeast England. Sediment. Geol., **114**. 305-319.

Van Biljon, W.J. (1977a): An introduction to the Limpopo Mobile Belt. Bull. geol. Surv. Botswana. **12**. 3-8.

Van Biljon, W.J. (1977b): Plate tectonics and ancient mobile belts. Bull. geol. Surv. Botswana. **12**. 211-218.

Van Eeden, O.R., Visser, H.N., van Zyl, J.S., Coertze, F.J. and Wessels, J.T. (1955): The geology of the eastern Soutpansberg and the Lowveld to the north. Expl. Sheet 42. Dept. Mines.

Van der Neut, M. (1994): Lithological description of the Waterberg Group as observed in a borehole drilled on the farm Vleypan 411, North Western Transvaal. Geological Survey of South Africa Report, **137**. 22p. (Unpubl.).

Van der Neut, M. and Eriksson, P.G. (1999): Palaeohydrological parameters of a Proterozoic braided fluvial system (Wilgerivier Formation, Waterberg Group, South Africa) compared with a Phanerozoic example. Spec. Publs. Int. Ass. Sediment., **28**. 381-392.

Van der Neut, M., Eriksson, P.G. and Callaghan, C.C. (1991): Distal alluvial fan sediments in early Proterozoic red beds of the Wilgerivier Formation, Waterberg Group, South Africa. J. Afr. Earth. Sci. **12**. 537-547.

Van Reenen, D.D. (1978): Metamorfe studies van granolite en verwante hoë-graadse gesteentes in die suidelike grenssone van die Limpopo-metamorfekompleks in Suid-Afrika. Ph.D. Thesis, Rand Afrikaans University, Johannesburg. 478p. (Unpubl.).

Van Reenen, D.D. (1983): Cordierite + garnet + hypersphene + biotite-bearing assemblages as a function of changing metamorphic conditions in the Southern Marginal Zone of the Limpopo Metamorphic Complex, South Africa. In: W.J. van Biljon and J.H. Legg (Eds.), The Limpopo Belt. Spec. Publ. Geol. Soc. S. Afr, **8.** 143-168.

Van Reenen, D.D. and Du Toit, M.C. (1977): Mineral reactions and the timing of metamorphic events in the Limpopo Metamorphic Complex south of the Soutpansberg. Bull. geol. Surv. Botswana, **12**. 107-128.

Van Reenen, D.D. and Du Toit, M.C. (1978): The reaction garnet + quartz = hypersthene in granulites of the Limpopo Metamorpic Complex in northern Transvaal. Spec. Publ. geol. Soc. S. Afr., **4**. 149-177.

Van Reenen, D.D., Barton, J.M., Jr., Roering, C., Smit, C.A. and Van Schalkwyk, J.F. (1987): Deep crustal response to continental collision: the Limpopo belt of southern Africa. Geology, **15**. 11-14.

Van Reenen, D.D., Roering, C., Brandl, G., Smit, C.A., van Schalkwyk, J.F. and Barton, J.M., Jr. (1990): The granulite facies rocks of the Limpopo Belt, southern Africa. In: D. Veilzeuf and P. Vidal (Eds.), Granulites and crustal evolution. NATO ASI, **c311**. Kluwer, Dordrecht. 257-289.

Van Reenen, D.D., Roering, C., Ashwal, L.D. and de Wit, M.J. (1992): Regional geological setting of the Limpopo Belt. Precambrian Res., **55**. 1-5.

Vos, R.G. and Eriksson, K.A. (1977): An embayment model for tidal and wave-swash deposits occurring in a fluvially dominated Proterozoic sequence in South Africa. Sediment. Geol., **18**. 161-173.

Wadge, G., Archer, D.J. and Millington, A.C. (1994): Monitoring playa sedimentation using sequential radar images. Terra Nova, **6**. 391-396.

Walraven, F. Armstrong, R.A. and Kruger, F.J. (1990): A chronostratigraphic framework for the north-central Kaapvaal craton, the Bushveld Complex and the Vredefort structure. Tectonophysics, **171**. 23-48.

Watkeys, M.K. and Armstrong, R.A. (1985): The importance of being Alkaline-deformed late Archaean lamprophyric dykes, Central Zone, Limpopo belt. Trans.geol. Soc.S. Afr., **88**. 195-206.

Watkeys, M.K., Light, M.P.R. and Broderick, T.J. (1983): A retrospective view of the Central Zone of the Limpopo Belt, Zimbabwe. In: W.J. van Biljon and J.H. Legg (Eds.), The Limpopo Belt. Spec. Publ. Geol. Soc. S. Afr, **8.** 65-80.

Wentworth, C.K. (1922): A scale of grade class terms for clastic sediments. J. Geol., **30**. 377-392.

Wilke, D.P. (1963): Die geologie van die suidelike gedeelte van blad 2428B/2: Rep. geol. Surv.S.Afr., **1963-0066**. (Unpubl.).

Willemse, J., Schwellnus, C.M., Brandt, J.W., Russel, H.D. and van Rooyen, D.P. (1944): Lead deposits in the Union of South Africa and South-West Africa. Mem. geol. Surv.S. Afr., **39**.

Williams, G.P. (1978): Bank-full discharge of rivers. Water Resour. Res., **14**. 1141-1154.

Wilson, M. (1989): Igneous Petrogenesis. Harper Collins, London. 466p.

APPENDIX 1: GEOLOGICAL MAPS OF THE STUDY AREA.

Index of Field Map sheets in Appendix 1

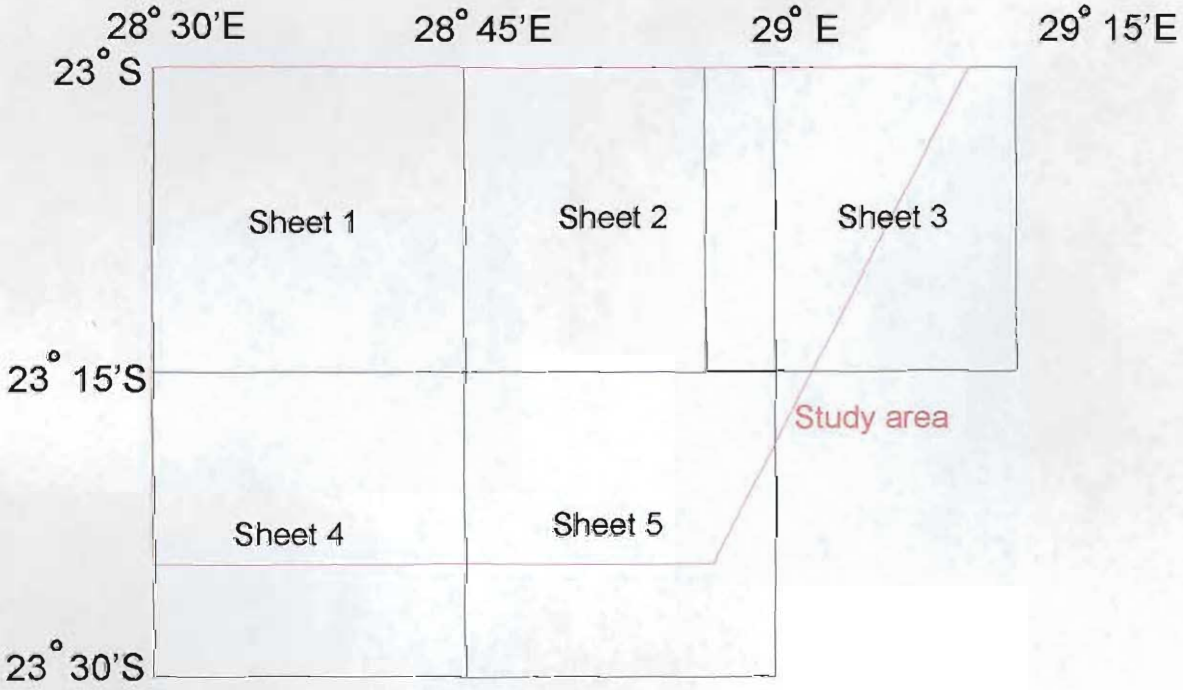

Maps are in folder in back cover

A	B	C	D	E	F	G	H	I	J	K	L	M	N	O	P	Q	R	S	T	U	V
m						%	%	%	%	%			%	%	%	m	cm	cm	cm	cm	cm
87	18					6					24	18	6	18	6	87	3				
86	12					6					18	12	6	12	6	86	2				
85	48					12					60	48	12	48	12	85	4				
84	12					3					15	12	3	12	3	84	4				
83	8					2					10	8	2	8	2	83	4				
82											0	0	0	0	0	82					
81											0	0	0	0	0	81					
80	15					5					20	15	5	15	5	80	3				
79	0					0					0	0	0	0	0	79					
78	30					6					36	30	6	30	6	78	5				
77	25					5					30	25	5	25	5	77	5				
76	10					5					15	10	5	10	5	76	2				
75	4					2					6	4	2	4	2	75	2				
74	2					1					3	2	1	2	1	74	2				
73	65					13					78	65	13	65	13	73	5				
72	35					7					42	35	7	35	7	72	5				
71	48					8					56	48	8	48	8	**71**	6				
70	60					10					70	60	10	60	10	70	6				
69	12.5					5					17.5	12.5	5	12.5	5	69	2.5				
68	84					12					96	84	12	84	12	68	7				
67	20					5					25	20	5	20	5	67	4				
66	12					6					18	12	6	12	6	66	2				
65	16					4					20	16	4	16	4	65	4				
64	72					12					84	72	12	72	12	64	6				
63	4					2					6	4	2	4	2	63	2				
62	3					1					4	3	1	3	1	62	3				
61	5					1					6	5	1	5	1	61	5				
60	6					2					8	6	2	6	2	60	3				
59	28					7					35	28	7	28	7	59	4				
58	28					7					35	28	7	28	7	58	4				
57	28					7					35	28	7	28	7	57	4				
56	21					7					28	21	7	21	7	56	3				
55	21					7					28	21	7	21	7	55	3				

A	B	C	D	E	F	G	H	I	J	K	L	M	N	O	P	Q	R	S	T	U	V
m						%	%	%	%	%			%	%	%	m	cm	cm	cm	cm	cm
54	32					8					40	32	8	32	8	54	4				
53	28					7					35	28	7	28	7	53	4				
52	9					3					12	9	3	9	3	52	3				
51	12					4					16	12	4	12	4	51	3				
50	68		28			14		7			117	96	21	45.5	10.5	50	7		4		
49	28		48			7		6			89	76	13	38	6.5	49	4		8		
48	14		45			7		9			75	59	16	30	8	48	2		5		
47	17.5		90			5		9			121.5	107.5	14	54	7	47	3.5		10		
46	6		32			3		8			49	38	11	19	5.5	46	2		4		
45	12		32			4		8			56	44	12	12	6	45	3		4		
44	12.5		30			5		6			53.5	42.5	11	21	5.5	44	2.5		5		
43	7		15			2		5			29	22	7	11	3.5	43	3.5		3		
42	4		24			2		4			34	28	6	14	3	42	2		6		
41	20		55			4		11			90	75	15	37.5	7.5	41	5		5		
40	14		3			4		1			22	17	5	8.5	2.5	40	3.5		3		
39	10		30			5		5			50	40	10	20	5	39	2		6		
38	91					14					105	91	14	91	14	38	6.5				
37	10					4					14	10	4	10	4	37	2.5				
36	24		6			6		3			39	30	9	15	4.5	36	4		2		
35	8		20			4		4			36	28	8	14	4	35	2		4		
34	8		72			4		12			96	80	16	40	8	34	2		6		
33	12		28			3		7			50	40	10	20	5	33	4		4		
32	10	12	36			4	3	9			74	58	16	19	5.3333333	32	2.5	4	4		
31	2	12	28			1	3	7			53	42	11	14	3.6666666	31	2	4	4		
30	19.5	6	30			3	3	5			66.5	55.5	11	19	3.6666666	30	6.5	2	6		
29	60	15	9			10	5	3			102	84	18	28	6	29	6	3	3		
28	72	64	8			11	16	4			175	144	31	48	10.333333	28	6.5	4	2		
27	9	36	84			3	9	12			153	129	24	43	8	27	3	4	7		
26	56	54	10			8	9	5			142	120	22	40	7.3333333	26	7	6	2		
25	20	176	8			5	22	4			235	204	31	68	10.333333	25	4	8	2		
24	6		6			3		3			18	12	6	6	3	24	2		2		
23	30		28			5		7			70	58	12	29	6	23	6		4		
22	9	12	60			3	3	6			93	81	12	27	4	22	3	4	10		
21	4	24	30			1	4	6			69	58	11	19	4	21	4	6	5		
20	12	25	42			3	5	7			94	79	15	26	5	20	4	5	6		

A	B	C	D	E	F	G	H	I	J	K	L	M	N	O	P	Q	R	S	T	U	V
m						%	%	%	%	%			%	%	%	m	cm	cm	cm	cm	cm
19		45	119				5	17			186	164	22	82	11	19		7	7		
18		424	4				53	2			483	428	55	214	27.5	18		8	2		
17		6	24				3	6			39	30	9	15	4.5	17		2	4		
16		56	16				14	8			94	72	22	36	11	16		4	4		
15		36	63	40			6	9	8		162	139	23	46	8	15		6	7	5	
14		16	77	30			4	11	6			123	21	41	7	14		4	7	5	
13		72	42	960	105		6	8	48	7		1179	69	295	17	13		12	6	20	15
12		6	96	160	70		3	16	16	7		332	42	83	11	12		2	6	10	10
11		60	110	210	56		10	11	21	7		436	49	109	12.25	11		6	10	10	8
10		28	180	650	480		7	12	26	32		1338	77	335	19.25	10		4	15	25	15
9		10	78	5	48		5	13	3	12		141	33	35	8.25	9		2	6	2	4
8		6	440	12	600		3	22	4	24		1058	53	265	13	8		2	20	3	25
7		36	130	27	72		9	13	9	9		265	40	66	10	7		4	10	3	8
6		84	12	14	60		14	2	7	6		170	29	43	7	6		6	6	2	10
5		100	20	12	96		20	5	4	12		228	41	57	10	5		5	4	3	8
4		90	18	48	190		15	6	8	19		346	48	87	12	4		6	3	6	10
3		171	32	24	64		19	8	8	8		291	43	73	11	3		9	4	3	8
2		470	70	27	35		47	10	9	5		602	71	151	17.75	2		10	7	3	7
1		110	12	680	740		11	6	24	37		1542	78	386	20	1		10	2	20	20

A = Stratigraphic height above base
B = Product of i/a and % (Masebe)
C = Product of i/a and % (Sadu)
D = Product of i/a and % (Tsolametse S)
E = Product of i/a and % (Tsolametse N)
F = Product of i/a and % (Blackhill)
G = % of clasts >1cm (Masebe)
H = % of clasts >1cm (Sadu)
I = % of clasts >1cm (Tsolametse S)
J = % of clasts >1cm (Tsolametse N)
K = % of clasts >1cm (Blackhill)

L = Sum of (% of clasts)+(Product x %)
M = Total product for specific height
N = Total % clasts for specific height
O = Average product of i/a x % for specific height (M/n)
P = Average % of clasts for specific height (N/n)
Q = Stratigraphic height above base
R = i/a of largest clast(Masebe)
S = i/a of largest clast (Sadu)
T = i/a of largest clast (Tsolametse S)
U = i/a of largest clast (Tsolametse N)
V = i/a of largest clast (Blackhill)

Location of cross-section is shown on Sheet 3, Appendix 1

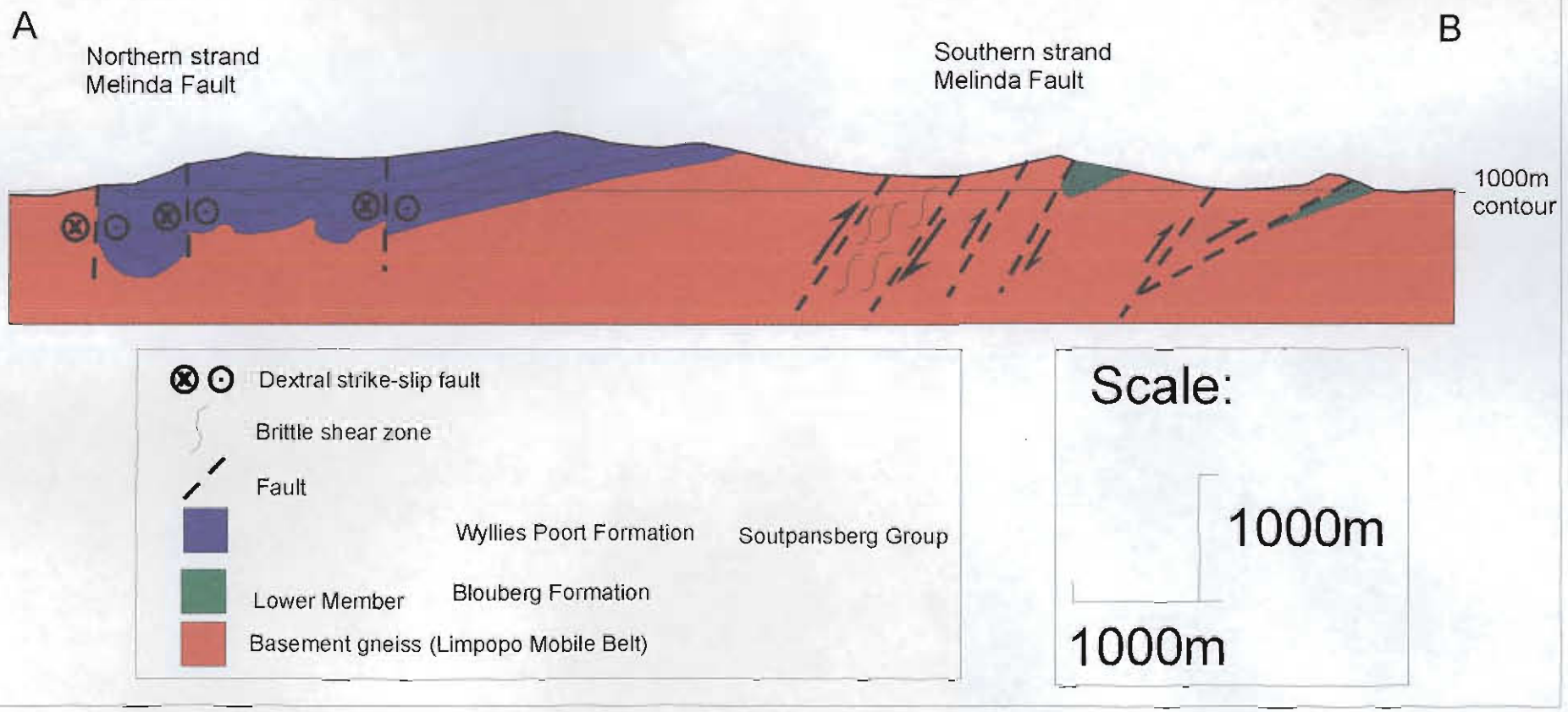

APPENDIX 3a.

Location of cross-section is shown on Sheet 2, Appendix 1

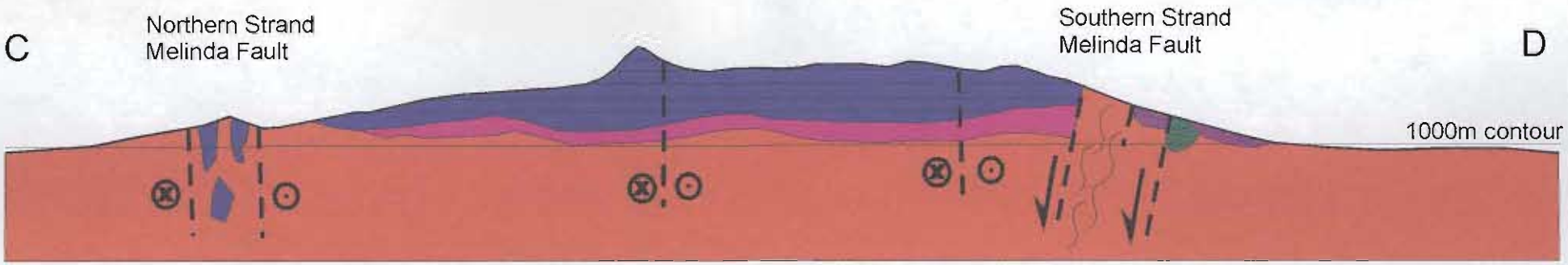

Dextral strike-slip fault

Brittle shear zone

Fault

Wyllies Poort Formation — Soutpansberg Group

Coarse sandstone and granulestone

Conglomerate

Mogalakwena Formation — Waterberg Group

Lower Member — Blouberg Formation

Basement gneiss (Limpopo Mobile Belt)

Scale:

1000m

1000m

APPENDIX 3b.

Location of cross-section is shown on Sheet 2, Appendix 1

Reactivated fault (⚡=most recent movement)

Dextral strike-slip fault

Brittle shear zone

Fault

Wyllies Poort Formation		Soutpansberg Group
Coarse sandstone and granulestone	Mogalakwena Formation	Waterberg Group
Conglomerate		
	Makgabeng Formation	
Lower Member	Blouberg Formation	
Basement gneiss (Limpopo Mobile Belt)		

Scale:

1000m

1000m

APPENDIX 3c.